5-2013

CHARACTERIZATION OF DIFFERENTIATION AND PROGNOSTIC BIOMARKERS ON CD8+ TUMOR-INFILTRATING LYMPHOCYTES IN METASTATIC MELANOMA

Richard C. Wu

CHARACTERIZATION OF DIFFERENTIATION AND PROGNOSTIC BIOMARKERS ON CD8$^+$ TUMOR-INFILTRATING LYMPHOCYTES IN METASTATIC MELANOMA

By

Richard ChengHan Wu, B.S.

APPROVED:

_____

Laszlo Radvanyi, Ph.D.
Supervisory Professor

_____

Qing Ma, Ph.D.

_____

Qing Yi, M.D., Ph.D.

_____

Dapeng Zhou, M.D., Ph.D.

_____

Russell Broaddus, M.D., Ph.D.

APPROVED:

_____

Dean, The University of Texas
Graduate School of Biomedical Sciences at Houston

CHARACTERIZATION OF DIFFERENTIATION AND PROGNOSTIC BIOMARKERS ON CD8$^+$ TUMOR-INFILTRATING LYMPHOCYTES IN METASTATIC MELANOMA

A

DISSERTATION

Presented to the Faculty of

The University of Texas

Health Science Center at Houston

And

The University of Texas

M.D. Anderson Cancer Center

Graduate School of Biomedical Sciences

in Partial Fulfillment

of the Requirements

for the Degree of

DOCTOR OF PHILOSOPHY

in

Immunology

By

Richard ChengHan Wu, Bachelor of Science

Houston, Texas

May, 2013

-DEDICATION-

To my parents, my brother Henry, and my dearest girlfriend, Victoria.

-ACKNOWLEDGEMENTS-

I would like to thank my supervisory professor, Dr. Laszlo Radvanyi, for his superb guidance, mentorship, encouragement, and supervision throughout this thesis work.

I would also like to thank my Advisory Committee members: Drs. Laurence Cooper, Dapeng Zhou, Sandeep Agarwal, and Stephanie Watowich, and my Supervisory Committee members: Drs. Qing Yi, Qing Ma, Dapeng Zhou, and Russell Broaddus, for the support, ideas, and inspirations they provided me throughout this thesis work. I would also like to express my gratitude to the National Center for Research Resources and UT-Health Science Center at Houston's Center for Clinical and Translational Sciences (CCTS) T32 Training Program for three years of research funding support.

Thank you to the Radvanyi Lab and the TIL Clinical Therapy Lab for their support.

I would like to especially thank my family, friends, and loved ones for their continuous support and encouragement.

-TABLE OF CONTENTS-

-List of Illustrations-

-List of Tables-

-ABBREVIATIONS-

ACT: Adoptive T-cell Therapy

AICD: Activation-induced cell death

pAPC: Professional antigen-presenting cells

Akt/PKB: v-akt murine thyomoma viral oncogene homolog 1/Protein kinase B

BTLA: B- and T- Lymphocyte Attenuator

CD: Cluster of Differentiation

CFSE: carboxyfluorescein succinimidyl ester

CTL: Cytotoxic T-Lymphocytes

DC: Dendritic cells

EBV: Epstein-Barr virus

ELISA: Enzyme-linked Immunosorbent Assay

EOMES: eomesodermin (a T-box transcription factor)

FACS: Fluorescent-Activated Cell Sorting

FDA: Federal Drug Administration

FOXP3: forkhead helix box P3

GB: Granzyme B

HCMV: Human cytomegalovirus

HLA: Human Leukocyte Antigen

HNK-1: Human natural killer carbohydrate antigen-1

HVEM: Herpesvirus entry mediator

IDO: Indoleamine-2,3-dioxygenase

IL: Interleukin

IFN-α(γ): Interferon-α(-γ)

ITAMs: Immunoreceptor tyrosine-based activation motifs

ITIMs: Immunoreceptor tyrosine-based inhibitory motifs

KIRs: Killer-cell immunoglobulin-like receptors

KLRG-1: Killer-cell lectin-like receptor G1

LIGHT: homologous to **L**ymphotoxins, exhibits **I**nducible expression,
and competes with HSV **G**lycoprotein D for **H**erpesvirus entry mediator,
a receptor expressed by **T** lymphocytes, a ligand for the TNF receptor superfamily

mAb: Monoclonal antibody

MFI: Mean fluorescence intensity

MHC: Major Histocompatibility Complex

MIP-1β: Macrophage inflammatory protein-1β

NCAM: Neural cell adhesion molecule

NFATc1: Nuclear factor of activated T-cells, cytoplasmic 1

NK: Natural-killer cells

NKR: Natural killer receptor (aNRK – activating, iNKR – inhibitory)

Perf: Perforin

PBMC: Peripheral Blood Mononuclear Cells

PD-1: Programme death 1

PD-L (-1 or -2)/B7-H(-1 or -2): Programmed death ligand (-1 or -2)

PI3K: Phosphoinositide 3-kinase

REP: Rapid-Expansion Protocol

SHP (-1 or -2): the Src-homology 2 domain (SH2)-containing phosphatase (-1 or -2)

TCR: T-cell Receptor

T_{EM}: Effector-Memory T cells

T_{CM}: Central Memory T cells

T_{EMRA}: Terminally-Differentiated CD45RA-Expressing T cells

T_{EFF}: Effector T-cells

TIL: Tumor-infiltrating Lymphocytes

TIL-CM: TIL culture medium

TIM-3: T-cell immunoglobulin- and mucin-domain-containing molecule-3

TNF-α: tumor necrosis factor-α

T_N: Naïve T cells

Treg: T regulatory cells

T_{TDE}: Terminally-differentiated effector T cells

-Abstract-

$CD8^+$ cytotoxic T lymphocytes (CTL) frequently infiltrate tumors, yet most melanoma patients fail to undergo tumor regression. We studied the differentiation of the $CD8^+$ tumor-infiltrating lymphocytes (TIL) from 44 metastatic melanoma patients using known T-cell differentiation markers. We also compared $CD8^+$ TIL against the T cells from matched melanoma patients' peripheral blood. We discovered a novel subset of $CD8^+$ TIL co-expressing early-differentiation markers, CD27, CD28, and a late/senescent CTL differentiation marker, CD57. This $CD8^+CD57^+$ TIL expressed a cytolytic enzyme, granzyme B (GB), yet did not express another cytolytic pore-forming molecule, perforin (Perf). In contrast, the $CD8^+CD57^+$ T cells in the periphery were $CD27^-CD28^-$, and GB^{Hi} and $Perf^{Hi}$. We found this TIL subset was not senescent and could be induced to proliferate and differentiate into $CD27^-CD57^+$, $perforin^{Hi}$, mature CTL. This further differentiation was arrested by TGF-β1, an immunosuppressive cytokine known to be produced by many different kinds of tumors. Therefore, we have identified a novel subset of incompletely differentiated $CD8^+$ TIL that resembled those found in patients with uncontrolled chronic viral infections.

In a related study, we explored prognostic biomarkers in metastatic melanoma patients treated in a Phase II Adoptive Cell Therapy (ACT) trial, in which autologous TIL were expanded *ex vivo* with IL-2 and infused into lymphodepleted patients. We unexpectedly found a signficant positive clinical association with the infused $CD8^+$ TIL expressing B- and T- lymphocyte attentuator (BTLA), an inhibitory T-cell receptor. We found that $CD8^+BTLA^+$ TIL had a superior proliferative response to IL-2, and were more capable of autocrine IL-2 production in response to TCR stimulation compared to the

$CD8^+BTLA^-$ TIL. The $CD8^+BTLA^+$ TIL were less differentiated and resembled the incompletely differentiated $CD8^+$ TIL described above. In contrast, $CD8^+BTLA^-$ TIL were poorly proliferative, expressed CD45RA and killer-cell immunoglobulin-like receptors (KIRs), and exhibited a gene expression signature of T cell deletion. Surprisingly, ligation of BTLA by its cognate receptor, HVEM, enhanced the survival of $CD8^+BTLA^+$ TIL by activating Akt/PKB. Our studies provide a comprehensive characterization of $CD8^+$ TIL differentiation in melanoma, and revealed BTLA as a novel T-cell differentiation marker along with its unexpected role in promoting T cell survival.

Chapter 1

General Background

1.1 Melanoma and Current Approved Treatments

Melanoma is considered to the most aggressive form of skin cancer. The incidence rate has been increasing for the past 30 years (1). In 2012, there were 76,250 new cases of melanoma and 9,180 deaths in the U.S. (1) These tumors originate in the pigment-producing melanocytes, which are the melanin (pigment)-producing cells derived from neural crest cells that reside in the basal layer of the epidermis (2). Although melanoma commonly arise in the skin, they may also occur at mucosal sites to which neural crest cells migrate (2). There are two types of risk factors for developing melanoma: intrinsic, which is based on a person's family history and genetic predisposition, and environmental (3, 4). In the case of melanoma, the largest environmental risk factor is exposure to the ultraviolet (UV) radiation from the sun or other sources (3, 4). Although melanin functions to protect the deeper layer of skin from the sun's ultraviolet radiation, excessive exposure to UV radiations (UVA and UVB) can cause damage to melanocytes' DNA that, when not properly repaired, lead to mutations in the genes that control cell proliferation, differentiation, and apoptosis (3, 4). If these mutations occur within oncogenes or tumor suppressor genes, the cells will experience uncontrolled proliferation that drive tumor growth (4). Common mutation found in melanocytes progressing to maligant melanoma are point mutations in the *BRAF* and *NRAS* proto-oncogenes (5-8). Over-expression of anti-apoptotic gene, such as survivin, is also common in melanoma (5-8).

There are 5 different stages of melanoma. Stage 0 is melanoma *in situ*, where the tumor is in the epidermis and has not spread beyond to the dermis. Patients in this category have favorable 5-year survival rate of 99.9% after surgical excision of the tumor (9). Stage I melanoma is characterized by < 1.0 mm in thickness. Survival rates are between 92-97%

with surgery (9). Stage II melanomas have bigger primary lesion sizes that range between 1.0 mm in depth to 4.0 mm in depth. 5-year survival rates after surgery decreases in proportion with the size of the tumor (between 53% to 81%) (9). Stage III melanomas are characterized by having spread to regional lymph nodes, with 5 year survival rates between 40-78% (9). Finally, Stage IV melanoma involves metastases to distant organs, with 5-year survival rate between 15-20% (9).

Melanomas that have not spread beyond their site of origin are highly curable with surgery (2). Most of these are thin lesions that have not invaded beyond the papillary dermis (Breslow thickness $\leq$1 mm) (2). Melanomas with a Breslow thicknes of 2 mm or more are still curable by surgery in a significant number of patients, however the risk of lymph node or systematic metastases increase with increasing thickness of the primary lesion (2). Therefore patients also need to undergo sentinel lymph node biopsy followed by complete lymph node dissection if the sentinel node(s) are microscopically or grossly positive. Patients with $>$ 4 mm Breslow thickness will need to be considered for adjuvant therapy in addition to surgery. Melanomas that have spread to lymph nodes may be curable with wide-local excision of the primary tumor and removal of the involved regional lymph nodes. For patients with high-risk of relapse, systemic treatment with high dose and pegylated interferon alpha-2b (IFN-alpha-2b) are approved for the adjuvant treatment of patients who have already undergone a complete surgical resection (10). Prospective randomized controlled trials with both agents have shown an increase in relapse-free survival (RFS) but not overall-survival (OS) when compared to observation (11). However these regimens are associated with substantial side effects that require close monitoring of the patients (11). For patients with distant metastases, chemotherapeutic agents such as dacarbazine (DTIC), which was

approved by the FDA in 1970, has demonstrated, in a Phase III trial, an overall response rate of 10-20% with rare complete responders observed (CRs) (12), though no impact on OS was demonstrated in randomized trials (10). Temozolomide, an oral alkylating agent, appeared to be similar to DTIC (given intraveneously) in a randomized phase III trial (13). Another option includes an immuno-modulating cytokine, interleukin-2 (IL-2), which was approved by the FDA in 1998 on the basis of durable complete response (CR) rates in a minority of patients (0 to 8%) with previously treated metastatic melanoma in eight phase I and Phase II studies, though no improvement in OS has been demonstrated in randomized trials (10) . More recently, the newer agents, ipilimumab (14) and vermurafenib (15), have demonstrated improvement in both progression-free survival (PFS) and OS in international, multicenter, randomized trials in patients with advanced or unresectable disease, leading to the FDA's approval of these agents in 2011. Vemurafenib is a selective inhibitor of the mutant BRAF kinase (V600E); its indication is limited to patients with a demonstrated BRAF V600E mutation by an FDA-approved test (10). The mechanism of action of ipilimumab, a humanized monoclonal antibody against Cytotoxic T-Lymphocyte-4 (CTLA), an inhibitory receptor on T cells (16), will be discussed further in the next section.

1.2 **Cancer Immunotherapies**

The dismal prognosis associated with metastatic melanoma was often due to the highly radio and chemo-resistant nature of the tumor cells. A large study conducted by the Eastern Cooperative Oncology Group (ECOG) found that prior chemotherapy was associated with poorer prognosis (17). Even with the introduction of vemurafenib, which specifically targets a mutant protein kinase in a crucial cellular signaling pathway driving tumor cell divison, the clinical responses are often short-lived (6-8 month median progression-free

survival) due to the rapid development of resistance (18). However, melanoma is also highly immunogenic, since it frequently elicits lymphocytic infiltrates, and that the presence of tumor infiltrating lymphocytes (TIL) is one of the positive prognostic factors (19). The ECOG study has also shown that prior immunotherapy was associated with better survival (17). During the last decade, significant progress has been made in the identification and characterization of several MHC class I–restricted melanoma tumor-associated antigens (TAA) recognized by $CD8^+$ cytotoxic T lymphocytes (CTLs). These antigens belong to four main categories (20): melanocyte differentiation antigens (e.g., tyrosinase, Melan-A/MART-1, gp100, TRP-1, and TRP-2) (21), cancer-testis–specific antigens (e.g., MAGE, BAGE, GAGE, PRAME, and NY-ESO-1) (22), over-expressed self-antigens (e.g., survivin, Mcl-1, and other anti-apoptotic genes) (23), and antigens derived from mutated or aberrantly expressed proteins (e.g., MUM-1, CDK4, beta-catenin, gp100-in4, p15, and *N*-acetylglucosaminyl transferase V) (24). $CD4^+$ helper T cells can also recognize several MHC class II–restricted epitopes derived from melanoma antigens (25-29). Thus, the developments of immunotherapies for melanoma have come a long way from theoretical possibilities a few decades ago to real proven clinical successes. In fact, the tables are turning with various kinds of immunotherapies emerging to be among the most powerful approaches to treat metastatic melanoma.

One prominent example was the recent FDA's approval of the humanized monocloncal antibody anti-CTLA-4 (ipilimumab) as a single-agent therapy for Stage IV disease (30). CTLA-4 is expressed by activated $CD4^+$ and $CD8^+$ T lymphocytes. When T cells are activated by antigen, CTLA-4 is rapidly mobilized from the intracellular compartment to the immune synapse where it competes with co-stimulatory receptor, CD28,

for binding to its ligands, B7-1 and B7-2, on the antigen-presenting cells (APCs). As a result, T-cell's activation is attenuated. Administration of anti-CTLA-4 blocking mAb interrupts this key inhibitory checkpoint during T-cell activation and thus "takes the brakes off" of T cells, resulting in enhanced proliferation and effector activity against a large array of self-antigens, including tumor antigens (31, 32) (**Fig. 1-1**).

Figure 1-1: Enhancement of T-cell activation by blocking engagement of inhibitory receptors on T cells. (**a**) Antigenic presentation triggers T cell activation and occurs when a peptide derived from an antigen binds to Major Histocompatibility Complex (MHC) molecule on an antigen presenting cell (APC) and interacts with the T cell receptor (TCR) on the surface of a T cell. In order to achieve optimal activation, additional co-stimulatory signals are required and involve interaction between costimulatory receptor, CD28, on T cells, and B7-1 and B7-2 molecules on APCs. After T cell activation, a natural negative feedback exists to attenuate the degree of T cell activation. For example, cytotoxic T lymphocyte-associated protein (CTLA)-4 is mobilized after activation to the cell surface and binds to B7 molecules with greater affinity than CD28, which inhibits signaling through CD28. Inhibitory signals can also be provided by co-inhibitory receptors such as programmed cell death 1 (PD-1), which binds to PD-1 ligand 1 or 2 (PDL1/2). Other known inhibitory receptors expressed by T cells include V-domain immunoglobulin suppressor of T cell activation (VISTA) (33), T-cell immunoglobulin and mucin domain-containing protein-3 (TIM-3) (34), and B-and-T lymphocyte attenuator (BTLA) (35). (**b**) Sustaining T cell activation through blockade of negative co-inhibitory receptors. Blocking antibodies against CTLA-4 or PD-1 are currently used to neutralize co-inhibitory receptors and prevent dampening of the T cell response. Blockade of these inhibitory immune checkpoints results in enhanced and sustained activation of tumor-specific T cells that produce effector cytokines including TNF-α, interferon (IFN-γ), and granzyme B.

Reprinted from: *Trends in Immunology*, Volume 34, Issue 2, Gao J, Bernatchez C, Sharma P, Radvanyi L, and Hwu P. Advances in the development of cancer immunotherapies, p90-98, 2012, with permission from Elsevier.

Figure 1-1:

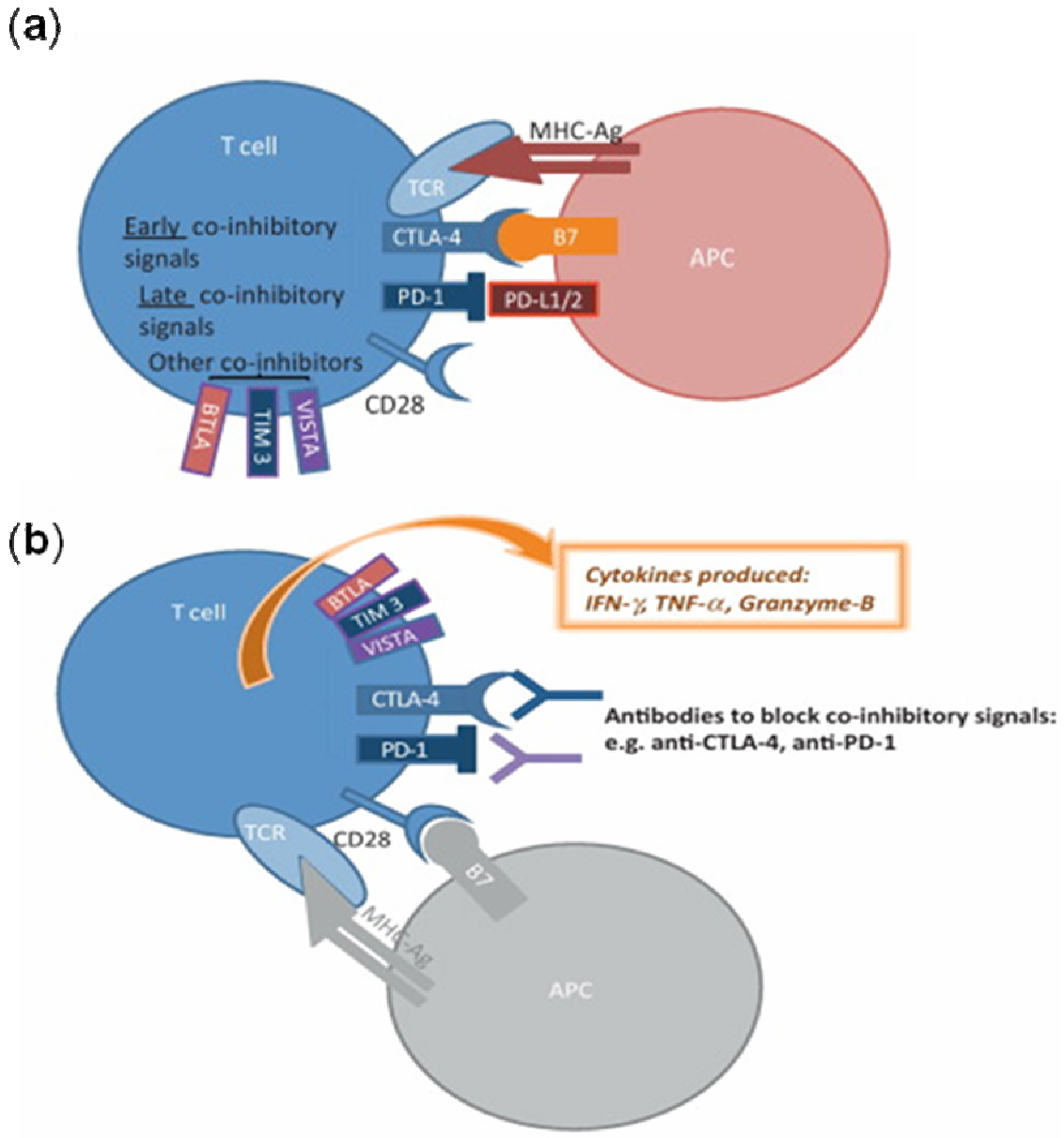
(a)
T cell
MHC-Ag
TCR
Early co-inhibitory signals
CTLA-4
B7
APC
Late co-inhibitory signals
PD-1
PD-L1/2
Other co-inhibitors
CD28
BTLA
TIM 3
VISTA
(b)
Cytokines produced:
IFN-γ, TNF-α, Granzyme-B
T cell
BTLA
TIM 3
VISTA
CTLA-4
Antibodies to block co-inhibitory signals:
e.g. anti-CTLA-4, anti-PD-1
PD-1
TCR
CD28
B7
MHC-Ag
APC

In addition to CTLA-4, another inhibitory receptor currently receiving intense interest is programmed death-1 (PD-1), which was reported to be expressed at high levels on activated T cells as well endogenous melanoma antigen-specific T cells and TIL (36, 37). The ligand for PD-1 are PD-L1 (B7-H1) and PD-L2 (B7-DC). PD-L1 is expressed by many normal non-hematopoietic tissues as well as dendritic cells as a self-tolerance mechanism, especially at sites of inflammation. However, this pathway has alsoo been usurped in cancer, with many types of cancer cells, including melanoma, found to express PD-L1. PD-L2 is mainly expressed by dendritic cells and other myeloid cells, such as macrophages (38). PD-L1 expression on tumor tumor cells has been postulated to cause immune suppression of tumor-infiltrating T cells (36) (**Fig. 1-1**). However, it is also possible that PD-L1 and PD-L2 expression in tumor resident dendritic cells and macrophages may also contribute to this T-cell suppression. The inhibitory role of PD-L1 on T-cell activation suggests that its expression would be a poor prognostic factor in cancer. Although initial immunohistochemistry studies in renal cancer and other cancers suggested that higher PD-L1 expression in tumor cells correlated with poorer progression-free and overall survival (39-42), more recent data suggests the contrary (43, 44). These contrasting data seems to be due to the degree of T-cell infiltration in the tumor microenvironment with T-cell associated cytokines such as IFN-γ, which is known to induce PD-L1 expression on cancer cells (45) as one of the mechanisms of "adaptive resistance" (43). Thus, paradoxically, higher PD-L1 expression may be an indicator of increased activated T-cell infiltration into tumor and a better prognosis as a result.

In a phase I trial in 39 patients with refractory metastatic melanoma, colorectal cancer, prostate cancer, non-small cell lung cancer (NSCLC), or renal cell carcinoma (RCC), anti-PD-1 blocking antibody (MDX-1106) resulted in complete or partial response in three

patients and less significant tumor regression in two others (46). A recent phase I clinical trial with a different anti-PD1 antibody (BMS-936558) showed durable objective response rates between 18-28% depending on tumor types in patients with advanced NSCLC, RCC, and melanoma (47). Another phase I trial with anti-PD-L1 antibody showed mild to modest antitumor activity in patients with advanced NSCLC, melanoma, and RCC (objective response rates between 6 to 17% with prolonged stabilization of disease) (48) . Blocking antibodies against other T cell co-inhibitory receptors, such as LAG-3 and TIM-3, are still at early stages of development as potential targets for immune checkpoint blockade (34, 49) (**Fig. 1-1**).

B- and T- lymphocyte attenuator (BTLA) is another inhibitory receptor with two immunotyrosine-based inhibitory motifs (ITIMs) that are similar to other well-known inhibitory receptors, PD-1 and CTLA-4 (50) (**Fig. 1-1; Chapter 3, Fig. 3-15**). Interestingly, unlike PD-1 and CTLA-4, the cytoplastmic domain of BTLA has been reported to contain a third conserved tyrosine-containing motif, which has been shown to recruit Grb-2 and p85 subunit of PI3K *in vitro* (51). BTLA signaling is generally considered to be suppressive, as ligation with its cognate receptor, Herpesvirus entry mediator (HVEM), results in the recruitment of SHP1/2 phosphatases and leads to decreases in T-cell's proliferation and cytokine secretion (50, 52). However, it is controversial whether BTLA expression truly marked "exhausted" $CD8^+$ T cells. Although it was reported that BTLA is up-regulated on exhausted, NY-ESO-1 tumor antigen-specific $CD8^+$ T cells (53), a number of studies on human $CD8^+$ T cells have shown that BTLA was already expressed at a high level on naïve $CD8^+$ T cells and was gradually down-regulated during normal differentiation (52, 54). A recent study has suggested a close relationship between the expressions of multiple inhibitory

receptors (e.g., PD-1, TIM3 and LAG3) and the antigen-specificity, anatomic localization, and differentiation of $CD8^+$ T cells in humans (**Chapter 3, Fig. 3-3**). In our phase II ACT trial with melanoma TIL, we found that that patients receiving more $CD8^+$ TIL expressing BTLA were significantly correlated to positive clinical responses (55) (**Chapter 3**, **Fig. 3-2**). However, we did not find clinical correlations with $CD8^+$ TIL's expressions of other inhibitory receptors such as PD-1 (programmed death-1) or TIM-3 (**T**-cell **i**mmunoglobulin domain and **m**ucin domain 3 receptor) (55) (**Chapter 3, Fig. 3-2**). It is not known whether BTLA's third signaling motif can modulate T cell survival *in vitro* and *in vivo*. If that is true, that may provide one of the explanations for our observed positive clinical correlations.

A number of other immunotherapy approaches have also been developed and improved over the last decades with incremental successes. These include IL-2 therapy (56), peptide vaccines together with IL-2 (57), and adoptive T-cell therapy using autologous expanded tumor-infiltrating lymphocytes (TIL) (58-60). In addition, agonistic monoclonal antibodies that enhance T cell response by activating co-stimulatory receptors [e.g., OX40 (CD134), 4-1BB (CD137)] are being tested (61-63). Moreover, rational combinations of these immunotherapies with chemotherapies or targeted therapies against the components of the MAPK signaling pathway are now making an entry into the clinic (15, 64, 65). These are based on the newly discovered synergistic mechanism of chemotherapies and targeted therapies in facilitating immune responses by activating innate immunity ("immunogenic chemotherapy") (66-68) or enhancing T-cells' recognition of tumor cells by inducing expressions of tumor antigens (65, 69).

1.3 Adoptive T-cell Therapy (ACT) using TIL for metastatic melanoma

To date, one of the most powerful immunotherapies against metastatic melanoma has been adoptive T-cell therapy (ACT) using autologous *ex vivo*-expanded TIL that are re-infused back into patients. Adoptive transfer of TIL for the treatment of human metastatic melanoma was initially described in 1988 (70) and has since yielded highly encouraging results since its initial development with >50% clinical responses; these clinical responses have been shown to be durable for years in recent clinical trials (58-60, 71). More recently, other forms of ACT using genetically-modified T cells are now being developed and tested clinically. Genetic modifications frequently involve modifying the affinity and avidity of the TCR for the targeted tumor antigen. A schematic of TCR, its signaling subunit, CD3, and a brief description of the signaling event downstream of TCR are shown (**Figure 1-2a**). The other ACT approaches include expanding tumor-associated antigens (TAA)-specific T-cells from peripheral blood mononuclear cells (PBMCs) through pAPC pulsed with tumor antigen peptides(72-74), engineering recombinant TCR α and β chains recognizing peptides derived from tumor-associated antigens (TAAs) (75, 76), and introducing into T-cells chimeric antigen receptors (CAR), which are composed of single-chain immunoglobulin variable regions (scFv) recognizing tumor antigens fused to a linker region followed by the signaling domains of the TCR ζ chain and costimulatory molecules, such as CD28 and CD137/4-1BB (77, 78) (**Figure 1-2b**). As a side note, a recent clinical trial from a group at the University of Pennsylvania has demonstrated impressive clinical efficacy of CAR-modified T-cells against a leukemic B-cell antigen, CD19 (79). **Table 1-I** provides a summary of different types of ACT that are currently being investigated for the treatment of metastatic melanoma, a brief descriptions of the methods, the antigens targeted, and the status of clinical development.

Figure 1-2: (**a**) Diagram of the TCR:CD3 complex. The T-cell receptor (TCR) is composed of two subunits, α and β subunits. The other four protein subunits (ε, δ, γ, ζ) assemble in three different dimers to form the CD3 complex. The square boxes on the CD3 subunits in cytoplasm represent the immunoreceptor tyrosine-based activation motifs (ITAMs). An early event in TCR activation is phosphorylation of ITAMs in the cytoplasm of TCR/CD3 complex by lymphocyte protein-tyrosine kinase (Lck). The CD45, which is a receptor tyrosine phosphatase, modulates the phosphorylation and activation of Lck and other Src family tyrosine kinases. ζ-chain associated protein kinase (ZAP-70) is recruited to the TCR/CD3 complex where it becomes activated, promoting recruitment and phosphorylation of downstream adaptor or scaffold proteins. More detailed TCR signaling events is at the following reference (80).

Reprinted with permission from: de Felipe, P., Skipping the co-expression problem: the new 2A "CHYSEL" technology. *Genet. Vaccines Ther.* 2004. 2(1):13. BioMed Central Open Access Article.

(**b**) Structure of chimeric antigen receptors (CARs)(81). CARs are composed of a single-fragment length antibody (scFv) containing the heavy (V_H) and light chain (V_L) variable regions derived from a murine hybridoma expressing a monoclonal antibody (mAb) targeting a desired TAA. CARs typically contain a scFv-based TAA binding domain fused to an inert transmembrane domain of the CD8 ("first generation"), or a signaling domain of CD28 receptor ("second generation") fused to a TCR ζ chain. "Third generation" CARs contain tandem cytoplasmic signaling domains from 2 co-stimulatory receptors (i.e., CD28-OX-40 and CD28-4-1BB).

Reprinted with permission from: Chekmasova, A. 2010. http://www.discoverymedicine.com/Alena-A-Chekmasova/2010/01/22/adoptive-t-cell-immunotherapy-strategies-for-the-treatment-of-patients-with-ovarian-cancer. Accessed January 27th, 2013.

Figure 1-2:

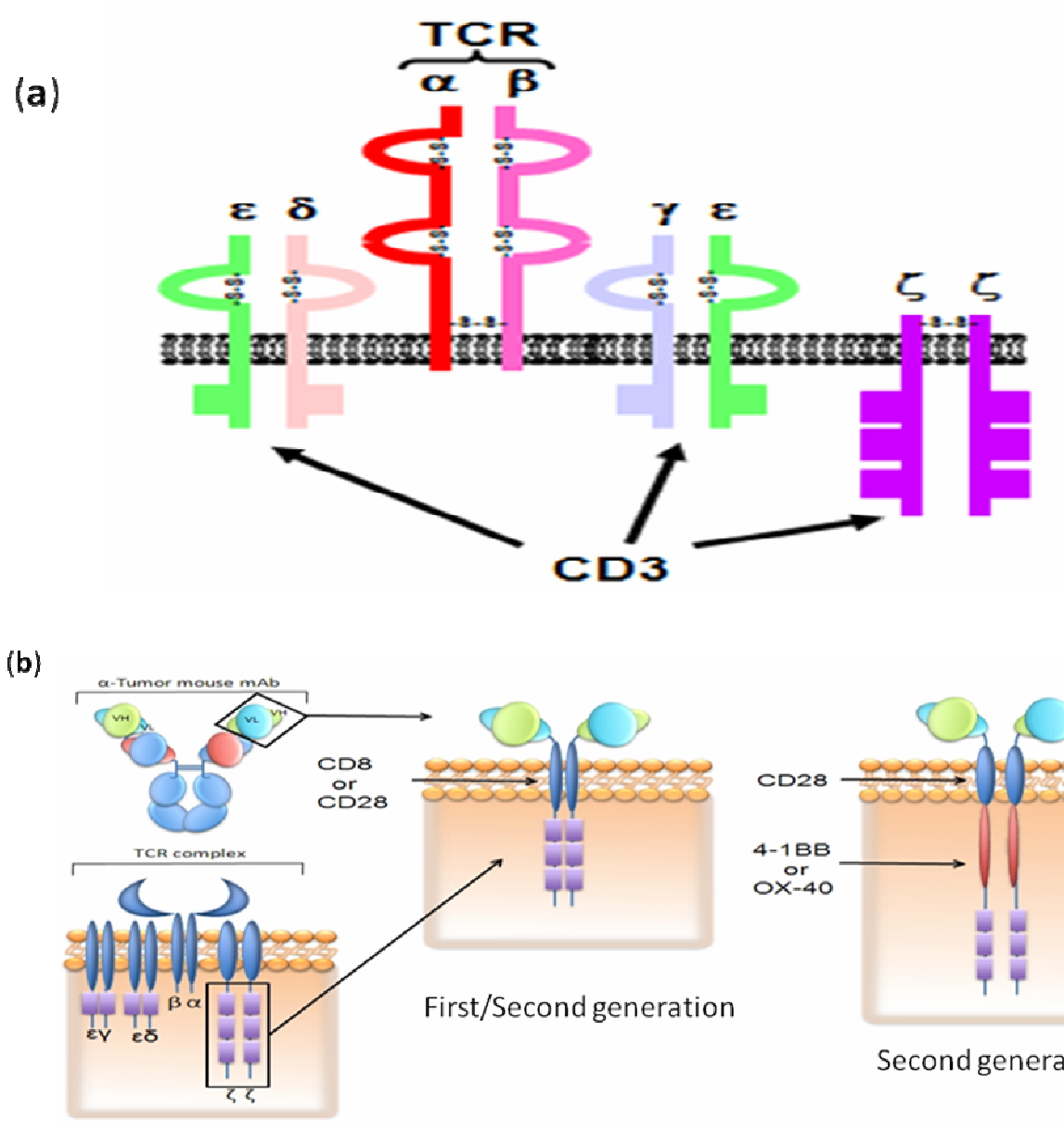
(a)
TCR
α β
ε δ
γ ε
ζ ζ
CD3
(b)
α-Tumor mouse mAb
VH
VL
CD8
or
CD28
TCR complex
β α
εγ εδ
ζ ζ
First/Second generation
CD28
4-1BB
or
OX-40
Second generation

Table 1-I: A summary of different types of ACT for the treatment of metastatic melanoma and the status of clinical development

Strategy for ACT	Brief Description	Targets	Clinical Status
Tumor infiltrating lymphocytes (TIL)	Isolation of T lymphocytes from primary or secondary tumors followed by *in vitro* expansion with IL-2	Polyclonal (shared melanoma differentiation antigens, antigens derived from mutated genes)	**Clinical (phase II)** Dudley, *et al.* (59, 82, 83) Rosenberg, *et al.* (84, 85) Radvanyi, *et al.* (60, 71) Besser, *et al.* (58, 86)
Antigen-expanded $CD8^+$ or $CD4^+$ T cells	*In vitro* reactivation and expansion of T lymphocytes specifically recognizing tumor-associated antigen (TAA)	MART-1, Tyrosinase, gp100, NY-ESO-1, or polyclonal	**Clinical (phase I/II)** Yee, *et al.* (74) Mitchell, *et al.* (73) Mackensen, *et al.* (72) Hunder, *et al.* (87) Verdegaal, *et al.* (88) Butler, *et al.* (89)
Engineered T cell receptor (TCR) expression in lymphocytes	Genetic modification of T cells for expression of second TCR (human or mouse) directed against TAA	MART-1, gp100, p53, and NY-ESO-1	**Clinical (phase I/II)** Morgan, *et al.* (75) Johnson, *et al.* (90) Robbins, *et al.* (91)
Chimeric antigen receptor (CAR) expression in lymphocytes	Genetic modification of T cells for expression of a chimeric receptor partly constituted of TAA-specific antibody and CD3/co-stimulatory molecule trans-membrane and cytoplasmic domains	Ganglioside GD2, GD3, and HMW-MAA (MCSP-1)	**Pre-clinical** Yvon, *et al.* (78) Lo, *et al.* (92) Burns, *et al.* (93)

Reprinted with permission from: Wu, R. Forgét, MA, Chacon J, Bernatchez C, Haymaker C, Chen JQ, Hwu P, and Radvanyi L. Adoptive T-cell Therapy Using Autologous Tumor-infiltrating Lymphocytes. 2012. *The Cancer J*. 18(2):160-75. doi: 10.1097/PPO.0b013e31824d4465.

Adoptive T-cell therapy (ACT) using autologous *ex vivo*-expanded TIL, which is the primary focus of this thesis, involves the expansion of TIL *ex vivo* in two stages. The steps in TIL expansion and treatment are summarized in **Fig. 1-3**. The first stage involves the initial expansion of TIL isolated from the tumor fragments over a 5-week period in culture medium with IL-2 (94-96). Medium exchanges with fresh IL-2 are done regularly to ensure continued T-cell division and survival during this time. This first stage yields a product ("pre-REP" TILs) that is used to generate a final TIL infusion product following a "rapid expansion protocol" (REP) (94, 97). These pre-REP TILs can either be used immediately for secondary expansion with the REP, or they can cryo-preserved and used later. The REP involves activating the TILs through the CD3 complex using an agonistic anti-CD3 mAb (OKT3) in the presence of a 200:1 ratio of irradiated (5,000 cGy) PBMC feeder cells obtained from the patient (autologous feeders), or pooled from 3 to 6 healthy donors (allogeneic feeders). Two days after initiation of the REP, IL-2 (6,000 U/mL) is added to drive rapid cell division in the activated TIL (94, 98, 99). The TIL are then expanded for another 12 days and diluted, as needed, with 1:1 culture medium containing fresh IL-2 (94, 98, 99).

A typical REP results in 1,000-fold to 2,000 fold expansion of TIL during a 14-day culture period. The TIL are harvested, concentrated, and infused intravenously into the patient along with high-dose IL-2 to drive further TIL survival and expansion *in vivo* (94, 98, 99). Prior to infusing the TIL back into the patient, the patient is lympho-depleted using a cocktail of drugs to deplete all endogenous T and B cells. IL-2 is systemically administered in order to help support the transferred TIL following lymphodepletion and TIL infusion (56, 100, 101) (**Fig. 1-3**). Treatment with IL-2 at this point supports the persistence of the infused

TIL *in vivo*; this is critical for the short-term survival of the TIL which contributes to tumor regression (84, 102, 103).

Lymphodepleting patients prior to infusion with autologous TIL has contributed to the improved clinical efficacy of ACT. Metastatic melanoma patients were initially treated with TIL and IL-2 without lymphodepletion, resulting in an objective response rate of 39% (59, 83, 104, 105). However, a series of Phase II clinical trials in humans conducted by Dudley *et al.* at the National Cancer Institute in 2002 used a preparative lymphodepleting chemotherapy regimen (cyclophosphamide and fludarabine) in melanoma patients prior to TIL and IL-2 infusions, resulting in an unprecedented 50% clinical response rate (59, 83, 104, 106, 107). Lymphodepleting patients prior to TIL infusion improves persistence of the TIL by eliminating endogenous lymphocytes that can compete with the infused TIL for homeostatic cytokines such as interleukin-7 (IL-7) and interleukin-15 (IL-15) (59, 83, 104, 106, 107). Lymphodepletion also eliminates endogenous $CD4^{+}Foxp3^{+}$ T regulatory cells (Tregs) and myeloid-derived suppressor cells (MDSCs) that can inhibit proliferation and effector functions of the infused TIL *in vivo* (108-111). Although chemotherapeutic lymphodepletion has led to improved clinical responses in ACT, a potential problem that may occur is the post-treatment recovery of endogenous T-cells, in particular the re-emergence of Tregs that could suppress the anti-tumor activity of the infused TIL. In order to overcome this issue, total-body irradiation (TBI), at different dosages (2 Gy and 12 Gy), plus cyclophosphamide and fludaribine, have been tested (83, 85). They reported a significant enhancement of objective clinical response rate to 72% with the 12 Gy TBI plus chemotherapy preparative regimen, together with 40% complete responders (59, 83, 85, 99, 112). The NCI group has recently provided a summary of their 10-year experience with the

Phase II ACT trials using different preparative regimens. In sum, these trials have demonstrated a response rate of 51%, and 13% rate of durable and complete regression past 5 years (85, 113).

Different centers have now utilized ACT with TIL to treat metastatic melanoma patients and have reported promising results. At the M.D. Anderson Cancer Center (Houston, TX), our group is currently conducting a phase II trial of TIL therapy in metastatic melanoma patients that have not responded to first-line and second-line therapies (60, 71). We have treated over 70 patients to date and have achieved a 48% overall response rate (60, 71). These responses have been durable, with a majority of responders having relapse-free survival over 12 months. The Sheba Cancer Center (Jerusalem, Israel) has reported an overall response rate of 50% using TIL therapy in their clinical trials (58, 86). In summary, these impressive rates of positive clinical response from various groups around the world have shown that ACT with TIL is a powerful approach for the treatment of metastatic melanoma.

Figure 1-3. Schematic representation of the process of TIL expansion and TIL therapy for metastatic melanoma. Suitable tumors from eligible stage IIIc-IV melanoma patients are resected and taken to the lab under sterile conditions where they are cut up into small 3-5 mm^2 fragments and placed in culture plates or small culture flasks with growth medium and high-dose (HD) IL-2. The TILs are initially expanded for 3-5 weeks during this "pre-rapid expansion protocol" (pre-REP) phase to at least 50 x 10^6 cells. The cells are then subjected to a rapid expansion protocol (REP) over two weeks by stimulating the T cells using an agonistic anti-CD3 mAb (OKT3) in the presence of PBMC feeder cells and IL-2. The expanded TIL are washed, pooled, and infused into the patient followed by one or two cycles of HD IL-2 therapy. Before TIL transfer, the patient is treated with a preparative regimen using cyclophosphamide (Cy) and fludaribine (Flu) that transiently depletes host lymphocytes. Lymphodepletion plays an important role in enhancing the efficacy of the ACT using TIL, by providing space for the infused TIL to expand, reducing the competition between TILs and endogenous T cells for homeostatic cytokines (e.g., IL-7, IL-15), and removing regulatory T cells.

Reprinted with permission from: Wu, R. Forgét, MA, Chacon J, Bernatchez C, Haymaker C, Chen JQ, Hwu P, and Radvanyi L. Adoptive T-cell Therapy Using Autologous Tumor-infiltrating Lymphocytes. 2012. *The Cancer J*. 18(2):160-75. doi: 10.1097/PPO.0b013e31824d4465.

Figure 1-3:

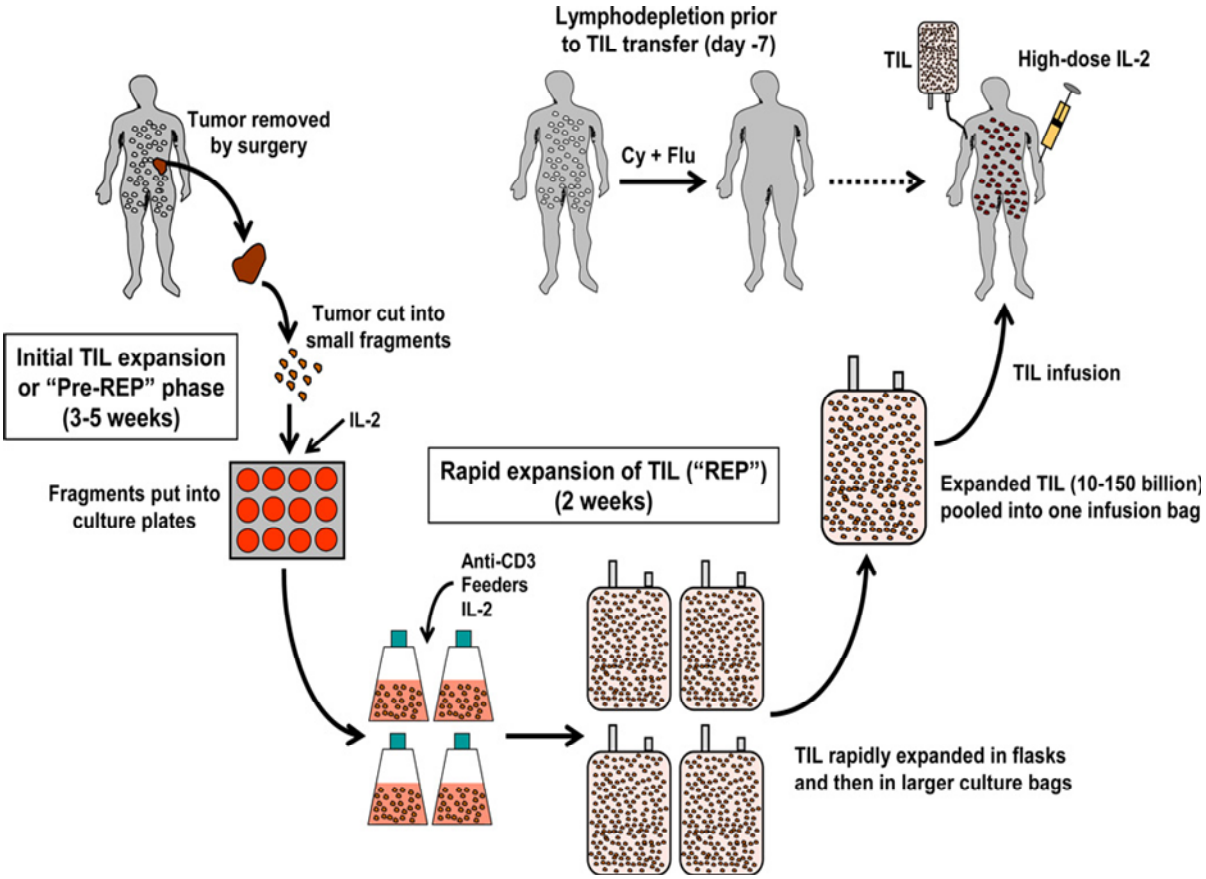
Lymphodepletion prior
to TIL transfer (day -7)
TIL
High-dose IL-2
Tumor removed
by surgery
Cy + Flu
Tumor cut into
small fragments
Initial TIL expansion
or "Pre-REP" phase
(3-5 weeks)
IL-2
TIL infusion
Rapid expansion of TIL ("REP")
(2 weeks)
Fragments put into
culture plates
Expanded TIL (10-150 billion)
pooled into one infusion bag
Anti-CD3
Feeders
IL-2
TIL rapidly expanded in flasks
and then in larger culture bags

1.4 $CD8^+$ CTL differentiation and anti-tumor immune response

A significant part of the adaptive immune system is consisted of two types of T lymphocytes, $CD8^+$ and $CD4^+$ T cells, which operate by reacting specifically to viral or tumor antigens. $CD8^+$ cytotoxic T lymphocytes (CTL) play a major role in anti-tumor responses and carry out the antigen-specific cytolysis of tumor cells through the action of granzymes (e.g., granzyme B), which belong to a family of serine proteases that cleave at aspartate residues in the substrate, and perforin (114, 115). Perforin forms pores in the plasma membrane of target cells, which allows granzymes to enter the target cell and activate caspases (e.g., caspase 3), causing apoptosis in the target tumor cells (114). The Fas-Fas ligand interaction may also be important for the tumor cell killing, although the extent this pathway contributes to tumor killing is not known (116). Although the clinical data from NCI was less conclusive about the importance of $CD8^+$ TIL (59, 83, 117), the reports from the melanoma ACT trials by Besser, *et al*. (58), and at M.D. Anderson Cancer Center (60, 71) have revealed a positive correlation between a higher number of infused $CD8^+$ TIL and positive clinical response in a majority of Stage IIIc/IV metastatic melanoma patients.

Although $CD8^+$ T cells are emerging to be the dominant cell type in adoptive cell therapy, the role of $CD4^+$ T cells cannot simply be ignored. $CD4^+$ T cells play a central role in coordinating many elements of the adaptive immunity (118). They participate not only in priming $CD8^+$ T cells, but they can also induce tumor eradication by a number of direct and indirect mechanisms: direct killing of MHC class II^+ tumor cells presenting TAA, the activation of pAPC cross-presenting TAA, the activation of tumor-cytolytic macrophages and eosinophil, and the provision of survival signal (lymphokines) for the transferred $CD8^+$ CTL (119). $CD4^+$ T cells in some healthy donors have been reported to express cytolytic

molecules typically associated with $CD8^+$ cytotoxic T lymphocyte (CTL), such as granzyme B and perforin, in chronic viral infections (120). Recent data suggest a possible pathway of differentiation of a subset of $CD4^+$ T-cells into highly tumor-cytolytic cells expressing the transcription factor Eomesodermin (Eomes) that drives granzyme and perforin expression (121). We have observed in our phase II clinical trial that a small percentage of patients (about 8-10%) who had a $CD4^+$ T-cell dominated TIL product for adoptive transfer nevertheless underwent dramatic clinical responses and even complete remissions in some patients (60, 71). It is a likely that a subset of "cytotoxic" $CD4^+$ T cells may exist in some of melanoma patients' TIL. However, in the majority of cases, patients receiving $CD4^+$ T-cell dominated TIL tended to be nonresponders (60, 71). It is also possible that in these responding patients that recived a $CD4^+$ T-cell dominated TIL product, the few $CD8^+$ T cells expanded *in vivo* and mediated tumor regression. Detailed tracking of T-cell clones *in vivo* from the infused TIL products will be required to address this possibility.

Therefore, $CD8^+$ T cells have been the subject of the most intense research in melanoma ACT. $CD8^+$ T cells are heterogeneous with respect to anatomic localization, proliferative and engraftment capabilities, and different profiles of cytokine secretion, metabolism, and gene expression. Each of these parameters may have influence on a CD8+ T-cell's ability to mediate cancer regression after ACT. Many of these properties tend to cluster together in discrete populations defined by characteristic patterns of expression of cell-surface markers detectable by flow cytometry. An important discovery in the classification of $CD8^+$ T-cell subsets in humans was the full-length form of the protein tyrosine phosphatase CD45, CD45RA (122). It is expressed on the surface of human naive T cells (T_N) (123), the recently identified memory stem T cells (T_{SCM}) (124), and the

terminally-differentiated, CD45RA-re-expressing T cells (T_{EMRA}) (123). The shorter isoform, CD45RO, is expressed by the antigen-experienced central-memory (T_{CM}) (123) and effector-memory T cells (T_{EM}) (123) (**Fig. 1-4a**). T-cell subsets can be further classified functionally for the co-expressions of the lymphoid homing molecules, L-selectin (CD62L) and CC-chemokine receptor 7 (CCR7) (123) (**Fig. 1-4a**). T-cells that express these molecules on their surface can home to secondary lymphoid structures, where they can survey pAPC for the presence of foreign antigen. Cells in this category include naive T cells (T_N) and two memory T-cell populations, T_{SCM} (124) and T_{CM} (123) (**Fig. 1-4a**). Although both T_N and T_{SCM} express the RA isoform of CD45, T_{SCM} can be distinguished from T_N by its unique expressions of the IL-2/IL-15β chain receptor (CD122) and Fas (CD95) (124). $T_{CM,}$ on the other hand, express the prototypical human Ag-experienced T-cell marker, CD45RO. In addition to their localization in lymphoid organs, all three T-cell subsets possess high proliferative and engraftment capacities upon adoptive transfer (125). In contrast, T_{EM} and T_{EMRA} are antigen-experienced T cells that have down-regulated CD62L and CCR7 and therefore reside in peripheral rather than lymphoid tissues (123). These T-cell subsets are poised to rapidly execute effector functions upon activation, as shown by their ability to release high levels of inflammatory cytokines, such as IFN-γ and TNF-α, and their ability to lyse antigen-expressing targets (123). However, they may also possess a relatively limited proliferative and engraftment capacities, which correlate with their shorter telomere length, as compared to the $CCR7^+CD62L^+$ counterparts (125) (**Fig. 1-4a**).

Figure 1-4: **A current model of $CD8^+$ T cell differentiation in humans**. (**a**) During an immune response, naive T cells (T_N) are primed by professional antigen-presenting cells (pAPC) in secondary lymphoid organs. Depending on the strength and quality of stimulatory signals, proliferating T cells progress along a differentiation pathway. Naive T cells (T_N) express the full-length CD45, CD45RA, and, when primed, develop into T_{CM} or effector T cells that can self-renew. Primed effector T cells express the CD45, RO isoform, and when antigen is eliminated, are rescued as memory T cells. Central-memory T cells (T_{CM}) express lymphoid homing receptors, CCR7 (CC-chemokine receptor 7) and CD62L (also known as L-selectin), and undergo homeostatic proliferation in lymphoid tissues. Effector-memory T cells (T_{EM}) express low levels of CD62L, do not express CC-chemokine receptor 7 (CCR7) or home to lymphoid tissues, and are less proliferative than T_{CM}. Senescent, terminally-differentiated effector T cells (T_{EMRA}) reacquire expression of CD45RA and are derived from T_{EM} cells. T_{SCM} is a newly discovered memory T cell type that is distinct from the previously characterized T_{CM} and T_{EM} cells. T_{SCM} cells are less differentiated and share several markers, including CD45RA, with the naive T cells. T_{SCM} cells self-renew and differentiate in response to cytokines (dotted black arrows) or antigen (solid black arrows) and, in adoptive transfer experiments in murine models, have the highest reconstitution and antitumor capacity (124). Reprinted with permission from Macmillan Publishers Ltd: *Nature Medicine.* Sallusto F, Lanzavecchia A. 17(10):1182-3. 2011.

(**b**) Costimulatory molecules have been the first markers used to dissect the heterogeneity of memory T cells. CD27 and CD28, which are expressed on naive T cells, are also expressed on some memory T cells, but are absent in a subset of $CD8^+$ T_{EMRA} cells characterized by high effector function. The $CD27^-CD45RA^+$ CD8 T cell population largely overlaps with T_{EMRA}. However, some cells within T_{EMRA} express CD27 and display phenotypic and functional features that are intermediate between naive and effector T cells.

Figure 1-4:

(**a**)

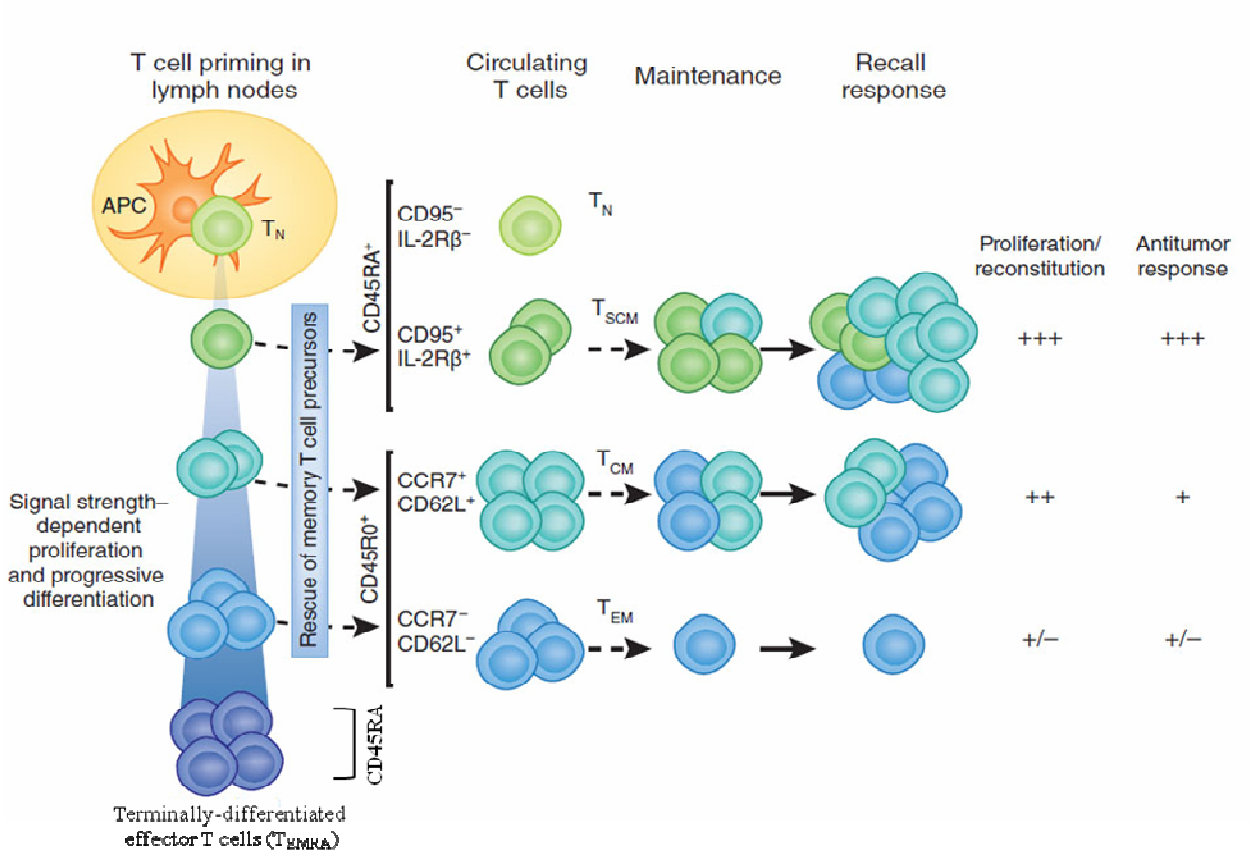
T cell priming in lymph nodes
Circulating T cells
Maintenance
Recall response
APC
T_N
CD95⁻ IL-2Rβ⁻
CD95⁺ IL-2Rβ⁺
CD45RA⁺
T_N
T_{SCM}
Proliferation/ reconstitution
Antitumor response
+++
+++
Rescue of memory T cell precursors
Signal strength–dependent proliferation and progressive differentiation
CCR7⁺ CD62L⁺
CD45RO⁺
T_{CM}
++
+
CCR7⁻ CD62L⁻
T_{EM}
+/–
+/–
CD45RA
Terminally-differentiated effector T cells (T_{EMRA})

(**b**)

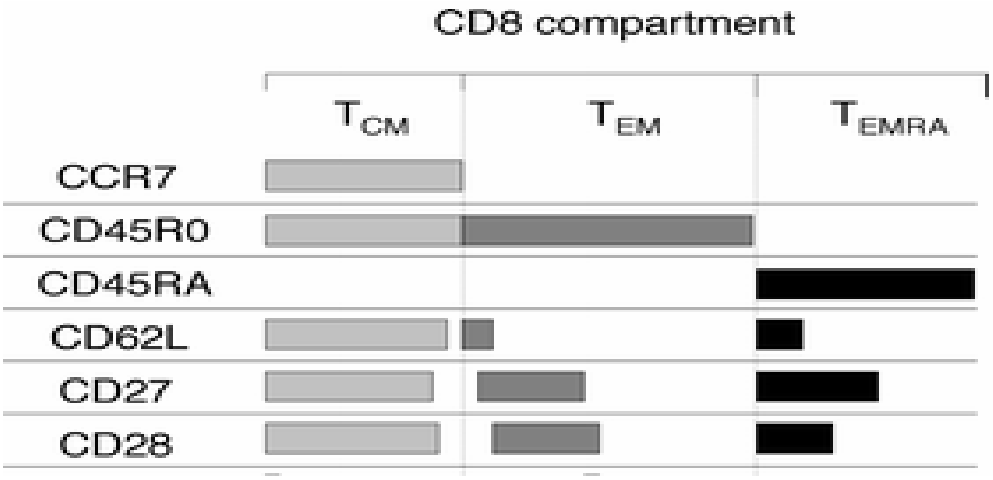
CD8 compartment
T_{CM}
T_{EM}
T_{EMRA}
CCR7
CD45RO
CD45RA
CD62L
CD27
CD28

Costimulatory receptors, CD27 and CD28, have also been used to delineate the heterogeneity of memory T cells. These receptors are expressed on naïve T cells and on some memory T cells, but are lost on terminally-differentiated T cells (**Fig. 1-4b**). The loss of CD28 expression has been associated with the emergence of oligoclonal, senescent, and natural-killer (NK)-like $CD8^+$ T cells with shortened telomere length in humans (126) (**Fig. 1-5**). Expression of CD27 may further identify $CD8^+$ $CD28^-$ T cells that are closest to terminal differentiation and senescence(127). It was shown that $CD27^-$ $CD8^+$ $CD28^-$ T cells have the shortest telomeres, decreased telomerase activity, and reduced capacity to proliferate after activation with anti-CD3 and irradiated professional APC (pAPC) compared with $CD27^+$ T cells, indicating that $CD27^-$ $CD8^+$ $CD28^-$ T cells have differentiated to an extent where co-stimulatory signals are no longer sufficient to induce telomerase activity (128). The $CD27^-CD45RA^+$ $CD8^+$ T cell population largely overlaps with T_{EMRA}. However, some cells within T_{EMRA} express CD27 and display functional features that are in between naïve and terminally-differentiated effector T cells(123). Therefore, Plunkett, *et al*., (128) postulated a linear differentiation pathway of $CD8^+$ T cells from $CD28^+CD27^+$ (early-differentiated) to $CD28^-CD27^+$ (intermediate-differentiated) and finally to $CD28^-CD27^-$ (late-differentiated) upon repeated stimulation *in vitro*. The same pattern of CD28 and CD27 expressions during the differentiation of $CD8^+$ T cells was also described *in vivo*, where human immunodeficiency virus (HIV)-specific $CD8^+$ T cells, during the early phase of infection, differentiated within 2-4 weeks from a $CD27^+CD28^+$ to a $CD28^-CD27^+$ phenotype (129, 130). This was associated with the acquisition of a carbohydrate epitope HNK-1 (human natural-killer-1, also known as CD57, synthesized by β-1,3-glucuronyltransferase 1),

a proposed marker of replicative senescence of $CD8^+$ T-cells in chronic viral infection (130, 131).

Figure 1-5: Loss of CD28 expression is a central event in the progression from polyclonal naïve T cells to highly oligoclonal, senescent natural killer (NK)-like T cells. Results of studies with various *in vitro* replicative senescence systems have consistently demonstrated that the loss of CD28 expression is a central event in the senescence pathway of human $CD4^+$ and $CD8^+$ T cells. Replicative pressure such as activation by common persistent Ags and by chronic inflammation leads to down-regulation of CD28 and to telomere length shortening that limits T-cell proliferation. Coincident with these processes are the loss and/or gain of function, such as the loss of perforin among $CD8^+$ T cells and the acquisition of natural killer cell (NK)-related receptors (NKR), killer cell immunoglobulin (Ig)-like receptor (KIR), and an activating NK receptor, NKG2D. Expression of inhibitory forms of KIR and of members of the Ig-like transcripts (ILT) family could also confer suppressive activity. Similar to that seen with *in vitro* replicative senescence systems, normal chronological aging results in the accumulation of long-lived, terminally differentiated, oligoclonal $CD28^-$ NK-like T-cell effectors.

Figure 1-5:

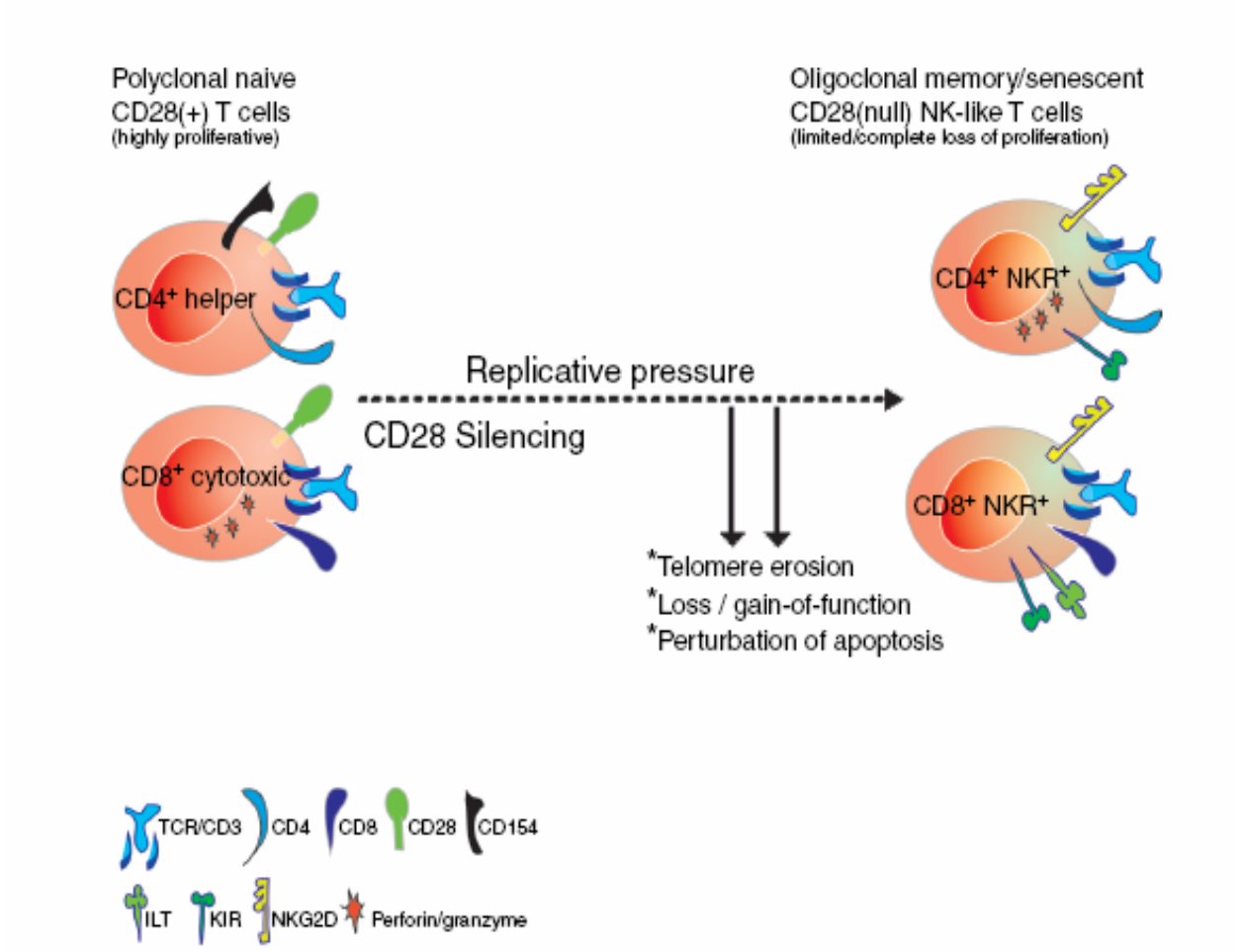
Polyclonal naive
CD28(+) T cells
(highly proliferative)
Oligoclonal memory/senescent
CD28(null) NK-like T cells
(limited/complete loss of proliferation)
CD4+ helper
CD8+ cytotoxic
CD4+ NKR+
CD8+ NKR+
Replicative pressure
CD28 Silencing
*Telomere erosion
*Loss / gain-of-function
*Perturbation of apoptosis
TCR/CD3
CD4
CD8
CD28
CD154
ILT
KIR
NKG2D
Perforin/granzyme

It is not clear which subset(s) of $CD8^+$ TIL contribute more to the long term control of tumor growth. The aforementioned differentiation/memory T-cell markers have been used to gain an understanding into these questions, but the data has been inconsistent and confusing. In a murine B16 melanoma tumor model, the adoptive transfer of T_{SCM} cells exhibited the most effective control of melanoma tumor growth among all different T-cell subsets (132) (**Fig. 1-4a**). Although such T_{SCM} $CD8^+$ T cells exist in the peripheral blood in humans, they have not been found in melanoma TIL populations. The other T-cell subset, T_{CM}, can migrate to lymph nodes, where they may encounter activated pAPC (e.g., dendritic cells) presenting TAA either derived from vaccination or from dying tumor cells (133). Although an adoptive transfer of melanoma TAA-specific T_{CM} have been shown in murine models to be superior T cells for ACT (125), it must be noted this effect occurs only when a vaccination with the specific TAA is given concurrently following cell transfer. Thus, T_{CM} may not be useful for ACT without concurrent vaccination with TAA, since these T cells have limited homing to tissue or tumor, and exhibit no anti-tumor cytolytic activity unless re-stimulated by mature pAPC (133). Also, only a very few central memory $CD8^+$ T-cells (T_{CM}) are found TIL, especially after the extensive expansion with REP used to generate TIL infusion products, which were mainly consisted of T_{EM} (early, intermediate, and late) and T_{EMRA} $CD8^+$ T cell subsets (60, 71). Early T_{EM} cells are capable of proliferation, have longer telomere length, and have some capacity for self-renewal (133). However, they have a limited capacity as cytolytic effector cells, as they express granzymes, but very low to no expressions of perforin and other critical killing proteins, such as granulysin (133). On the other hand, late-differentiated T_{EM} cells and T_{EMRA}, which express much higher amounts of granzymes and perforin, have been reported as the most potent cells for inducing effective

cytotoxic killing of tumor cells (133). However, these $CD8^+$ T cells have shorter telomeres and less T-cell costimulatory receptors, causing them to be less proliferative following TCR stimulation than T_{EM} cells (133). They are also more sensitive to activation-induced cell death (AICD) and cannot traffic to lymph nodes (133). At the present time, there is no clear evidence that they mediate long-term memory response against tumors after ACT.

NCI's phase II clinical trials have reported that early-differentiated T_{EM} cells expressing CD27 are associated with clinical response to TIL therapy (85, 134). These studies, however, only show a positive correlation when reported as total $CD8^+CD27^+$ infused, but not as a percentage of the $CD8^+$ T cells infused. Thus, higher numbers of $CD8^+$ T cells infused may account for this correlation. On the other hand, earlier reports from NCI showed that the persistence of TIL *in vivo* was correlated with positive clinical responses, and that the subset of TIL showing persistence *in vivo* was $CD8^+CD28^+$, not $CD27^+$ TIL (103, 135, 136). Our group has also reported that MART-1 (TAA)-specific $CD8^+CD28^+$ TIL after the REP possessed longer telomere length, proliferated better, survived better, and responded better to re-stimulation with pAPC than $CD8^+CD28^-$ TIL, whereas no difference was found between $CD27^+$ and $CD27^-$ TIL (96). Thus there was no clear mechanistic basis for the clinical correlation with $CD8^+CD27^+$ TIL. To confuse matters more, in the ongoing Phase II ACT clinical trial at MD Anderson Cancer Center where over 70 patients have been treated, we have found that the more differentiated $CD8^+CD27^-$ T cells were significantly correlated with positive clinical response to TIL, while the correlation with $CD8^+$ T_{EM} did not reach statistical significance (60, 71). It must be noted that many of these $CD8^+CD27^-$ T cells had retaind at least some CD28 expression. Also many of these cells were positive for another activation marker called B- and T- lymphocyte attenuator (BTLA), a marker for less-

differentiated $CD8^+$ TIL that we have found to be positively correlated to clinical response to adoptive cell therapy using melanoma TIL (**Chapter 3**, also *manuscript in preparation*).

A different way in thinking about the relationship between $CD8^+$ T-cell differentiation and anti-tumor activity is that a cooperation between early differentiated and late differentiated $CD8^+$ memory and effector subsets are needed to maximize the therapeutic potential of ACT with TIL for melanoma (**Fig. 1-6**). According to this view, late-differentiated T_{EM} or T_{EMRA}, which highly express granzymes and perforin, yet are poorly persisting *in vivo*, provide immediate control of tumor growth, while early-differentiated T_{EM} cells maintain more long-term tumor control by having the capacity to divide and replenish a pool of more differentiated T cells after adoptive transfer. This model is a new conceptual framework for ACT with TIL which, if proven correct, suggests that the adoptive transfer of different types of TIL products enriched in $CD8^+$ T cells with appropriate early and late differentiation phenotypes at different times into patients may be a new approach to ACT. This also fits in line with how $CD8^+$ cytotoxic T-cell populations against chronic viral infections, such as cytomegalovirus (CMV), are maintained over decades in humans. Here, younger CMV-specific T_{EM} $CD8^+$ T cells are thought to turn over and differentiate into terminally-differentiated $CD8^+CD28^-CD57^+$ populations that have immediate cytotoxic potential, can survive for extended periods of time, and turn over more slowly than their younger less-differentiated precursors (127, 137).

Figure 1-6: Model for the cooperation of $CD8^+$ T-cells at different stages of differentiation in controlling tumors *in vivo* following ACT with TIL. The model proposes that early, T_{EM}, late T_{EM}, and T_{EMRA} may all play a critical role in adoptive cell therapy at different times to control tumor growth. In order for CD8+ TIL to become cytolytic effector cells against tumor cells, this requires differentiation into late T_{EM} and T_{EMRA} cells. In contrast, early T_{EM} cell are long-lived, but have low cytolytic potential. The late T_{EM} and T_{EMRA} subsets, which are more oligoclonal (**Fig. 1-5**), execute an early wave of tumor killing. These cells are relatively short-lived and can be replaced by the more polyclonal early T_{EM} that possess a higher intrinsic proliferative capacity and can differentiate later into cytolytic effector cells. In addition to these infused TIL subsets, endogenous T cells re-appearing in the patients after transient lymphodepletion may also play a role at these later times by recognizing tumor antigens initially released from early waves of tumor killing.

Reprinted with permission from: Wu, R. Forgét, MA, Chacon J, Bernatchez C, Haymaker C, Chen JQ, Hwu P, and Radvanyi L. Adoptive T-cell Therapy Using Autologous Tumor-infiltrating Lymphocytes. 2012. *The Cancer J*. 18(2):160-75. doi: 10.1097/PPO.0b013e31824d4465.

Figure 1-6:

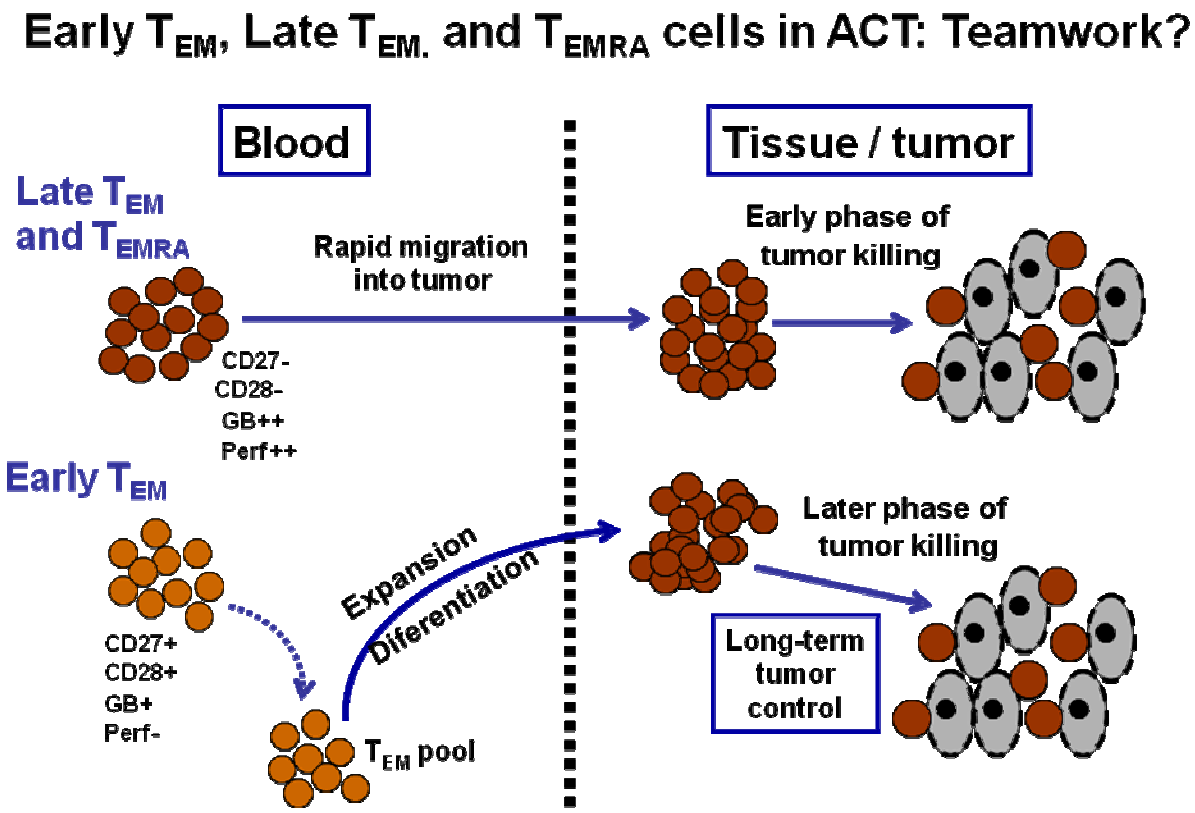
Early T_{EM}, Late $T_{EM.}$ and T_{EMRA} cells in ACT: Teamwork?
Blood
Tissue / tumor
Late T_{EM} and T_{EMRA}
Rapid migration into tumor
Early phase of tumor killing
CD27-
CD28-
GB++
Perf++
Early T_{EM}
Expansion
Diferentiation
Later phase of tumor killing
CD27+
CD28+
GB+
Perf-
Long-term tumor control
T_{EM} pool

Chapter 2

Detection and characterization of a novel subset of $CD8^+CD57^+$ T cells in metastatic melanoma with an incompletely differentiated phenotype

Partially reproduced and adapted for this doctoral dissertation with permission from the publisher (*American Association for Cancer Research*):

Wu R, Liu S, Chacon JA, Wu S, Li Y, Sukhumachandra P, Murray JL, Molldrem JJ, Hwu P, Pircher H, Lizée G, Radvanyi L. 2012. *Clin. Can. Res.* 18(9): 2465-77.

Introduction

$CD8^+$ cytotoxic T lymphocytes (CTL) play a major role in anti-tumor responses by lysing tumor cells in an antigen-specific manner through the action of granzymes [e.g., granzyme B (GB)], which belong to a family of serine proteases that cleave at aspartate residues in the substrate, and perforin (Perf) (114, 115). Perforin forms pores in the plasma membrane of target cells, which allows granzymes to enter the target cell and activate caspases (e.g., caspase 3), causing apoptosis in the target tumor cells (114). Uncovering how $CD8^+$ T cells' differentiation and effector function can be altered in the tumor microenvironment is critical to understand why most tumors continue to progress, despite being infiltrated with $CD8^+$ T cells.

Terminally-differentiated effector (T_{TDE}) $CD8^+CD57^+$ CTL, which express high levels of GB and Perf, have been reported as the most potent type of CTL for combating chronic viral infections, as well as inducing effective cytotoxic killing of tumor cells(138-143). Most healthy adults contain a population of persisting, long-lived CMV-specific $CD8^+$ $CD27^-CD28^-$ $CD57^+$, and GB^{Hi} $Perf^{Hi}$ lymphocytes in the peripheral blood that exhibit spontaneous anti-viral CTL activity (142-145). Differentiation of $CD27^+$ CTL precursors have been shown to be critical for maintaining a pool of mature $CD57^+$ CTL, which controls CMV and EBV infections in humans (131, 141, 145, 146). However, differentiation towards such mature CTL phenotype can be affected in situations where $CD8^+$ T cells undergo chronic antigen stimulation, as has been reported for patients having re-activation of HIV and EBV infections (144, 147), where an accumulation of incompletely differentiated $CD8^+CD27^+CD57^+$ CTL leads to a loss of control of viral replication (145).

In cancer patients, the role of the $CD8^+CD57^+$ T cells in the control of tumor growth has not been clearly defined (148). In malignant melanoma, renal cell carcinoma, and gastric carcinoma, it was reported that patients who harbored higher percentages of $CD8^+CD57^+$ lymphocytes in their peripheral blood had shorter overall survival (149-151). However, in those studies, other differentiation markers (e.g., CD27, CD28, CD45RA) that could be expressed by the $CD8^+CD57^+$ T lymphocytes were not further characterized. $CD8^+CD57^+$ T cells in the peripheral blood of advanced gastric carcinoma patients have been shown to have lower Perf expression and IFN-γ production as compared to healthy individuals (152). In contrast, $CD8^+CD57^+$ cells with a late-differentiated phenotype ($CD27^-CD28^-GB^{high}Perf^{high}$) accumulate in the peripheral blood of normal aged individuals and are the main IFN-γ-producing $CD8^+$ T cell subset (153). $CD8^+CD57^+$ T cells have also been positively associated with potent anti-tumor and anti-viral (CMV in particular) effector functions and longer relapse-free survival in leukemia patients after stem-cell transplant (138, 154).

Little is known about the frequency and function of the $CD8^+CD57^+$ CTL within the tumor-infiltrating lymphocytes (TIL) populations in solid tumors, such as melanoma or breast cancer. Recently, a distinct population of $CD8^+$ CTL in human peripheral blood with late-differentiation characteristics ($CD27^-CD28^-GB^{Hi}Perf^{Hi}$) was found to express another natural-killer (NK) cell marker, CD56 (also known as NCAM, **N**eural **C**ell **A**dhesion **M**olecule) (142, 143, 155). $CD8^+CD56^+$ CTL ($CD3^+$) that did not co-express CD57 exhibited an even higher spontaneous cytolytic activity than $CD57^+$ CTL against tumor targets; they re-express CD45RA as well as high levels of Perf and GB expression (155). It is not known whether $CD8^+$ TIL preferentially differentiate to become $CD56^+$ or $CD57^+$ effector CTLs.

In this study, we conducted a detailed analysis of the phenotypic differentiation of $CD8^+$ TILs in 44 melanoma metastases (lymph-node (LN) and non-LN) and 5 breast cancer metastases using multicolor flow cytometry. A similar study previously reported by others focused exclusively on T-cells infiltrates in lymph mode metastases (156). In our studies here, we included a large number of non-lymph node visceral melanoma metastases in order to exclude contributions from non-tumor specific, resident lymph node immune cells. Our study was also important because melanoma patients frequently die from visceral, non-lymph node metastases. We did not find a population of $CD8^+CD56^+$ CTL in freshly-isolated melanoma TIL, but instead observed a significant population of $CD8^+CD57^+$ TILs. Moreover, we found that the majority of the $CD57^+$ TIL in melanoma and breast cancer pleural effusions also co-expressed CD27 and CD28, markers of effector-memory T cells (T_{EM}) (123, 147, 157) with intermediate levels of GB expression and low-to-absent Perf expression, similar to that of the $CD8^+CD27^+CD57^+$ T-cell population that was recently described in HIV-infected patients who were progressors (145). These $CD8^+CD27^+CD57^+$ T-cells could be induced to differentiate into late-differentiated $CD27^-CD57^+$, $Perf^{Hi}$ CTL after short-term TCR stimulation and recovered high cytolytic activity. In addition, we showed that the differentiation of this unique subset in TIL could be inhibited by TGF-β1, a cytokine with potent immunosuppressive activity and is known to be produced by many types of tumor cells, including melanoma (158-161). These results suggest that the differentiation pathway of $CD8^+$ TIL to a late-differentiated, mature $CD8^+CD57^+$ CTL lineage is blocked, which may be caused by the presence of immunosuppressive factors within the tumor microenvironment.

Materials and Methods

Reagents. Flow cytometry antibodies were purchased from BD Biosciences (San Jose, CA), eBioscience (La Jolla, CA), or Beckman-Coulter (Brea, CA). Human recombinant IL-2 (ProLeukin™) was a generous gift from Novartis (East Hanover, NJ). KLRG1-Alexa 488 mAb was a gift from Dr. H. Pircher (Freiburg, Germany).

Patient TIL and PBMC samples. TIL and blood samples for laboratory studies were obtained from patients with Stage IIIc to Stage IV melanoma who were undergoing surgery at The University of Texas MD Anderson Cancer Center according to an Institutional Review Board–approved protocol and patient consent. The resected melanoma metastases were cut up into 3-5 mm^2 fragments after trimming away fat and connective tissue and disaggregated in cold RPMI 1640 using gentle mechanical pulverization using a Seward Stomacher device (Fisher, Pittsburgh, PA). This process rapidly produces a single cell suspension without enzymatic digestion. The cell suspension was filtered through a 75 μm pore-size screen (BD Biosciences, San Jose CA) and washed culture medium. A portion of the cells used for immediate staining and analysis by flow cytometry were washed in culture medium and the cell suspension layered over a discontinuous 70% followed by a 100% Ficoll Isopaque gradient, and centrifuged separate the tumor cells (70% interface) from the enriched TIL (100% interface). Typically 0.5 x 10^6 to 5 x10^6 lymphocytes were isolated initially from tumor fragments, depending on the size of tumors. In cases where cultured TIL were studied, the TIL from tumor samples were expanded in TIL culture medium (TIL-CM) consisting of RPMI 1640 with Glutamax (Invitrogen), 10% human AB serum (Sigma, St. Louis, MI), 50 mM 2-mercaptoethanol (Invitrogen), 1 mM pyruvate, 1X Penicillin/Streptomycin

(Invitrogen) using high-dose (HD) 3,000 IU/mL recombinant IL-2, as described previously (96).

Peripheral blood mononuclear cells (PBMC) were isolated by density gradient separation with Ficoll-Isopaque from normal donors from buffy coats obtained from the Gulf Coast Regional Blood Center (Houston, TX) or peripheral blood from Stage IV melanoma patients collected in heparizined tubes (BD Biosciences). The PBMC were cryopreserved in 10% DMSO, 90% human AB serum until analysis.

Pleural effusions were also collected from metastatic breast cancer patients under an IRB-approved protocol. Lymphocytes in pleural effusions were isolated by centrifugation over 70% and 100% Ficoll-Isopaque double layers to separate tumor cells from lymphocytes. The lymphocytes were collected at the 100% Ficoll-Isopaque layer and washed in TIL-CM before flow cytometry staining.

Surface and intracellular staining by flow cytometry. Freshly-isolated TIL and TIL cultured and expanded with IL-2, as well as thawed normal donor or patient PBMC, were washed twice in D-PBS and stained using Live/Dead® Fixable Aqua Dead Cell Stain Kit (Life Technologies, CA) according to manufacturer's instruction (**Fig. 2-1A**). Cells were then washed twice in FACS wash buffer (D-PBS + 1% BSA) and stained for 30 min at 4°C with antibodies conjugated with fluorochromes against different T-cell cell surface and intracellular markers. In the cases of HLA-A2.1$^+$ patients, the TIL suspensions were additionally stained with MART-1 peptide (ELAGIGILTV) HLA-A2.1 tetramer, gp100 peptide (IMDQVPFSV) HLA-A2.1 tetramer, or control HLA-A2.1 tetramer containing HIV-*gag* peptide (SLYNTVATL) (Beckman Coulter, Brea, CA) (**Fig. 2-2**). The cells were

finally fixed in D-PBS, 1% p-formaldehyde and 0.25% ethanol. Intracellular staining for GB and Perf was done by according to manufacturer's protocol (BD Biosciences). Flow cytometric analysis was performed using a FACSCanto II flow cytometer (Becton-Dickinson, San Jose, CA). The positive and negative regions of the staining of the indicated surface markers were determined by comparing against the unstained samples (**Fig. 2-1B**). Data was analyzed using FACSDiva (BD Biosciences) or FlowJo software (Tree Star Inc, Ashland, OR). Proliferation was assessed by intracellular staining for Ki67 using an anti-Ki67-APC antibody (BD Biosciences).

Figure 2-1: Methods for distinguishing between live and dead cells in TIL freshly isolated from melanoma metastases and defining the positive and negative regions of the indicated surface markers. (**A**) TIL were isolated from tumor fragments as described in Supplementary Methods. Typically 0.5 x 10^6 to 5 x 10^6 lymphocytes were isolated, depending on the size of the tumor fragments. Freshly-isolated TIL were stained with Live/Dead® Aqua cell exclusion dye (Invitrogen) followed by staining for the indicated surface markers. At least 100,000 light scatter events were acquired by the flow cytometer. Live cells were gated on in the Aqua-negative region. (**B**) The expressions of the indicated surface markers were determined by comparing the stained (**A**) versus unstained (**B**) TIL sample from the same patient.

Reprinted with permission from: Wu R, Liu S, Chacon JA, Wu S, Li Y, Sukhumachandra P, Murray JL, Molldrem JJ, Hwu P, Pircher H, Lizée G, Radvanyi L. 2012. *Clin. Can. Res.* 18(9): 2465-77. doi:10.1158/1078-0432.CCR-11-2034

Figure 2-1:

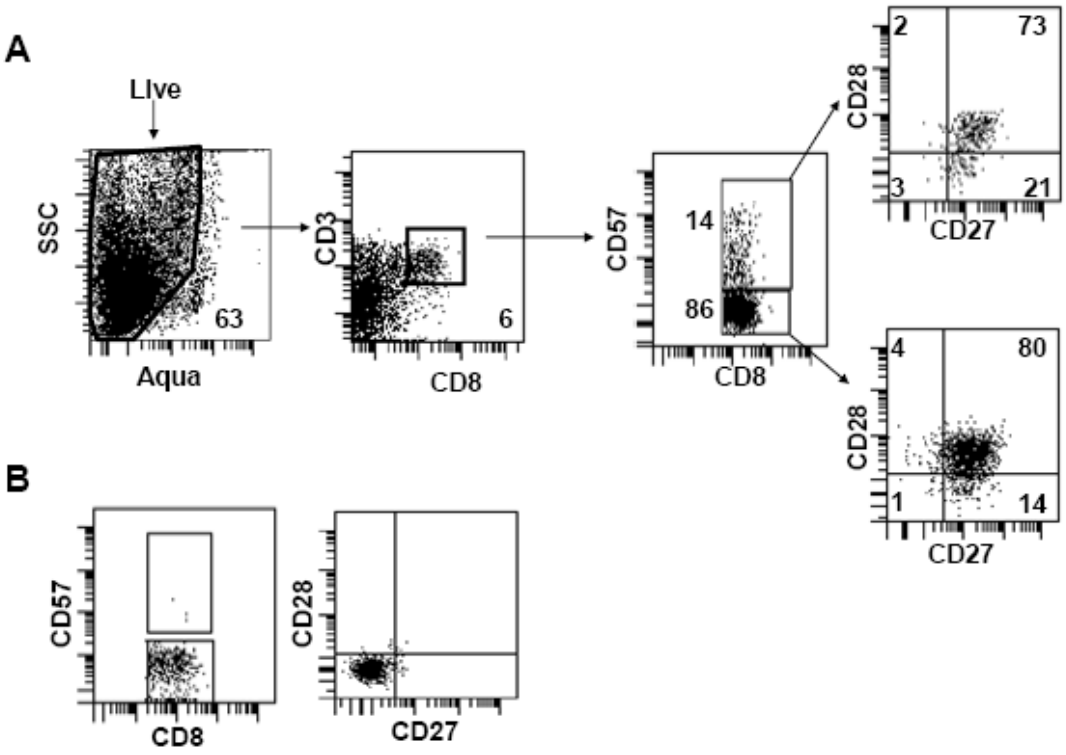
A
LIve
SSC
Aqua
63
CD3
CD8
6
CD57
CD8
14
86
CD28
CD27
2
73
3
21
CD28
CD27
4
80
1
14
B
CD57
CD8
CD28
CD27

Figure 2-2. Method for determination of tumor antigen-specific $CD8^+$ population in TIL. In order to determine the actual vs. background staining of $CD8^+$ melanoma TIL for the HLA-A2 tetramers loaded with MART-1 or gp100 peptides (Beckman Coulter, see Material and Methods), a comparison was made between TIL samples from a HLA-$A2^+$patient against a HLA-$A2^-$ patient. A minimum of 100,000 gated light scatter events were acquired for each sample. (**A**) Flow cytometry plot of a HLA-$A2^+$ TIL patient having low frequencies of tumor antigen-specific $CD8^+$ TIL for MART-1 (0.5%) or gp100 (0.2%). (**B**) Flow cytometry plot of a HLA-$A2^-$ patient whose $CD8^+$ TIL did not react with HLA-A2 tetramers.

Reprinted with permission from: Wu R, Liu S, Chacon JA, Wu S, Li Y, Sukhumachandra P, Murray JL, Molldrem JJ, Hwu P, Pircher H, Lizée G, Radvanyi L. 2012. *Clin. Can. Res.* 18(9): 2465-77. doi:10.1158/1078-0432.CCR-11-2034

Figure 2-2:

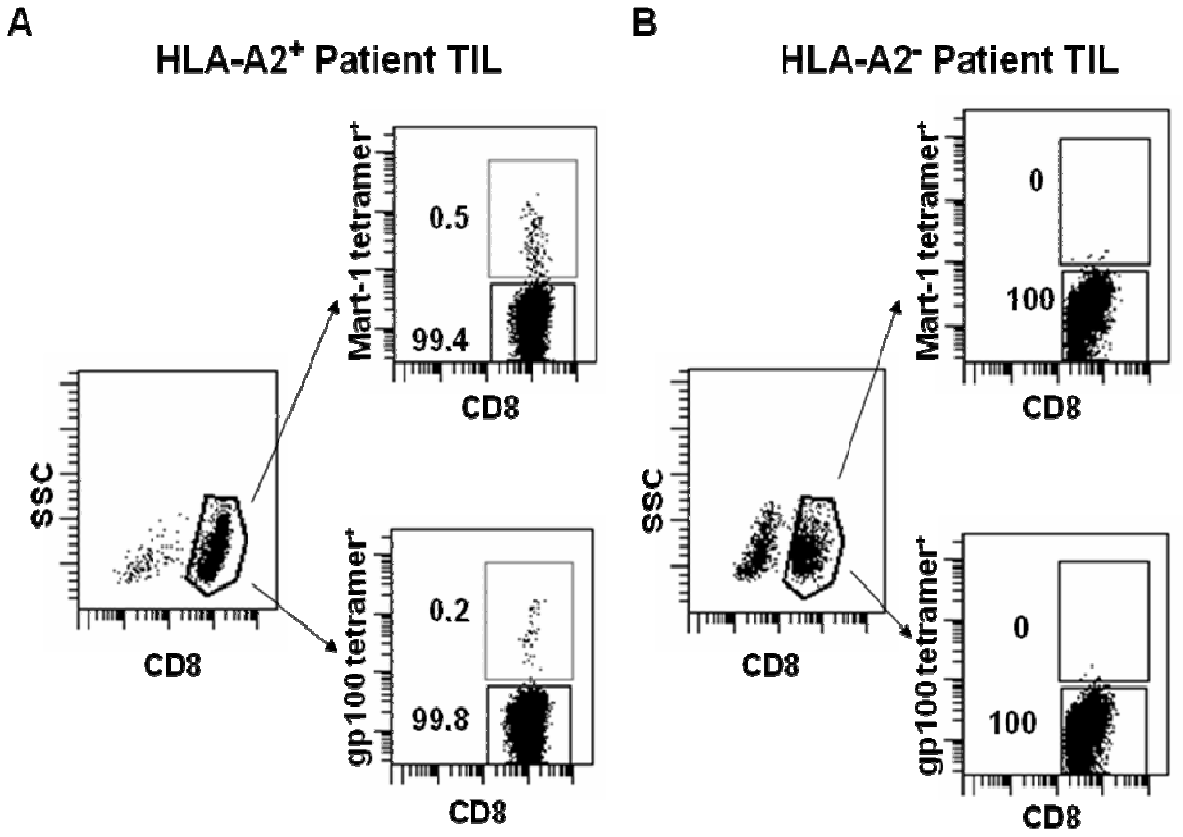
A
HLA-A2+ Patient TIL
SSC
CD8
Mart-1 tetramer+
0.5
99.4
CD8
gp100 tetramer+
0.2
99.8
CD8
B
HLA-A2- Patient TIL
SSC
CD8
Mart-1 tetramer+
0
100
CD8
gp100 tetramer+
0
100
CD8

Sorting and ^{3}H-thymidine incorporation assay. IL-2-cultured TILs were stained with anti-CD8-Pacific Blue, anti-CD27-APC-Cy7 and anti-CD57-FITC in PBS containing 1% BSA and 5% goat serum. The $CD8^{+}CD27^{+}CD57^{-}$ and $CD8^{+}CD27^{+}CD57^{+}$ subsets were sorted using an InFlux® cell sorter (BD Biosciences). 5 x 10^{4} viable cells per well were plated into 96-well Costar 3361 High-bind plates (Sigma-Aldrich, St. Louis, MO) precoated overnight with anti-CD3 (OKT3; Ortho Biotech, Raritan, NJ) or anti-CD3 and anti-CD28 (eBioscience, La Jolla, CA) agonistic antibodies. After 3 days, the cells were pulsed with 1 μCi of [^{3}H]-thymidine (methyl-T-thymidine, PerkinElmer Inc., Boston, MA) for 18 h. The incorporated [^{3}H] thymidine was determined as counts per minute by using a beta liquid scintillation counter (Beckman Coulter, Brea, CA).

Human Th1/Th2 multiplex cytokine analysis. The tissue culture supernatants from a triplicate wells of sorted, TIL subsets from unstimulated and stimulated conditions were collected and plated on the multiplex ELISA plate configured to detect a panel of human Th1/Th2 cytokines (IFN-γ, IL-2, IL-4, IL-5, IL-10, IL-12 p70, and IL-13), according to the manufacturer's instructions (Meso Scale Discovery, Gaithersburg, MD). The signals were captured and analyzed by the SECTOR Imager 2400 (Meso Scale Discovery, Gaithersburg, MD). The concentration of each cytokine was calculated from its each respective standard curves. For analysis using a multiplex cytokine bead assay, the tissue culture supernatants from a triplicate wells of sorted, TIL subsets from unstimulated and stimulated conditions were collected, diluted to 1:3 ratio, and added to magnetic beads coated with immobilized antibodies against selected human cytokines (IFN-γ, IL-5, IL-13 and TNF-α) in a Milliplex® MAP human multiplex cytokine kit, according to the manufacturer's instructions (EMD Millipore, Billerica, CA). The signals from the Strepavidin-Phycoerythrin (PE) coated beads

were acquired and analyzed by the Luminex® 100 IS System (Luminex® Corporation, Austin, TX). The concentration of each cytokine was calculated from its each respective standard curves.

TCR Vβ spectratyping. RNA was isolated from sorted $CD8^+$ TIL subsets with RNA-STAT 60 reagent (Isotex Diagnostics, Friendswood, TX) according to manufacturer's instructions. After reverse-transcription of 1 μg of RNA to cDNA with SuperScript®III reverse transcriptase (Invitrogen, Carlsbad, CA), TCR Vβ mRNA expression profiling and size spectratyping of the 23 antigen-binding Vβ CDR3 regions was performed as previously reported (162). Primer sequences for each of the 23 Vβ families are available upon request. CDR3 spectratypes were assessed using the OpenGene® System (Bayer, Berkeley, CA).

In vitro differentiation assay. $CD8^+$ TIL were sorted into subsets as described previously and stimulated with anti-CD3 or anti-CD3 and anti-CD28 antibodies precoated on Nunc® plates (Thermo Fisher Scientific, NY). IL-2 (200 IU/ml) was added to each culture to maintain cell viability. Human TGF-β1 (R&D Systems, Minneapolis, MN) was used at 1 ng/ml for the TGF-β1-treated group. After 7 days, the cells were stained for CD8, CD27, CD28, CD56, and CD57. Intracellular staining for GB and Perf was done as described above.

Redirected cytotoxic T-cell assay. Analysis of CTL activity on the sorted $CD8^+$ subsets was done according to a novel flow cytometric method measuring the cleavage of caspase-3 in anti-CD3 coated target cells as described previously (163). Briefly, 5×10^6 murine mastocytoma target cells (P815) were labeled with a fixable, far-red fluorescent tracer, CellTrace® Far Red DDAO-Succinimidyl Ester (DDAO-SE; Invitrogen, Carlsbad, CA)

according to manufacturer's instructions, washed, resuspended at a density of 2.5 x 10^6/mL, and pulsed with 200 μg/mL of anti-CD3 mAb in a low-serum containing media (RPMI 1640 with 2% FBS) at RT for 30 min. Unpulsed target cells served as controls. Labeled, pulsed P815 target cells were added to the sorted TIL subsets at E:T ratios of 1:1 and 3:1, or 1:10 and 1:20 in a round-bottom 96-well plate and spun down for 5 min at low centrifuge speed (300 RPM) in order to maintain optimal contact between target cells and effector T cells. The cells were co-incubated for 3 h before harvesting. The 3 hour time point was chosen to prevent the apoptotic target cells from becoming necrotic and losing the cleaved caspase-3 signal. The cells were stained intracellularly with an anti-cleaved caspase-3-PE mAb (BD Biosciences). Target cells were distinguished from effector T cells by the far-red tracer DDAO-SE (which fluoresce in the APC channel), and the extent of the caspase-3 cleavage in the target cell population was analyzed by the FACSanto II flow cytometer (BD Biosciences).

Statistical analysis. The two-tailed, paired Wilcoxon rank-sum test was used to analyze the statistical significance in differences between two groups, and two-tailed nonparametric Kruskal-Wallis test followed by Dunn's multiple comparison test were used for more than two sample groups. $p \leq 0.05$ was deemed to be statistically significant. GraphPad Prism version 5.0 (GraphPad Software, La Jolla, CA) was used for graphing and statistical analysis.

Results

Patient tumor samples and experimental approach

In this study, tumors were surgically excised from Stage III/IIIc and Stage IV (M1a-M1c) melanoma patients as part of an ongoing adoptive T-cell therapy clinical trial at MD Anderson Cancer Center (Houston, TX). A supplemental table, showing the characteristics of the melanoma patients, including patient age, sex, tumor location, disease stage, and anatomical sites, is available online as part of the following publication: Wu R, *et al*. 2012. *Clin. Can. Res*. 18(9): 2464-77. The tumors were processed immediately after surgery for multicolor flow cytometry staining and expansion of TIL.

Presence of a $CD8^+CD57^+$ subset highly positive for CD27 and CD28 and absence of $CD8^+CD56^+$ T cells in TIL freshly isolated from melanoma tumors

As $CD8^+$ T cells transition from T_{EM} into fully-differentiated (T_{TDE}) CTL, they generally acquire GB and Perf expression, down-regulate CD27 and CD28, and express CD57, or in some cases, CD56. This T_{TDE} phenotype ($CD27^-CD28^-CD56^+$ or $CD27^-CD28^-CD57^+$) is associated with immediate cytolytic activity, with no requirement for antigenic re-stimulation to induce CTL function (140, 143, 155, 157). To determine the extent of the T_{TDE} phenotype in tumors, we first gated on the live $CD8^+$ lymphocytes, as determined by the Aqua Live/Dead® exclusion dye (Invitrogen), on TIL freshly isolated from tumors (**Fig. 2-1**). We then analyzed them for CD4, CD8, CD27, CD28, CCR7 and CD45RA expressions using multicolor flow cytometry. A majority of the bulk as well as tumor antigen-specific $CD8^+$ TIL from melanoma tumors displayed a T_{EM} phenotype ($CD27^+$, $CD28^+$, $CCR7^-$, $CD45RA^-$) (123, 157) (**Fig. 2-3 and 2-4**)

Figure 2-3: Melanoma metastases contained bulk and tumor antigen-specific $CD8^+$ T cells with a $CD27^+CD28^+CD45RA^-$ effector-memory phenotype. Single cell suspensions, isolated from surgically-removed LN and non-LN melanoma metastases were stained with a panel of fluorochrome-conjugated antibodies against human CD4, CD8, CD27, CD28, CD57, CCR7, and CD45RA. Results were shown by gating on the live cells as described previously. (**A**) FACS dot plots of one representative bulk TIL preparation from Tumor #2276 is shown. $CD8^+$ T-cells or $CD8^-$ cells were identified in dot plots of side scatter (SSC) versus CD8 after dead cell removal; each gated subset was then analyzed for the indicated markers shown. (B) Isolated cell suspensions from involved LN and non-LN melanoma metastases of HLA-$A2.1^+$ patients were stained with antibodies for the same markers as in panel A, in addition to an HLA-A2.1 tetramer containing either Melan-A/MART-1 peptide, gp100 peptide, or CMV peptide (negative control, not shown). The $CD8^+$ T-cell subset was gated and analyzed for MART-1 or gp100 $tetramer^+$ cells. The $tetramer^+$ cells were then gated and analyzed for CD27 and CD28 expression. Figure shown in panel **B** represents the tetramer staining of two different tumor antigen specificities (Mart-1 and gp100) from the same patient. (**C**) Tetramer staining of a different HLA-$A2.1^+$ patient with antigen specificity to gp100 only, which showed the majority of antigen-specific TIL being $CD27^+CD28^+$. The HIV *gag* peptide tetramer in each case stained <0.05% of the $CD8^+$ cells (not shown).

Reprinted with permission from: Wu R, Liu S, Chacon JA, Wu S, Li Y, Sukhumachandra P, Murray JL, Molldrem JJ, Hwu P, Pircher H, Lizée G, Radvanyi L. 2012. *Clin. Can. Res.* 18(9): 2465-77. doi:10.1158/1078-0432.CCR-11-2034

Figure 2-3:

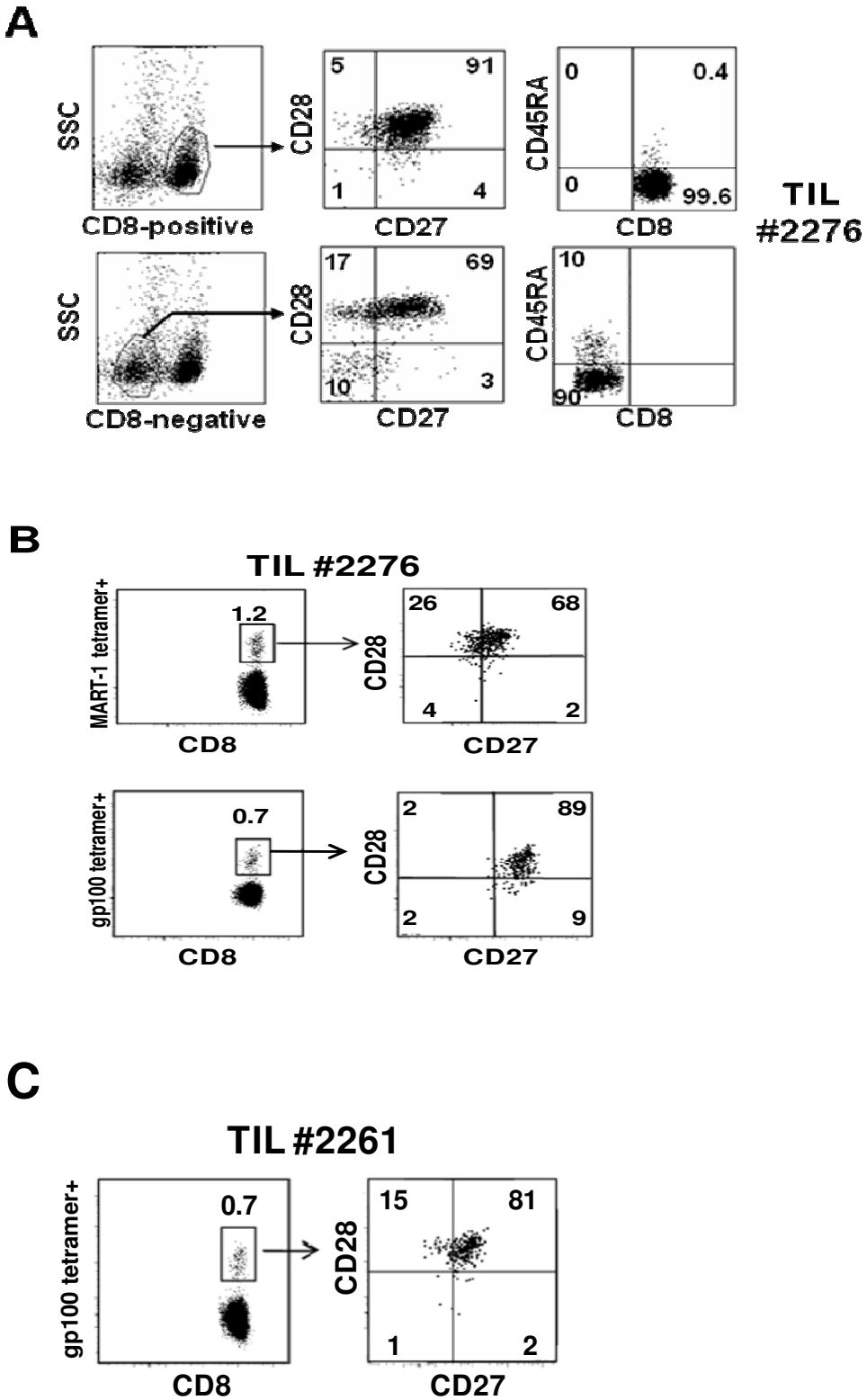
A
SSC
CD8-positive
CD28
CD27
5
91
1
4
CD45RA
CD8
0
0.4
0
99.6
TIL #2276
SSC
CD8-negative
CD28
CD27
17
69
10
3
CD45RA
CD8
10
90
B
TIL #2276
MART-1 tetramer+
CD8
1.2
CD28
CD27
26
68
4
2
gp100 tetramer+
CD8
0.7
CD28
CD27
2
89
2
9
C
TIL #2261
gp100 tetramer+
CD8
0.7
CD28
CD27
15
81
1
2

Figure 2-4: Summary of CD27 and CD28 expression in the $CD8^+$ TIL subsets (n=39) and in the $CD8^+$MART-1 $tetramer^+$ TIL subset (n=11) of metastatic melanomas showing a lack of $CD27^-CD28^-$ fully differentiated T cells and the preponderance of $CD27^+CD28^+$ T_{EM}. Isolated TIL were stained in a panel of fluorochrome-conjugated antibodies against (**A**) CD4, CD8, CD27, CD28, CD57, CCR7, CD45RA, and (**B**) MART-1 tetramer in HLA-$A2^+$ patients. Results were shown by gating on the live cells as described previously. They were analyzed for $CD27^+$, $CD28^+$, $CD27^+CD28^+$, $CD27^-CD28^-$, and $CCR7^+$ cells as indicated. Each dot represents a single patient sample with the bars indicating the averages for all samples. Results for gated $CD8^+$ (**A**) and $CD8^+$MART-1 $tetramer^+$ (**B**) subsets are shown.

Reprinted with permission from: Wu R, Liu S, Chacon JA, Wu S, Li Y, Sukhumachandra P, Murray JL, Molldrem JJ, Hwu P, Pircher H, Lizée G, Radvanyi L. 2012. *Clin. Can. Res.* 18(9): 2465-77. doi:10.1158/1078-0432.CCR-11-2034

Figure 2-4:

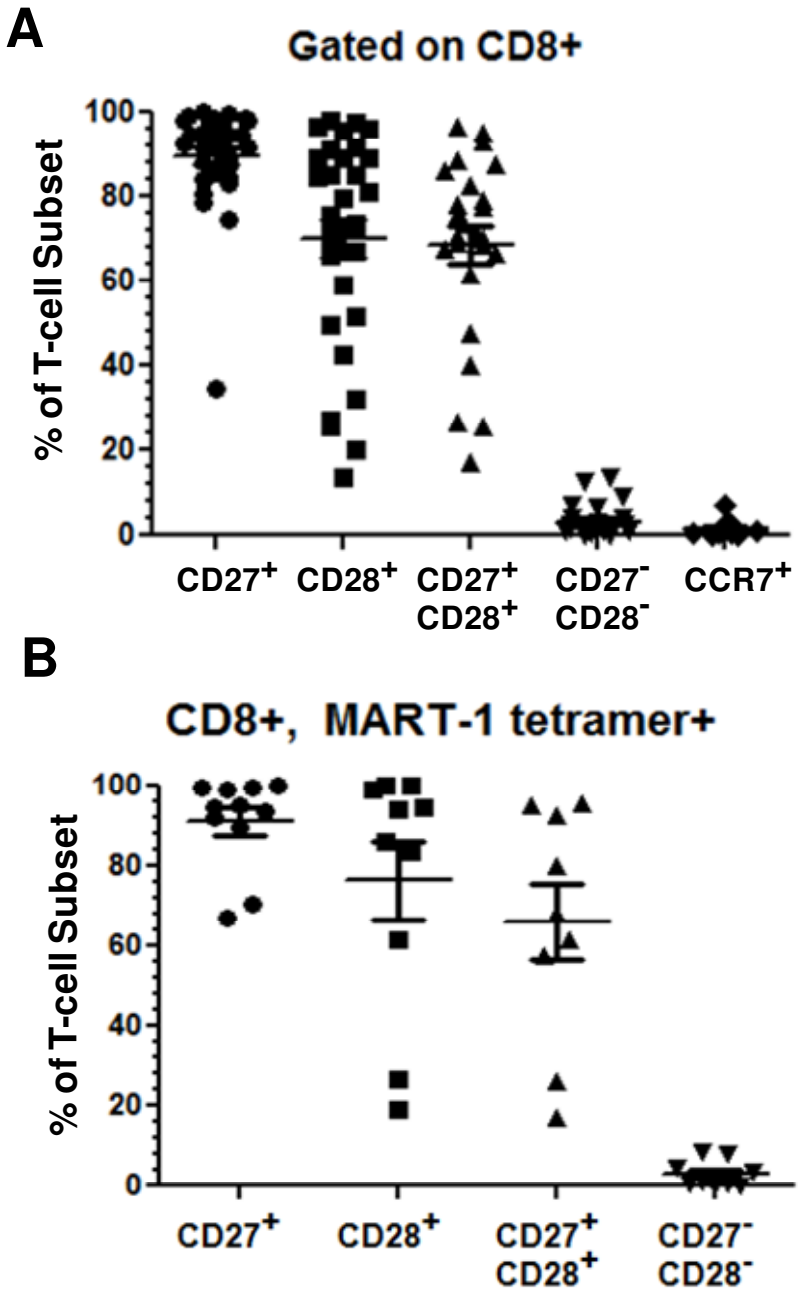
A
Gated on CD8+
% of T-cell Subset
100
80
60
40
20
0
CD27+
CD28+
CD27+ CD28+
CD27- CD28-
CCR7+
B
CD8+, MART-1 tetramer+
% of T-cell Subset
100
80
60
40
20
0
CD27+
CD28+
CD27+ CD28+
CD27- CD28-

The specificity of the MART-1 and gp100 tetramer staining was verified against a negative control, HIV *gag* tetramer (data not shown) as well as comparing against HLA-A2$^-$ patients (**Fig. 2-2**). We then stained the TIL for CD8, CD27, CD28, CD56, and CD57 and analyzed the relationship between end-stage CTL markers (CD57 and CD56) vs. T_{EM} markers (CD27 and CD28). We found that a significant population of CD57 single positive cells was seen without CD56 expression (see **Fig. 2-5A** for a representative example). **Fig. 2-5B** shows this predominance of CD8$^+$CD57$^+$ cells (mean percentage ± SEM = 16.2 ± 3.5) over CD8$^+$CD56$^+$ cells (mean percentage ± SEM: 1.0 ± 0.6) (paired Wilcoxon rank-sum test; $p < 0.005$) in the CD8$^+$ subset in freshly-isolated TIL for ten separate patient samples. Upon further analysis of the staining profiles from the freshly-isolated TIL samples, we found that many CD8$^+$CD57$^+$ T cells co-expressed CD27 and CD28, which could be considered as a hybrid of late-stage CTL and early T_{EM} markers (**Fig. 2-5C**). We also found that PD-1, a marker for antigen-experienced CD8$^+$ T cells, exhausted CD8$^+$ T cells, or CD8$^+$ T_{EM} in normal donor PBMC (164-166), was more enriched in the CD27$^+$CD57$^+$ than the CD27$^+$CD57$^-$ subset (**Fig. 2-6**; Kruskal-Wallis test, $p < 0.05$), in the tumors from ten different metastatic melanoma patients, which suggests that the CD27$^+$CD57$^+$ "hybrid" phenotype may represent a more differentiated effector phenotype than that of the CD27$^+$CD57$^-$ TIL subset.

Figure 2-5: Lack of CD56-expressing end-stage CTL and the appearance of a novel subset of $CD8^+CD57^+$ melanoma TIL co-expressing CD27 and CD28. (**A**) Fresh TIL isolates were stained with a panel of fluorochrome-conjugated antibodies for CD4, CD8, CD27, CD28, CD56, and CD57. Results were shown by gating on the live cells as described previously. A minimum of 100,000 gated light scatter events per sample were acquired on the flow cytometer. CD56 and CD57 expression in the $CD8^+$ subset in a representative patient TIL sample is shown. (**B**) A summary of the $CD8^+CD56^+$ and $CD8^+CD57^+$ populations in 10 freshly-isolated TIL from melanoma tumors. Significant difference was calculated by a two-tailed, paired Wilcoxon rank-sum test. (**C**) The gated $CD8^+CD57^+$ and $CD8^+CD57^-$ sub-populations were further analyzed separately for CD27 versus CD28 expression. Examples of TIL from two melanoma patient tumor samples are shown.

Reprinted with permission from: Wu R, Liu S, Chacon JA, Wu S, Li Y, Sukhumachandra P, Murray JL, Molldrem JJ, Hwu P, Pircher H, Lizée G, Radvanyi L. 2012. *Clin. Can. Res.* 18(9): 2465-77. doi:10.1158/1078-0432.CCR-11-2034

Figure 2-5:

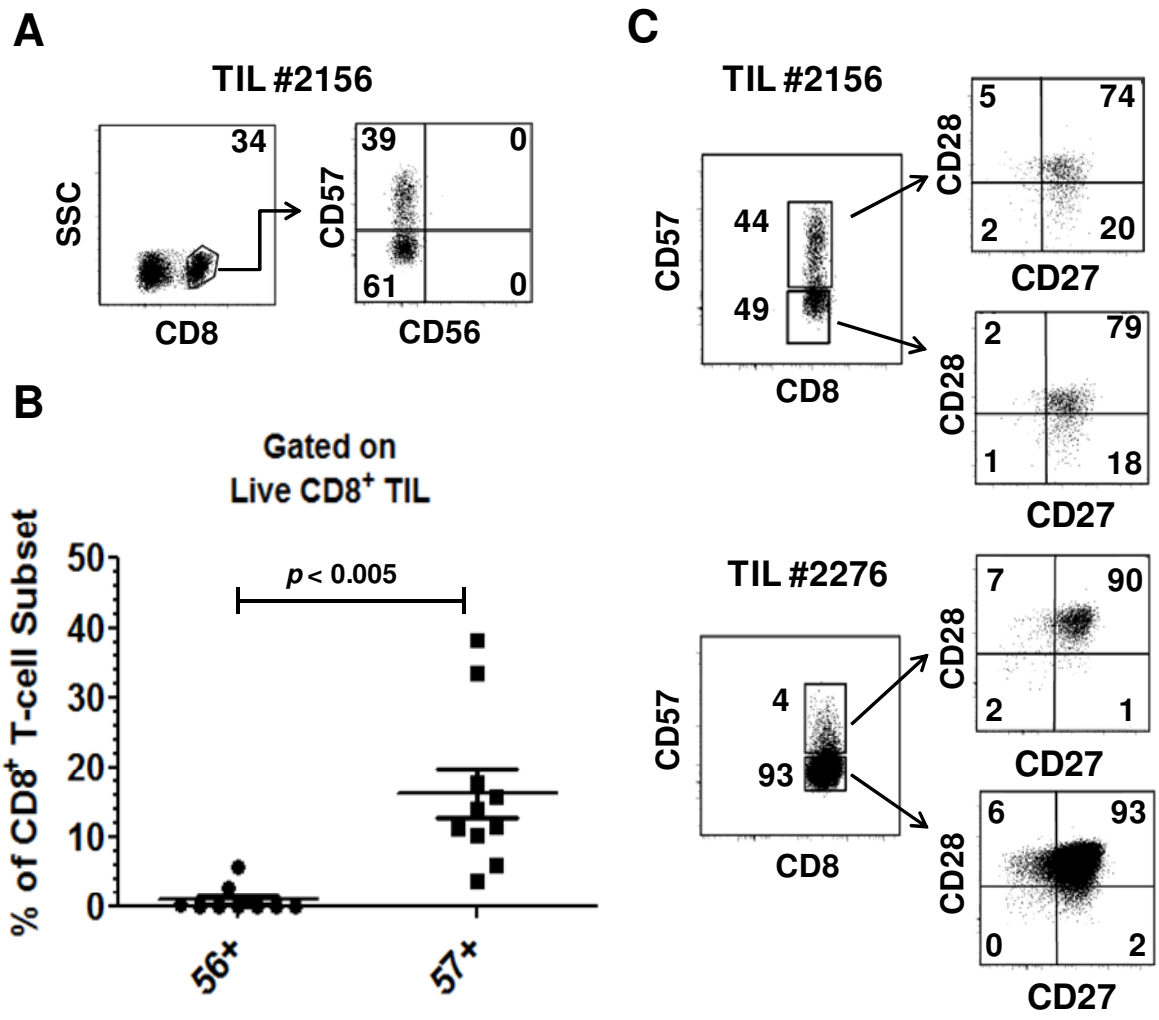
A
TIL #2156
34
SSC
CD8
39
0
61
0
CD57
CD56
B
Gated on
Live CD8+ TIL
p < 0.005
% of CD8+ T-cell Subset
50
40
30
20
10
0
56+
57+
C
TIL #2156
CD57
44
49
CD8
5
74
2
20
CD28
CD27
2
79
1
18
TIL #2276
4
93
7
90
2
1
6
93
0
2

Figure 2-6: PD-1 expression is enriched in the $CD8^+CD27^+CD57^+$ TIL subset freshly isolated from melanoma metastases (n=10). (**A**) Fresh TIL isolates from 10 melanoma patients were stained in a panel of fluorochrome-conjugated antibodies against CD4, CD8, CD27, CD28, CD57, and PD-1. . A minimum of 100,000 gated light scatter events per sample were acquired on the flow cytometer. Results were shown by gating on the live cells that were determined using Live/Dead® Fixable Aqua Dead Cell Stain Kit (Life Technologies, CA). PD-1 expression in the each gated $CD8^+$ TIL subset from patients' TIL samples are shown. Significant differences between the groups were calculated by a two-tailed, nonparametric Kruskal-Wallis test followed by Dunn's multiple comparison test. ns: not significant.

Reprinted with permission from: Wu R, Liu S, Chacon JA, Wu S, Li Y, Sukhumachandra P, Murray JL, Molldrem JJ, Hwu P, Pircher H, Lizée G, Radvanyi L. 2012. *Clin. Can. Res.* 18(9): 2465-77. doi:10.1158/1078-0432.CCR-11-2034

Figure 2-6:

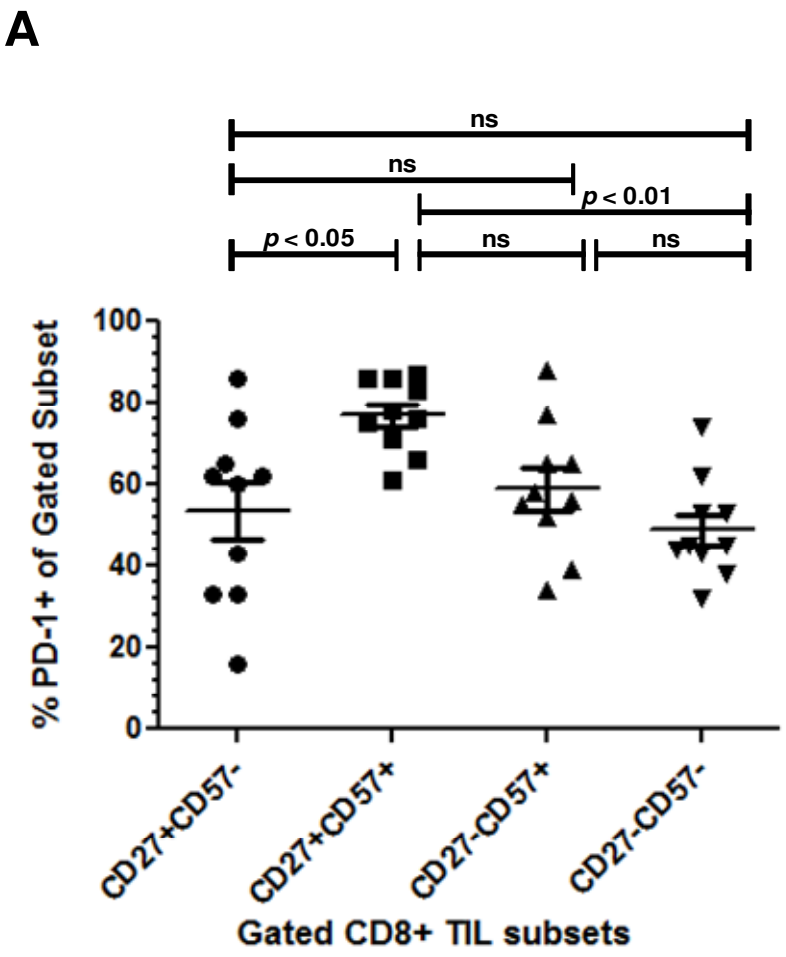
A
ns
ns
p < 0.01
p < 0.05
ns
ns
% PD-1+ of Gated Subset
100
80
60
40
20
0
CD27+CD57-
CD27+CD57+
CD27-CD57+
CD27-CD57-
Gated CD8+ TIL subsets

We also stained PBMC from patients and normal donors to determine the extent of $CD27^+CD28^+$ $CD8^+CD57^+$ T cells. Comparing TIL and PBMC from the same patient, we found that the $CD8^+$ T cells in the PBMC had only a few (<5%) of $CD57^+$ T cells co-expressing CD27 and CD28, while almost 60% of the $CD8^+CD57^+$ TIL co-expressed CD27 and CD28 (**Fig. 2-2A**). Similarly, only a few (<5%) of the $CD8^+CD57^+$ in PBMC of normal donors co-expressed CD27 and CD28 (**Fig. 2-7A**). In contrast, melanoma TIL contained, on average, >20% of the $CD8^+CD57^+$ subset co-expressing CD27 and CD28 in samples analyzed from a larger number of patients (**Fig. 2-7B**). An examination of the melanoma antigen-specific $CD8^+$ subsets (MART-1 and gp100) in fresh TIL isolates by using tetramer staining revealed these $tetramer^+$ cells were either $CD27^+CD57^-$ or $CD27^+CD57^+$, with a negligible fraction of cells having a $CD27^-CD57^+$ or $CD57^-CD27^-$ phenotype (**Fig. 2-7C**).

Figure 2-7: Relatively few fully differentiated $CD8^+CD27^-CD28^-CD57^+$ TIL were found in metastatic melanomas compared to peripheral blood of patients and normal donors. TIL isolated from melanoma metastases and PBMC from Stage III/IV melanoma patients were stained in a panel of fluorochrome-conjugated antibodies against CD4, CD8, CD27, CD28, CD56, and CD57. PBMC from 2 normal donors were similarly stained for comparison. Results were shown by gating on the live $CD8^+$ lymphocytes, as described previously, and analyzed for CD27 and CD28 expressions. (**A**) The results from one representative TIL isolate from tumor #2163, one representative patient PBMC sample, and two normal donors. (**B**) Analysis of the $CD57^+$ subset co-expressing CD27 and CD28 in the $CD8^+$ T-cell population in a larger group of melanoma TIL samples (n=18), melanoma patient PBMC (n=12), and normal donor PBMC (n=6) samples. The percentage of gated $CD8^+CD57^+$ subset co-expressing CD27, CD28, or both, was plotted for each sample type. Each dot represents a single sample with bars indicating the averages for each sample group. Results of a Student's t-test between the TIL and patient PBMC are shown for each subset ($p< 0.05$ indicates statistical significance). (**C**) Melanoma metastases from HLA-$A2.1^+$ patients were stained with antibodies for the same markers as in panel **A** together with tetramer containing either a human HLA-A2.1 MART-1 epitope or the human gp100 epitope. The $CD8^+$ T-cell subset was gated and analyzed for MART-1 or gp100 $tetramer^+$ cells. The $tetramer^+$ cells were then gated and analyzed for CD27 and CD57 expression. Shown are two examples of the analysis done using TIL from two different patient metastases (#2058 and #2276).

Reprinted with permission from: Wu R, Liu S, Chacon JA, Wu S, Li Y, Sukhumachandra P, Murray JL, Molldrem JJ, Hwu P, Pircher H, Lizée G, Radvanyi L. 2012. *Clin. Can. Res.* 18(9): 2465-77. doi:10.1158/1078-0432.CCR-11-2034

Figure 2-7:

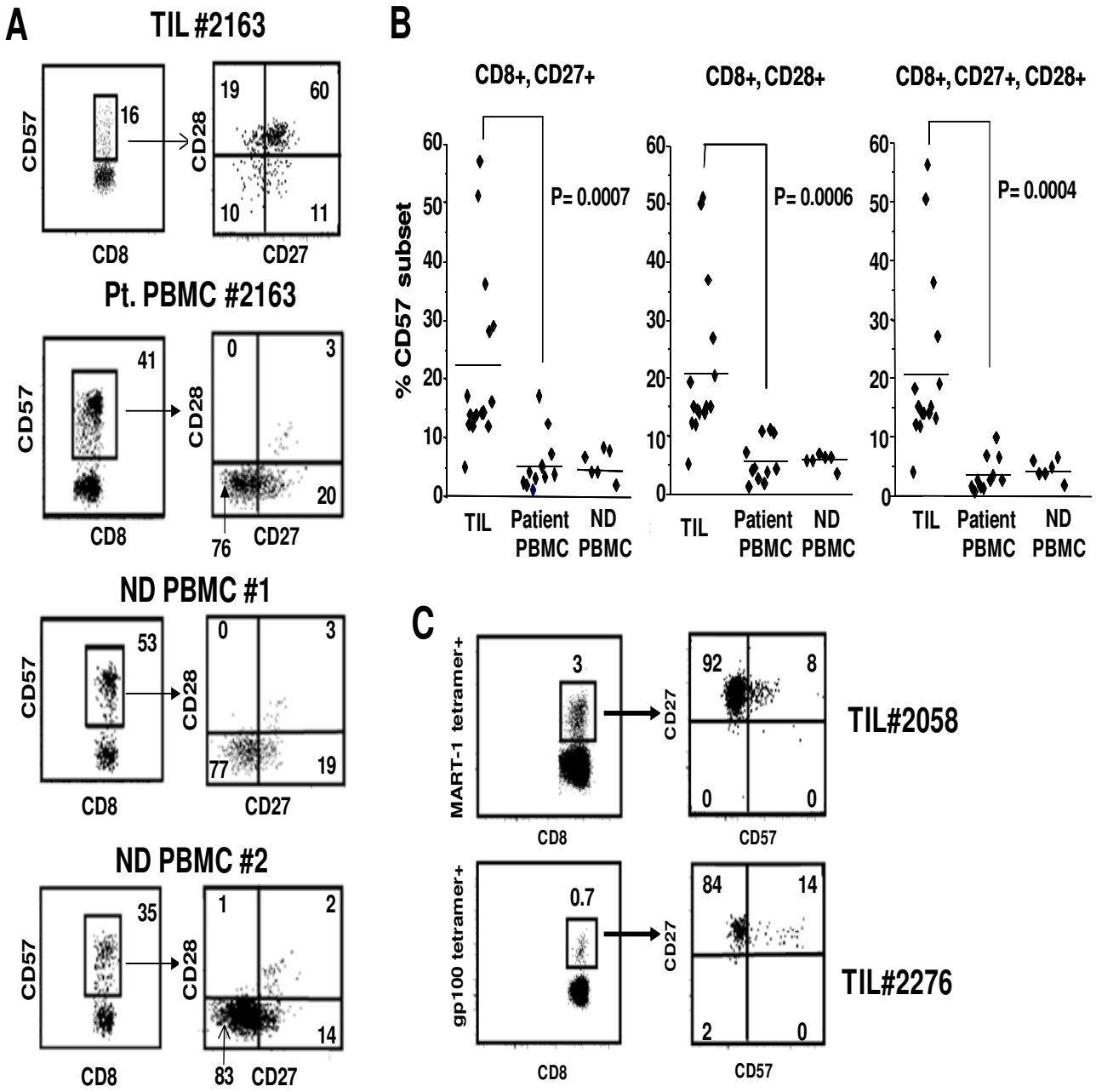
A
TIL #2163
CD57
CD28
16
19
60
10
11
CD8
CD27
Pt. PBMC #2163
41
0
3
20
76
ND PBMC #1
53
77
19
ND PBMC #2
35
1
2
14
83
B
CD8+, CD27+
CD8+, CD28+
CD8+, CD27+, CD28+
% CD57 subset
P= 0.0007
P= 0.0006
P= 0.0004
TIL
Patient PBMC
ND PBMC
C
MART-1 tetramer+
gp100 tetramer+
92
8
TIL#2058
84
14
TIL#2276

$CD8^+CD57^+CD27^+$ melanoma TIL are GB^+, but $Perf^{-/low}$

We next determined the intracellular GB and Perf expression, markers used to identify end-stage (T_{TDE}) CTL, in $CD8^+CD27^+CD57^+$ TIL in melanoma. We also obtained pleural effusions from newly diagnosed metastatic breast cancer patients to determine whether $CD8^+CD57^+$ co-expressing CD27 and CD28 were also found in other forms of cancer, and what their GB and Perf expression might be. First, in melanoma TIL, we found that the majority of gated $CD8^+CD27^+CD57^+$ and $CD8^+CD27^+CD57^-$ cells expressed GB, but most of the cells in both subsets had low or negative Perf expression (**Fig. 2-8A**). Using the same gating approach, we analyzed fresh melanoma TIL samples from 7 Stage IV melanoma patients, PBMC samples from 17 Stage IV melanoma patients, and PBMC from 6 normal donors. Shown in **Fig. 2-8B** was an example of the analysis that compared $CD8^+CD57^+$ T lymphocytes' GB and Perf contents in a patient's TIL against the same patient's PBMC and that of a normal donor. In Fig. 3C, 48.0 ± 8.6 % (mean ± SEM) of $CD8^+CD27^+CD57^+$ TIL from 7 patients were found to express GB, whereas only 20.5 ± 6.0 % expressed Perf. In contrast, averages of 94 ± 1.7 % and 80.9 ± 4.2 %, of the $CD8^+CD57^+$ lymphocytes in the peripheral blood of 17 melanoma patients were positive for GB and Perf, respectively. The difference was statistically significant for both GB and Perf ($p<0.001$, respectively; Kruskal-Wallis test). When we analyzed lymphocytes isolated from breast cancer pleural effusions, we also found that many $CD8^+CD57^+$ cells co-expressed CD27 and CD28, and that these cells were predominantly GB^+ with very little or no Perf expression (**Fig. 2-9**).

Figure 2-8: $CD8^+CD57^+$ subset in the melanoma microenvironment has a unique $GB^+Perf^{-/low}$ phenotype compared to the same subset in patient and normal donor PBMC. (**A**) TIL isolates were stained for CD8, CD27, CD28, CD57, GB, and Perf expression, as described in Material and Methods. Results were shown by gating on the live cells as described previously. The gated $CD8^+CD57^+$ and $CD8^+CD57^-$ sub-populations were further analyzed separately for GB and Perf expression. One representative melanoma TIL sample is shown. (**B**) Results comparing GB and Perf expression in the $CD8^+CD57^+$ TIL and $CD8^+CD57^+$ T cells in PBMC from the same patient (#2163) and in a representative normal donor. (**C**) Summary of GB and Perf expression in $CD8^+CD57^+$ TIL subsets from a number of melanoma metastases (n=7) compared to PBMC of patients (n=17) and PBMC from a group of normal donors (n=16). The percentages of $CD8^+CD57^+$ T-cells expressing GB or Perf are shown. Each dot represents a single sample with the bars indicating the averages and standard error on the means (SEM) for each TIL's $CD8^+$ subset. Significant differences between the groups were calculated by the two-tailed, nonparametric Kruskal-Wallis test followed by Dunn's multiple comparison test. ns: not significant.

Reprinted with permission from: Wu R, Liu S, Chacon JA, Wu S, Li Y, Sukhumachandra P, Murray JL, Molldrem JJ, Hwu P, Pircher H, Lizée G, Radvanyi L. 2012. *Clin. Can. Res.* 18(9): 2465-77. doi:10.1158/1078-0432.CCR-11-2034

Figure 2-8:

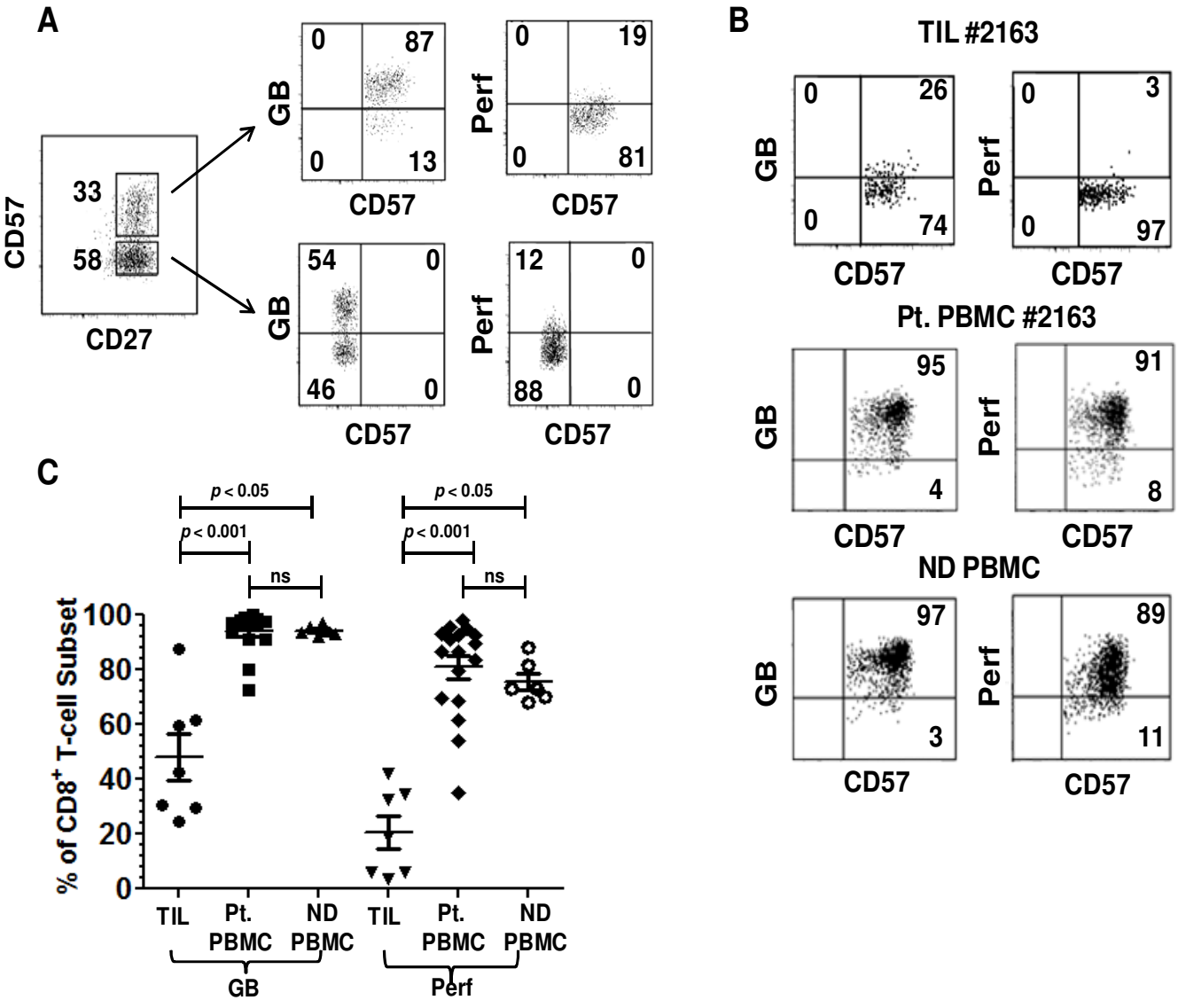
A
CD57
CD27
33
58
GB
Perf
CD57
0
87
0
13
0
19
0
81
54
0
46
0
12
0
88
0
B
TIL #2163
Pt. PBMC #2163
ND PBMC
GB
Perf
CD57
0
26
0
74
0
3
0
97
95
4
91
8
97
3
89
11
C
% of CD8+ T-cell Subset
p < 0.05
p < 0.001
ns
TIL
Pt. PBMC
ND PBMC
GB
Perf

Figure 2-9: Accumulation of incompletely differentiated $CD8^+CD27^+CD28^+$ effector-memory (T_{EM}) lymphocytes co-expressing CD57 with high GB and low Perf expression in pleural effusions of metastatic breast cancer patients. Isolated lymphocytes were stained for CD4, CD8, CD27, CD28, CD57, GB, and Perf expression. The gated $CD8^+CD57^+$ subset was further analyzed separately for surface CD27 or CD28 expression, or intracellular GB or Perf expression. Shown in each FACS plot are the percentages out of the gated subsets as indicated in the figure. Results of two of five pleural effusion samples with similar results are shown.

Figure 2-9:

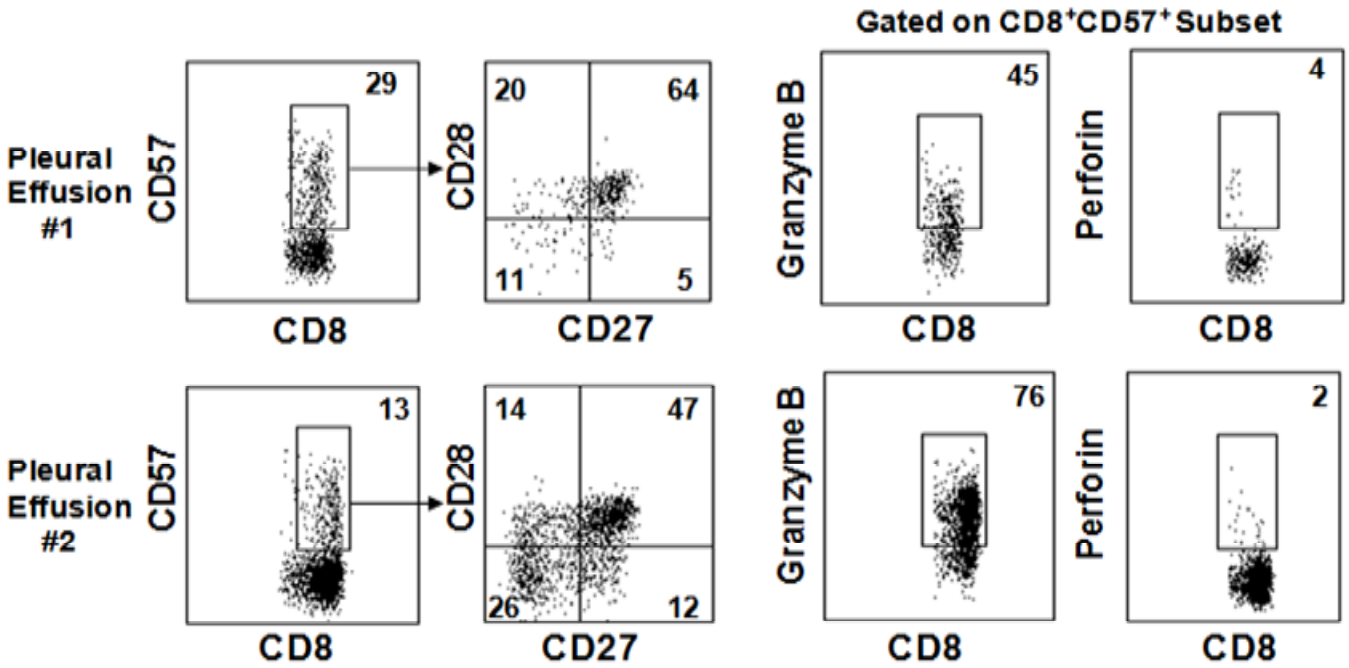
Gated on CD8+CD57+ Subset
Pleural Effusion #1
CD57
CD8
29
CD28
CD27
20
64
11
5
Granzyme B
45
Perforin
4
Pleural Effusion #2
13
14
47
26
12
76
2

$CD8^+CD27^+CD57^+$ TIL persist in culture with IL-2, can be induced to enter cell cycle, and are potent IFN-γ producers after TCR stimulation.

Several studies have demonstrated that $CD8^+CD57^+$ cells do not divide appreciably, or at all, in response to TCR stimulation, indicating that they are senescent cells (131, 167). We therefore asked whether the $CD8^+CD27^+CD57^+$ cells found in melanoma TIL were capable of further proliferation and cytokine production in the presence of IL-2. Culturing of isolated melanoma TIL in culture medium with high-dose (HD) IL-2 (3,000 IU/ml) is a standard method to expand TIL for adoptive cell therapy (96, 168). Routinely, we find that a two-week culture period of isolated TIL with IL-2 expands the $CD8^+$ T cells between 200- to 300- fold (data not shown). We stained 2-week IL-2-expanded TIL for CD8, CD27, CD57, and Perf. The percentage of the $CD27^+CD57^+$ subset increased from 4% to 20% of the gated $CD8^+$ subset (**Fig. 2-10A**). A small percentage of cells (~10%) in both $CD27^+CD57^+$ and $CD27^+CD57^-$ subsets expressed another marker for senescence and terminal differentiation, KLRG-1 (data not shown) (169-171). To further examine the proliferative capacity of these cells, we stained the cultured TIL with Ki67 at the end of the 2-week culture period and found that both $CD8^+CD27^+CD57^+$ and $CD8^+CD27^+CD57^-$ subsets contained a significant frequency of $Ki67^+$ cells (**Fig. 2-10B**).

Figure 2-10: $CD8^+CD27^+CD57^+$ subset in TIL can persist, proliferate, and expand *ex vivo* in high-dose IL-2 culture. TIL were isolated from the indicated patients' melanoma metastases and cultured in high-dose (HD) IL-2 (3,000 U/mL) as described in the Material and Methods. (**A**) Surface phenotype of the TIL after two weeks of HD IL-2 culture. By gating on the $CD8^+$ TIL, a population $CD27^+CD57^+$ subset increased in frequency as compared to the freshly-isolated TIL. Also, HD IL-2 did not appreciably induce down-modulation of CD27 on either the $CD27^+CD57^-$ or $CD27^+CD57^+$ subset. The percentages of the each indicated subsets were out of the total gated $CD8^+$ population. (**B**) Histograms of the intracellular Ki67 staining of the indicated $CD8^+$ subsets in TIL. Bulk TIL were stained with antibody against an intracellular proliferation marker, Ki67, as described in the Material and Methods. Both of the $CD27^+CD57^+$ and $CD27^+CD57^-$ subsets expressed high levels of Ki67 after high-dose IL-2 culture. The percentages indicated in B were determined by (the number of $Ki67^+$ cells as compared to the isotype control in each gated subsets)/(the total number of cells in each subset) X 100.

Reprinted with permission from: Wu R, Liu S, Chacon JA, Wu S, Li Y, Sukhumachandra P, Murray JL, Molldrem JJ, Hwu P, Pircher H, Lizée G, Radvanyi L. 2012. *Clin. Can. Res.* 18(9): 2465-77. doi:10.1158/1078-0432.CCR-11-2034

Figure 2-10:

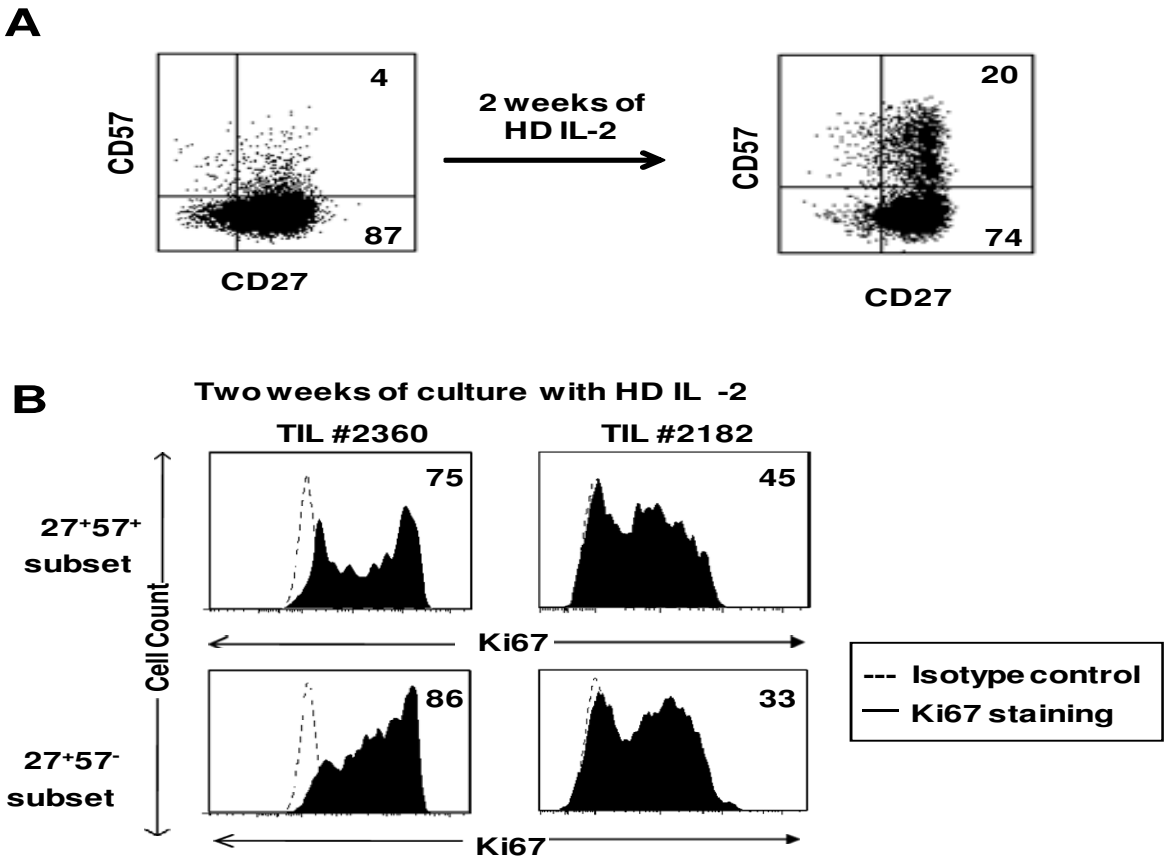
A
4
87
CD57
CD27
2 weeks of
HD IL-2
20
74
CD57
CD27
B
Two weeks of culture with HD IL -2
TIL #2360
TIL #2182
27+57+
subset
75
45
Ki67
Cell Count
27+57-
subset
86
33
Ki67
--- Isotype control
— Ki67 staining

We then asked whether the $CD8^+CD27^+CD57^+$ TIL could enter cell cycle and produce cytokines after TCR stimulation. Two-week IL-2-cultured TIL were isolated, washed and then re-cultured with low-dose (LD) IL-2 (200 IU/ml) alone (to prevent apoptosis due to cytokine withdrawal), or re-stimulated with LD IL-2 plus plate-bound anti-CD3 or anti-CD3 plus anti-CD28 mAb for 7 days followed by Ki67 staining (all $CD8^+CD27^+CD57^+$ T cells were $CD28^+$; see earlier results in **Fig. 2-5** and **2-7**). The gated $CD8^+CD27^+CD57^+$ cells re-cultured with LD IL-2 alone were negative for Ki67 staining. However, a significant proportion of these cells were $Ki67^+$ following stimulation with anti-CD3 or anti-CD3 and anti-CD28 (**Fig. 2-11A**).

The results above indicate that the $CD8^+CD27^+CD57^+$ T-cells in isolated melanoma TIL have proliferative capacity, but it could also be that $CD8^+CD27^+CD57^-$ T cells proliferated and induced CD57 expression when cultured with IL-2. Thus, to more directly examine the proliferative capacity of $CD8^+CD27^+CD57^+$ TIL, we sorted these cells and examined their response to TCR stimulation and IL-2. The $CD8^+CD27^+CD57^+$ and $CD8^+CD27^+CD57^-$ TIL subsets from four different melanoma patients were each stimulated with anti-CD3 plus anti-CD28 mAbs, and labeled with [^{3}H]-thymidine after 3 days. Both sorted subsets showed a marked induction of [^{3}H]-thymidine incorporation after TCR stimulation, although the sorted $CD8^+CD27^+CD57^-$ subset demonstrated a higher proliferative capacity than the sorted $CD8^+CD27^+CD57^+$ subset in response to CD3 and CD28 stimulation, in a majority of patients (**Fig. 2-11B**). Analysis of the supernatants from a parallel set of cultures of activated cells found that both the sorted $CD8^+CD27^+CD57^+$ and $CD8^+CD27^+CD57^-$ TIL produced Th1/Th2 cytokines (IFN-γ, IL-5 and IL-13) upon TCR stimulation, with the $CD27^+CD57^+$ subset producing significantly more IFN-γ compared to

the $CD27^{+}CD57^{-}$ subset in TIL in 3 out of the 4 patients studied (**Fig. 2-11C**). Thus, the $CD8^{+}CD27^{+}CD57^{+}$ T lymphocytes found in melanoma TIL were capable of continued cell division and were potent IFN-γ producers.

Figure 2-11: The $CD8^+CD27^+CD57^+$ subset in melanoma TIL was not anergic and could be induced to proliferate and produce a high level of IFN-γ and other Th2 cytokines (IL-5, IL-13) after TCR stimulation with CD28 co-stimulation. **(A)** Bulk TIL were rested overnight with low-dose IL-2 and stimulated the next day with a combination of plate-bound anti-CD3 or anti-CD3 with anti-CD28 antibodies for 7 days. Proliferation was determined by the percentage of $Ki67^+$ cells as compared to the isotype control out of the total gated $CD8^+CD27^+CD57^+$ subset. (**B**) $CD8^+CD27^+CD57^+$ and $CD8^+CD27^+CD57^-$ TIL subsets from four different patients were purified by sorting and an equal number of both sorted subsets in triplicate were stimulated with anti-CD3 and anti-CD28 antibodies. [^{3}H]-thymidine was added for 18 h on day 4 of the stimulation before harvesting and counting. The negative control was sorted TIL treated with low-dose (LD) of IL-2 (200 U/mL) only, which induced very low level of proliferation. Results shown were means ± standard error on the means. Note for patient #2184, no error bar was shown for the assay performed on sorted $CD8^+CD27^+CD57^+$ TIL due to insufficient number of cells for triplicate wells after sorting. Relevant patient information for TIL #2544 and #2545 are available online. (**C**) The tissue culture supernatants from 5 x 10^4 cells in each subset in triplicate wells after stimulation were collected on day 4 of the stimulation and cytokine levels were determined using MSD® human Th1/Th2 cytokine multiplex assay as described in Material and Methods. Results shown were means ± standard errors on the means on experiments done on two different patients (#2182 and #2206).

Reprinted with permission from: Wu R, Liu S, Chacon JA, Wu S, Li Y, Sukhumachandra P, Murray JL, Molldrem JJ, Hwu P, Pircher H, Lizée G, Radvanyi L. 2012. *Clin. Can. Res.* 18(9): 2465-77. doi:10.1158/1078-0432.CCR-11-2034

Figure 2-11:

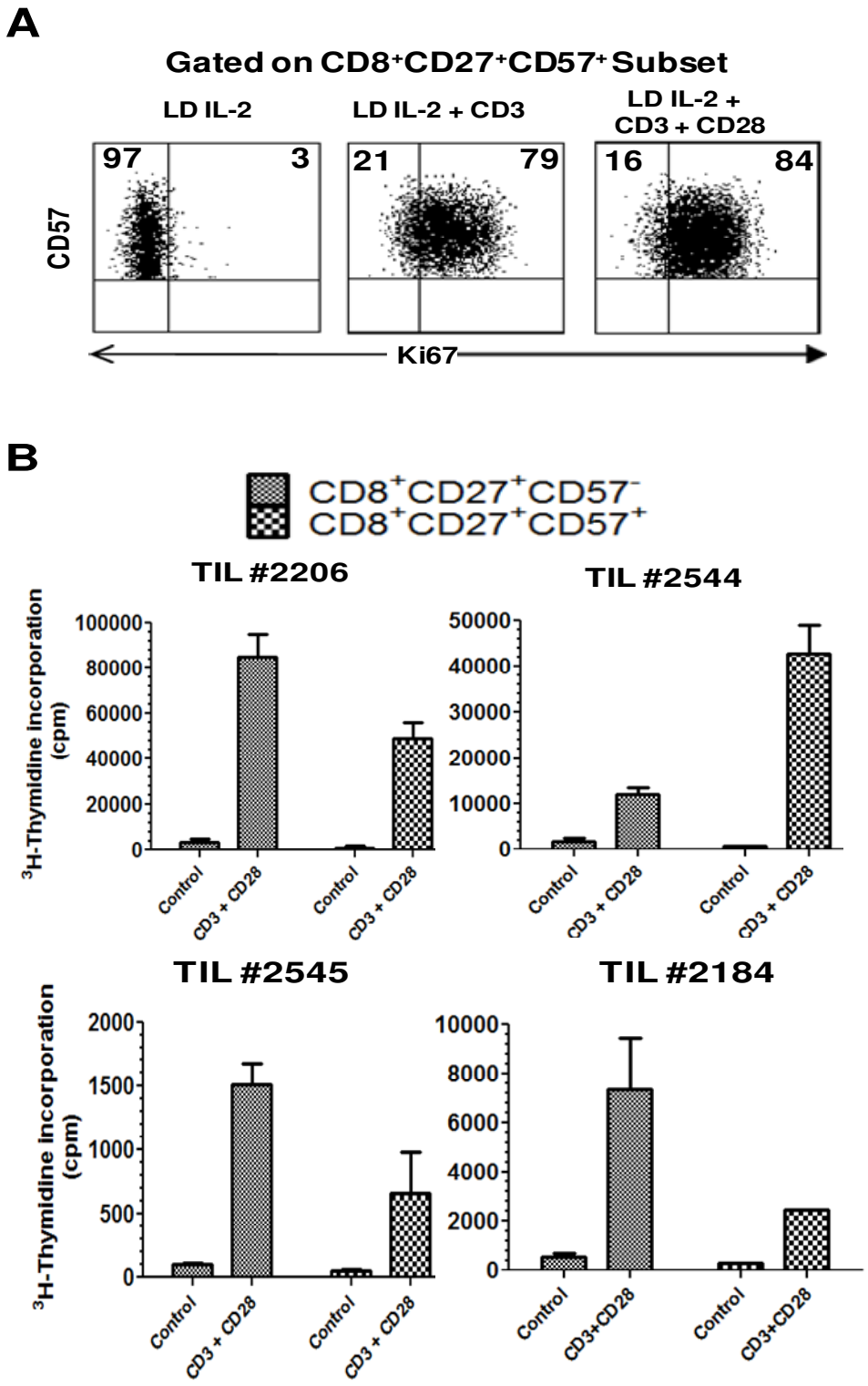
A
Gated on CD8+CD27+CD57+ Subset
LD IL-2
LD IL-2 + CD3
LD IL-2 + CD3 + CD28
97
3
21
79
16
84
CD57
Ki67
B
CD8+CD27+CD57-
CD8+CD27+CD57+
TIL #2206
TIL #2544
TIL #2545
TIL #2184
3H-Thymidine incorporation (cpm)
Control
CD3 + CD28
CD3+CD28

Figure 2-11. con't.

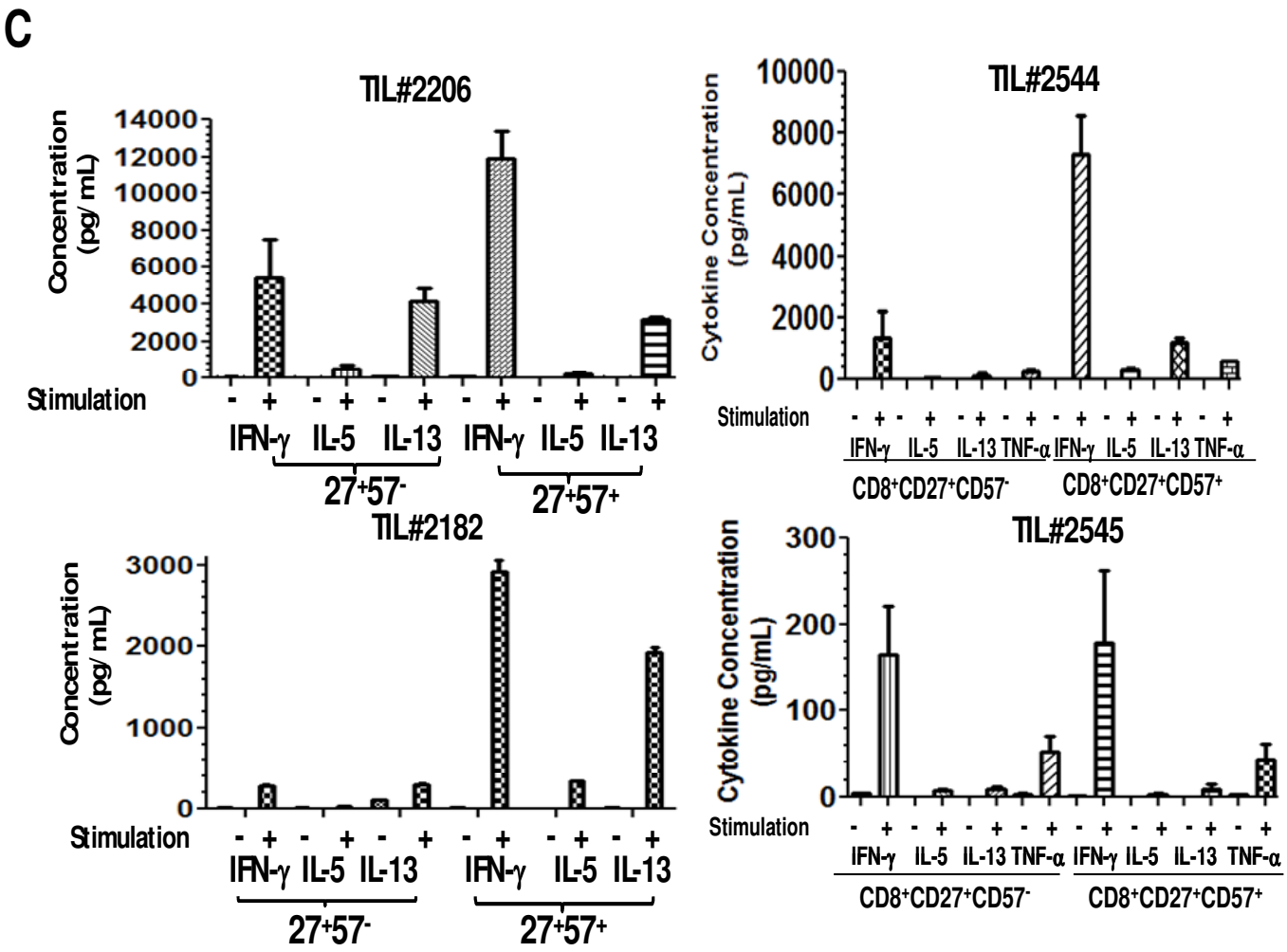

$CD8^+CD27^+CD57^+$ TIL are more oligoclonal than $CD8^+CD27^+CD57^-$ TIL

$CD8^+CD57^+$ T cells in some pathologic situations have been shown to have a more restricted Vβ TCR diversity (154, 172). However, since most of these T cells in the periphery do not co-express CD27 or CD28, we asked what the relative Vβ TCR diversity was in tumor-associated $CD8^+CD27^+CD57^+$ TIL versus the dominant subset of $CD8^+CD27^+CD57^-$ TIL. We performed Vβ TCR spectratyping after sorting these T-cell subsets obtained from two samples of melanoma TIL and a breast cancer pleural effusion sample. The sorted $CD8^+CD27^+CD57^+$ TIL from representative melanoma and breast cancer pleural effusion samples (minimum of 1×10^6 sorted cells each analyzed) had a significantly less Vβ TCR diversity and oligoclonality in some Vβ families than the $CD8^+CD27^+CD57^-$ TIL (**Fig. 2-12B and C**). In addition, the Vβ peaks did not overlap between these two sorted subsets. Thus, the $CD8^+CD27^+CD57^+$ TIL of melanoma and breast cancer seem to be an oligoclonal and a subset that is distinct from the $CD8^+CD27^+CD57^-$ subset, the other major population in TIL

Figure 2-12: (**A**) a schematic representation of a TCR Vβ chain spectratype analysis, illustrating typical spectratype profiles of polyclonal, oligoclonal, and monoclonal T cell populations. (**B**) Vβ TCR spectratype analysis on the sorted T-cell subsets from a representative sample of melanoma TIL, or (**C**) a breast cancer pleural effusion sample. mRNAs were isolated from at least 1 x 10^6 cells from each sorted $CD8^+$ TIL subsets as indicated in the figure. After reverse transcription of the RNA to cDNA, TCR Vβ mRNA expression profiling and size spectratyping of the 23 antigen-binding Vβ CDR3 regions were performed as CDR3 spectratypes were assessed on the Bayer OpenGene® System. Sorted $CD8^+CD27^+CD57^+$ TIL subset from melanoma or breast cancer pleural effusions displays reduced Vβ repertoire and less TCR diversity within most Vβ receptor families as compared to the $CD8^+CD27^+CD57^-$ TIL subset. Oligoclonal expansion in some TCR Vβ families is also observed in the $CD8^+CD27^+CD57^+$ subset.

Figure 2-12:

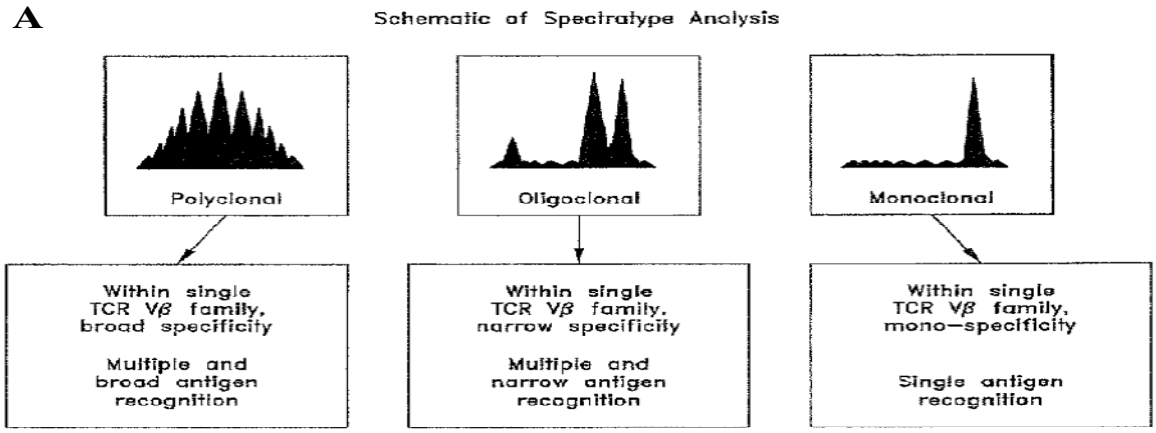
A
Schematic of Spectratype Analysis
Polyclonal
Oligoclonal
Monoclonal
Within single TCR Vβ family, broad specificity
Multiple and broad antigen recognition
Within single TCR Vβ family, narrow specificity
Multiple and narrow antigen recognition
Within single TCR Vβ family, mono-specificity
Single antigen recognition

B

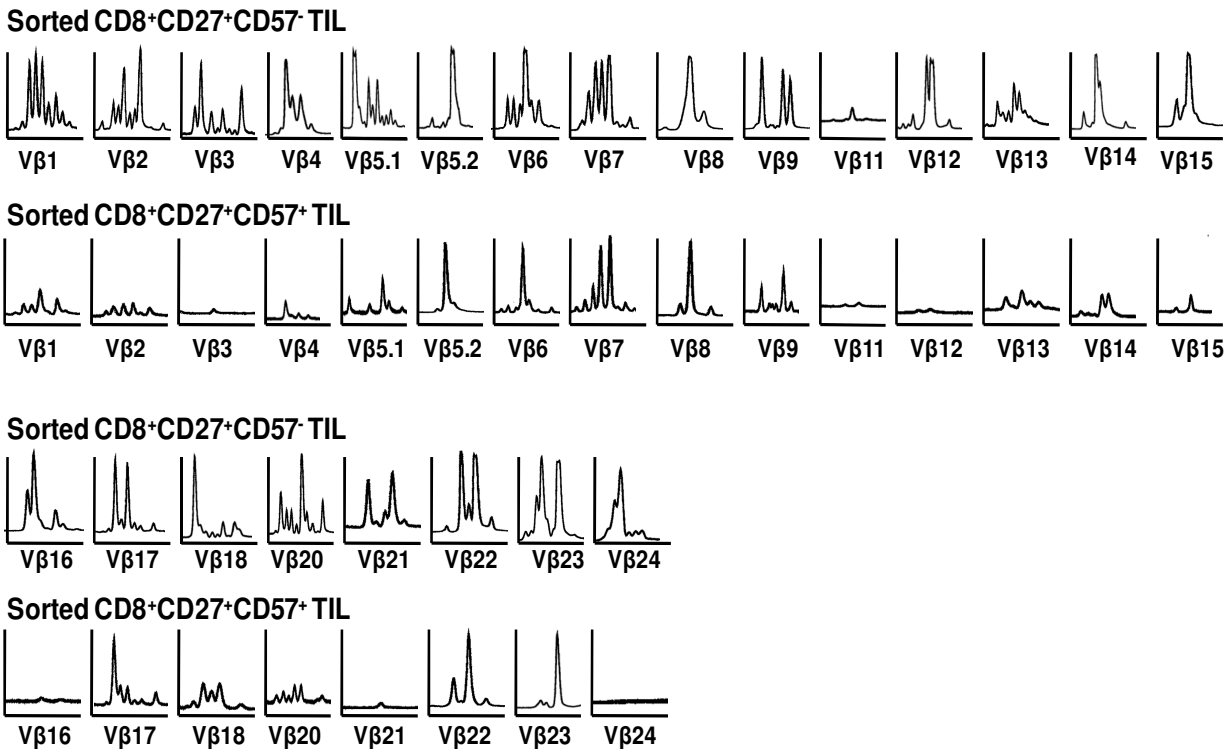
Sorted CD8+CD27+CD57- TIL
Vβ1 Vβ2 Vβ3 Vβ4 Vβ5.1 Vβ5.2 Vβ6 Vβ7 Vβ8 Vβ9 Vβ11 Vβ12 Vβ13 Vβ14 Vβ15
Sorted CD8+CD27+CD57+ TIL
Vβ1 Vβ2 Vβ3 Vβ4 Vβ5.1 Vβ5.2 Vβ6 Vβ7 Vβ8 Vβ9 Vβ11 Vβ12 Vβ13 Vβ14 Vβ15
Sorted CD8+CD27+CD57- TIL
Vβ16 Vβ17 Vβ18 Vβ20 Vβ21 Vβ22 Vβ23 Vβ24
Sorted CD8+CD27+CD57+ TIL
Vβ16 Vβ17 Vβ18 Vβ20 Vβ21 Vβ22 Vβ23 Vβ24

Figure 2-12 con't.

C

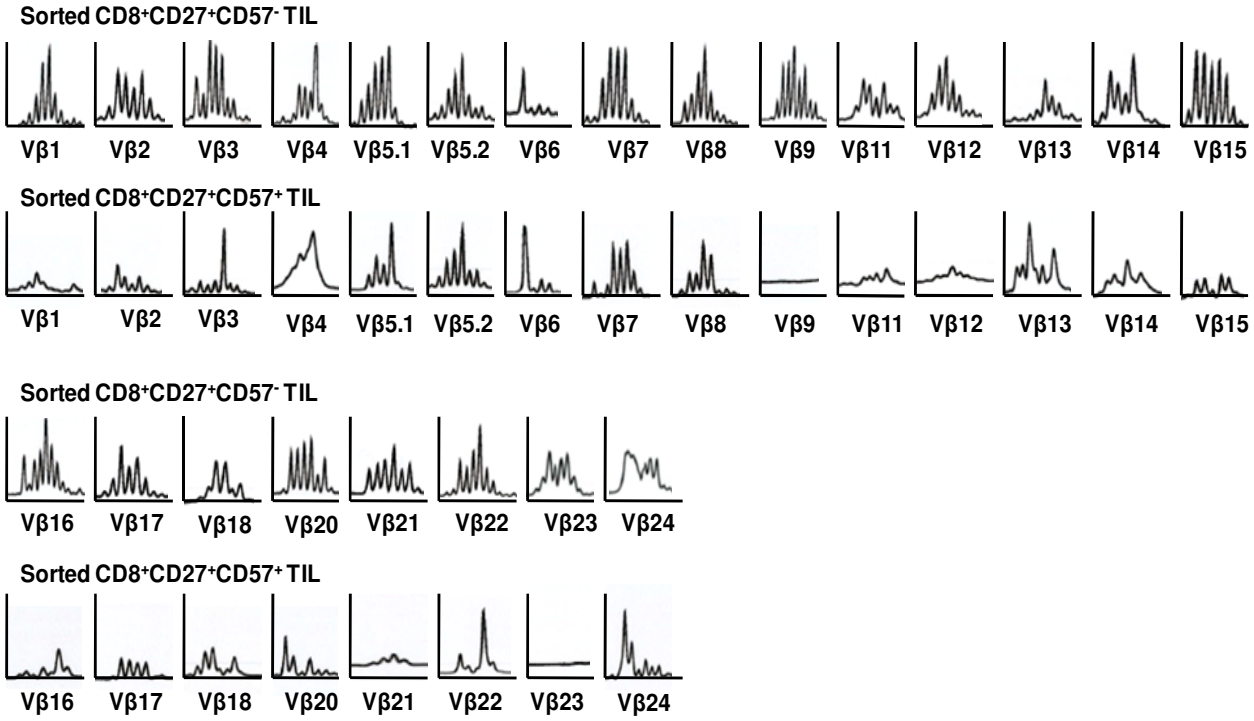

TCR stimulation drives $CD8^+CD27^+CD57^+$ TIL to differentiate into $CD8^+CD27^-CD57^+Perf^{high}$ cells that are inhibited by TGF-β

We asked whether $CD8^+CD27^+CD57^+$ TIL were capable of further differentiation towards $CD8^+CD27^-CD57^+$ CTL expressing increased Perf. We first took bulk TIL in vitro and activated them in LD IL-2 medium with anti-CD3 plus anti-CD28 and tracked the fate of the cells after 7 days by staining and analyzing for changes in CD27, CD57 and Perf expression in the $CD8^+$ subset. This process induced further cell division associated with a decrease in the frequency of the $CD27^+CD57^+$ and $CD27^+CD57^-$ $CD8^+$ cells and an increase in the percentage of the $CD27^-CD57^+$ and $CD27^-CD57^-$ populations (**Fig. 2-13A**). Both the percentage and level (MFI) of Perf expression was also increased in each cell subset (**Fig. 2-13B**).

Figure 2-13: $CD8^+CD57^+$ T cells in TIL can further differentiate into $CD27^-CD57^+$, $Perf^{Hi}$ effector cells *ex vivo.* Freshly isolated TIL from melanoma metastases were cultured in 3,000 U/mL of IL-2. After two weeks of expansion, bulk TILs were maintained in low dose IL-2 (200 U/mL) or re-stimulated with CD3 plus CD28 for 7 days as described in the Material and Methods. (**A**) Surface expression of CD27 and CD57 on gated $CD8^+$ TIL was determined by FACS staining. Low-dose (LD) IL-2 culture did not appreciably down-modulate CD27, whereas CD3 + CD28 stimulation down-modulated CD27 on either the $CD27^+CD57^+$ subset (6% $CD27^-$ compared to 2% with IL-2 alone), or the $CD27^+CD57^-$ subset (33% $CD27^-$ compared to 7% with IL-2 alone). (**B**) Histograms of the intracellular Perf staining versus isotype control (shown in gray). Bulk $CD8^+$ TIL from both stimulation conditions were stained for Perf expression. Both IL-2 culture alone and CD3 plus CD28 stimulation increased Perf expression on both $CD27^+CD57^-$ and $CD27^+CD57^+$ subsets. Perf expression, however, was increased to a greater extent by CD3 plus CD28 re-stimulation. The newly emerging $CD27^-CD57^+$ and $CD27^-CD57^-$ subsets from CD3 + CD28 stimulation also acquired high level of Perf expression/cell (MFI). (**C**) Corrected MFI for Perf was calculated by subtracting the MFI of the isotype control from that of the perforin staining. The values are shown by gating on the indicated subsets. Results from two different TIL isolates are shown.

Reprinted with permission from: Wu R, Liu S, Chacon JA, Wu S, Li Y, Sukhumachandra P, Murray JL, Molldrem JJ, Hwu P, Pircher H, Lizée G, Radvanyi L. 2012. *Clin. Can. Res.* 18(9): 2465-77. doi:10.1158/1078-0432.CCR-11-2034

Figure 2-13:

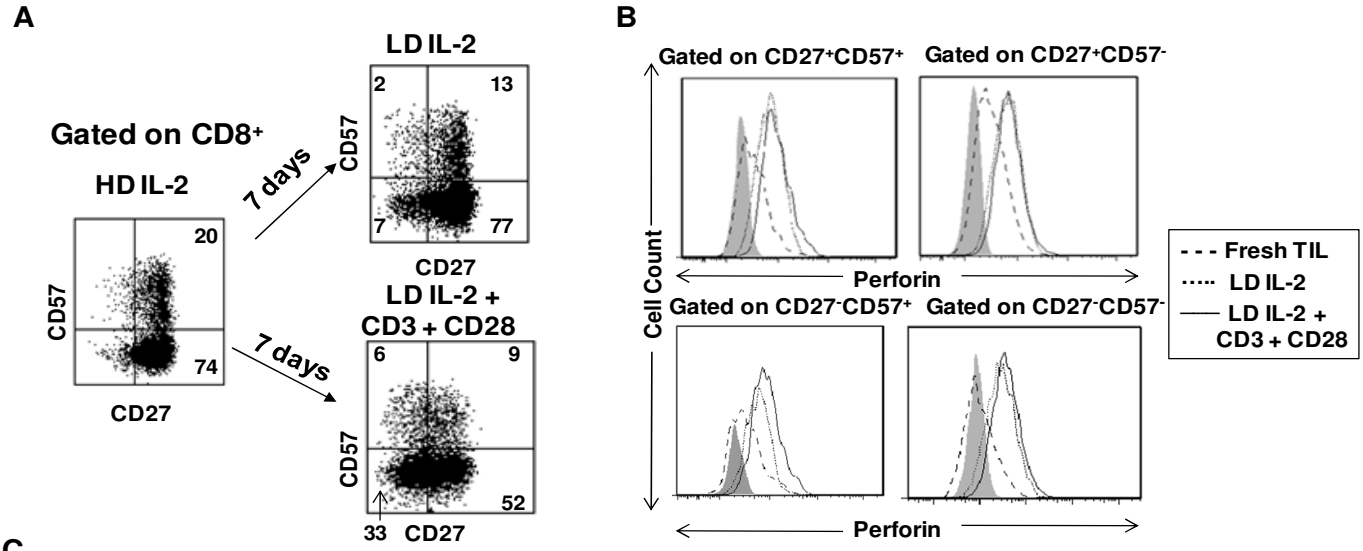

C

TIL #2276

MFI / Subset	Fresh	LD IL-2	LD IL-2 + CD3 + CD28
$CD27^+CD57^+$	133	403	599
$CD27^+CD57^-$	144	384	425
$CD27^-CD57^+$	133	345	551
$CD27^-CD57^-$	113	370	465

TIL #2261

MFI / Subset	Fresh	LD IL-2	LD IL-2 + CD3 + CD28
$CD27^+CD57^+$	N.D.	682	3428
$CD27^+CD57^-$	N.D.	739	2610
$CD27^-CD57^+$	N.D.	590	2006
$CD27^-CD57^-$	N.D.	805	1605

To better delineate how TCR stimulation specifically affects the predominant $CD8^+CD27^+CD57^+$ and $CD8^+CD27^+CD57^-$ subsets in TIL, we sorted these subsets from melanoma TIL and re-cultured the sorted cells with LD IL-2 or IL-2 and anti-CD3 plus anti-CD28. The post-sort purity of the two populations was verified (**Fig. 2-14**). The sorted cells were also verified to have CD3 and CD28 expression. The 7-day TCR stimulation induced a large decrease in the percentage of the sorted $CD8^+CD27^+CD57^+$ cells from 72% to 37% (**Fig. 2-15A**) or 66% to 6% (**Fig. 2-15B**), with a concomitant increase in the percentage of $CD8^+CD27^-CD57^+$ cells from 6% to 49% (**Fig. 2-15A**, **bottom panel**), or $CD8^+CD27^-CD57^-$ cells from 4% to 54% in other patient (**Fig. 2-15B**, **bottom panel**). On the other hand, the sorted $CD8^+CD27^+CD57^-$ cells differentiated into a $CD8^+CD27^-CD57^-$ population with TCR stimulation (increase from 6% to 34% and 13% to 73%, respectively, in two different patients), although a minor subpopulation converted into $CD8^+CD27^+CD57^+$ cells in LD IL-2 culture alone (**Fig. 2-15A and B, top panel**).

Figure 2-14: Flow cytometry plots of the purity of the TIL subsets after cell sorting. TIL lines from patients were sorted by fluorescence-activated cell sorting using Influx® cell sorter (BD Biosciences) as described in Material and Methods. The purity of each sorted $CD8^+$ TIL subsets were determined by acquiring the samples through the flow cytometer immediately after sorting. . A minimum of 30,000 gated light scatter events per sample were acquired on the flow cytometer. Shown here are sorted TIL subsets from two representative patients whose cells were used in experiment described in **Fig. 2-15**.

Reprinted with permission from: Wu R, Liu S, Chacon JA, Wu S, Li Y, Sukhumachandra P, Murray JL, Molldrem JJ, Hwu P, Pircher H, Lizée G, Radvanyi L. 2012. *Clin. Can. Res.* 18(9): 2465-77. doi:10.1158/1078-0432.CCR-11-2034

Figure 2-14:

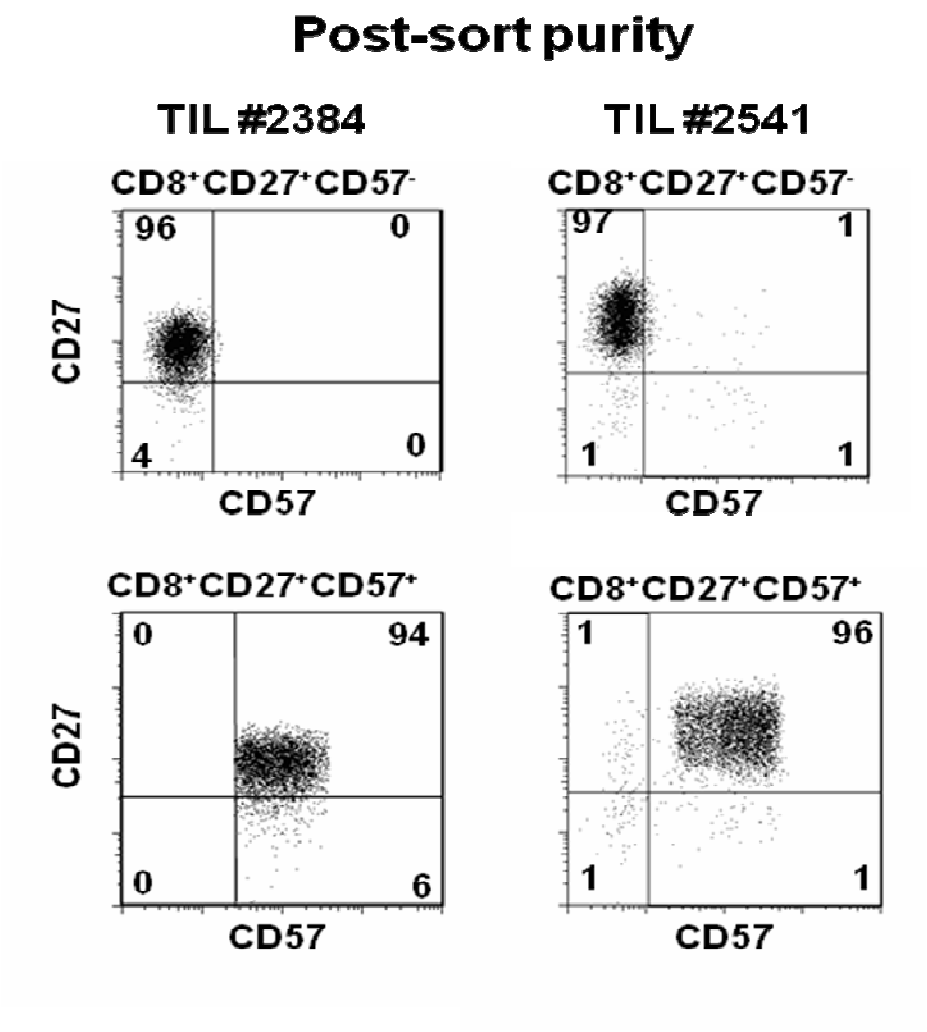
Post-sort purity
TIL #2384
TIL #2541
CD8+CD27+CD57-
96
0
4
0
CD27
CD57
CD8+CD27+CD57-
97
1
1
1
CD57
CD8+CD27+CD57+
0
94
0
6
CD27
CD57
CD8+CD27+CD57+
1
96
1
1
CD57

Figure 2-15: Sorted $CD8^+CD27^+CD57^+$ T cells in TIL could further differentiate into $CD27^-$ $CD57^+$ CTL upon TCR stimulation, which was inhibited by the addition of TGF-β1. TIL were sorted into $CD8^+CD27^+CD57^+$ and $CD8^+CD27^+CD57^-$ subsets as before. Post-sort purity of the sorted populations is shown in **Fig. 2-14**. (**A**) The sorted TIL subsets (from patient #2384) were stimulated with anti-CD3 and anti-CD28 antibodies for 7 days. The cells were then re-stained for CD8, CD27, and CD57 expression and analyzed by flow cytometry. To some cultures of sorted, re-stimulated cells, 1 ng/mL of TGF-β1 was added on day 0 with CD3 and CD28. Cells were harvested similarly on day 7 of the stimulation and stained for CD8, CD27, and CD57. (**B**) Similar experiment performed on TIL from a different patient (#2541).

Reprinted with permission from: Wu R, Liu S, Chacon JA, Wu S, Li Y, Sukhumachandra P, Murray JL, Molldrem JJ, Hwu P, Pircher H, Lizée G, Radvanyi L. 2012. *Clin. Can. Res.* 18(9): 2465-77. doi:10.1158/1078-0432.CCR-11-2034

Figure 2-15:

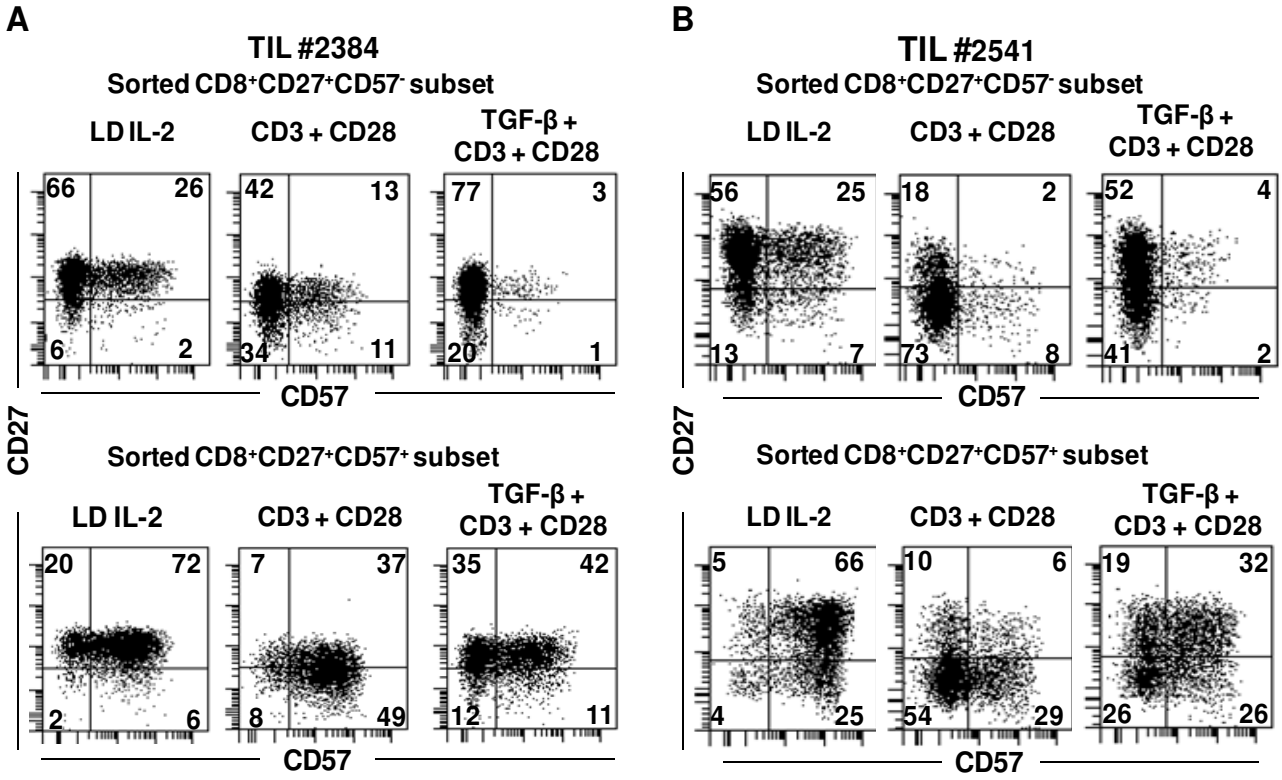
A
TIL #2384
Sorted CD8+CD27+CD57- subset
LD IL-2
CD3 + CD28
TGF-β + CD3 + CD28
66
26
6
2
42
13
34
11
77
3
20
1
CD27
CD57
Sorted CD8+CD27+CD57+ subset
LD IL-2
CD3 + CD28
TGF-β + CD3 + CD28
20
72
2
6
7
37
8
49
35
42
12
11
CD57
B
TIL #2541
Sorted CD8+CD27+CD57- subset
LD IL-2
CD3 + CD28
TGF-β + CD3 + CD28
56
25
13
7
18
2
73
8
52
4
41
2
CD27
CD57
Sorted CD8+CD27+CD57+ subset
LD IL-2
CD3 + CD28
TGF-β + CD3 + CD28
5
66
4
25
10
6
54
29
19
32
26
26
CD57

We also tracked changes in GB and Perf expression and found that both proteins increased in the sorted $CD8^+CD27^+CD57^+$ and $CD8^+CD27^+CD57^-$ TIL populations following TCR stimulation for 7 days, although the extent of the increase in Perf expression was greater in the sorted $CD8^+CD27^+CD57^+$ subset in three different patients (**Fig. 2-16A**). The increase in Perf expression in both sorted subsets led to an enhanced cytotoxic activity, in a redirected lysis assay using anti-CD3 antibody coated P815 target cells (**Fig. 2-16B**). We chose the redirected lysis assay to assess the cytotoxic activity between the TIL subsets to avoid erroneous interpretation of any differences due to differences in the percentages of tumor antigen-specific T lymphocytes in each subset. The sorted and TCR-activated $CD8^+CD27^+CD57^+$ subset also exhibited higher or similar levels of cytotoxic activity against P815 target cells as compared to sorted $CD8^+CD27^+CD57^-$ subset in TIL from two different melanoma patients (**Fig. 2-16B**). Thus, TCR stimulation induces the phenotypic and functional maturation of the $CD8^+$ $CD27^+CD57^-$ and $CD27^+CD57^+$ subsets into more differentiated $CD27^-CD57^-$ and $CD27^-CD57^+$ T cell populations with high Perf expression and cytotoxic activity.

Figure 2-16: CD3 and CD28 stimulation of melanoma TIL subsets induced Perf and GB expression and increased cytotoxic killing function of the sorted $CD8^+$ TIL subsets, which was abrogated in the presence of TGF-β1. Intracellular flow cytometry staining for GB and Perf was performed as described in the Material and Methods. **(A)** Graphs show the percentage of GB^+ and $Perf^+$ cells in the sorted $CD8^+CD27^+CD57^+$ and $CD8^+CD27^+CD57^-$ subsets, from three different patients, before and after CD3 and CD28 stimulation for 7 days. TGF-β1 (1 ng/ml) was added to some cultures as indicated and the cells incubated and then stained in the same way. *ND: Not determined (due to insufficient cell number). **(B)** A caspase-3 cleavage assay was used to assess the CTL killing activity. Sorted $CD8^+$ TIL subsets, cultured with LD IL-2 alone, or after TCR re-stimulation with anti-CD3 and anti-CD28, with or without added TGF-β1 (1 ng/ml) for 7 days, were co-incubated for 3 h at the indicated Effector: Target (E:T) ratios with P815 (murine mastocytoma) target cells, which were previously pulsed with 200 ug/mL of anti-CD3 antibody, in a redirected lysis assay. Target cells were distinguished from effector T cells by labeling with a fixable, far-red fluorescent tracer, CellTrace® Far Red DDAO-Succinimidyl Ester (DDAO-SE) at the beginning of the assay. Non-pulsed P815 cells were used as negative controls. Results were expressed as percent cleaved caspase-3 positive target cells out of the total target cell population. Results shown were from experiments done on sorted TIL subsets from two different patients as indicated.

Reprinted with permission from: Wu R, Liu S, Chacon JA, Wu S, Li Y, Sukhumachandra P, Murray JL, Molldrem JJ, Hwu P, Pircher H, Lizée G, Radvanyi L. 2012. *Clin. Can. Res.* 18(9): 2465-77. doi:10.1158/1078-0432.CCR-11-2034

Figure 2-16:

A

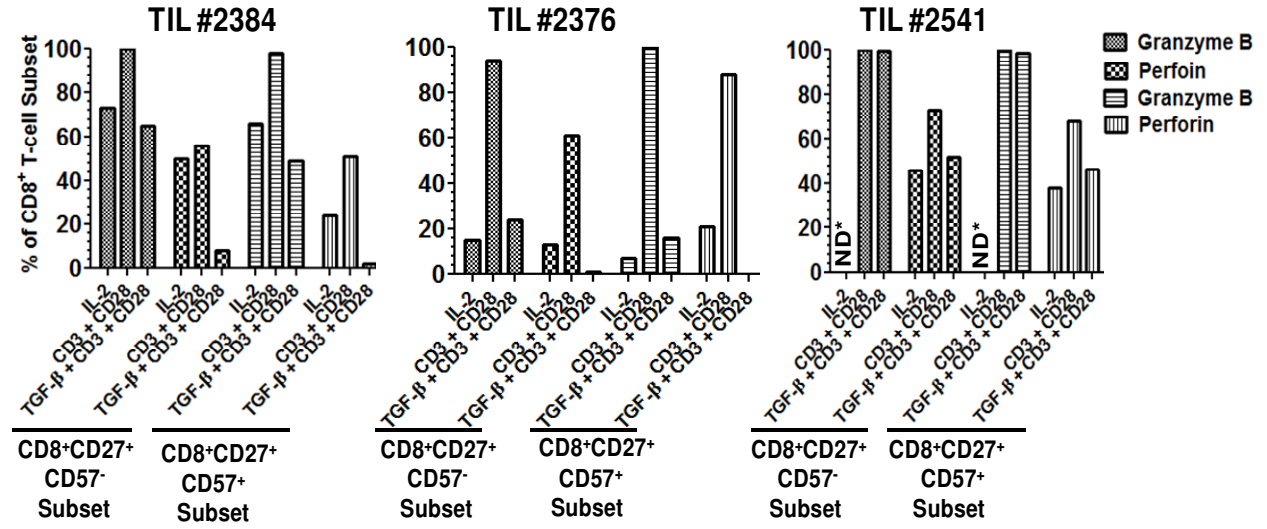

B

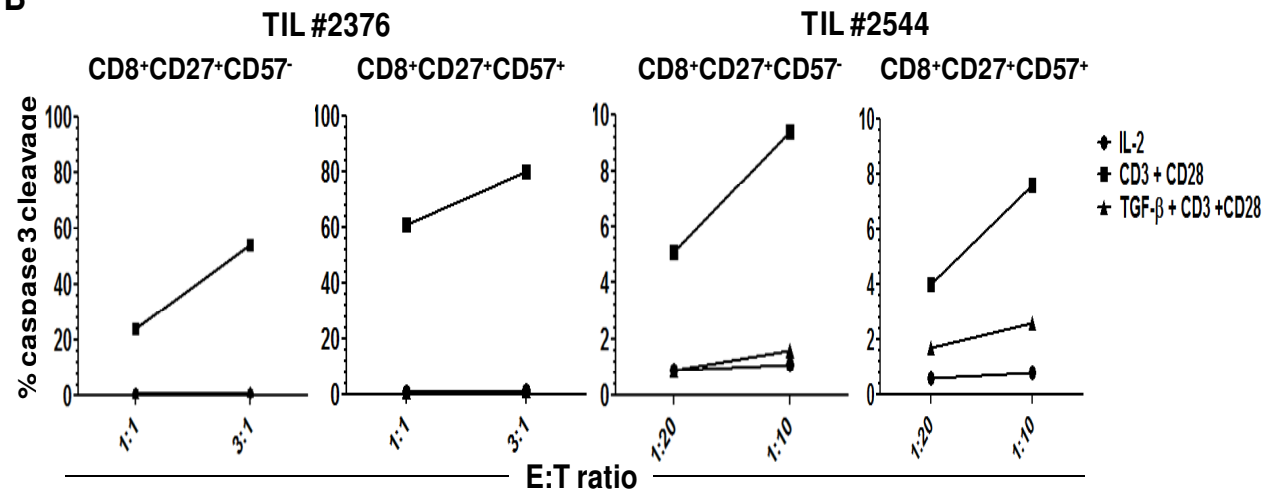

TGF-β1 is an immunosuppressive factor produced by melanoma cells and is found in about 50% of metastatic melanomas (159-161). It has also been shown to inhibit CTL differentiation in human peripheral blood $CD8^+$ T cells and inhibit the induction of Perf expression (158, 173-175). We reasoned that TGF-β may also affect the further differentiation of the $CD8^+CD27^+CD57^+$ cells found in melanoma TIL. We first tested the effect of adding TGF-β to bulk TIL stimulated with anti-CD3 and anti-CD28, and found that the differentiation of $CD8^+CD27^+$ T cells subsets were arrested, with attenuated perforin expression (**Fig. 2-17**). We then sorted $CD8^+CD27^+CD57^+$ and $CD8^+CD27^+CD57^-$ melanoma TIL and treated them with TGF-β during TCR stimulation. In sorted TIL from two different melanoma patients, addition of TGF-β increased the frequency of the $CD8^+$ $CD27^+CD57^-$ memory-effector TIL (**Fig. 2-15A** and **B**, **top panels**) as well as maintained the $CD27^+CD57^+$ "hybrid" phenotype (**Fig. 2-15A** and **B**, **bottom panels**), which were both associated with low GB expression and more attenuated Perf expression (**Fig. 2-16A**). TGF-β prevented the loss of CD28 expression (data not shown). TGF-β1 also strongly diminished the cytotoxic activity of $CD8^+$ $CD27^+CD57^+$ and $CD27^+CD57^-$ TIL subsets after stimulation with anti-CD3 and anti-CD28 for 7 days, as seen in two different melanoma patients (**Fig. 2-16B**). Thus, the differentiation of the $CD27^+CD57^+$ and $CD27^+CD57^-$ $CD8^+$ TIL into mature $CD27^-$ $GB^{Hi}Perf^{Hi}$ CTL *in vitro* was blocked by TGF-β1, which resembled the phenotype of the $Perf^{Lo}$, $CD8^+$ TIL freshly isolated from melanoma tumors.

Figure 2-17: $CD8^+CD27^+CD57^-$ and $CD8^+CD27^+CD57^+$ subsets in bulk TIL could further differentiate into $CD27^-CD57^-$ and $CD27^-CD57^+$ subsets, respectively, and up-regulate perforin expression upon TCR stimulation, which were both inhibited by the addition of TGF-β1. Bulk TIL #2276 were re-stimulated with anti-CD3 and anti-CD28 antibodies for 7 days. The cells were then re-stained for CD8, CD27, and CD57 expressions and intracellular perforin expression, and were analyzed by flow cytometry. As a control, bulk TILs were cultured in LD IL-2 (200 U/mL) only without TCR stimulation. To some cultures of re-stimulated cells, 1 ng/mL of TGF-β1 was added on day 0 with CD3 and CD28. Cells were harvested similarly on day 7 of the stimulation and stained for CD8, CD27, CD57, and perforin.

Reprinted with permission from: Wu R, Liu S, Chacon JA, Wu S, Li Y, Sukhumachandra P, Murray JL, Molldrem JJ, Hwu P, Pircher H, Lizée G, Radvanyi L. 2012. *Clin. Can. Res.* 18(9): 2465-77. doi:10.1158/1078-0432.CCR-11-2034

Figure 2-17

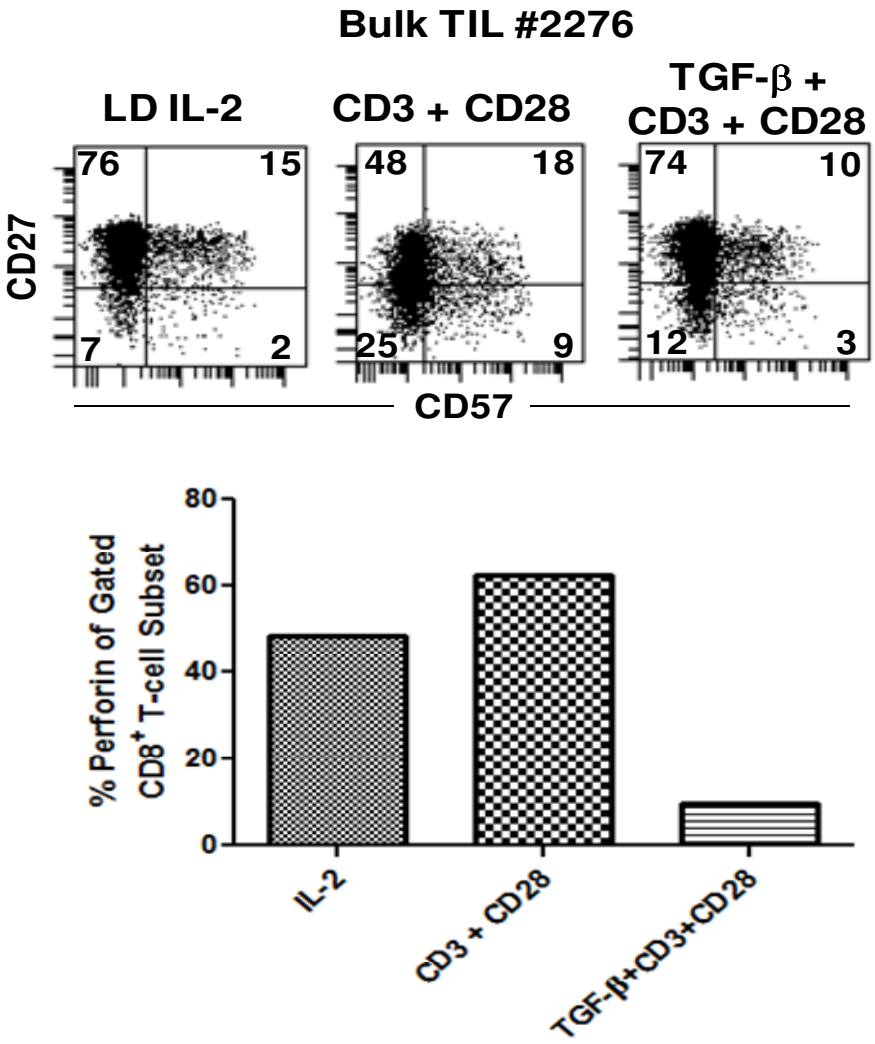
Bulk TIL #2276
LD IL-2
CD3 + CD28
TGF-β + CD3 + CD28
76
15
7
2
48
18
25
9
74
10
12
3
CD27
CD57
% Perforin of Gated CD8+ T-cell Subset
80
60
40
20
0
IL-2
CD3 + CD28
TGF-β+CD3+CD28

Discussion

We found that the majority of $CD8^+$ TIL in metastatic melanomas in a large number of patients had a $CD27^+CD28^+GB^+Perf^{-/Lo}$ phenotype, reminiscent of early T_{EM} cells (123, 144, 157). Importantly, in this study, most of the tumors analyzed were from non-LN visceral metastases. We only found a very few highly-differentiated $CD8^+$ TIL ($CD27^-CD28^-$) with high Perf and GB co-expressions. Many of the high CD27-expressing $CD8^+$ TIL also co-expressed CD57 (HNK-1), a marker previously proposed to mark highly differentiated end-stage CTL with high Perf and GB levels and potent cytolytic activity (142, 143, 157, 167). We also found a similar subset of $CD8^+$ T-cells having this unusual early T_{EM} phenotype co-expressing CD57 in pleural effusions of metastatic breast cancer patients. Some of these $CD8^+CD27^+CD28^+CD57^+$ melanoma TIL were specific for tumor antigens, as demonstrated by co-staining with MART-1 and gp100 peptide tetramers, suggesting that they were not non-tumor antigen specific, bystander $CD8^+$ T cells. However, many of the other $CD8^+CD27^+CD28^+CD57^+$ TIL may also have been tumor-specific, recognizing other undefined tumor antigens; this will need to be addressed in future studies. The existence of this subset in metastatic cancer patients bears resemblance to a population of $CD8^+CD27^+CD28^+CD57^+$ T cells found to accumulate in the peripheral blood of patients unable to control HIV, EBV, or CMV infections (141, 145, 146). The circulating gp100 $tetramer^+$ $CD8^+$ T cells containing a $CD27^+CD57^+$ subset has also been previously described in the peripheral blood of early stage melanoma patients receiving gp100 peptide vaccination (176). Although it is important to further explore the relationship between tumor stage(s), the state of $CD8^+$ TIL's differentiation, and the appearance of this $CD8^+CD27^+CD28^+CD57^+$, our study was hampered by the lack of access to early-stage melanoma tissue samples. We

did not find detectable level of Foxp3 expression in the $CD8^+CD27^+CD57^+$ TIL subset (data not shown), indicating that these were not "regulatory" $CD8^+$ T cells with immunosuppressive activities. Furthermore, Anichini, *et al*. reported that a subpopulation of $CD8^+Foxp3^+$ T cells residing in melanoma-invaded lympho nodes were $CD57^-$ (177).

Our findings suggest that the $CD8^+$ TIL's differentiation into potent $Perf^{Hi}$ killer cells in the melanoma tumor microenvironment may have been arrested at the early T_{EM} stage ($CD8^+CD27^+CD28^+CD57^-$). Although $CD8^+$ TIL started to express CD57 (a marker for late-differentiated CTL), they failed to down-modulate CD27 and CD28 and induce Perf. Another explanation may be that $CD8^+CD57^+$ TIL with properties of T_{TDE} do arise, but these cells are too short-lived to be detectable *ex vivo*. The reason why these cells begin to express CD57 is unclear at present. CD57 (HNK-1) was originally found to be a marker of human NK cells. Recently, it has been shown to be most highly expressed by the most mature $CD8^-CD56^{lo}CD16^{hi}$ human NK cell sub-population (178). CD57 antigen is a terminally sulfated glycan carbohydrate epitope, and little is known about its actual function in T cells, although studies on other cell types (e.g., motor neurons) have found that it appears to function as a cell adhesion molecule (179). One study reported that CD57 exhibits binding activity to IL-6 *in vitro* (180).

Previous studies have shown that the highly-differentiated $CD8^+CD27^-CD28^-CD57^+$ CTL in the peripheral blood accumulated with aging and was a senescent population incapable of further cell division and prone to activation-induced cell death after TCR ligation (131, 167). $CD8^+CD57^+$ T cells in humans have also been reported to be oligoclonal, resulting from multiple expansions of specific clones as a consequence of aging or chronic viral infections by EBV and CMV (141, 143, 153, 172). In our study, we found

that the $CD8^+CD27^+CD57^+$ TIL in both melanoma and breast cancer pleural effusion were also more oligoclonal than the $CD8^+CD27^+CD57^-$ TIL, which suggested that the $CD8^+CD27^+CD57^+$ TIL subset were more differentiated than the $CD8^+CD27^+CD57^-$ TIL (loss of TCR diversity and oligoclonality is a natural consequence of T-cell differentiation and aging; see **Fig. 1-5**). However, whether CD57 marks truly senescent $CD8^+$ T cells in humans have come under debate, with newer studies demonstrating that these cells could be induced to divide and produce cytokines after TCR stimulation (127, 181).

Based on these previous findings, we examined whether $CD8^+CD27^+CD57^+$ melanoma TIL were capable of further cell division when compared to $CD8^+CD27^+CD57^-$ T cells, the other major TIL subset in melanoma. Several lines of evidence in the present study support that the $CD8^+CD57^+$ TIL were not senescent and were also capable of further cell division and differentiation *in vitro*. First, $CD8^+CD27^+CD57^+$ subset in the fresh TIL isolates persisted and expanded over a number of weeks in culture with IL-2. However, these IL-2-cultured $CD8^+$ TIL did not show evidence of further differentiation into $CD27^-CD57^+$ or $CD27^-CD57^-$ cells, but did up-regulate Perf expression slightly, which has been described after IL-2 signaling (182). Second, in bulk TIL cultures and sorted populations of $CD8^+CD27^+CD57^+$ TIL, we found that stimulation with agonistic anti-CD3 and CD28 antibodies also stimulated their cell cycle entry and divisions. Third, the sorted $CD8^+CD27^+CD57^+$ TIL produced IFN-γ, IL-5, and IL-13 after TCR stimulation, with significantly higher IFN-γ production than those of the $CD27^+CD57^-$ subset. Interestingly, TILs in breast and kidney carcinoma have also been observed to produce IL-13, which has been shown to negatively regulate IDO (indoleamine-2,3-dioxygenase) expression in tumors (183). Of note, IDO is the first and rate-limiting enzyme of tryptophan catabolism through

kynurenine pathway, thereby depleting tryptophan, which can halt the growth of T cells (184). Lastly, our sorting experiments revealed that TCR stimulation induced sorted $CD8^+CD27^+CD57^+$ T cells to differentiate into $CD8^+CD27^-CD57^+GB^{Hi}Perf^{Hi}$ T cells, reminiscent of T_{TDE} $CD57^+$ CTL in the peripheral blood; this observation was not due to $CD8^+CD27^+CD57^-$ TIL contaminants, since sorted $CD8^+CD27^+CD57^-$ T cells did not differentiate into $CD27^-CD57^+$ T cells, but rather, differentiated directly into $CD27^-CD57^-$ T cells, which further supports that $CD8^+CD57^-$ and $CD8^+CD57^+$ TIL belong to distinct lineages. It is not known whether these $CD8^+CD27^+CD57^+$ TIL persist as short-lived effector cells at the tumor site or re-circulate in the periphery. Addressing this question requires an *in vivo* study using a murine model, but this $CD8^+CD57^+$ T cell subset does not exist in mice (185).

Based on our initial observation that incompletely differentiated $Perf^{Lo}$ $CD8^+$ TIL accumulate in the tumor microenvironment, we reasoned that the existence of certain immunosuppressive factors may affect $CD8^+$ TIL's further differentiation. TGF-β1 is known to be secreted by many tumors, including melanoma cells and certain types of tumor-associated macrophages (158-160). Previous studies have shown that TGF-β1 inhibited the differentiation of naïve $CD8^+$ T cells into effector cells (173, 175), attenuated the production of inflammatory cytokines such as IFN-γ and TNF-α by effector $CD8^+$ T cells (158), and significantly decreased Perf expression in lymphokine-activated killer (LAK) cells and murine $CD8^+$ T cells (174, 186). The inhibitory effect of TGF-β1 on CTL's effector function was apparent in studies showing enhanced tumor eradication in mice with T-cells lacking TGF-β signaling (173, 187). In our study, we found that TGF-β1 prevented the differentiation of $CD8^+CD27^+$ subsets into more mature $CD8^+CD27^-$ CTL. This cytokine

also inhibited the expressions of Perf and, to a lesser extent, GB in $CD8^+$ TIL. In addition to TGF-β1, other factors in the tumor microenvironment, such as a lack of adequate cytokine signaling (e.g, IL-2, IL-15), or the absence of proper costimulatory signals (e.g., through 4-1BB), or the presence of co-inhibitory signaling through PD-1, BTLA, or TIM-3 following TCR activation (52, 164), could also contribute to this arrest of CTL differentiation. Alternatively, the presence of other immunosuppressive cytokines, such as IDO, PGE_2, or IL-10, may also play a role (161, 188).

In sum, we have identified a unique stage in which $CD8^+$ CTL differentiation was blocked in the tumor microenvironment, in both metastatic melanoma and breast cancer pleural effusions. This was associated with the appearance of an unusual early $CD8^+$ T_{EM} subset co-expressing a late CTL differentiation marker, CD57. These $CD8^+CD27^+CD28^+CD57^+$ TIL, though expressing GB, had little or no Perf expression and therefore were a unique T_{EM} subset in cancer (**Fig. 2-18**). Immunosuppressive factors, such as TGF-β, might affect the CTL differentiation and led to the appearance of this unique $CD57^+$ subset (**Fig. 2-18**). It was possible that these unique $CD57^+$ cells might also represent a subpopulation of $CD8^+CD27^+CD57^-$ TIL that have attempted to differentiate into $CD57^+$ cells, but were blocked from further differentiation into $CD27^-Perf^{Hi}$ cells in the tumor microenvironment. On the other hand, the $CD8^+$ $CD27^+CD57^-$ T_{EM} TIL, which were the dominant $CD8^+$ TIL population, might represent a putative CTL precursor subset, which, like the hybrid $CD27^+CD57^+$ subset, was also functionally suppressed by the immunosuppressive factors in the tumor microenvironment. Finally, tumor antigen-specific $CD8^+$ populations could be found in both $CD27^+CD57^-$ and $CD27^+CD57^+$ subsets. Thus, further studies will be needed to examine whether the more differentiated $CD8^+CD27^-$ TIL exhibit better control of

tumor growth *in vivo* than their $CD27^+$ precursors. In addition, it will be of interest to determine whether $CD8^+CD27^+CD57^+$ TIL can differentiate into long-lived $CD8^+CD27^-CD57^+$ cells *in vivo,* which are reminiscent of the long-lived $CD57^+$ T cells in the periphery of healthy individuals that effectively control CMV and EBV infections (141, 146).

Figure 2-18: Differentiation pathway of the tumor-infiltrating $CD8^+$ T cells in metastatic cancer. In situations where $CD8^+$ T cells encounter persistent, chronic antigenic stimulation such as metastatic cancer or uncontrolled chronic viral infections, $CD8^+$ effector-memory T (T_{EM}) cells fail to coordinately down-regulate of CD27 and up-regulate an end-stage CTL marker, CD57 and acquire a more cytolytic phenotype. Thus T_{EM} fail to transition from a granzyme B (GB^+) $perforin^{Lo}$ ($Perf^{Lo}$) cells into $Perf^{Hi}$, highly cytotoxic end-stage CTL. This resulted in accumulation of $CD8^+$ T cells at a transitional stage where markers for early T_{EM} (CD27, CD28) are co-expressed with CD57, even though the cells remain $Perf^{Lo}$. We also found that TGF-β1, an immunosuppressive cytokine frequently found in the microenvironment of metastatic cancer, could also contribute to the arrested differentiation and accumulation of $CD27^+CD57^-$ precursor T cells and $CD27^+CD57^+$ T cells. Other yet-to-be identified immunosuppressive factors may also contribute to this arrested state of $CD8^+$ TIL's differentiation.

Figure 2-18:

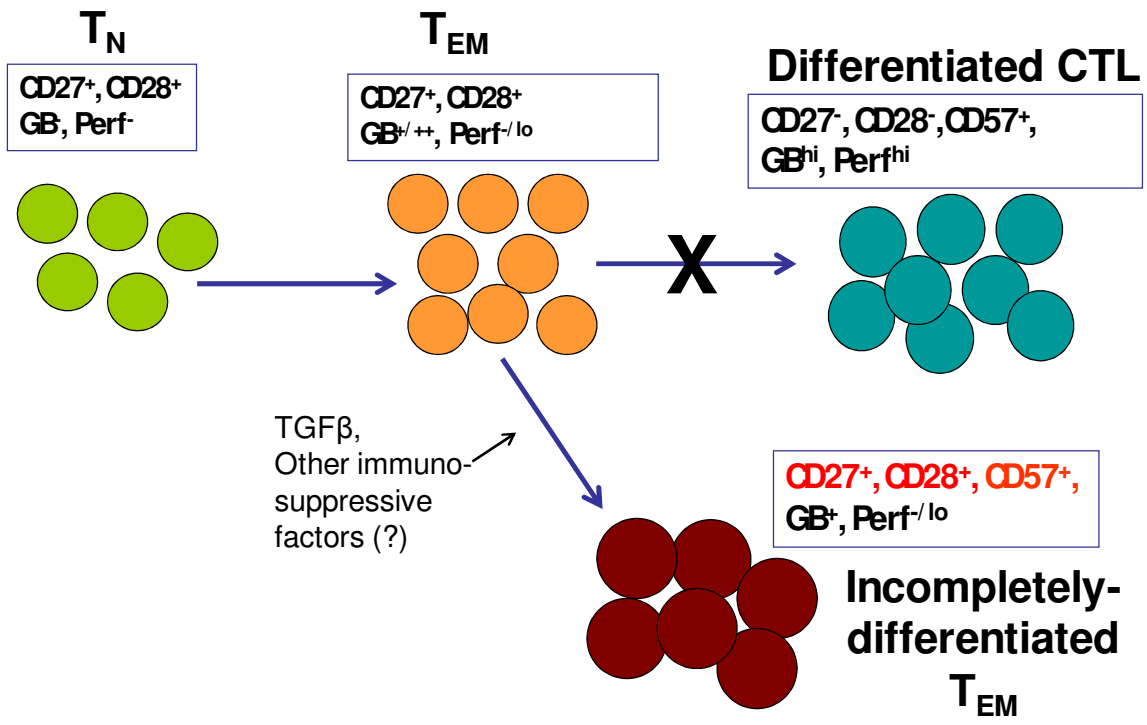
T N
CD27+, CD28+
GB-, Perf-
T EM
CD27+, CD28+
GB+/ ++, Perf-/ lo
Differentiated CTL
CD27-, CD28-, CD57+,
GBhi, Perfhi
X
TGFβ,
Other immuno-
suppressive
factors (?)
CD27+, CD28+, CD57+,
GB+, Perf-/ lo
Incompletely-
differentiated
T EM

Chapter 3

Phenotypic and functional characterization of a $CD8^+$ TIL subset expressing **B-** and **T- L**ymphocyte **A**ttenuator (**BTLA**) associated with melanoma regression during adoptive T-cell therapy

Partially reproduced and adapted for this doctoral dissertation from the following manuscript in preparation:

*Wu R, *Haymaker C, *Bernatchez C, Chen JQ, Liu H, Wang E, Marincola F, Davies MA, Hwu P, and Radvanyi L. 2013. BTLA Promotes Survival of Young $CD8^+$ Melanoma TIL via Akt.

*These authors contributed equally

Introduction

Adoptive T cell therapy (ACT) has emerged as a promising treatment for metastatic cancers such as melanoma. This process involves expanding melanoma patients' autologous tumor- infiltrating lymphocytes (TIL) *in vitro* for a period of 4-5 weeks, followed by a rapid-expansion protocol (REP) and re-infusion into lympho-depleted patients along with high-dose IL-2 (59). Multiple institutions, including our group at M.D. Anderson Cancer Center, have conducted ongoing Phase II studies for patients with Stage IIIc/IV metastatic melanoma, with reported clinical response rates between 48 to 51% based on the RECIST criteria (55, 59, 189).

Our group has previously reported that positive clinical response of this therapy and the degree of melanoma tumor shrinkage post-treatment were significantly correlated to the amount of $CD8^+$ cytotoxic T cells, not $CD4^+$ T cells, that were infused into patients (55) (**Fig. 3-1**).

Figure 3-1: Comparison of total cells infused and major T-cell subsets in the infused TIL product between responders (**CR**, complete responders, and **PR**, partial responders) and non-responders (**PD**, patients with progressive disease, and **SD**, patients with stabilization of disease). Clinical response was assessed using Response evaluation criteria in solid tumors (RECIST 1.1) (190)**.** (**A**) Responding patients were infused with significantly more TIL (median 99×10^9 cells) than nonresponders (median 55×10^9; $p = 0.0003$). (**B**) We further analyzed the different subsets of T cells using multicolor flow cytometry for the content of $CD3^+CD8^+$ and $CD3^+CD4^+$ T cells, which revealed that both the percentage and total number of $CD8^+$ T cells infused were significantly associated with clinical response ($p = 0.001$ and 0.0003, respectively). (**C**) Non-responders had significantly higher percentages of $CD4^+$ TIL ($p = 0.001$; Fig. 3C). (**D**) We further analyzed the role of total $CD8^+$ TIL as a continuous predictor of percentage change in tumor burden ($p = 0.0003$). Linear regression shows the relationship between total $CD8^+$ infused and percentage change in tumor burden ($P = 0.0003$), with the solid line in showing the best fit, the broken line representing the 95% prediction limits, and the gray area indicating the 95% confidence limits.

Reprinted with permission from: Radvanyi, LG, Bernatchez C, Zhang M, *et al*. 2012. Specific Lymphocyte Subsets Predict Response to Adoptive Cell Therapy Using Expanded Autologous Tumor-infiltrating Lymphocytes in Metastatic Melanoma Patients. *Clin. Cancer Res.* 18(24):6758-6770. doi:10.1158/1078-0432.CCR-12-1177.

Figure 3-1:

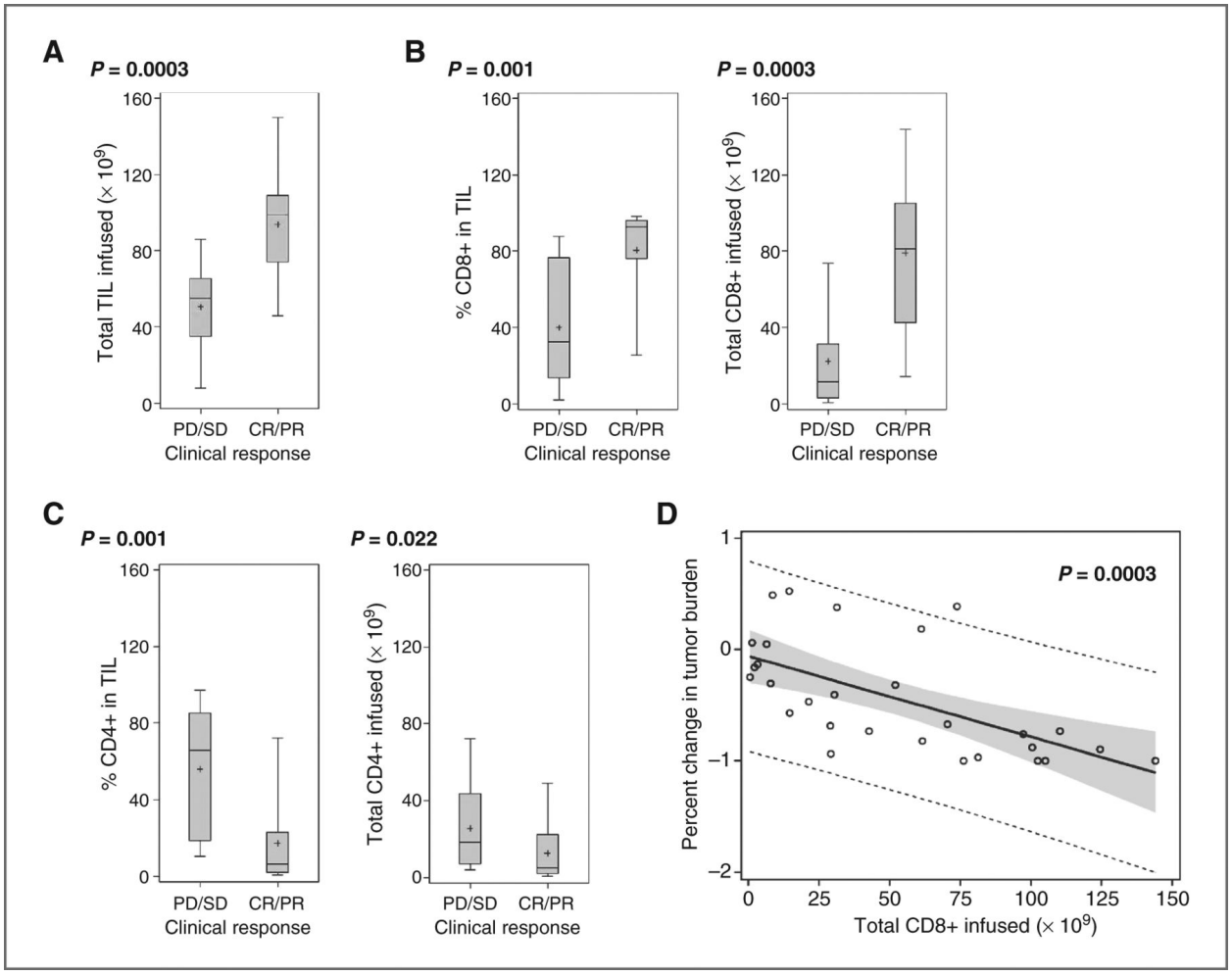
A
P = 0.0003
Total TIL infused (× 10^9)
160
120
80
40
0
PD/SD
CR/PR
Clinical response
B
P = 0.001
% CD8+ in TIL
P = 0.0003
Total CD8+ infused (× 10^9)
C
P = 0.001
% CD4+ in TIL
P = 0.022
Total CD4+ infused (× 10^9)
D
P = 0.0003
Percent change in tumor burden
1
0
−1
−2
0
25
50
75
100
125
150
Total CD8+ infused (× 10^9)

However it is still controversial which phenotypic markers expressed by $CD8^+$ T cells and what state(s) of differentiation are correlated to clinical response. Others have shown in a murine B16 melanoma tumor model that the adoptive transfer of the least differentiated, stem-like memory CD8+ T cells (T_{SCM}) exhibited the most effective control of melanoma tumor growth (132). Although T_{SCM} $CD8^+$ T cells have been found in the peripheral blood in humans (124), they could not be found among tumor-infiltrating lymphocyte populations within melanoma patient tumors, which were consisted of more differentiated T_{EM} and T_{EMRA} $CD8^+$ T cell subsets (55). One study reported that infusion of higher numbers of $CD8^+CD27^+$ melanoma TIL, which marked early-differentiated cells within the T_{EM} populations, correlated with positive clinical response (191). However, CD27 cannot stably and reliably define the $CD8^+$ T cell differentiation state since its expression is prone to be affected by IL-2 or interaction with its cognate ligand, CD70 (134). Thus, it is critical to explore additional biomarkers in order to better define the subset and the differentiation state of the $CD8^+$ TILs contributing to a positive clinical response to ACT. Identification of such a subset of $CD8^+$ TIL could lead to efforts to selectively expand these T cells prior to infusion into patients, which has the potential to further improve the efficacy of ACT (192).

We found that melanoma patients receiving higher numbers of $CD8^+$ TIL expressing B-and-T lymphocyte attenuator (BTLA), an inhibitory receptor with two immunotyrosine-based inhibitory motifs (ITIMs) that are similar to other well-known inhibitory receptors, PD-1 and CTLA-4 (50), were significantly correlated to positive clinical responses to ACT (55) (**Fig. 3-2**). However, we did not find clinical correlations with $CD8^+$ TIL's expressions of other inhibitory receptors such as PD-1 (programmed death-1) or TIM-3 (**T**-cell **i**mmunoglobulin domain and **m**ucin domain 3 receptor) (55) (**Fig. 3-2**).

Figure 3-2: Comparison of PD-1, BTLA, and TIM-3 expressions on $CD8^+$ TIL in responders (CR/PR) and nonresponders (PD/SD) in metastatic melanoma patients treated with ACT. (**A**) Results shown were the percentage of cells in the total $CD8^+$ TIL population expressing PD-1, BTLA, and TIM-3 in all treated patients. (**B**) The percentages of $CD8^+PD\text{-}1^+$, $CD8^+BTLA^+$, and $CD8^+TIM\text{-}3^+$ subsets in the infused TIL was compared between responders and nonresponders. Wilconxon rank-sum test was used to assess statistical significance differences. There were highly significant differences in BTLA expression between responders and non-responders (p=0.0006), while the differences in PD-1 or Tim-3 expressions did not reach statistical significance (p=0.070 and p=0.004, respectively) after Bonferroni correction for multiple comparisons were applied.

Reprinted with permission from: Radvanyi, LG, Bernatchez C, Zhang M, *et al*. 2012. Specific Lymphocyte Subsets Predict Response to Adoptive Cell Therapy Using Expanded Autologous Tumor-infiltrating Lymphocytes in Metastatic Melanoma Patients. *Clin. Cancer Res.* 18(24):6758-6770. doi:10.1158/1078-0432.CCR-12-1177.

Figure 3-2:

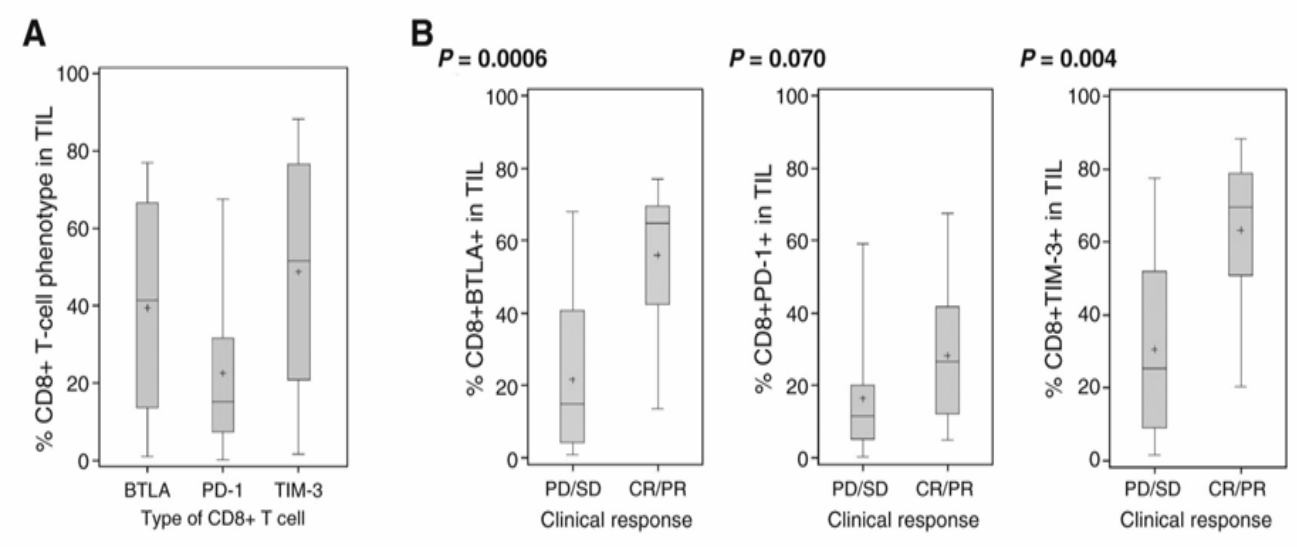
A
% CD8+ T-cell phenotype in TIL
100
80
60
40
20
0
BTLA
PD-1
TIM-3
Type of CD8+ T cell
B
P = 0.0006
% CD8+BTLA+ in TIL
PD/SD
CR/PR
Clinical response
P = 0.070
% CD8+PD-1+ in TIL
PD/SD
CR/PR
Clinical response
P = 0.004
% CD8+TIM-3+ in TIL
PD/SD
CR/PR
Clinical response

This finding was surprising since signaling through BTLA has been shown to inhibit proliferation and cytokine production in melanoma tumor antigen-specific (MART-1-reactive) $CD8^+$ T cells (52). However, BTLA has also been reported to harbor a third conserved tyrosine-containing motif within the cytoplasmic domain, which has been shown to recruit Grb-2 and p85 subunit of PI3K *in vitro* (51). The functional significance of this interaction in enhancing T cell survival has not been previously explored in the literature.

It is also not clear whether BTLA expression truly marked exhausted, dysfunctional $CD8^+$ T cells. Although it was reported that BTLA is up-regulated on exhausted, NY-ESO-1 tumor antigen-specific $CD8^+$ T cells (53), a number of studies on human $CD8^+$ T cells have shown that BTLA was already expressed at a high level on naïve $CD8^+$ T cells and was gradually down-regulated during normal differentiation (52, 54). A recent study has suggested a close relationship between the expressions of multiple inhibitory receptors (e.g., PD-1, TIM3 and LAG3) and the antigen-specificity, anatomic localization, and differentiation of $CD8^+$ T cells in humans (193) (**Fig. 3-3B**) . Therefore, we hypothesize that BTLA may mark a specific stage of differentiation in $CD8^+$ melanoma TIL.

Figure 3-3: Expression profiles of inhibitory receptors with human $CD8^+$ T cell's differentiation. Peripheral blood mononuclear cells (PBMC) from melanoma patients were stained with antibodies specific for these inhibitory receptors, as well as for CD8, CD45RA and CCR7. (**A**) $CD8^+$ T cells subsets were further classified into naive (N), central memory (CM), effector memory (EM) and effector memory $CD45RA^+$ (EMRA) cells as defined by CCR7 and CD45RA expression. (**B**) Naive cells were frequently BTLA positive and many of them also co-expressed TIM-3. In contrast, all other inhibitory receptors were up-regulated along with progressive differentiation. While T_{EMRA} cells were frequently positive for 2B4, KLRG-1 and CD160, they expressed less PD-1 and BTLA than T_{EM} cells.

Reprinted with permission from: Baitsch L, Legat A, Barba L, Fuertes Marraco SA, Rivals J-P, *et al*. (2012) Extended Co-Expression of Inhibitory Receptors by Human CD8 T-Cells Depending on Differentiation, Antigen-Specificity and Anatomical Localization. *PLoS ONE*. 7(2): e30852. doi:10.1371/journal.pone.0030852.

Figure 3-3:

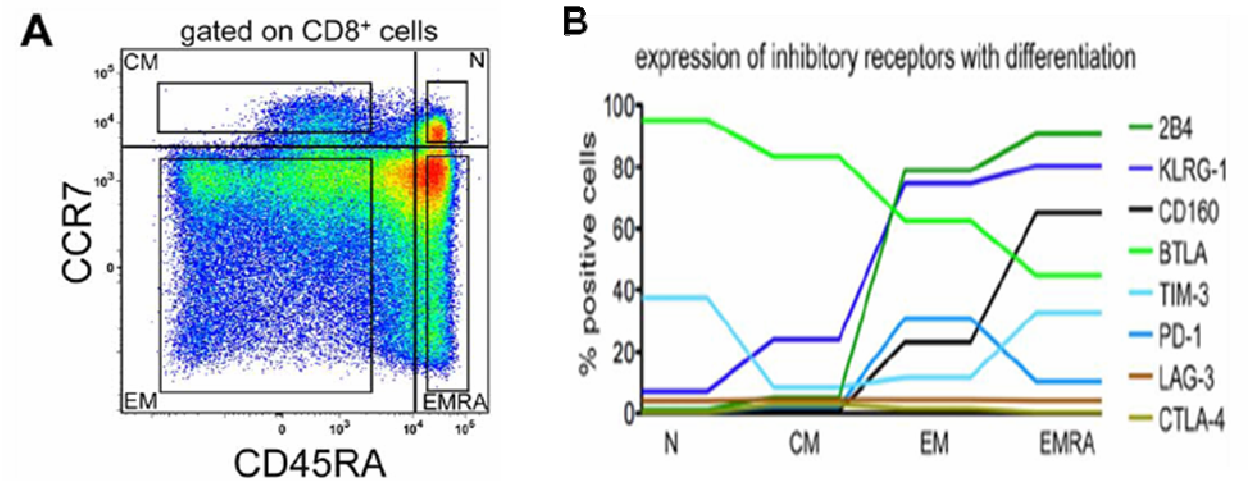
A
gated on CD8⁺ cells
CM
N
EM
EMRA
CCR7
CD45RA
B
expression of inhibitory receptors with differentiation
% positive cells
100
80
60
40
20
0
N
CM
EM
EMRA
2B4
KLRG-1
CD160
BTLA
TIM-3
PD-1
LAG-3
CTLA-4

In this study, we have characterized the $CD8^+BTLA^+$ and $CD8^+BTLA^-$ subsets in melanoma TIL in terms of their effector functions and global gene expression profiles. We discovered that BTLA was a stable marker that defined a subset of less-differentiated, highly proliferative effector-memroy (T_{EM}) TIL responsive to IL-2 and TCR signals. In contrast, the absence of BTLA expression on $CD8^+$ TIL defined a distinct subset consisting of late-differentiated T_{EM} and T_{EMRA} TIL that was poorly responsive to IL-2 or TCR signals. This subset expressed receptors belonging to the killer-cell immunoglobulin-like receptor family, which were typically expressed by natural killer (NK) cells (194) and highly-differentiated or senescent $CD8^+$ T cells (66, 166, 195, 196), and exhibited a molecular signature of T-cell deletion (197, 198). We also found that the ligation of BTLA on $CD8^+$ TIL with its cognate receptor, herpes virus entry mediator (HVEM), though exerted inhibitory effect on proliferation and cytokine production, nevertheless promoted phosphorylation of Akt and improved TIL survival. Therefore, our findings provide an explanation for the positive clinical association with the $CD8^+BTLA^+$ TIL subset, and suggest that the $CD8^+BTLA^+$ TIL may be selectively harnessed to improve the persistence of the TIL in patients undergoing Adoptive T cell Therapy (ACT).

Materials and Methods

Expansion of tumor infiltrating lymphocytes from human melanoma tumors. Briefly, TIL were separated from tumor cells by centrifugation over 75% and 100% Ficoll double layers following enzymatic digestion with collagenase type I (0.375%, Sigma-Aldrich), hyaluronidase (75µg/ml, Gibco) and DNase I (250 U/ml). TIL lines were cultured in TIL-CM [RPMI 1640, 10% human Ab serum, 1 mM glutamine, 1 mM sodium pyruvate, 50 µM 2-mercaptoethanol, 1× penicillin-streptomycin (Invitrogen, Carlsbad, CA)] and expanded in high-dose IL-2 (6,000 IU/mL, Novartis) as described previously (66). Autologous primary melanoma tumor lines were also established by collecting the cells at the 75% Ficoll layer and used as targets in CTL assays.

Flow Cytometry. Freshly-isolated or IL-2 cultured T cells were washed twice in D-PBS and stained using Live/Dead® Fixable Aqua Dead Cell Stain Kit (Life Technologies, CA) according to manufacturer's instruction. Cells were then washed twice in FACS wash buffer (D-PBS + 1% BSA) and stained with CD3 FITC (SK7), CD4 PerCP-Cy5.5 (RPT-T4), CD8 PB (RPT-T8), BTLA PE (J168), TIM3 APC (F38-2E2), PD-1 PerCP-Cy5.5 (EH12.2H7), CD27 APC-H7 (M-T271), CD28 PE-Cy7 (CD28.2), CD45RA (HI100), and MART-1 APC or gp100 APC (HLA-A02$^+$ cells only) (Beckman Coulter). For KIR phenotyping, TIL were stained with CD3 PerCP-Cy5.5 (SK7), CD8 PB (RPT-T8), BTLA PE (J168), CD158a (KIR2DL1) (FITC), CD158b (KIR2DL2/3) (FITC), NKAT2 (KIR2DL3) (FITC), and CD158e/NKB1 (KIR3DL1) (FITC). For tetramer staining, TIL were initially stained with 3ul tetramer for 15 minutes in 100ul of FACS buffer. Cells were then stained for other markers without washing between steps. Cells were stained on ice for 30 minutes in 100 µl of

FACS buffer. 5% goat serum was added to the FACS buffer when staining fresh tumor isolated T cells to block Fc receptors.

Cell sorting. TIL were harvested, washed in FACS buffer, and stained for CD8, BTLA, and CD27 for 30 min on ice. Cells were then washed and re-suspended in FACS buffer for cell sorting. Sorts were performed using an Aria I (BD Biosciences) or Influx (BD Biosciences) cell sorter. Cells were sorted directly into TIL media. Only populations with a ≥ 95% post-sort purity were used for experiments.

Proliferation and survival assays. 1 μM of CFSE (Molecular Probes™/Invitrogen, Carlsbad, CA) was used for labeling sorted TILs in order to monitor the number of cell divisions they undergo in response to different concentrations of IL-2 (200 U/mL and 3,000 U/mL) after 5 days. In experiments where there was conflict between CFSE and other flurochrome-conjugated antibodies, 1 μM of eFluor® 670 Cell Proliferation Dye (eBioscience, San Diego CA), which was detected by the flow cytometer's APC channel, was used to label the TILs according to the manufacturer's protocol. The sorted TILs were washed in D-PBS and re-suspended in PBS containing CFSE. Labeling was done at RT for 5-7 minutes followed by washing three times with TIL-CM. After 5 days of stimulation with IL-2, the cells were harvested and stained with anti-CD8 mAb. Data were acquired using using FACScanto II cytometer (BD Biosciences). The number of cell divisions was estimated using a curve-fitting method from the FlowJo software's Proliferation Tool (Treestar v7.6.5). Apoptosis of the TILs was monitored the Apoptosis Detection Kit (BD Biosciences). The cells were harvested, washed in cold D-PBS, re-suspended in the 100 μL 1X Binding Buffer (supplied with the kit), and stained with anti-CD8 mAb, Annexin V-PE, and 7-AAD for 20 minutes. The cells were washed with 2 mL of 1X Binding Buffer, re-

suspended in 0.3 mL of 1X Binding Buffer, and analyzed by flow cytometer within 1 hour. For [^{3}H]-thymidine incorporation assay, a total of 5×10^4 sorted cells per well were plated into 96-well Costar 3361 High-bind plates (Sigma-Aldrich) pre-coated overnight with anti-CD3 (OKT3; Ortho Biotech) or anti-CD3 and anti-CD28 (eBioscience) agonistic antibodies. After 3 days, the cells were pulsed with 1 μCi of [^{3}H]-thymidine (methyl-T-thymidine; PerkinElmer Inc.) for 18 hours. The incorporated [^{3}H] thymidine was reported as counts per minute (cpm) by a β liquid scintillation counter (Beckman Coulter).

Phospho-flow staining. Sorted cells were stimulated with escalating doses of IL-2 (50 U/mL, 200 U/mL, and 3,000 U/mL) for 20 minutes. Unstimulated cells served as the control. At the end of the stimulation, cells were fixed in a pre-warmed BD™ Cytofix Buffer for 10 min. Cells were then permeabilized by chilled BD™ Phosphoflow™ Perm Buffer III for 20 min at 4°C. Cells were washed twice with BD™ Pharmingen™ Stain Buffer and stained with fluorochrome-conjugated anti phospho-Stat5 (Tyr694; BD Biosciences) or anti phospho-Akt (Ser473; Cell Signaling Technology, Danvers, MA) antibodies for 20 min at 4°C and washed twice with Stain Buffer. Data were acquired using using FACSCanto II cytometer (BD Biosciences) and analyzed using FlowJo (Treestar version 7.6.5).

Intracellular cytokine staining. The sorted cells were stimulated with 25 ng/mL of PMA and 1 μg/mL of ionomycin. Unstimulated cells serve as the control. At the same time, BD™ GolgiStop™ (monensin) was added to each culture according to the manufacturer's instruction. At the end of the 4-hour stimulation period, cells were fixed and permeabilized using BD Cytofix/Cytoperm^{TM} kit and subsequently stained with IL-2 PerCP-Cy5.5, IFN-γ PE-Cy7, and TNF-α APC mAbs (BD Biosciences). Data were acquired using using

FACScanto II cytometer (BD Biosciences), and analyzed using FlowJo software (Treestar version 7.6.5).

Cytotoxic T cell assays. Analysis of CTL activity of the sorted $CD8^+$ subsets was done according to a flow cytometric method measuring the cleavage of caspase-3 in anti-CD3 coated target cells or in autologous melanoma tumor cells as described previously (163). Briefly, 5 x 10^6 murine mastocytoma target cells (P815) or autologous melanoma tumor cells were labeled with a fixable, far-red fluorescent tracer, CellTrace® Far Red DDAO-Succinimidyl Ester (DDAO-SE; Invitrogen, Carlsbad, CA) according to manufacturer's instructions, washed, resuspended at a density of 2.5 x 10^6/mL. For redirected lysis assay with P815 target cells, these were additionally pulsed with 200 μg/mL of anti-CD3 mAb in a low-serum containing media (RPMI 1640 with 2% FBS) at RT for 30 min. Unpulsed target cells served as controls. Labeled target cells were added to the sorted TIL subsets at E:T ratios of 1:3, 1:1 and 3:1 in a round-bottom 96-well plate and spun down for 5 min at low centrifuge speed (300 RPM) in order to maintain optimal contact between target cells and effector T cells. The cells were co-incubated for 3h before harvesting. The 3 hour time point was chosen to prevent the apoptotic target cells from becoming necrotic and losing the cleaved caspase-3 signal. The cells were stained intracellularly with an anti-cleaved caspase-3-PE mAb (BD Biosciences). Target cells were distinguished from effector T cells by the far-red tracer DDAO-SE, and the extent of the caspase-3 cleavage in the target cell population was analyzed by the FACSCanto II flow cytometer (BD Biosciences). For CD107a and IFN-γ co-release assay, sorted T cells were co-cultured with autologous melanoma tumor cells at the same E:T ratios for 4 hours. Fluorochrome-conjugated CD107a-PE mAb (eBioscience) and BD™ GolgiStop™ were added at the beginning of the cultures. At the end culture

period, cells were fixed and permeabilized using BD Cytofix/Cytoperm™ kit and subsequently stained with CD8-Pacific Blue and IFN-γ PE-Cy7 mAbs (BD Biosciences). Data were acquired using using FACScanto II cytometer (BD Biosciences), and analyzed using FlowJo software (Treestar version 7.6.5).

Cytokine multiplex assays. Pre-REP TIL were harvested and washed twice in TIL-CM to remove any excess IL-2 and plated for 24h in 96 well plates pre-coated with or without 30 ng/ml agonistic anti-CD3 mAb and 1 μg/mL of agonistic anti-CD28 mAb. The tissue culture supernatants from triplicate wells of each condition were collected, diluted at a 1:3 ratio, and added to magnetic beads coated with immobilized antibodies against selected human cytokines (IFN-γ, TNF-α, MIP-1β) Milliplex® MAP human multiplex cytokine kit, according to the manufacturer's instructions (EMD Millipore, Billerica, CA). The signals from the Strepavidin-Phycoerythrin (PE) coated beads were acquired and analyzed by the Luminex® 100 IS System (Luminex® Corporation, Austin, TX). The concentration of each cytokine was calculated from its each respective standard curves.

Microarray. Total RNA was isolated from $1.0x10^6$ or less of the sorted $CD8^+$ TIL subsets using RNeasy Mini Kit (Qiagen, Valencia, CA) with DNAase digestion according to manufacturer's instruction, and eluted in 40 μl of elution buffer. RNA quality was assessed by Agilent Bioanalyzer (Santa Clara, CA) and quantified by Nanodrop 2000 (ThermoScientific, Wilmington, DE). 300 ng of total RNA were amplified using Ambion WT expression kit (Life Technologies, Grand Island, NY) according to the manual. Briefly, mRNA was reverse transcription into cDNA and followed by second strand cDNA synthesis, which was used as a template for *in vitro* transcription for cRNA synthesis. After purification, the cRNA were converted into cDNA and removed by RNase H treatment. The

single strand cDNA was fragmented by restriction digestion and terminal labeled using GeneChip WT Terminal Label kit in the presence of controls. Samples were hybridized to Human Gene ST 1.0 Arrays (Affymetrix, Santa Clara, CA) in a GeneChip Hybridization Oven 640 for >16 hours, at +45°C, 60 rpm, stained on a GeneChip Fluidics Station 450, and scanned by GeneChip Scanner 3000 7G (Affymetrix, Santa Clara, CA). Raw data passed QC assessment were generated with Affymetrix GeneChip Command Console, and the data were imported into BRB-ArrayTools v4.2.1 (NCI, Bethesda, MD), normalized with robust multi-array average (RMA) algorithm, and $\log_2$ transformed. The microarray data has been deposited into the NCBI GEO database (Accession #GSE43260; http://www.ncbi.nlm.nih.gov/geo/query/acc.cgi?acc=GSE43260).

Generation of CD32$^+$HVEM$^+$ L cells. L cells transfected with CD32 (low-affinity Fc receptor) in a retroviral vector were a gift from Yong-Jun Liu and have been described previously (199). In order to generate CD32$^+$HVEM$^+$ L cells, L cells transfected with CD32 in a retroviral vector were a gift from Yong-Jun Liu. RNA was isolated from a HVEM-expressing human melanoma tumor cells (52) using RNeasy Mini Kit (Qiagen) and reverse-transcribed into cDNA using Superscript First-Strand Synthesis System (Life technologies, Grand Island, NY). Using the cDNA as a template, the human HVEM gene was cloned using high-fidelity DNA polymerase (BioRad, Hercules, CA) and the following primers: forward primer: 5'- CACCATGGAGCCTCCTGGAGA-3'; reverse primer: 5'-TCAGTGGTTTGGGCTCCTCCCCGTGAA-3' with the following settings for PCR: 98°C for 10s, 58°C for 30s, and 72°C for 30s for 30 cycles. The resulting PCR product was ligated into a pcDNA™3.1D/V5-His-TOPO® vector provided by the Directional Topo® Expression Kit (Life Technologies, Grand Island, NY) according to the manufacturer's instructions, and

transfected into TOP10® Competent E. coli bacteria (Life technologies, Grand Island, NY). The amplified vectors were isolated from grown E. coli bacteria, and DNA sequencing of the vector was performed to verify insertion of the HVEM gene. The vector product was subsequently introduced into $CD32^+$ L cells. The transfected $CD32^+$ $HVEM^+$ L cells were grown in L-cell medium [RPMI 1640 (Life technologies, Grand Island, NY), 10% fetal bovine serum (FBS)] and selected with 500 μg/mL of Geneticin® (Life technologies, Grand Island, NY). When L cells have grown to $10x10^7$ cells, they were stained with anti-HVEM-FITC (Ancell, Bayport, MN) and purified by fluorescent-activated cell sorter. The cell sorting, selection, and culturing were repeated two more times to achieve a >97% purity (**Fig. 3-4**).

Figure 3-4: Flow cytometry staining of the $CD32^+$ L cells and $CD32^+HVEM^+$ L cells. Murine fibroblasts (L cells) that have been transduced with a retroviral containing human CD32 (low-affinity Fc receptor) gene has been described previously (199). (**Left panel**) Flow cytometry staining of the $CD32^+$ L cells, showing >98% purity. (**Right panel**) $CD32^+$ L cells were transfected with human HVEM gene. Stable $CD32^+HVEM^+$ L cell line was obtained by repeated cell sorting using anti-HVEM-FITC mAb, selection with G418 (Geneticin®), and culturing in L-cell medium until >97% purity was achieved, as described in Material and Methods.

Figure 3-4:

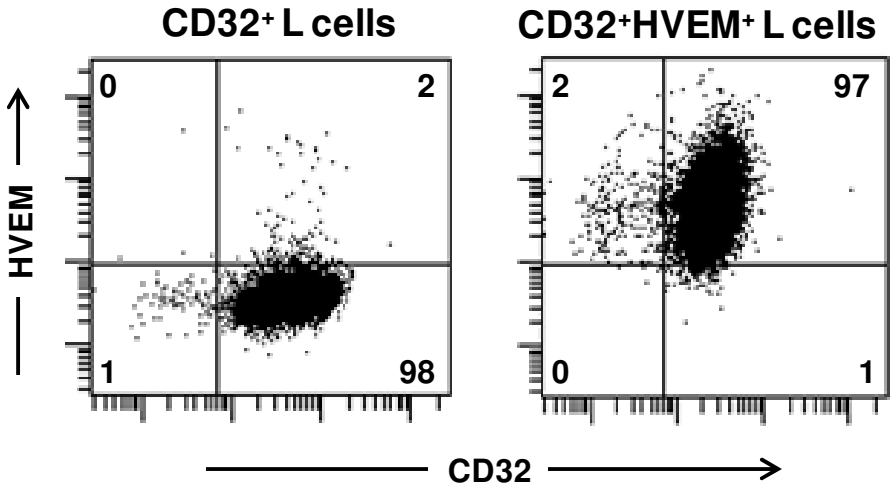

Costimulation of TIL with HVEM$^+$ L cells or HVEM-Fc fusion protein. Generation of CD32$^+$ (low-affinity Fc receptor), HVEM$^+$ L cells (murine fibroblast) was described in Supplemental Methods online. 1x10^6 of CD32$^+$ or CD32$^+$HVEM$^+$ L cells were harvested and pulsed with 30 ng/mL of OKT3 mAb in low-serum media (RPMI 1640, 2% fetal bovine serum) for 30 min. The L cells were seeded in a 24-well tissue culture plate and allowed to adhere to the plastic for 3h. 1x10^6 bulk TIL cells were added to OKT3-pulsed L cells in a 1:1 ratio. As an additional specificity control, BTLA on TIL was pre-blocked by incubation of 10 μg/mL of soluble anti-BTLA blocking mAb clone 3B1 (200), a gift from Genentech (San Francisco, CA), in serum-free TIL media for 30 min at room temperature, and were then co-incubated with CD32$^+$HVEM$^+$ L cells. At the end of the 5-day co-culture, the survival of TIL was tracked by staining for CD8, 7-AAD, and Annexin-V-FITC as described previously, and analyzed by FACSCanto™ II flow cytometer (BD Biosciences). Additionally, sorted CD8$^+$ BTLA$^+$ and BTLA$^-$ TILs were washed free of IL-2 and stimulated with 30 ng/mL of plate-bound OKT3 and 10 μg/ml control human Ig, OKT3 and 10 μg/ml HVEM-Fc with or without 10 μg/ml of soluble anti-BTLA blocking mAb (3B1) or 10 nM of a pan class I PI3K inhibitor, GSK2126458 (kindly provided by GlaxoSmithKline), or HVEM-Fc alone for 3 or 6 hours. TIL cultured in the absence of IL-2 were included as a negative pAkt control. The TILs were harvested, fixed, and stained for phospho-Akt using a Phospho-flow protocol described previously. In some cases, sorted TIL were labeled with CFSE and cultured for three days with OKT3 and HVEM-Fc or OKT3 and the control Ig as above. CFSE dilution was measured using a FACsCanto II (BD) and analyzed using FlowJo software version 7.6.5. Supernatants were also collected and analyzed for inflammatory cytokine production as described above.

Statistics. For quantitative comparisons between 2 paired groups, Wilcoxon signed-rank test (2-sample, 2-tailed comparisons) was performed with Graph Pad Prism v5.0 (La Jolla, CA) with column statistics reported as mean ± S.E.; $p < 0.05$ was considered statistically significant. *p* values and FDRs for gene sets used in GSEA were calculated with 1,000 permutations by phenotype, which was the more stringent criteria, in the online tool. Enrichment of a particular gene set in an indicated subset of $CD8^+$ TIL was considered significant if $p < 0.05$ and FDR < 0.25, as suggested in the online tool. We also used a comprehensive software package, BRB-ArrayTools v4.2.1 (NCI, Bethesda, MD), to determine statistically significant genes ($p < 0.05$) between $CD8^+BTLA^+$ and $CD8^+BTLA^-$ TIL subsets using a paired Student's *t* test.

Results

Patient tumor samples and experimental approach.

Tumor samples were obtained from Stage IIIc to Stage IV melanoma patients undergoing surgery at The University of Texas MD Anderson Cancer Center according to an Institutional Review Board–approved protocol and patient consent (IRB# LAB06-0755). Supplemental Table 1 shows the characteristics of the melanoma patients, including patient age, sex, tumor location, disease stage, and anatomical sites. The tumors were processed immediately after surgery for TIL isolation, multicolor flow cytometry staining, and expansion with high-dose IL-2 as described in Methods.

BTLA is expressed on melanoma-specific T cells and co-expressed with PD-1 and TIM3 ex vivo.

First, we wanted to determine BTLA expression levels on TIL freshly isolated *ex vivo* as well as on the known melanoma antigen-specific populations (MART-1 and gp100). Shown in **Fig. 3-5A** was the staining of the TIL with control HLA-A02 tetramer. We stained freshly-isolated $CD3^+CD8^+$ TIL from two different HLA-A02 patients with MART-1 and gp100 tetramers and assessed for co-expressions with BTLA. Interestingly, BTLA expression was observed to be enriched in the $CD8^+$MART-1^+ population (TIL 2385; 86% and TIL 2616; 80%) as compared to the corresponding tetramer negative population (TIL 2385; 71% and TIL 2616; 36%) (**Fig. 3-5B**). This trend was also observed in the $CD8^+gp100^+$ (TIL 2385; 85% and TIL 2616; 88%) populations as compared to the tetramer negative population (TIL 2385; 69% and TIL 2616; 44%) (**Fig. 3-5B**). The expression of BTLA on melanoma antigen-specific cells has been previously demonstrated in the

peripheral blood (52, 53). However, BTLA was strongly co-expressed with another inhibitory receptor, PD-1, on both tetramer positive populations in $CD8^+$ TIL. In fact, the overall percentages of freshly isolated, MART-1^+ or $gp100^+$ TIL that co-expressed BTLA and PD-1 were at least twice of the tetramer-negative population [$MART1^+$ vs. MART-1^- TIL 2385: 72% vs 35%, TIL 2616: 48% vs 4%; $gp100^+$ vs. $gp100^-$: TIL 2385; 71% vs 32%, TIL 2616: 67% vs 15%] (**Fig. 3-5B**). Overall, this data provides evidence that BTLA expression can be found on freshly-isolated melanoma antigen specific $CD8^+$ TIL, which also co-expressed PD-1 *ex vivo*. Because a previous report has shown that a majority of melanoma antigen-specific $CD8^+$ TIL was found in the PD-1^+ population in TIL, and that BTLA was known to be co-expressed with PD-1 and TIM-3, on melanoma antigen-specific $CD8^+$ T cells in the periphery (53), we wanted to determine their co-expression pattern on TIL. To this end, freshly-isolated, bulk $CD3^+CD8^+$ TIL were examined for co-expressions of BTLA and PD-1 (**Fig. 3-5C, top row**) or TIM-3 (**Fig. 3-5C, bottom row**). Indeed, we found that the $CD8^+BTLA^+$ population co-expressed PD-1 and TIM-3 in five patient TIL samples tested (**Fig. 3-5B**), though the extent of pattern of co-expression was variable from patient to patient.

Figure 3-5: **BTLA is expressed on $CD3^+CD8^+$ melanoma TIL *ex vivo*.** Melanoma tumor samples were first mechanically segregated using glass slides. The isolated TILs were then stained with Aqua® dead-cell exclusion dye, anti-CD3, anti-CD8, anti-BTLA, anti-PD-1, MART-1 tetramer (HLA-A02 restricted patients), gp100 tetramer (HLA-A02 restricted patients), and anti-TIM3. (**A**) As a control, live $CD3^+CD8^+$ TIL ($Aqua^-$) were stained with control tetramer. No appreciable staining was observed. (**B**) TIL from two HLA-A02 patients were stained with the tetramers, gated similarly as in (**A**), and analyzed for co-expressions of BTLA and PD-1. MART-1 $tetramer^+$ cells are shown on the left, and gp100 $tetramer^+$ cells are shown on the right. The top contour plot is gated on the $tetramer^+$ population, while the bottom is gated on the $tetramer^-$ population as depicted by the arrow. (**C**) BTLA, PD-1, and TIM3 expression from both HLA-A02 and non-HLA-A02 patients with TIL line numbers at the top of the contour plot. Gates were drawn based on FMO (fluorescence minus one) controls and negative tetramer controls. The numbers indicate percent expression for each marker.

Figure 3-5:

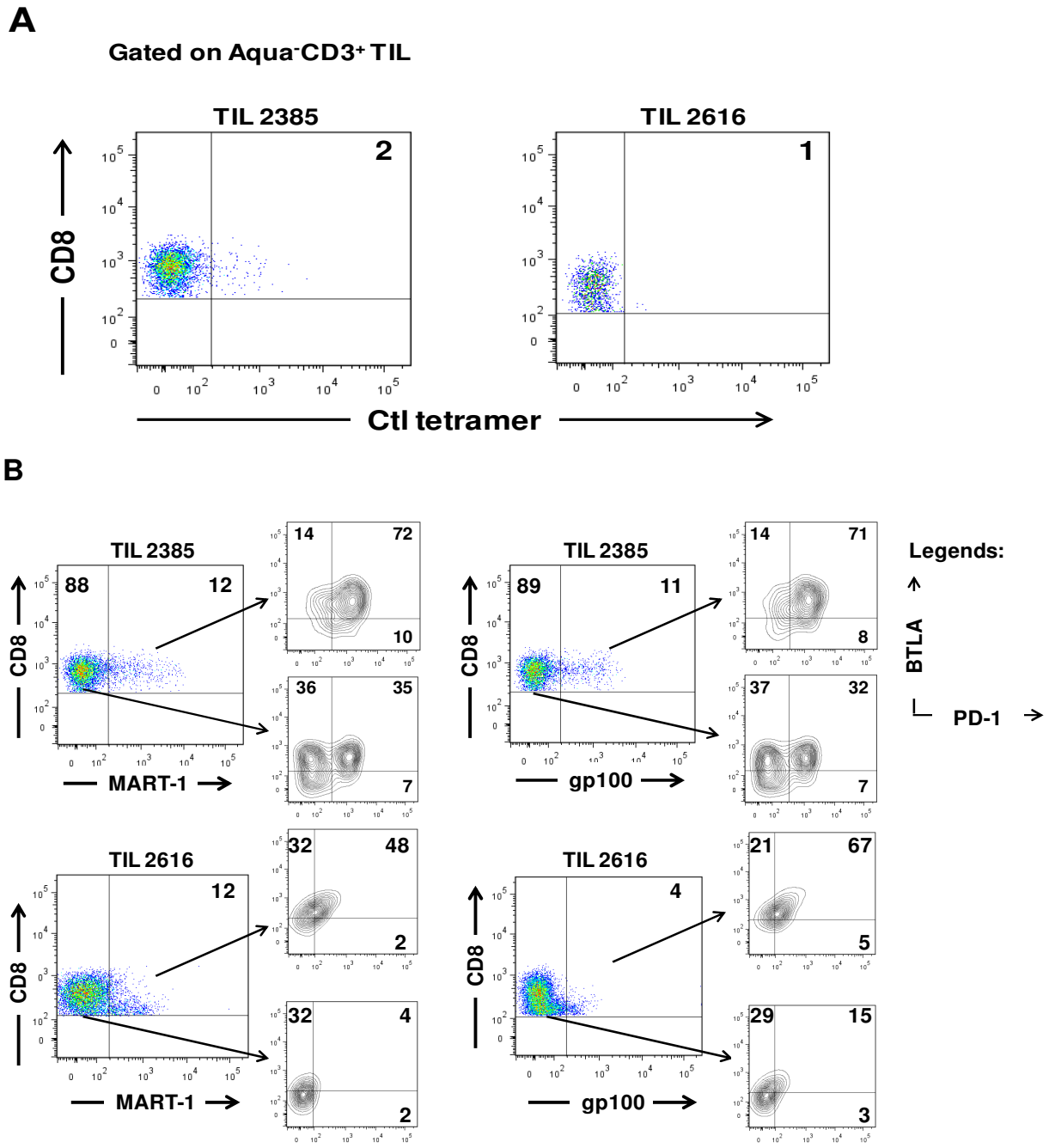
A
Gated on Aqua-CD3+ TIL
TIL 2385
TIL 2616
CD8
Ctl tetramer
B
TIL 2385
TIL 2616
CD8
MART-1
gp100
Legends:
BTLA
PD-1

Figure 3-5 con't.

C

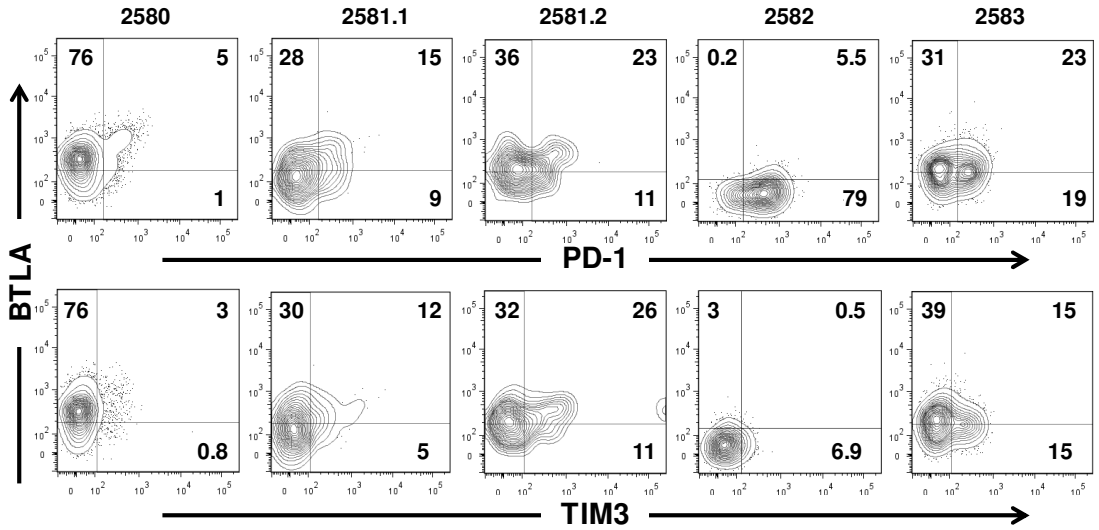

$CD8^+BTLA^+$ TIL are effector cells enriched in CD28, CD57, PD-1 and TIM-3 expressions.

A number of studies on human $CD8^+$ T cells showed that BTLA was expressed at a high level on naïve $CD8^+$ T cells and was gradually down-regulated during normal differentiation (52, 54, 201). Therefore we set out to determine the differentiation state of the $CD8^+BTLA^+$ and $CD8^+BTLA^-$ subsets in cultured TIL. TIL from 13 patients that had been cultured in IL-2 for 2 weeks were examined for expression of the major differentiation markers, CD45RA and CCR7. Differentiation subsets were broadly defined as follows: naïve T cells (T_N – $CD45RA^+CCR7^+$), central memory T cells (T_{CM} – $CD45RA^-$ $CCR7^+$), effector memory T cells (T_{EM} – $CD45RA^-CCR7^-$), and terminally differentiated effector T cells re-expressing CD45RA (T_{TDE} – $CD45RA^+CCR7^-$) (123). These markers provide a framework for comparing the differentiation state of the $CD8^+BTLA^+$ and $CD8^+BTLA^-$ populations. Analysis of a representative TIL is shown (**Fig. 3-6A**, **left panel**). Indeed, while there was no statistically significant difference in the percentages of T_{EM} cells within the $CD8^+BTLA^+$ and $BTLA^-$ subsets (**Fig. 3-6A, right panel**), the percentages of T_{EMRA} cells were significantly more enriched in the $CD8^+BTLA^-$ subset than the $CD8^+BTLA^+$ subset (**Figure 3-6A, right graph**).

To further define the surface phenotypes of the $CD8^+BTLA^+$ subset, TIL were stained for CD28, CD27, CD57, CD25, PD-1, TIM3, Granzyme B (GB), and perforin (**Fig. 3-6B**). Within the T_{EM} subset, CD28 and CD27 are markers of early $CD8^+$ effector-memory T (T_{EM}) cells. Based on studies on virus-specific T cells in humans, it was postulated that $CD8^+$ T_{EM} cells differentiate in a linear pathway from $CD28^+CD27^+$ (early-differentiated) to $CD28^-$ $CD27^+$ (intermediate-differentiated) to $CD28^-CD27^-$ (late-differentiated) (127). As $CD8^+$ T_{EM} differentiates further, the loss of CD28 and gain of CD57 is an immunological

characteristic of humans and primates (127). In addition, we and others have previously reported that the loss of CD28, not CD27, expression marked senescent $CD8^+$ T cells and TILs in humans (66, 195). We found significantly higher expression of CD28 in the $BTLA^+$ subset compared to the $BTLA^-$ subset (61 ± 6.2% vs. 45 ± 6.8%; p=0.0008; **Fig. 3-6B**). However, the difference in the level of CD27 expression between the two subsets was not statistically significant (33 ± 4.6% vs 36 ± 4.6%, respectively, *p*=0.455) (**Fig. 3-6B**) Therefore the $CD8^+BTLA^+$ subset belongs to the early-differentiated T_{EM} population.

We also examined the difference in CD57 expression, a reported marker for late T cell differentiation and senescence (131), in the $CD8^+BTLA^+$ and $CD8^+BTLA^-$ subset. We found that the $CD8^+BTLA^+$ subset was enriched in cells expressing CD57 (28 ± 4.1%) as compared to their $BTLA^-$ counterpart (17 ± 2.4%, $p = 0.001$) (**Fig. 3-6B**). The notion of CD57 as a senescent marker has been challenged by recent studies showing that $CD8^+CD57^+$ T cells could still maintain proliferative capacity (127, 181). Our group has previously reported that a subset of $CD8^+$ TIL co-expressing early T_{EM} markers (CD27 and CD28) and CD57 are able to exhibit CTL activity and production of cytokines [**Chapter 2** and ref. (202)]. Therefore the enrichment of CD57 in the $CD8^+BTLA^+$ subset suggests similarity to the T_{EM} TIL subset we described previously, which was only found within the TIL population and not in the peripheral blood. We also examined the expression of CD25 (IL-2Rα), which was reportedly a marker of potent memory T cells in humans (203). We found that the $CD8^+BTLA^+$ subset expressed slightly more CD25; the expression level was 29 ± 3.9 % as compared to 25 ± 3.8% for the $CD8^+BTLA^-$ subset (p=0.049) (**Fig. 3-6B**).

Two reported inhibitory markers, PD-1 and TIM3 were also found to be significantly expressed on the $CD8^+BTLA^+$ subset as compared to the $CD8^+BTLA^-$ population. In fact,

PD-1 expression was 42 ± 4.1% on the $BTLA^+$ populations versus 29 ± 3.4% on the $BTLA^-$ cells (p=0.0002) (**Fig. 3-6B**). Similarly, TIM3 expression on the $BTLA^+$ subset was 22 ± 7.1% as compared to 13 ± 4.8% on the $BTLA^-$ subset (p= 0.015) (**Fig. 3-6B**). Finally, we examined protein expressions of Granzyme B and perforin as markers associated with cytolytic activity. Of the six independent lines tested, there was no significant difference between the $BTLA^+$ and $BTLA^-$ subsets for either cytolytic marker (GB: 95 ± 3.4% vs 95 ± 2.4%, p=0.438; Perforin: 50 ± 9% vs 55 ±10%, p=0.688) (**Fig. 3-6B**). Overall our phenotypic data suggests that $CD8^+BTLA^+$ TIL subset has a less-differentiated and a more activated phenotype, but may exhibit a similar level of CTL activity as compared to the $CD8^+BTLA^-$ subset.

Figure 3-6: $CD8^+BTLA^+$ TIL exhibit a less differentiated, more activated phenotype than the $BTLA^-$ counterparts. TIL were isolated from melanoma tumors and were cultured with high-dose (3,000 IU/mL) IL-2 for 2 weeks. TILs were stained for expression of CD8, BTLA, CD45RA, CCR7, CD28, CD27, CD57, CD25 (IL2Rα), PD-1, TIM-3, and cytolytic granule proteins, Granzyme B and Perforin. Dead cells were excluded using Aqua® dead cell exclusion dye. (**A, left panel**) CD45RA and CCR7 expression on the $CD8^+BTLA^+$ (left dot plot) and $CD8^+BTLA^-$ (right dot plot) populations on a representative TIL from patient #2360 (left panel). (**A, right panel**) A summary of CD45RA and CCR7 expressions within each $CD8^+BTLA^+$ or $CD8^+BTLA^-$ subset (n=13). Differentiation subsets are defined as follows: T_N: $CD45RA^-CCR7^+$; T_{CM}: $CD45RA^+CCR7^+$; T_{EM}: $CD45RA^-CCR7^-$; T_{EMRA}: $CD45RA^+CCR7^-$. The results are shown by determining the percentages of T_{EM} or T_{EMRA} subsets within each gated $CD8^+BTLA^+$ or $BTLA^-$ subsets. T_N and T_{CM} are omitted since no significant populations were found. (**B**) A summary of the expressions of surface markers, CD28, CD27, CD57, CD25, PD-1, TIM3, and intracellular proteins, granzyme B and perforin, by the $CD8^+BTLA^+$ and $CD8^+BTLA^-$ subsets (n ranges from 6 – 42 per marker). Statistical significance between the subsets was determined using Wilcoxon signed-rank test. The *p* value for each marker is shown at the top of each graph. $*p<0.05$, $**p<0.01$, and $***p<0.001$.

Figure 3-6:

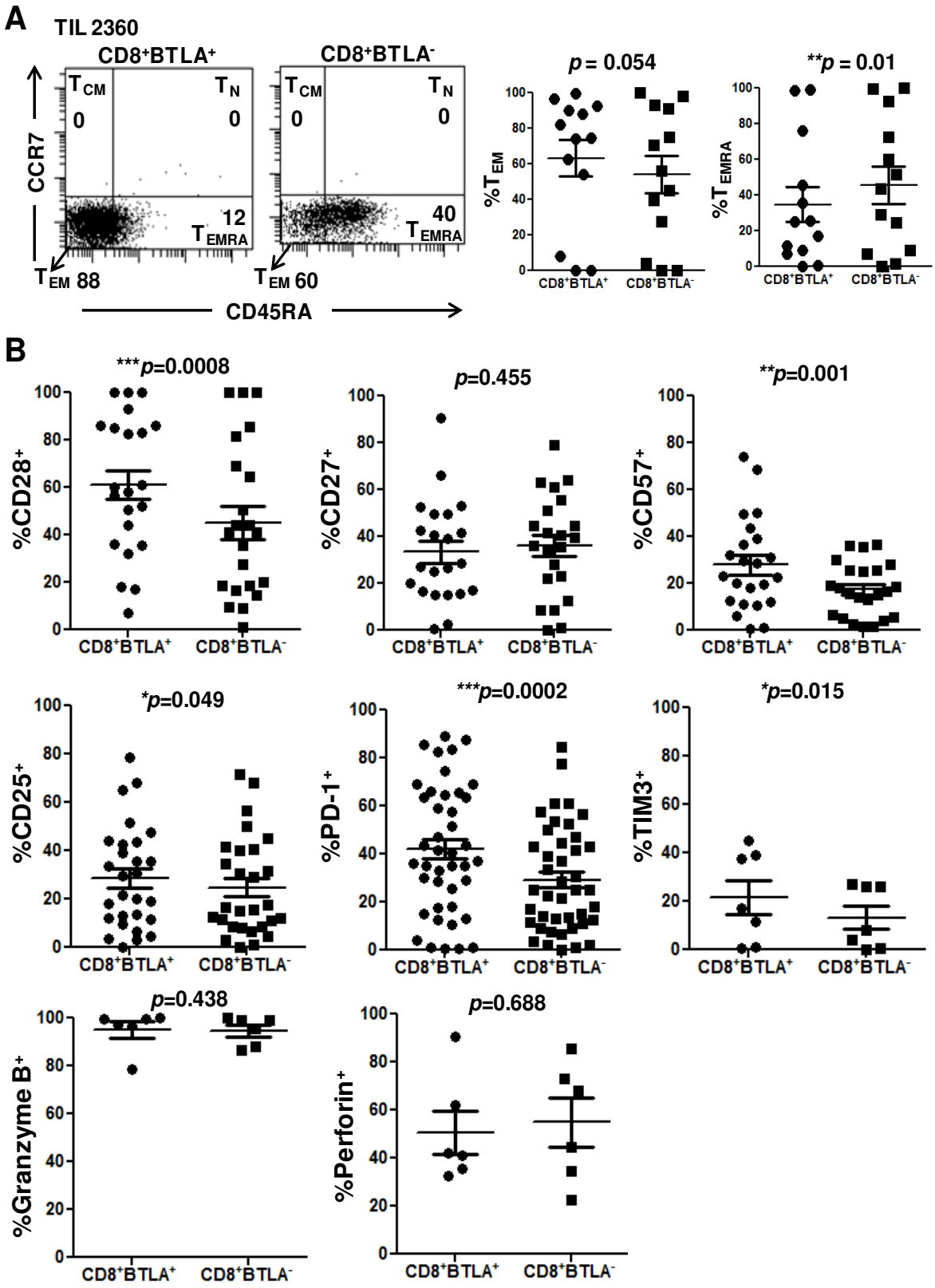
A
TIL 2360
CD8+BTLA+
CD8+BTLA-
TCM
TN
0
0
12
40
TEMRA
TEM 88
TEM 60
CCR7
CD45RA
p = 0.054
**p = 0.01
%TEM
%TEMRA
B
***p=0.0008
p=0.455
**p=0.001
%CD28+
%CD27+
%CD57+
*p=0.049
***p=0.0002
*p=0.015
%CD25+
%PD-1+
%TIM3+
p=0.438
p=0.688
%Granzyme B+
%Perforin+

Stability of BTLA expression on bulk TIL and sorted CD8$^+$BTLA$^+$ and BTLA$^-$ TIL subsets.

While a number of reports have shown high BTLA expression on naïve and less-differentiated CD8$^+$ T cells (52, 54, 201), one study reported its up-regulation on "exhausted" melanoma antigen-specific CD8$^+$ T cells in the periphery (53). Therefore, we wanted to examine the stability of BTLA's expression during *in vitro* culture with IL-2 as well as during TCR activation. We maintained bulk TILs either with low-dose (LD) IL-2 (200 IU/ml) or stimulated them with LD IL-2 plus agonistic αCD3 antibody (OKT3) (30 ng/ml) for three days. LD IL-2 was used in order to clearly distinguish the effect of TCR stimulation. TIL were subsequently stained for CD8, BTLA, CD25, and LIGHT; CD25 and LIGHT (homologous to **L**ymphotoxins, exhibits **I**nducible expression, and competes with HSV **G**lycoprotein D for **H**erpesvirus entry mediator, a receptor expressed by **T** lymphocytes, a ligand for the TNF receptor superfamily) were known to be up-regulated on activated T cells and hence served to indicate TCR stimulation (204, 205). On two separate TIL lines, we found that TCR stimulation, when compared to LD IL-2, did not significantly alter the expression of BTLA on CD8$^+$ TILs (TIL 2430: change from 82% to 89%; TIL 2425: change from 100 to 98%), whereas there were significant increases in CD25 (TIL 2430: change from 4% to 98%; TIL 2425: change from 86 to 100%) and LIGHT (TIL 2430: change from 9% to 79%; TIL 2425: change from 35 to 62%) (**Fig. 3-7)**.

Next, we sorted CD8$^+$BTLA$^+$ and CD8$^+$BTLA$^-$ subsets and assessed the effect of IL-2 on each subset's BTLA expression. The purity sort purity was shown on a representative TIL line (95% purity in the BTLA$^+$ subset and 99% purity in the BTLA$^-$ subset) (**Fig. 3-7C**). After 3 days of culture with LD IL-2, we found that a significant percentage of the CD8$^+$BTLA$^+$ subset became CD8$^+$BTLA$^-$ (26% BTLA$^+$ and 72% BTLA$^-$) (**Fig. 3-7C**). In

contrast, the sorted $CD8^+BTLA^-$ TIL remain $BTLA^-$ (1% $BTLA^+$ and 98% $BTLA^-$) (**Fig. 3-7C**). We were unable to compare the effect of TCR stimulation on sorted TILs due to limitations in the number of sorted $CD8^+BTLA^-$ TILs obtained from multiple TIL lines. In sum, our data demonstrated that $CD8^+BTLA^+$ TILs maintained stable expression of BTLA in response to TCR stimulation, and that they differentiated into $BTLA^-$ TIL when cultured with IL-2. $CD8^+BTLA^-$ TILs, on the other hand, did not up-regulate BTLA in response to TCR stimulation or differentiate into $BTLA^+$ TIL with IL-2. Our results are similar to a previous report demonstrating the stability of BTLA expression on peripheral melanoma antigen-specific $CD8^+$ T cells stimulated with cognate antigen (53).

Figure 3-7: **BTLA expression is stable upon TCR stimulation and is not up-regulated on the $CD8^+BTLA^-$ subset.** (**A**) Bulk TIL ($0.5x10^6$ cells) were cultured with 200 IU/ml IL-2 or IL-2 plus 30 ng/ml αCD3 mAb (OKT3) for 3 days. Cells were then stained for expression of CD8, BTLA, CD25 and LIGHT. Dead cells were excluded using Aqua® live/dead dye. The numbers indicate percentages of each marker within the gated $CD8^+$ TIL population. (**B)** A summary table of MFI of the BTLA, PD-1, LIGHT, and CD25 with low-dose (LD) IL-2 culture or with stimulation using OKT3 mAb, in TIL from two different patients. (**C, left panel**) the post-sort purity of the $CD8^+BTLA^+$ and $CD8^+BTLA^-$ subsets from a representative TIL line after cell sorting as described in *Material and Methods.* Each sorted subset was re-stained for expression of CD8 and BTLA. (**C**, **right panel**) shows the phenotype of the sorted TIL subsets five days after culturing with 200 IU/ml IL-2 *in vitro*.

Figure 3-7:

A

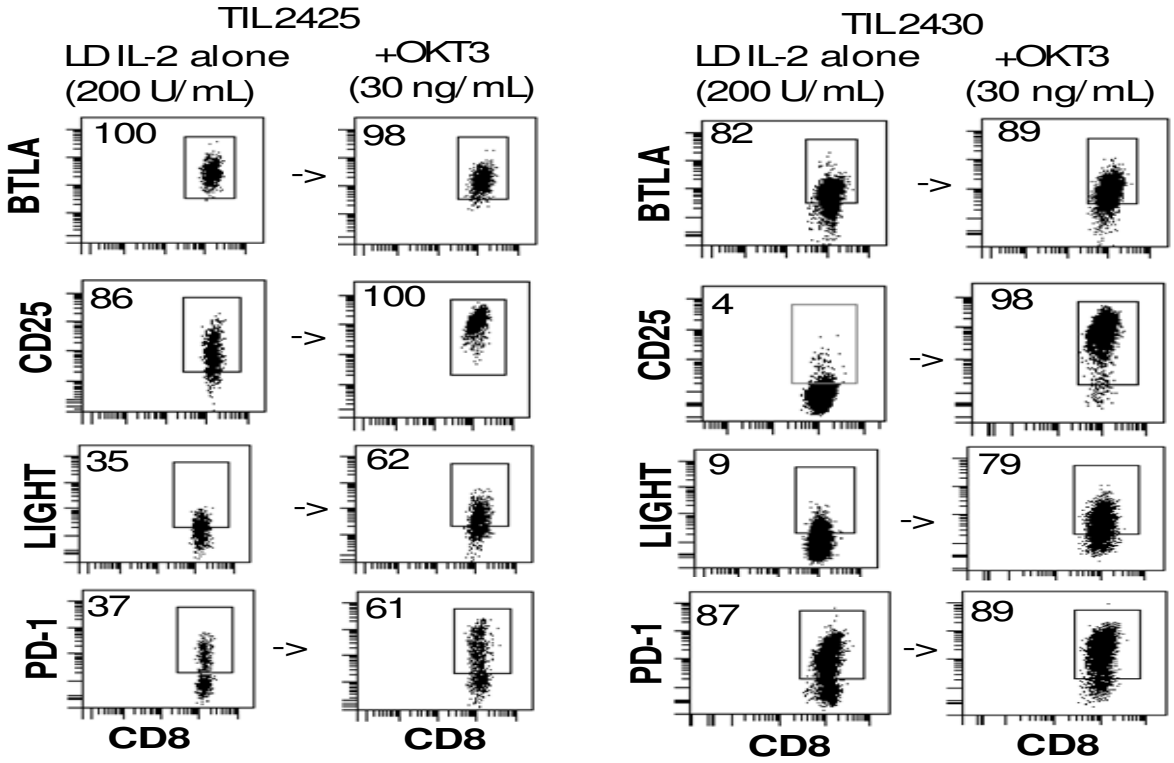

B

MFI / Marker(s)	TIL 2430		TIL 2425	
Stimulation Condition	**LD IL-2 alone**	**LD IL-2 + OKT3 (30 ng/mL)**	**LD IL-2 alone**	**LD IL-2 + OKT3 (30 ng/mL)**
BTLA	**653**	**975**	**3,319**	**1,841**
PD-1	**1695**	**2762**	**556**	**2,286**
CD25	**88**	**10,677**	**1,341**	**11,559**
LIGHT	**108**	**686**	**204**	**514**

Figure 3-7 con't.

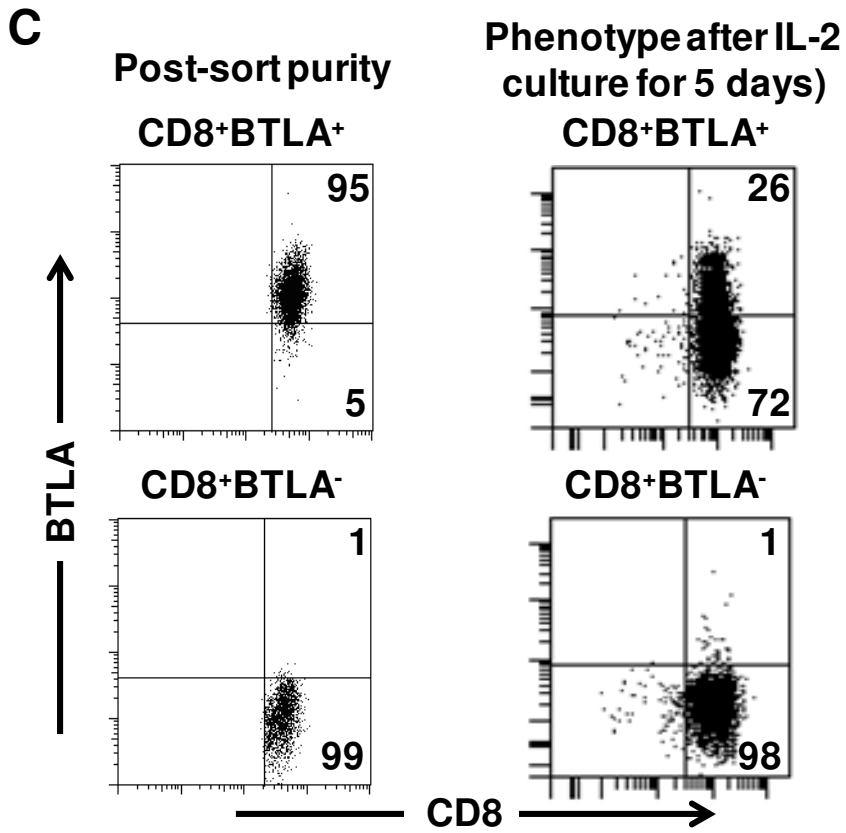

Enhanced proliferation of CD8$^+$BTLA$^+$ TIL with IL-2 culture in vitro.

Less-differentiated CD8$^+$ T cells are known to proliferate more rapidly than highly-differentiated T cells (124, 132, 191). Since our data on the surface phenotypes of the CD8$^+$BTLA$^+$ subset seemed to suggest it was less differentiated than the BTLA$^-$ subset (**Fig. 3-6**), we hypothesized that the CD8$^+$BTLA$^+$ TIL exhibited a higher proliferative capability than the CD8$^+$BTLA$^-$ TIL. In order to test this hypothesis, we sorted the CD8$^+$BTLA$^+$ and CD8$^+$BTLA$^-$ TIL, labeled them with CFSE, and tracked the extent of proliferation in each subset with cultured with 3,000 IU/ml IL-2. In fact, CD8$^+$BTLA$^+$ TIL from four different patients had higher fractions of proliferating cells and had undergone more cell divisions than the CD8$^+$BTLA$^-$ subset (TIL 2486: 58% vs. 36%, Division Index: 1.90 vs. 1.43; TIL 2488: 30% vs 18%, Division Index: 1.44 vs. 1.28; TIL 2605B: 84% vs. 53%, Division Index: 2.67 vs 1.31; TIL 2612: 73% vs. 8%, Division Index: 0.8 vs 0.18; **Fig. 3-8A** and **Fig. 3-9**). Furthermore, manual cell counting based on trypan blue exclusion after 6 days in culture showed that, CD8$^+$BTLA$^+$ TIL, on average, had higher fold expansion than the CD8$^+$BTLA$^-$ TIL (TIL 2425: 5.4-fold vs. 1.4-fold; TIL 2396: 2.2-fold vs. 0.9-fold; TIL 2486: 1.7-fold vs. 0.45-fold; **Fig. 3-8A** and **Fig. 3-9**). However, the lack of proliferation in response to IL-2 was not due to apoptosis of the CD8$^+$BTLA$^-$ subset as staining with Annexin-V did not show consistent difference in the survival between the subsets (TIL 2486: 36% vs 37% Annexin-V$^+$ cells; TIL 2488: 6% vs. 11% Annexin-V$^+$ cells) (**Fig. 3-8B**).

Next, when we compared the proliferation of the sorted CD8$^+$BTLA$^{+/-}$ subsets stimulated with plate-bound αCD3 Ab (OKT3) or αCD3 + αCD28 (OKT3+aCD28) in a ^{3}[H]-thymidine incorporation assay in the absence of exogenous IL-2, we consistently noted significantly more proliferation in the CD8$^+$BTLA$^+$ subset in four different TIL lines (**Fig. 3-**

8C). Although others have shown that $CD8^+CD27^+$ tumor antigen-specific T cells in the periphery proliferated more and possessed longer telomere length (191), a previous study from our group found that a difference in proliferation existed between the $CD8^+$ $CD28^{+/-}$ TIL subsets, not between the $CD8^+CD27^{+/-}$ TIL subsets (66). Therefore, we also compared the proliferative capacity of the sorted $CD8^+$ $BTLA^{+/-}$ vs. $CD27^{+/-}$ TIL subsets from two patients. We found that there was significantly more differences in the proliferating fractions between the sorted $CD8^+$ $BTLA^{+/-}$ subsets than the $CD27^{+/-}$ subsets (TIL 2605B: $BTLA^{+/-}$: 84% vs. 53%, $CD27^{+/-}$: 92% vs. 81%; TIL 2612 $BTLA^{+/-}$: 73% vs. 8%, $CD27^{+/-}$: 81% vs. 100%) (**Fig. 3-9**). In sum, our data suggest that the $CD8^+BTLA^+$ TIL consistently proliferate more than the $CD8^+BTLA^-$ TIL in response to IL-2 or TCR signaling, and that the difference in CD27 expression did not correspond to difference in $CD8^+$ TIL's proliferation.

Figure 3-8: **$CD8^+BTLA^+$ TIL have enhanced proliferation in response to IL-2 or TCR stimulation compared to the $CD8^+BTLA^-$ subset.** Sorted $CD8^+BTLA^{+/-}$ TIL subsets were labeled with CFSE and cultured (1 x 10^6/ml) with HD IL-2 for 5 days (3,000 IU/mL) (n=4). (**A**) shows the percentages of proliferating cells from two lines (top histograms). The absolute number of cells per subsets was determined using trypan blue exclusion and graphed as fold expansion (bottom graph). (**B**) Sorted cells from each were also stained CD8, Annexin-V, and 7-AAD. Two representative TIL lines are shown. The numbers indicate percent expression of each marker within the $CD8^+BTLA^{+/-}$ subsets. (**C**) Sorted $CD8^+BTLA^+$ and $CD8^+BTLA^-$ cells were stimulated with plate-bound anti-CD3 (OKT3), ant-CD3 and anti-CD28 (OKT3+aCD28) or not stimulated (NIL) in the absence of IL-2 for 3 days. Cells were pulsed with 1 μCi of [^{3}H]-thymidine for the last 18 hours of culture. Results were shown as counts per minute (cpm) from triplicate wells (mean ± S.D.). * indicates significance ($p<0.05$) as determined by Student's *t* test.

Figure 3-8:

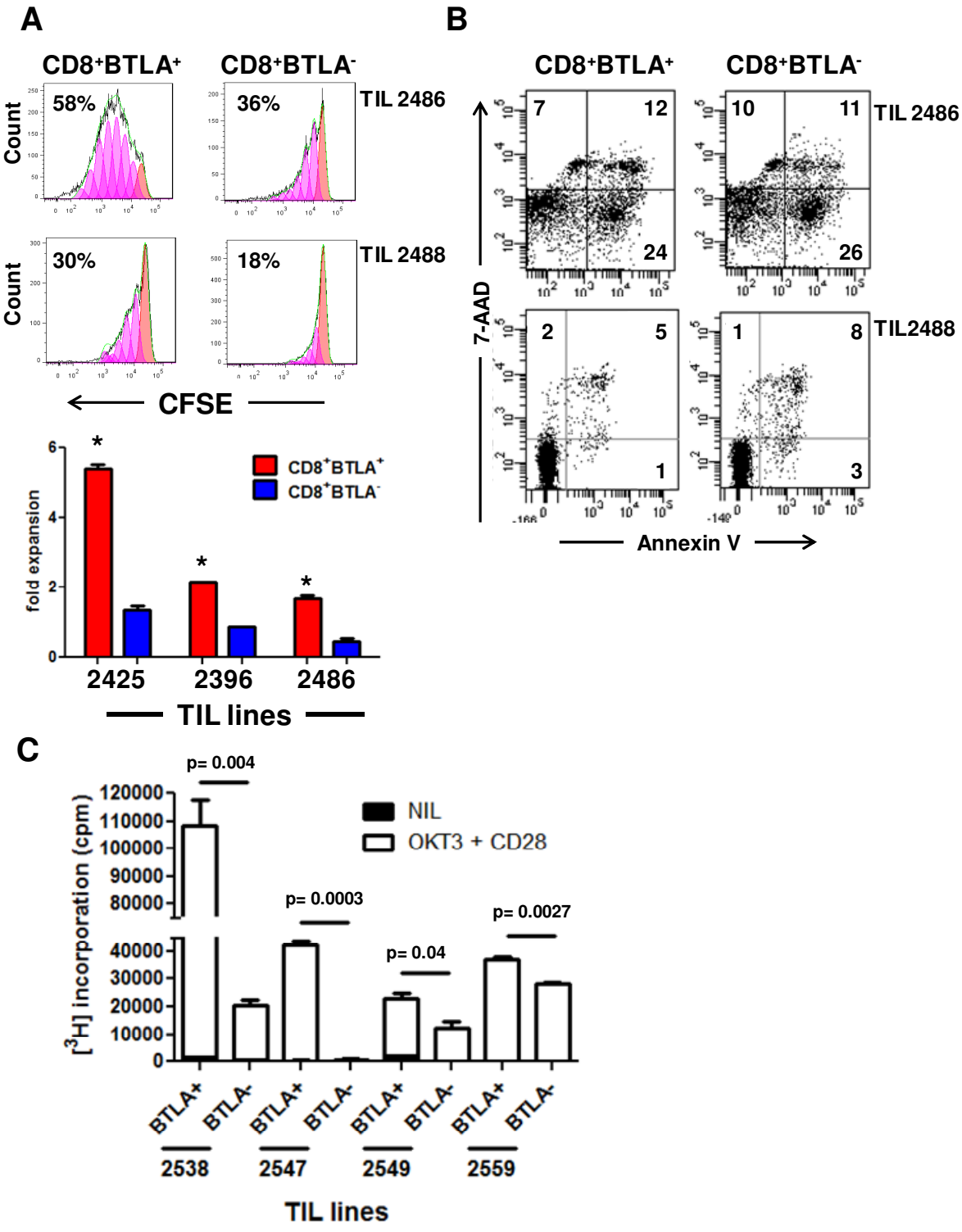
A
CD8+BTLA+
CD8+BTLA-
58%
36%
TIL 2486
Count
30%
18%
TIL 2488
CFSE
CD8+BTLA+
CD8+BTLA-
fold expansion
2425
2396
2486
TIL lines
B
CD8+BTLA+
CD8+BTLA-
7
12
24
10
11
26
TIL 2486
2
5
1
1
8
3
TIL2488
7-AAD
Annexin V
C
p= 0.004
p= 0.0003
p= 0.04
p= 0.0027
NIL
OKT3 + CD28
[3H] incorporation (cpm)
BTLA+
BTLA-
2538
2547
2549
2559
TIL lines

Figure 3-9: **Differences in proliferative capacity in response to IL-2 exists between $CD8^+BTLA^{+/-}$ TIL subsets, not between $CD8^+CD27^{+/-}$ TIL subsets.** Sorted $CD8^+BTLA^{+/-}$ or $CD8^+CD27^{+/-}$ TIL subsets were labeled with CFSE and cultured (1 x 10^6/ml) with HD IL-2 for 5 days (3,000 IU/mL) (n=4). (**A and B**) the percentages of proliferating cells from the indicated sorted subsets from two different TIL lines (**middle histograms**). The absolute number of cells per subsets was determined using trypan blue exclusion and graphed as fold expansion, with error bars denoting SEM (**rightmost graphs**).

Figure 3-9:

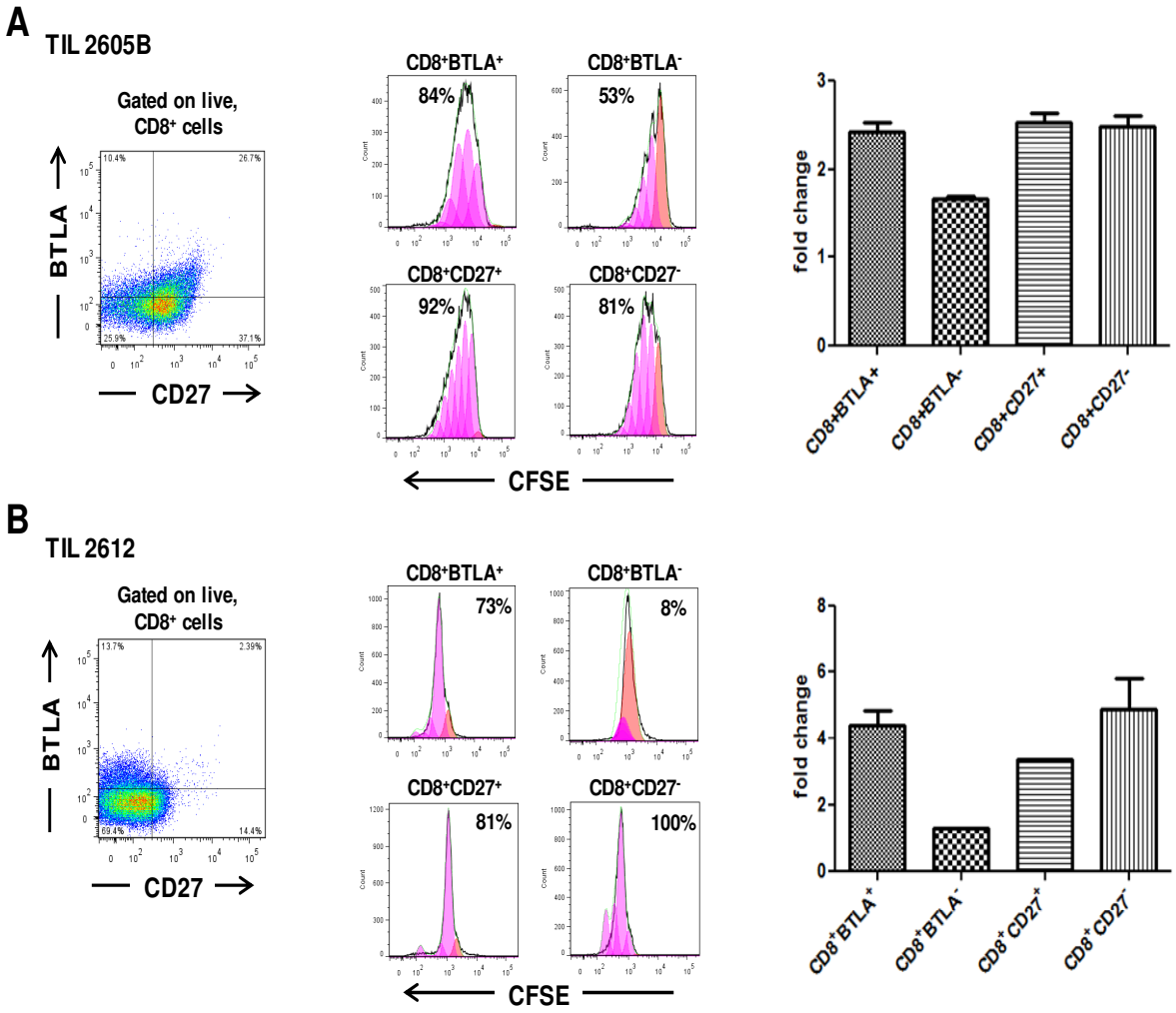
A
TIL 2605B
Gated on live,
CD8+ cells
BTLA
CD27
CD8+BTLA+
84%
CD8+BTLA-
53%
CD8+CD27+
92%
CD8+CD27-
81%
CFSE
fold change
CD8+BTLA+
CD8+BTLA-
CD8+CD27+
CD8+CD27-
B
TIL 2612
Gated on live,
CD8+ cells
BTLA
CD27
CD8+BTLA+
73%
CD8+BTLA-
8%
CD8+CD27+
81%
CD8+CD27-
100%
CFSE
fold change
CD8+BTLA+
CD8+BTLA-
CD8+CD27+
CD8+CD27-

The production of and responsiveness to IL-2 drives CD8$^+$BTLA$^+$ TIL's superior proliferation.

In order to explain the preferential expansion of the CD8$^+$BTLA$^+$ subset in response to IL-2, we hypothesized that the CD8$^+$BTLA$^+$ subset might express a higher level of the high-affinity IL-2 receptor, CD25 (IL2Rα), than the BTLA$^-$ subset as suggested by **Fig. 3-5**. Indeed, we found that a subset of CD25 expression was enriched within the CD8$^+$BTLA$^+$ subset in TIL from a representative patient, whereas there was very little CD8$^+$BTLA$^-$CD25$^+$ TIL (1%) within the BTLA$^-$ subset (**Fig. 3-10A, dot plot**). Furthermore, analysis of TIL from 28 patients, showed that there was a statistically significant difference in the MFI of CD25 expression between the CD8$^+$BTLA$^{+/-}$ subsets (**Fig. 3-10A**; $p = 0.002$; bottom panel).

Next, we hypothesized that the higher expression of CD25 in the CD8$^+$BTLA$^+$ subset might confer more responsiveness to IL-2. In order to this answer this question, we first sorted out CD8$^+$ BTLA$^{+/-}$ TIL subsets, treated them with different doses of IL-2 (none, 50 U/mL, 200 U/mL, and 3,000 U/mL), and determined the activation status of STAT5, which is activated downstream of the IL-2 receptor (206). We found that the CD8$^+$BTLA$^+$ subset had higher expression and MFI of phospho-Stat5 (pStat5) than those of the CD8$^+$BTLA$^-$ subset at all doses of IL-2 tested (**Fig. 3-10B, top panel**). Furthermore, when treated with 200 IU/mL of IL-2 for 20 minutes, CD8$^+$BTLA$^+$ TILs had higher levels of phospho-Stat5 (ΔMFI: 205) and phospho-Akt (ΔMFI: 74) than those of the CD8$^+$BTLA$^-$ TIL (**Fig. 3-10B, bottom panel**). We also explored the possibility whether the CD8$^+$BTLA$^+$ TIL could produce IL-2 in an autocrine fashion, since this has been reported as a feature of early-differentiated CD8$^+$ memory T cells in humans (203, 207). In sorted CD8$^+$ BTLA$^{+/-}$ subsets from two different patients, we found that the CD8$^+$BTLA$^+$ TIL produced more IL-2 than the

$CD8^+BTLA^-$ subset when stimulated with PMA and ionomycin (TIL 2547 ΔMFI: 274; TIL 2538 ΔMFI: 652) (**Fig. 3-10C**). Lastly, to further confirm that the autocrine production of IL-2 by the $CD8^+BTLA^+$ TIL contributed to its superior proliferation, we compared the proliferation of the TCR-stimulated $CD8^+BTLA^+$ TIL with or without anti-human IL-2 neutralizing mAb. We found that IL-2 neutralization significantly reduced the proliferation of the $CD8^+BTLA^+$ TIL to the same level as the $BTLA^-$ counterparts (**Figure 3-10D, bottom panel**). TCR-stimulated $CD8^+BTLA^-$ TIL did not proliferate as well as the $CD8^+BTLA^+$ TIL in the absence of IL-2 (**Fig. 3-10D, top panel**), and hence neutralization of IL-2 in the culture affected its proliferation to a lesser extent than that of the $CD8^+BTLA^+$ TIL (**Fig. 3-10D, bottom panel**). Therefore, the superior proliferation of the $CD8^+BTLA^+$ TIL subset could be partially explained by its higher level of autocrine IL-2 production and better responsiveness to IL-2 signaling than those of the $CD8^+BTLA^-$ TIL.

Figure 3-10: $CD8^+BTLA^+$ TIL's autocrine IL-2 production and higher responsiveness to IL-2 contributes to its superior proliferation. (**A, top panel**) TIL were stained for expression of CD8, BTLA, and CD25 along with the Aqua® live/dead viability dye. The dot plot shows representative staining of TIL 2559. The numbers indicated percent expression within the $CD8^+$ TIL population. (**A, bottom panel**) a summary graph of the CD25 MFI between the $CD8^+BTLA^{+/-}$ subsets (n=23). *p* value was calculated using Wilcoxon signed-rank test. (**B**) TIL were sorted into $CD8^+BTLA^+$ (**red**) and $CD8^+BTLA^-$ (**blue**) subsets. Cells were subsequently cultured with increasing concentrations of IL-2 for 20 minutes, fixed, permeabilized and stained for pStat5 (Y694) and pAkt (S473). The top panel shows the percent pStat5 expression as well as the MFI between the subsets in TIL 2538. The bottom histograms show the level of pStat5 and pAkt expression after treatment with 200 IU/ml IL-2 for 20 minutes. The change in MFI (Δ MFI) between the subsets is shown. (**C**) Sorted $CD8^+BTLA^{+/-}$ subsets were stimulated with PMA and ionomycin for 4 hours and stained for IL-2 intracellularly. The numbers indicate the MFI for each subset from 2 TIL lines. (**D**) The sorted subsets were labeled with a cell proliferation dye, eFluor670®, and stimulated with increasing doses of anti-CD3 (OKT3) for 3 days with or without 10 μg/ml of an anti-human IL-2 neutralizing antibody. (**D, top panel**) the extent of proliferation of the $CD8^+BTLA^+$ (**circles**) vs. $CD8^+BTLA^-$ (**squares**) subsets in response to OKT3 alone as percent eFluor dilution. (**D, top panel**) The bottom panel shows proliferation of the subsets with IL-2 blockade.

Figure 3-10:

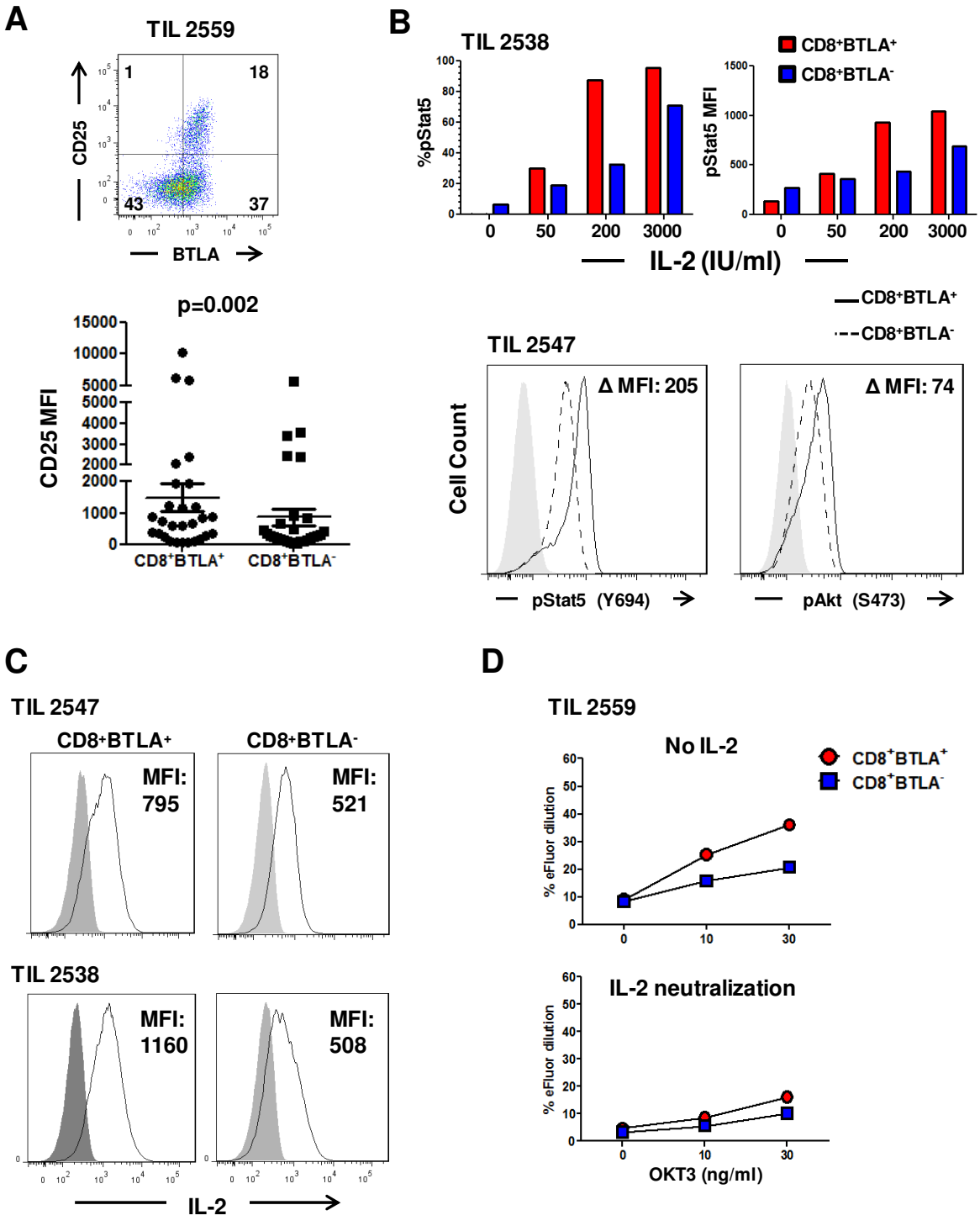
A
TIL 2559
1
18
43
37
CD25
BTLA
p=0.002
CD25 MFI
CD8+BTLA+
CD8+BTLA-
B
TIL 2538
%pStat5
pStat5 MFI
CD8+BTLA+
CD8+BTLA-
IL-2 (IU/ml)
TIL 2547
Δ MFI: 205
Δ MFI: 74
Cell Count
pStat5 (Y694)
pAkt (S473)
C
TIL 2547
CD8+BTLA+
CD8+BTLA-
MFI: 795
MFI: 521
TIL 2538
MFI: 1160
MFI: 508
IL-2
D
TIL 2559
No IL-2
% eFluor dilution
IL-2 neutralization
OKT3 (ng/ml)

$CD8^+BTLA^+$ TIL display a higher degree of polyfunctional cytokines production than the $CD8^+BTLA^-$ subset.

One measurement of $CD8^+$ T cells' polyfunctionality is their ability to produce multiple cytokines at high levels simultaneously (208). Thus, we were interested to further examine whether $CD8^+BTLA^+$ TILs were capable of producing high levels of cytokines other than IL-2. To this end, we collected tissue culture supernatants from 5 x 10^4 cells of each sorted $CD8^+$ $BTLA^{+/-}$ subset, from four different patients, stimulated with agonistic αCD3 Ab (OKT3) or αCD3 + αCD28 Abs (OKT3 + CD28) for three days. We used a multiplex cytokine assay to measure the concentrations of IFN-γ, TNF-α, and MIP-1β, which are cytokines known to be produced by human $CD8^+$ T cells (208). In fact, sorted $CD8^+BTLA^+$ TIL subset from 4 out of the 4 patients tested produced more IFN-γ after CD3 (OTK3) and CD28 stimulations than the $CD8^+BTLA^-$ subset (**Figure 3-11A and Table 3-I**). $CD8^+BTLA^+$ TIL from 3 out of 4 patients produced more MIP-1β, and the same TIL from 2 out of 4 patients produced more TNF-α. Therefore the $CD8^+BTLA^+$ TIL subset are in a more activated state after TCR stimulation and are more polyfunctional than the $CD8^+BTLA^-$ TIL subset.

Figure 3-11: $CD8^+$ $BTLA^+$ TIL are more polyfunctional than their $BTLA^-$ counterparts. $CD8^+BTLA^+$ (red) and $CD8^+BTLA^-$ (blue) TIL were sorted and stimulated with plate-bound anti-CD3 (30ng/ml) (OKT3), anti-CD3 and anti-CD28 (1μg/ml) (OKT3 + CD28) or left unstimulated (TIL alone) for 3 days. Supernatants were collected, diluted 1:3 and tested for the presence of IFN-γ, TNF-α, and MIP-1β using Multiplex technology. Data is shown as mean ± SD from triplicate wells for each condition. (n=4)

Figure 3-11:

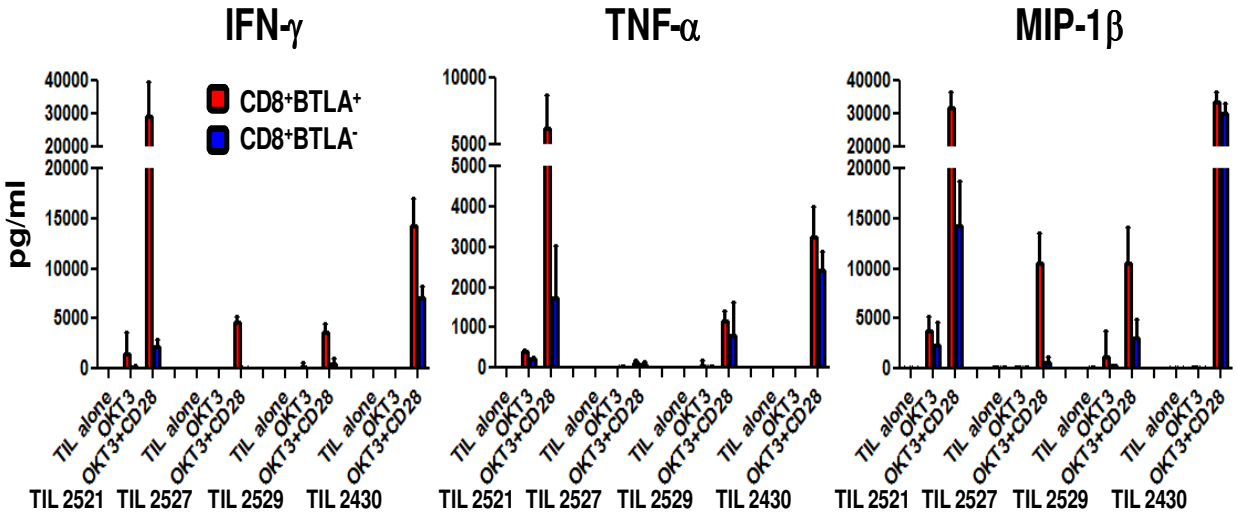
IFN-γ
TNF-α
MIP-1β
CD8+BTLA+
CD8+BTLA-
pg/ml
TIL alone
OKT3
OKT3+CD28
TIL 2521
TIL 2527
TIL 2529
TIL 2430

Table 3-I: Concentrations of cytokines before and after stimulation(s)

IFN-γ (pg/mL)		$CD8^+BTLA^+$		$CD8^+BTLA^-$	
	Stimulation Conditions	Mean Conc.	SEM	Mean Conc.	SEM
TIL 2521	TIL alone	5.5	1	6.1	1.6
	OKT3	1493	511.2	191.4	19.1
	OKT3 + CD28	29208.5	2394.6	2207.2	149.1
TIL 2527	TIL alone	11.4	0.8	10.6	0.8
	OKT3	14.2	5.9	14.8	2.9
	OKT3 + CD28	4602.5	156.8	36.2	8.8
TIL 2529	TIL alone	6.1	1.6	4.9	0.6
	OKT3	166.8	109.4	13.1	2.9
	OKT3 + CD28	3600.4	214.1	396.7	147
TIL 2430	TIL alone	7.3	0	10.5	1.3
	OKT3	9.8	1.7	17.7	5.2
	OKT3 + CD28	14261.5	642.2	7075.6	265.5
TNF-α (pg/mL)					
	Stimulation Conditions				
TIL 2521	TIL alone	3.5	0.6	0.3	0
	OKT3	409.9	5.9	214.9	10
	OKT3 + CD28	6248.6	573.6	1754.8	296.1
TIL 2527	TIL alone	0.6	0	1.7	1.1
	OKT3	0.4	0.2	10.5	4.1
	OKT3 + CD28	122.1	11.3	74.7	18.7
TIL 2529	TIL alone	2.3	0	0.3	0
	OKT3	55.3	28.3	20.1	3.1
	OKT3 + CD28	1155.7	59.4	810.3	186.7
TIL 2430	TIL alone	0.3	0	0	0
	OKT3	0.3	0	0.3	0
	OKT3 + CD28	3258.1	174.9	2428.2	107.9
MIP-1β (pg/mL)					
	Stimulation Conditions				
TIL 2521	TIL alone	65.9	5.7	81.4	2.9
	OKT3	3812.2	323.3	2364.4	539.7
	OKT3 + CD28	31996.9	1032	14351	1031.6
TIL 2527	TIL alone	96.4	8	83.7	4.6
	OKT3	113.9	19.6	86.4	15.6
	OKT3 + CD28	10558.8	704.7	600.2	135
TIL 2529	TIL alone	12	0	75	8.7
	OKT3	1182.2	587.7	263.6	22.9
	OKT3 + CD28	10530.9	835.1	3085.6	440.4
TIL 2430	TIL alone	33.5	5.2	33.5	5.2
	OKT3	101.6	21.2	42.7	8
	OKT3 + CD28	33749.7	694.2	30126.6	679.2

$CD8^+BTLA^+$ and $CD8^+BTLA^-$ TIL subsets exhibit similar levels of CTL activity.

We originally hypothesized that $CD8^+BTLA^+$ TIL might display a higher level of cytolytic activity against either αCD3-loaded targets or autologous melanoma tumor cells, which might explain the positive clinical association with this subset. To test this hypothesis, we sorted $CD8^+$ BTLA+/- TIL subsets from 6 different patients and co-cultured them for 3 hours with αCD3-loaded P815 target cells (murine mastocytoma cell lines) in a redirected lysis assay. Target cells were labeled prior to the co-culture with a fluorescent dye, DDAO-SE, in order to distinguish them from the effector T cells. Compared to the co-culture system with autologous tumor cells, the advantage of this system was that there was an activation of polyclonal T cells in each subset, so the CTL activity is not influenced by the frequencies of tumor antigen-specific populations in each subset. Contrary to our expectation, we did not find a significance difference in the percentage of the killed (DDAO-SE^+Caspase-3^+) P815 target cells co-cultured with either sorted $CD8^+BTLA^+$ or $BTLA^-$ TIL (**Fig. 3-12A**). We also co-cultured sorted $CD8^+$ $BTLA^{+/-}$ subsets with autologous tumor cells and tested their degranulation (CD107a) and release of IFN-γ as well as direct tumor killing via active-caspase-3 staining as before. In a representative TIL shown (**Fig. 3-12B**), we did not find significant difference in the percentages of $CD107^+$ populations ($BTLA^+$: 57% vs $BTLA^-$: 53%) or $CD107a^+IFN\text{-}\gamma^+$ double-positive populations between each subset ($BTLA^+$: 39% vs. $BTLA^-$: 34%) (**Fig. 3-12B**). Furthermore, the percentage of tumor targets killed (DDAO-SE^+Caspase-3^+) was similar between the two subsets ($BTLA^+$: 32% vs. $BTLA^-$: 29%). Notably, we have shown earlier that there were no significant differences in the levels of GB and Perf expressions between the two TIL subsets (**Fig. 3-12B**). Therefore, parameters of

$CD8^+$ T cells functions other than CTL activities between the two subsets may account for the observed positive clinical association with $CD8^+BTLA^-$ TIL.

Figure 3-12: No significant difference in CTL activities between $CD8^+BTLA^+$ vs $BTLA^-$ TIL subsets. (**A**) $CD8^+BTLA^+$ and $CD8^+BTLA^-$ TIL were sorted and co-cultured with P815 target cells pulsed with 300ng/ml OKT3 for 3 hours. Unpulsed targets were used as a negative control. Targets (T) were labeled with the far-red dye, DDAO-SE, to distinguish from effectors (E). E:T ratios of 1:3, 1:1 and 3:1 were used. After 3 hours, cells were permeabilized and stained for the presence of active caspase-3 by flow cytometry. The dot plots show representative staining of active caspase-3 on the DDAO-SE labeled targets (3:1 E:T ratio). The numbers indicate percent expression of caspase-3. The unpulsed control is shown on the bottom row. The right graph indicates the level of active caspase-3 staining from 6 TIL lines at each E:T ratio. The mean ± SE is shown for each ratio. (**B**) Sorted $CD8^+BTLA^{+/-}$ subsets were cultured 1:1 with autologous tumor cells labeled with DDAO-SE. After 3 hours, cells were harvested, permeabilized and stained for active caspase-3 as in (**A**). After 6 hours, cells were harvested, permeabilized and stained for surface CD8 and intracellular IFN-γ. CD107a PE antibody was added for the duration of the culture. Cells are gated on the $CD8^+DDAO\text{-}SE^-$ population. HLA-mismatched tumor from a different patient (2320) was used as a negative control.

Figure 3-12:

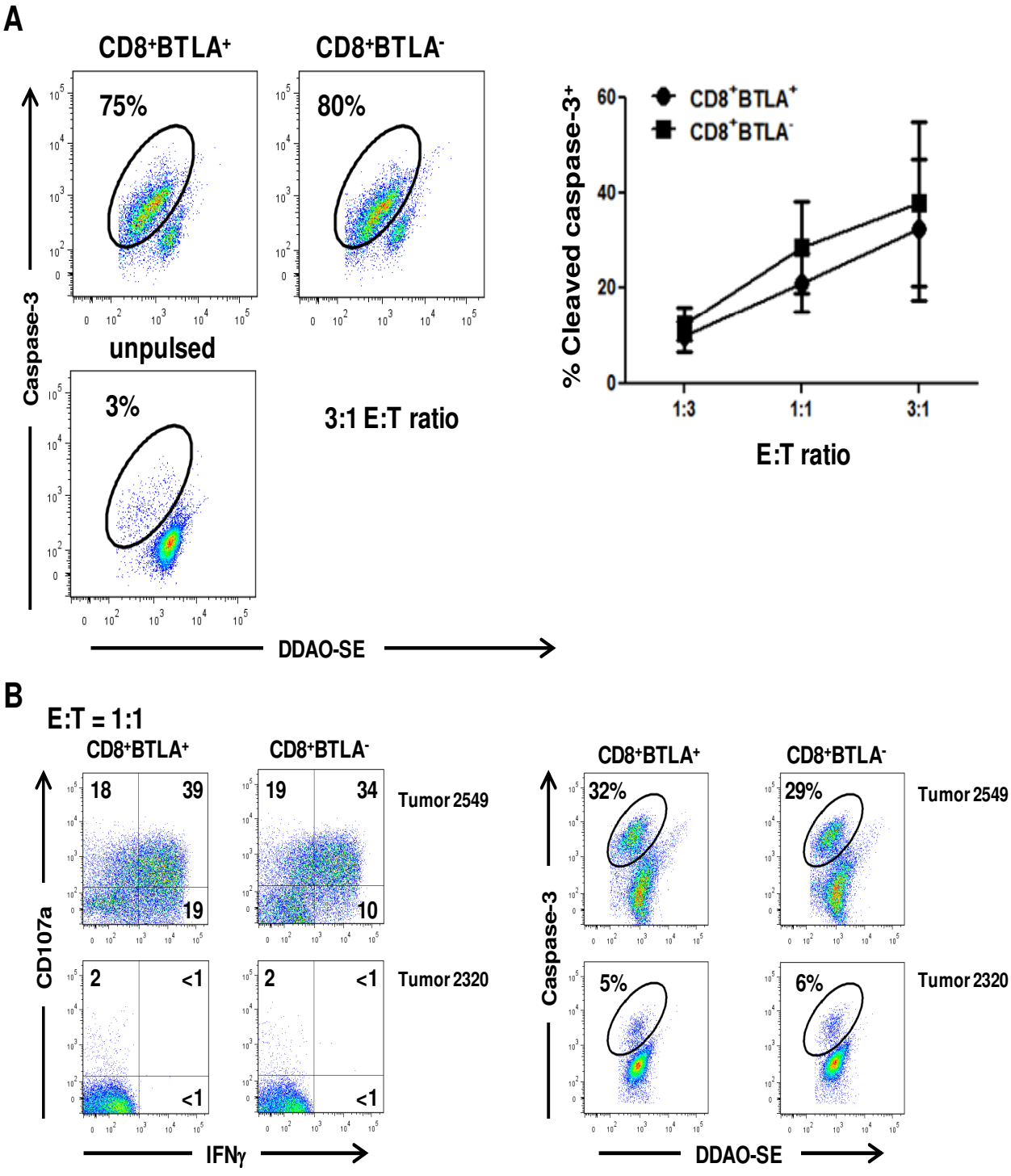
A
CD8+BTLA+
CD8+BTLA-
75%
80%
unpulsed
3%
Caspase-3
DDAO-SE
3:1 E:T ratio
% Cleaved caspase-3+
CD8+BTLA+
CD8+BTLA-
60
40
20
0
1:3
1:1
3:1
E:T ratio
B
E:T = 1:1
CD8+BTLA+
CD8+BTLA-
18
39
19
19
34
10
Tumor 2549
2
<1
<1
2
<1
<1
Tumor 2320
CD107a
IFNγ
CD8+BTLA+
CD8+BTLA-
32%
29%
Tumor 2549
5%
6%
Tumor 2320
Caspase-3
DDAO-SE

Differential gene expression profiles between $CD8^+BTLA^+$ and $CD8^+BTLA^-$ melanoma TIL.

A major aim of our study was to determine difference in the global gene expression profile between of $CD8^+$ $BTLA^+$ and $BTLA^-$ TIL. We used highly purified $CD8^+BTLA^+$ and $BTLA^-$ TIL from five different melanoma patients for gene expression studies using Affymetrix® Human Gene 1.0 ST Array containing 33,297 human transcripts. The microarray data has been deposited into the NCBI Gene Expression Omnibus (GEO) database (Accession # GSE43260). An example of post-sort analysis of $CD8^{Hi}BTLA^+$ and $BTLA^-$ TILs is shown (**Fig. 3-7C, left panel**). To confirm that the sorted cells are T cells (NK cells can express low levels of CD8), we did not find significant differences in the expression intensities of the TCR subunits, CD3ε and CD3δ, from the microarray data on the sorted $CD8^+BTLA^+$ and $BTLA^-$ TIL subsets (**Fig. 3-13**). As an internal control, we ascertained that the expression of the BTLA gene was significantly higher in the sorted $CD8^+BTLA^+$ subset (7.69-fold higher, $p = 8.80 \times 10^{-6}$; Student's paired *t* test) (**Table 3-II**). Using an arbitrary selection criteria to assess for significantly different genes between the two subsets (paired *t* test; fold change ≥ 1.45; $p < 0.05$), we determined that there were 406 differentially-expressed genes (DEGs). Among these, 171 genes were up-regulated in the $CD8^+BTLA^+$ subset, and 235 genes were up-regulated in the $CD8^+BTLA^-$ subset. In agreement with the surface phenotypes of the $CD8^+BTLA^+$ subset (**Fig. 3-6**), we found that there were significantly increased expressions of effector-memory genes [*CD28* (2.38-fold higher, $p = 0.025$), CD127 (IL7R) (2.08-fold higher, $p = 0.03$)], and late-differentiation genes [*B3GAT1* (CD57, or β-1,3-glucoronyltransferase 1; 1.79-fold higher, $p = 0.0008$). We also found CX3CR1 [a chemokine receptor for CX3CL1 (Fractalkine)] to be highly

expressed by the $CD8^+BTLA^+$ TIL (3.33-fold higher; $p = 8.18x10^5$)] (**Table 3-II**); CX3CR1 has been reported to be expressed by the senescent $CD8^+CD57^+$ T cells in the periphery (167) as well highly-differentiated $CD8^+$ and $CD4^+$ T cells (209). We did not find statistically significant difference in the expression of the *CD27* gene between the two TIL subsets. Interestingly, we also found increased expression of CD86 (2.0-fold higher, $p = 0.04$) and CD80 (1.45-fold higher, $p = 0.01$), which were costimulatory molecules expressed by antigen-presenting cells (APCs) and T cells (206), in the $CD8^+BTLA^+$ subset (**Table 3-II**). On the other hand, in the $CD8^+BTLA^-$ subset, there were significantly increased expressions of 13 members of the killer-cell immunoglobulin-like receptor (*KIR*) gene family, *KLRG-1* (killer-cell lectin-like receptor G1; 2.36-fold higher, p=0.04), and *TYROBP* gene (DAP12, an adaptor protein for the KIR receptors, ref. (210); 4.11-fold higher; $p = 0.0002$) (**Table 3-III**). KIR receptors are known to be expressed by NK cells (194), highly differentiated $CD8^+PD\text{-}1^-$ $CD45RA^+$ T_{EMRA} lymphocytes from normal donors' PBMC (166, 196), and senescent human $CD8^+CD28^-$ T cells (66, 195), while KLRG-1 is known to be expressed by NK cells and $CD8^+$ effector and memory T cells in humans with reduced proliferative capacity (170, 171, 211). We confirmed the preferential protein expressions of some KIR receptors in the $CD8^+BTLA^-$ subset by flow cytometry (**Fig. 3-14B**). We also found that the expressions of other genes typically associated with NK cells, such as *NCAM1* [(CD56; 3.42-fold higher, $p = 0.01$), *LYN* (2.41-fold higher, $p = 0.025$), and *SYK* (1.8-fold higher, $p = 0.02$)] (212, 213), were also significantly increased in the $CD8^+BTLA^-$ subset (**Table 3-III**). Lastly, we observed that the expressions of the genes associated with T cell deletion and anergy (197), such as *IKZF2* [IKAROS family zinc finger 2; 5.08-fold higher, $p = 0.00076$; ref. (198, 214)], *EGR2* [Early growth response 2; 1.82-fold higher, $p = 0.0185$; ref. (198, 215)], and

NR4A3 [(Nuclear receptor subfamily, group A, member 3; 1.8-fold higher, $p = 0.0014$; ref. (198, 215, 216)], were also significantly increased in $CD8^+BTLA^-$ TIL (**Table 3-II**). Similarly, others have shown that the $CD8^+$ T_{EMRA} ($PD\text{-}1^-$) lymphocytes from normal donor PBMC had increased expressions of the *IKZF2*, *NCAM1, LYN,* and *TYROBP* genes compared to the $PD\text{-}1^+$ T_{EM} subset (166).

Table 3-II: Partial list of genes significantly upregulated in $CD8^+BTLA^+$ TIL

Entrez ID	Gene Symbol	Fold change ($BTLA^+/BTLA^-$)	*p*-value
151888	BTLA	7.69	8.80E-06
1524	CX3CR1	3.33	8.18E-05
940	CD28	2.38	0.0254706
3575	IL7R	2.08	0.0300249
942	CD86	2.00	0.0411847
4345	CD200	1.89	0.0029873
27087	B3GAT1	1.79	0.0008077
3122	HLA-DRA	1.69	0.0112811
3577	CXCR1	1.69	0.0124128
57007	CXCR7	1.67	0.0003392
3119	HLA-DQB1	1.67	0.0003418
3122	HLA-DRA	1.67	0.0156466
3119	HLA-DQB1	1.67	0.024055
3111	HLA-DOA	1.64	0.0033466
3117	HLA-DQA1	1.61	0.004212
3108	HLA-DMA	1.54	0.0059107
50615	IL21R	1.52	0.0008461
3115	HLA-DPB1	1.52	0.0283427
3108	HLA-DMA	1.49	0.0029988
3118	HLA-DQA2	1.49	0.0080474
3127	HLA-DRB5	1.49	0.02435
3115	HLA-DPB1	1.49	0.038801
941	CD80	1.45	0.0100546
3113	HLA-DPA1	1.45	0.0266463
3684	ITGAM	1.45	0.0423103

Table 3-III: Partial list of genes significantly up-regulated in $CD8^{+}BTLA^{-}$ TIL

Entrez ID	Symbol	Fold change ($BTLA^{-}/BTLA^{+}$)	*p* -value
3805	KIR2DL4	7.8	0.003174
3804	KIR2DL3	7.78	0.007904
3813	KIR3DS1	6.67	0.009093
3802	KIR2DL1	6.56	0.002523
3805	KIR2DL4	6.38	0.003126
3812	KIR3DL2	6.08	0.004395
100132285	KIR2DS2	6.04	0.005326
3811	KIR3DL1	6.01	0.008326
3806	KIR2DS1	5.81	0.004101
3809	KIR2DS4	5.29	0.006637
3803	KIR2DL2	5.15	0.002984
22807	IKZF2	5.08	0.000761
3811	KIR3DL1	4.83	0.003344
3824	KLRD1	4.44	0.002406
3804	KIR2DL3	4.4	0.003473
100528032	KLRC4-KLRK1	4.35	0.027612
7305	TYROBP	4.11	0.000245
3822	KLRC2	3.91	0.008132
3821	KLRC1	3.62	0.007245
115653	KIR3DL3	3.57	0.00377
2207	FCER1G	3.43	0.000289
3823	KLRC3	3.43	0.012605
4684	NCAM1	3.42	0.011811
115653	KIR3DL3	3.29	0.005053
9173	IL1RL1	3.07	2.09E-05
55359	STYK1	2.78	0.003243
8302	KLRC4	2.66	0.048535
9437	NCR1	2.63	0.004604
10748	KLRAP1	2.61	0.00422
4067	LYN	2.41	0.02504
10219	KLRG1	2.36	0.039295
3595	IL12RB2	2.3	0.002999
3810	KIR2DS5	2.29	0.00413
57292	KIR2DL5A	2.17	0.008793
11126	CD160	2.08	0.017882
3460	IFNGR2	1.97	0.0153
3815	KIT	1.94	0.022978
343413	FCRL6	1.83	0.019832
1959	EGR2	1.82	0.018586
1958	EGR1	1.81	0.044018
8013	NR4A3	1.8	0.001398
6850	SYK	1.8	0.023553
952	CD38	1.71	0.000111
131450	CD200R1	1.56	0.000577
7422	VEGFA	1.55	0.017533
55801	IL26	1.47	0.0488

Figure 3-13: No find significant differences in the Log_2 normalized expression intensities of the TCR subunits, CD3ε and CD3δ, between $CD8^+BTLA^+$ vs $BTLA^-$ TIL, from the Affymetrix® Human Gene 1.0 ST microarray data on the sorted $CD8^+BTLA^+$ and $BTLA^-$ TIL subsets

Figure 3-13:

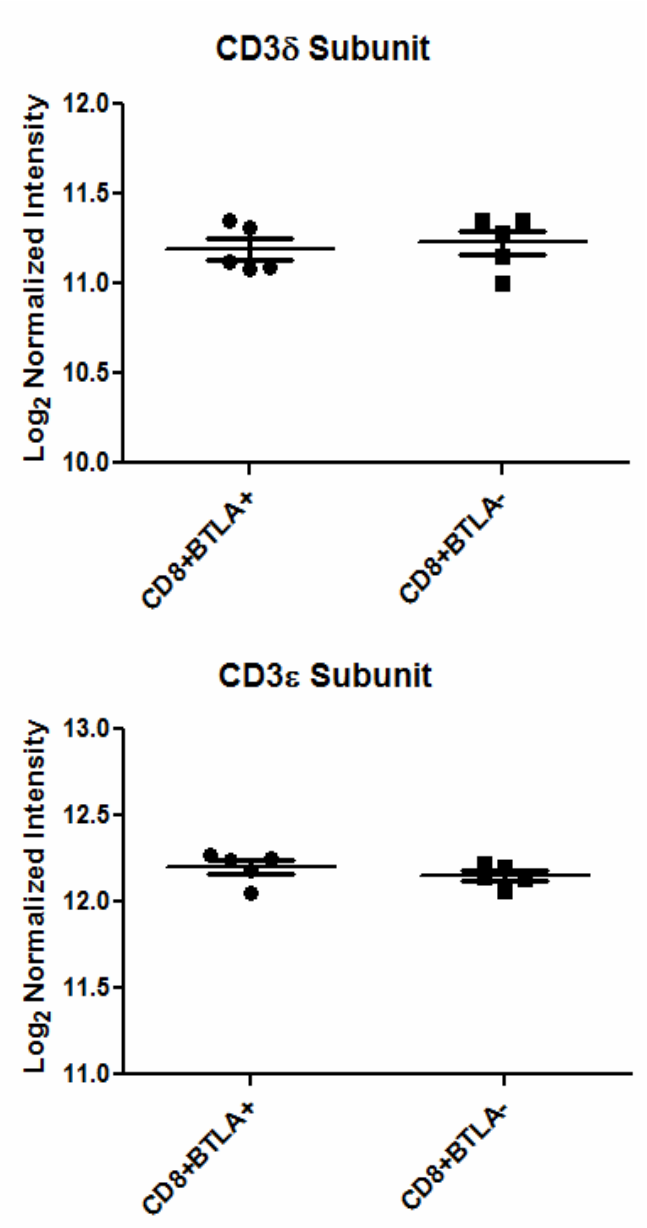
CD3δ Subunit
Log2 Normalized Intensity
12.0
11.5
11.0
10.5
10.0
CD8+BTLA+
CD8+BTLA-
CD3ε Subunit
Log2 Normalized Intensity
13.0
12.5
12.0
11.5
11.0
CD8+BTLA+
CD8+BTLA-

Enrichment of a molecular signature of T cell deletion in the CD8$^+$BTLA$^-$ TIL subset.

We also employed Gene set Enrichment Analysis (GSEA) to analyze our microarray data, which is a powerful approach to look for enrichment of global or pre-defined set of genes in either TIL subset. The top 50 genes ranked by the degree of enrichment in either the CD8$^+$BTLA$^+$ or CD8$^+$BTLA$^-$ subsets are shown (**Fig. 3-14**). Some of the genes listed in the heat map, such as CD28, IL7R, KIR receptors, showed agreement with the lists of DEGs described previously (**Tables 3-I and 3-II**). A complete list of genes ranked by the enrichment scores [-1 (enriched in CD8$^+$BTLA$^-$ subset) to +1 (enriched in CD8$^+$BTLA$^+$ subset)] are available (data not shown). We next asked which biologic processes could explain the lack of proliferation and responsiveness to TCR and IL-2 signals in the CD8$^+$BTLA$^-$ TIL subset (**Fig. 3-8** and **Fig. 3-10**). We set out to determine whether gene-set signatures deriving from CD8$^+$ T cells undergoing exhaustion in chronic viral infection or cancer (217, 218), deletion (198), or anergy (198), were enriched in our ranked-order list of DEGs. We did not find enrichment of exhaustion signature derived from Baitsch, L., *et al.* [p = 0.31; ref. (217)] or Wherry, E.J., *et al.* [(p = 0.50; ref. (218)] in either TIL subsets (**Fig. 3-14C, top panels**). We also did not find enrichment of T cell anergy signature in either TIL subsets (p = 0.53; **Fig. 3-14C**, **bottom left panel**). However, we discovered an enrichment of a molecular signature corresponding to T cell deletion (p = 0.00) in the CD8$^+$BTLA$^-$ TIL subset (**Fig. 3-14C, bottom right panel**). Our analysis of the microarray data provides further support that CD8$^+$BTLA$^+$ TIL is a less-differentiated T_{EM} subset, whereas CD8$^+$BTLA$^-$ TIL is a highly-differentiated, KIR-expressing subset within T_{EM} exhibiting molecular signature of T cell deletion, and hence lack of proliferation and responsiveness to IL-2 or TCR signals.

Figure 3-14: $CD8^+BTLA^+$ TIL have a less differentiated phenotype while $CD8^+BTLA^-$ TIL exhibit a T-cell deletion signature. (**A**) Enrichment analysis of a global set of genes from $CD8^+BLTA^+$ or $BTLA^-$ subsets. The top 50 genes, ranked by enrichment scores using gene-set enrichment analysis (GSEA), that are immunologically relevant in either $BTLA^+$ or $BTLA^-$ subset are shown. Red indicates over-expression and blue under-expression relative to the mean. Each row represents one gene and each column represents 1 sample of highly purified $CD8^+BTLA^+$ or $BTLA^-$ subset from 1 patient. (**B**) Flow cytometry plots of the $CD3^+CD8^+$ TIL from a representative patient showing the expression of BTLA and killer-cell immunoglobulin-like receptors (KIR): CD158a (KIR2DL1), CD158b (KIR2DL2/3), and NKAT2 (KIR2DL3). Percentages of KIR^+ population out of the total $CD3^+CD8^+$ TILs are shown. (**C, D**) GSEA of previously published gene-set signatures deriving from $CD8^+$ T cells undergoing exhaustion (217, 218), anergy (198), or deletion (198). Positions of selected example genes from statistically significant gene sets ($p < 0.05$ and FDR < 0.25, as suggested in the online tool) are indicated. Gene sets comprise genes enriched in "exhausted" T cells (**B**) or in anergic T cells or T cells undergoing deletion (**D**).

Figure 3-14:

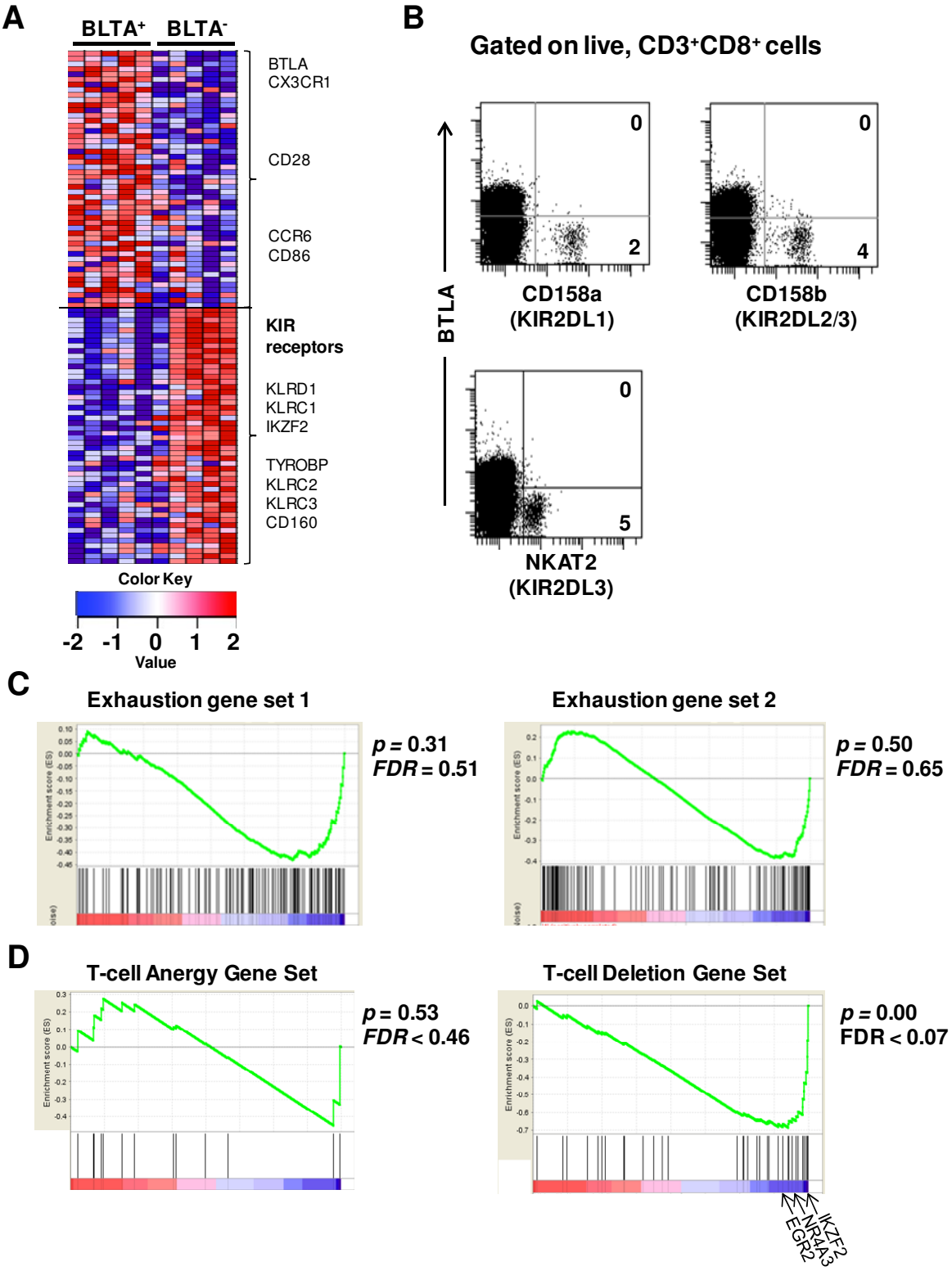
A
BLTA+
BLTA-
BTLA
CX3CR1
CD28
CCR6
CD86
KIR receptors
KLRD1
KLRC1
IKZF2
TYROBP
KLRC2
KLRC3
CD160
Color Key
-2 -1 0 1 2
Value
B
Gated on live, CD3+CD8+ cells
BTLA
0
2
CD158a (KIR2DL1)
0
4
CD158b (KIR2DL2/3)
0
5
NKAT2 (KIR2DL3)
C
Exhaustion gene set 1
p = 0.31
FDR = 0.51
Exhaustion gene set 2
p = 0.50
FDR = 0.65
D
T-cell Anergy Gene Set
p = 0.53
FDR < 0.46
T-cell Deletion Gene Set
p = 0.00
FDR < 0.07
IKZF2
NR4A3
EGR2

BTLA provides a survival signal in TIL correlating with enhanced persistence in vivo.

Our results so far underscore the fact that BTLA is a marker for less-differentiated cells that have an enhanced responsiveness to IL-2. However, BTLA signaling is considered to be suppressive as ligation results in the recruitment of SHP1/2 phosphatases and decreases in proliferation and cytokine secretion (50, 52). Given the strong, positive correlation we previously observed between the $CD8^+BTLA^+$ subset and responsiveness to ACT (55), we set out to determine whether BTLA signaling in TIL was still suppressive. In agreement wth a study on MART-1 specific $CD8^+$ T cells in the periphery (52), ligation of $CD8^+BTLA^+$ TIL *in vitro* using a plate-bound HVEM-Fc fusion protein along with OKT3 resulted in a marked decrease in proliferation (32% in OKT3 alone versus 8% in OKT3 + HVEM-Fc) and significant decrease in the production of pro-inflammatory cytokines, IFN-γ and TNF-α, as compared to the control human IgG after 3 days (**Fig. 3-15A and B).**

Figure 3-15: Ligation of BTLA on $CD8^+BTLA^+$ TIL with HVEM-Fc fusion protein significantly decreases proliferation and productions of IFN-γ and TNF-α. Sorted $CD8^+BTLA^+$ TIL from two different patients were plated in a flat-bottom 96-well plates, and stimulated with low-dose IL-2 (100 U/mL) and plate-bound 30 ng/ml OKT3 with control Ig (OKT3+ Ctl Ig), or with 10 μg/ml HVEM-Fc (plate-bound) (HVEM-Fc + OKT3). (**A**) Sorted $CD8^+BTLA^+$ TIL were labeled with a cell proliferation tracking dye, eFluor670®, and stimulated as described for 3 days. The cells were harvested and the percentages of the cells that have diluted eFluor670® in each stimulation condition are shown. (**B**) Sorted $CD8^+BTLA^+$ TIL were stimulated for 3 days, and the supernatants were collected for multiplex cytokine analysis as described in Materials and Methods. Shown are the concentrations (pg/mL) of IFN-γ and TNF-α produced by the $CD8^+BTLA^+$ TIL under different stimulation conditions: 0 ctl Ig (plate-bound control Ig alone), 0 HVEM (plate-bound 10 μg/mL of HVEM-Fc alone), 30 ctl Ig (plate-bound 30 ng/mL of OKT3 + control Ig), or 30 HVEM (plate-bound 30 ng/mL of OKT3 + 10 μg/mL of HVEM-Fc). Error bars with SEM are also shown.

Figure 3-15:

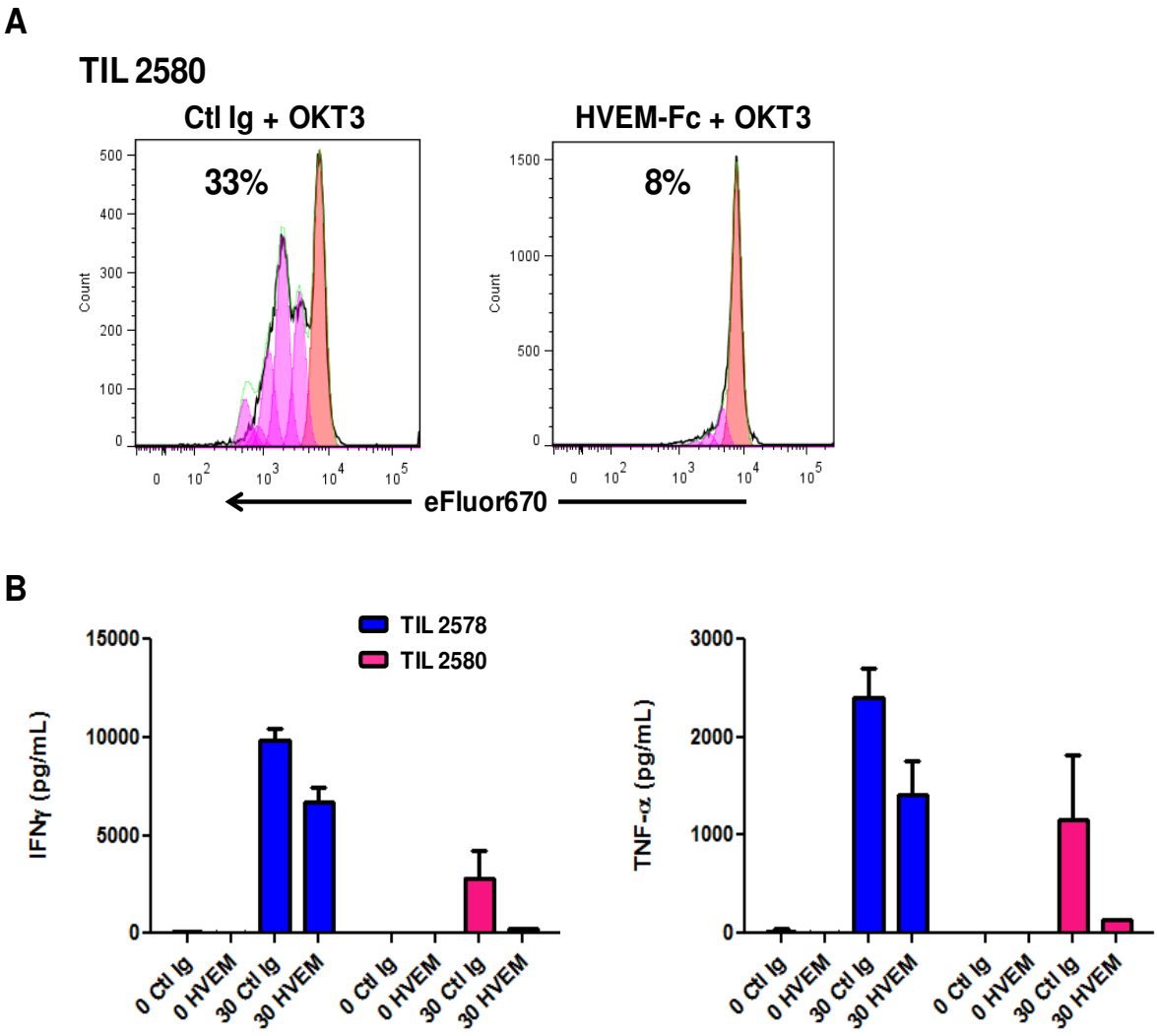
A
TIL 2580
Ctl Ig + OKT3
HVEM-Fc + OKT3
33%
8%
Count
eFluor670
B
TIL 2578
TIL 2580
IFNγ (pg/mL)
TNF-α (pg/mL)
0 Ctl Ig
0 HVEM
30 Ctl Ig
30 HVEM

Given that BTLA has a Grb-2 recruitment domain (51) and may potentially influence the survival of T cells (219), we next asked whether the ligation of BTLA on TIL by HVEM would impact their survival under low dose (LD) of IL-2 (100 U/mL) in order to diminish IL-2's survival-promoting effect. To answer this question, we first generated CD32-expressing and CD32/HVEM-expressing murine fibroblasts (L cells), and we co-cultured the bulk TIL with these L-cells loaded with OKT3 mAb. As shown in a representative TIL (**Fig. 3-16A**, **left panel**), we noticed a marked decrease in Annexin-V^+ 7-AAD^- (early apoptotic) cells in the $CD8^+$ TIL population when co-cultured for 5 days with HVEM-expressing L-cells under LD IL-2 (68% Annexin-V^+CD8^+ in $CD32^+$ L-cells co-culture vs. 19% Annexin-V^+CD8^+ in $CD32^+HVEM^+$ L-cells co-culture). We consistently noticed the same significant decrease in early-apoptotic $CD8^+$ TIL from five different patients (p=0.009; **Fig. 3-16A, right panel**). We next examined whether ligation of BTLA by HVEM could promote survival by enhancing Akt activation. Using a cleaner system where we stimulated sorted $CD8^+BTLA^+$ TIL from three patients with plate-bound OKT3 mAb and HVEM-Fc fusion protein for 2 hours, we found that there was significantly more phospho-Akt (S473) in $CD8^+BTLA^+$ TIL stimulated with OKT3 + HVEM-Fc, when compared to OKT3 + control Ig (p=0.017; **Fig. 3-16B**). This enhanced Akt activation was significantly abrogated when a specific BTLA blocking mAb [clone 3B1; ref. (200)] was added (p=0.02; **Fig. 3-16B**), or with the addition of a class I pan PI3K inhibitor (**Fig. 3-16B**). Histograms from a representative $CD8^+BTLA^+$ TIL are shown (**Fig. 3-16B, left panels**). In contrast, we did not observe significantly more Akt activation in $CD8^+BTLA^-$ TIL from three patients stimulated with OKT3 + HVEM-Fc, when compared to stimulation with OKT3 + control Ig (p = 0.61; **Fig. 3-16C**). Histogram from a representative $CD8^+BTLA^-$ TIL is shown (**Fig. 3-16C, left panel**)

Figure 3-16: BTLA ligation provides a pro-survival signal to TIL via Akt/PKB. (**A**) $CD32^+$ (CD32 L cells) or $CD32^+HVEM^+$ L cells (HVEM-L cells) were pulsed with 200ng/ml OKT3 and cultured with TIL ($1x10^6$/ml) along with 100 IU/ml IL-2. After 5 days, TIL were harvested and stained for CD8, Annexin-V and 7AAD. The dot plots show a representative TIL line staining gated on $CD8^+$ cells. The right graph shows the percent apoptosis among all lines tested (n=5). Statistical significance was determined using a Wilcoxen signed-ranked test. (**B, C**) TIL were sorted into $CD8^+BTLA^+$ and $CD8^+BTLA^-$ subsets. Sorted TIL were then plated in flat-bottom 96-well plates containing plate-bound 30 ng/ml OKT3 and 10 μg/ml HVEM-Fc (HVEM-Fc + OKT3), OKT3, HVEM, and 10 μg/ml anti-BTLA blocking antibody, 3B1 (HVEM-Fc + OKT3 + αBTLA). TIL alone without stimulation served as a negative control. As an additional negative control for Akt activation, 10 nM of a pan class I PI3K inhibitor, GSK2126458, was added to TIL stimulatd with OKT3 and HVEM (HVEM-Fc + OKT3 + PI3Ki). TIL were cultured for 2 hours, harvested, and were immediately fixed with pre-warmed Phosflow Fix buffer I for 10 min at 37C. Cells were then permeabilized with pre-chilled Phosflow Perm buffer III and stained with pAkt (S473) for 30 min on ice. The left histograms show representative staining from TIL 2619. The right graphs show the fold change in percent pAkt expression normalized to the TIL alone condition (set to 1) (n=3). Statistical significance was determined using a two-tailed, paired Student's *t* test.

Figure 3-16:

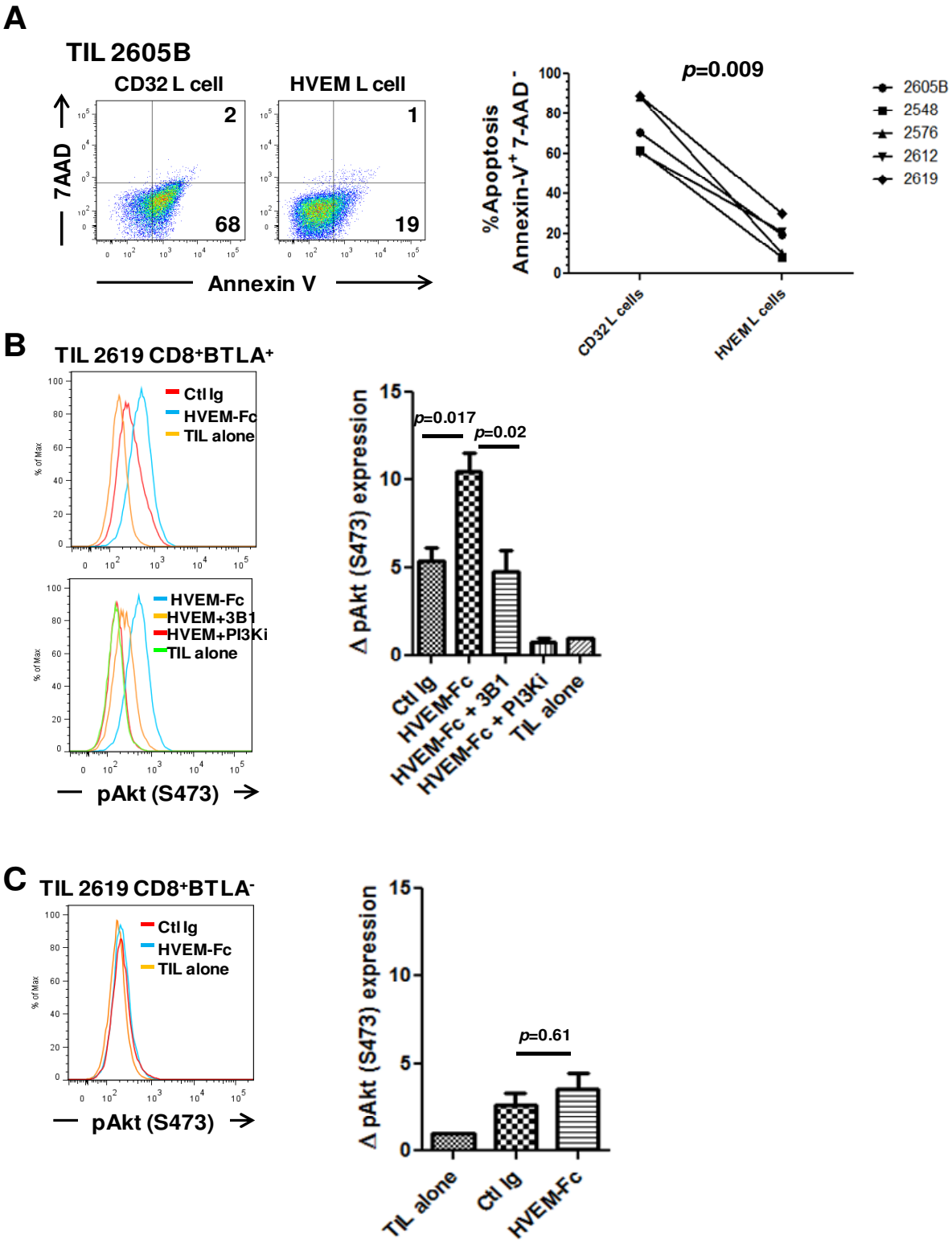
A
TIL 2605B
CD32 L cell
HVEM L cell
2
68
1
19
7AAD
Annexin V
p=0.009
% Apoptosis Annexin-V+ 7-AAD-
CD32 L cells
HVEM L cells
2605B
2548
2576
2612
2619
B
TIL 2619 CD8+BTLA+
Ctl Ig
HVEM-Fc
TIL alone
HVEM-Fc
HVEM+3B1
HVEM+PI3Ki
TIL alone
% of Max
pAkt (S473)
Δ pAkt (S473) expression
p=0.017
p=0.02
Ctl Ig
HVEM-Fc
HVEM-Fc + 3B1
HVEM-Fc + PI3Ki
TIL alone
C
TIL 2619 CD8+BTLA-
Ctl Ig
HVEM-Fc
TIL alone
% of Max
pAkt (S473)
Δ pAkt (S473) expression
p=0.61
TIL alone
Ctl Ig
HVEM-Fc

Discussion

T cell exhaustion, in which $CD8^+$ T cells progressively lose the ability to to proliferate in response to antigen, to lyse target cells efficiently *ex vivo*, and to produce IL-2, TNF-α or IFN-γ (220), has been described in chronic viral infections (220) and melanoma (217, 221). A characteristic feature often used to define exhausted $CD8^+$ T cells has been the co-expression of multiple inhibitory receptors such as PD-1, TIM-3, BTLA, LAG3, CD160, and 2B4 (53, 217, 221, 222). BTLA was proposed to mark exhausted tumor-specific $CD8^+$ T cells in melanoma because a recent report found that the melanoma antigen (NY-ESO-1)-specific $CD8^+$ T cells in the periphery expressed higher levels of BTLA, PD-1, and Tim-3 than those of the CMV-specific T cells from the same patient, and that the subset of $CD8^+$ T cells' co-expressing all three inhibitory receptors were the most deficient in producing IL-2, TNF-α, and IFN-γ (53). However, the concept of BTLA as a marker for exhaustion seemed incongruent with our previous clinical observation demonstrating a significant positive clinical correlation with metastatic melanoma patients receiving more $CD8^+BTLA^+$ TIL in an ACT trial (55). Also, other previous studies on $CD8^+$ T cells in chronic viral infections and on melanoma antigen-specific (MART-1) $CD8^+$ T cells isolated from tumor-invaded lymph nodes have shown that BTLA was not among a set of phenotypic markers or gene expression signatures used to define T cell exhaustion (217, 222).

In the present study, we have found that $CD8^+BTLA^+$ melanoma TIL (bulk and antigen-specific) frequently co-expressed PD-1 and TIM-3, and that $CD8^+BTLA^+$ TIL exhibits a significantly higher proliferative capacity in response to IL-2 compared to the $BTLA^-$ subset. An alternative explanation for the differing observations on the $CD8^+BTLA^+$ T cells between ours and others (53) could be the intrinsic difference between the melanoma

antigen-specific T cells in the peripheral blood and TIL in the tumor microenvironment. However, our findings are also similar conceptually to a different study, where it was shown that melanoma antigen-specific $CD8^+$ TIL were enriched in the $PD\text{-}1^+$ population, and that these $CD8^+PD\text{-}1^+$ TIL could recover function after culturing in IL-2 and subsequently become insensitive to suppression mediated by PD-L1 (223). Based on these observations, it is possible that T cell exhaustion could be overcome through *ex vivo* expansion with IL-2, much like how T cell anergy was classically shown to be overcome by IL-2-induced proliferation (224). However, adopting such a framework implies that T cell exhaustion is a transient, rather than a permanent state of $CD8^+$ T cell's differentiation as defined by others (220). A new concept is emerging that $CD8^+$ T cells, under normal immune activation, may naturally express inhibitory receptors, such as PD-1 and TIM-3, as a self-regulating mechanism to prevent hyper-responsiveness without eventual transition to T cell exhaustion (127, 225). Hence the anti-tumor activity of the monoclonal antibodies targeting PD-1 may be explained by relieving the suppressive signal via PD-1 and allowing the highly active $CD8^+PD\text{-}1^+$ cells to expand as well as migrate to the tumor (226, 227). We have shown in this study that PD-1 was up-regulated on $CD8^+$ TIL after TCR stimulation, while others have shown up-regulation of TIM-3 after TCR signaling in human T cells (228). Therefore the presence of PD-1 and TIM-3 on $CD8^+$ TIL could mark cells which have been previously activated through TCR by tumor antigens in the tumor microenvironment. In support of this concept, we have observed that $CD8^+BTLA^+$ TIL have significantly higher expressions of CD25, a classic marker of T cell activation (204), than that of the $BTLA^-$ TIL.

Furthermore, we reasoned that a likely relationship existed between expression of inhibitory receptors and a specific stage of $CD8^+$ TIL's differentiation. This concept was

suggested in a study by Duraiswamy, *et al.* (166), who found that $CD8^+PD\text{-}1^{Hi}$ T cells from normal donors did not share the same exhaustion gene signature as the T cells from HIV-infected patients. Instead, they exhibited similar phenotype and gene signature as the classic T_{EM} ($CCR7^-CD45RA^-$) $CD8^+$ T cells. In addition, other studies have shown a close relationship between BTLA and differentiation stages of human $CD8^+$ T cells: in normal and CMV-specific $CD8^+$ T cells in the periphery, naïve T cells constitutively expressed BTLA and down-regulated BTLA as they differentiated toward T_{EM} or T_{EMRA} phenotypes (54, 201). Several lines of evidence in our study provide support that $CD8^+BTLA^+$ are less-differentiated memory T cells compared to $CD8^+BTLA^-$ TIL. First, we found that T_{EM} subset ($CCR7^-CD45RA^-$) was found within the $CD8^+BTLA^+$ TIL, while significantly more T_{EMRA} subset ($CCR7^-CD45RA^+$) was found within $CD8^+BTLA^-$ TIL. Although there were three melanoma patients whose $CD8^+BTLA^+$ TIL express CD45RA, that was not unexpected since it has been reported that some cells within a T_{EMRA} subset could still retain T_{EM} marker, CD27, and displayed phenotypic and functional features that were intermediate between naïve and terminally-differentiated effector T cells (123). Secondly, we found that $CD8^+BTLA^+$ subset has significantly more CD28, not CD27, expression at the protein and mRNA levels than those of the $BTLA^-$ subset. CD28 has been reported as a key marker defining a less-differentiated, proliferative $CD8^+$ memory T cells in humans, whereas the loss of CD28 is one of the markers for T cell senescence in humans (195). Prior study from our group has determined that CD28, not CD27, was a key marker in defining a subset of TIL with superior proliferation and survival (66). Third, we found that $CD8^+BTLA^+$, compared to $CD8^+BTLA^-$ subset, had other features of early-differentiated memory T cells such as higher CD25 expression, a better response to IL-2 signal by activating more Stat5 and Akt,

higher production of autocrine IL-2 to sustain its own proliferation, and higher levels of polyfunctional cytokine (IFN-γ, TNF-α, and MIP-1β) productions. Our findings are consistent with a previous study on memory $CD8^+$ T cells in elderly individuals; it was found that memory $CD8^+CD25^+$ T cells displayed a polyclonal TCR repertoire and produced as well as responded to IL-2 and a variety of antigens, whereas the $CD8^+CD25^-$ memory T cell population had a more restricted TCR diversity, responded to fewer antigens, and did not proliferate in response to stimulation with IL-2 (203). Also, the cytokine profile of $CD8^+BTLA^+$ vs. $BTLA^-$ TIL subsets after stimulation with PMA and ionomycin were congruent with findings from another study, where it was reported that IL-2/IFN-gamma coproduction, a feature of early-differentiated memory T cells, was absent in human late memory ($CD27^-CD45RA^+$) $CD8^+$ T cells (207). Finally, the higher level of Akt activation in $CD8^+BTLA^+$ TIL in response to IL-2 was likely related to its early-differentiated state, as other study has shown a progressive decline in Akt phosphorylation (Ser473) as human $CD8^+$ T cells progressively differentiated from $CD28^+CD27^+$ to $CD28^-CD27^+$ to $CD28^-CD27^-$ that could not be reversed by the addition of IL-2 (128).

In contrast, we found that $CD8^+BTLA^-$ TIL poorly proliferate in response to IL-2 and TCR signals, and they showed enriched expressions of CD45RA and killer-cell immunoglobulin-like receptors (KIRs). We also found the enrichment of gene signature for T cell deletion, a cell fate defined by $CD8^+$ T cells' hyporesponsiveness due to TCR signaling defect and death by apoptosis triggered by the proapoptotic BH3-only protein, Bim (197), in the $CD8^+BTLA^-$ TIL. Deletion and anergy have considerable similarity at the molecular level. One of the features of anergic T cells is the upregulation of the transcription factor Egr-2 and Egr-3 by NFAT activation in the absence of AP-1 activation (197). Egr-2

and Egr-3 then promote the expression of immunosuppressive E3 ubiquitin ligases, such as Cbl-b, which degrades TCR signaling molecules (197). It is known that both Egr-2 and Cbl-b and other numerous anergy-associated genes were strongly upregulatd during deletion (198). A model depicting diverse $CD8^+$ T cells fates, such as anegy, deletion, exhaustion, senescence, or memory are shown in **Fig. 3-17.**

Figure 3-17: A model for generating diverse CD8$^+$ T cell fates. (**Top portion**) Naïve CD8$^+$ T cells (brown cell) that encounter antigen on steady state, tolerogenic DCs (**beige cell**) proliferate without acquiring effector functions (**dark blue cells**) in a process dependent on PD-1 and the molecules, Egr-2, Egr-3, and Cbl-b. Such tolerised T cells typically upregulate PD-1 and downregulate IL-7R as indicated, and either undergo deletion (**black cell**) or anergy (i.e., defects in TCR signalling as denoted by the **red cross**). Antigen (**Ag**) levels control this process, with high Ag levels promoting anergy, and low Ag levels causing deletion. (**Lower portion**) Immunogenic DCs (**red cell**), which have encountered pathogen-derived products, activate naïve CD8$^+$ T cells to form effector cells (cytotoxic granules and production of effector cytokines are indicated). This differentiation process is regulated by molecules such as Id2, Spi-6, Notch, T-bet and eomesodermin (Eomes). These effector cells can adopt multiple cell fates, such as memory precursor cell fates (characterised by IL-7R^{Hi}, KLRG-1^{Lo}, T-bet^{Lo}, Blimp-1^{Int}, Spi-2a^{Hi} and Bcl-2^{Hi} expression; bottom left) or short-lived effector cell fates (with IL-7R^{Lo}, KLRG1^{Hi}, T-bet^{Hi} and Blimp-1^{Hi} expression; middle). Such short-lived cells can either become senescent effectors and die by bim-dependent apoptosis, or persist into early memory as short-lived effector memory cells that are CCR7^{Lo}, CD62L^{Lo} and KLRG1^{Hi}. By contrast, memory precursor cells are long-lived and can be CCR7^{Lo}, CD62L^{Lo}, Blimp-1^{Int} effector memory cells, or CCR7^{Hi}, CD62L^{Hi}, Blimp-1^{Lo} central memory cells (driven by Bcl-6). Evidence exists that KLRG1^{Lo} effector cells can also give rise to KLRG1^{Hi} short-lived effector memory cells (denoted by broken arrow and question marks; NS Joshi, TW Hand and SMK, unpublished observations). In some chronic viral infections, PD-1, LAG-3 and IL-10 causes cells to acquire an exhausted phenotype (light blue cell) characterised by high PD-1 and LAG-3 expression and low IL-7R levels. Although the exhausted cell is depicted as sharing a common effector cell precursor with other cell fates, it is currently unclear at what point this fate occurs during effector cell's differentiation.

Reprinted with permission from: Ian A Parish, Susan M Kaech, Diversity in CD8$^+$ T cell differentiation, *Current Opinion in Immunology*, Volume 21, Issue 3, June 2009, Pages 291-297, ISSN 0952-7915, 10.1016/j.coi.2009.05.008.
(http://www.sciencedirect.com/science/article/pii/S0952791509000880)

Figure 3-17:

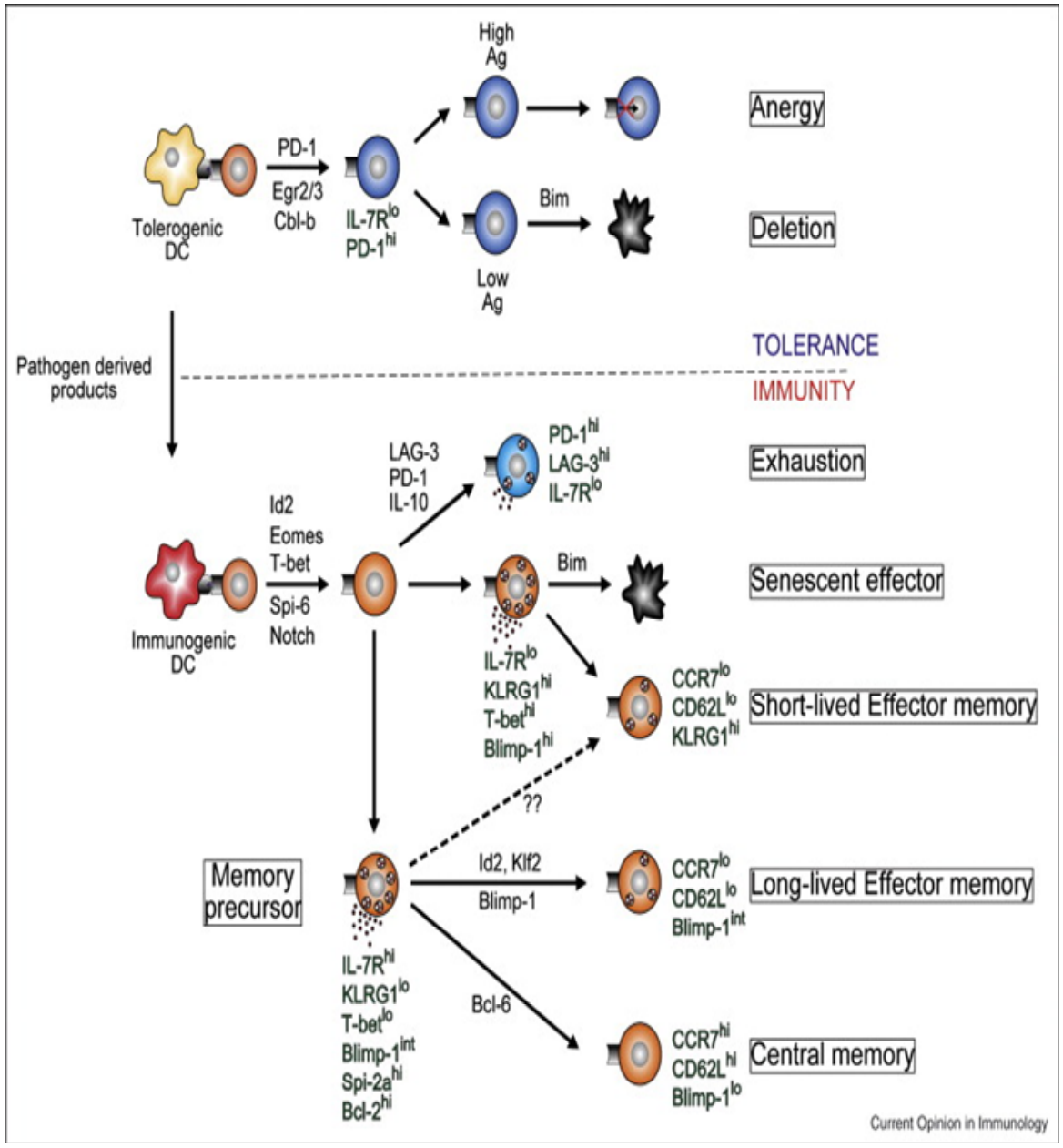
High Ag
Anergy
PD-1
Egr2/3
Cbl-b
Tolerogenic DC
IL-7R^{lo} PD-1^{hi}
Bim
Deletion
Low Ag
TOLERANCE
Pathogen derived products
IMMUNITY
LAG-3
PD-1
IL-10
PD-1^{hi} LAG-3^{hi} IL-7R^{lo}
Exhaustion
Id2
Eomes
T-bet
Spi-6
Notch
Immunogenic DC
Bim
Senescent effector
IL-7R^{lo} KLRG1^{hi} T-bet^{hi} Blimp-1^{hi}
CCR7^{lo} CD62L^{lo} KLRG1^{hi}
Short-lived Effector memory
??
Memory precursor
Id2, Klf2
Blimp-1
CCR7^{lo} CD62L^{lo} Blimp-1^{int}
Long-lived Effector memory
IL-7R^{hi} KLRG1^{lo} T-bet^{lo} Blimp-1^{int} Spi-2a^{hi} Bcl-2^{hi}
Bcl-6
CCR7^{hi} CD62L^{hi} Blimp-1^{lo}
Central memory
Current Opinion in Immunology

.

We think that enrichment of T-cell deletion signature in $CD8^+BTLA^-$ TIL is likely related to its highly-differentiated state, since it has been shown that $CD8^+$ TIL with highly-differentiated phenotypes failed to persist *in vivo* after adoptive transfer (136). Previously, we have reported expression of multiple KIRs in $CD8^+CD28^-$ TIL, and that this subset of TIL exhibited decreased telomere length and were hypo-responsive to proliferative signals (66). Others have found KIR expressions on $CD8^+PD\text{-}1^-$ T cells, which also co-expressed CD45RA, in the normal donor peripheral blood (166). Furthermore, we have re-analyzed microarray data from a previous study on the human $CD8^+$ T cell subsets in the peripheral blood (196) and have observed that T_{EMRA} had the highest expression of different KIRs, when compared with T_{EM} or T_{CM} (**Fig. 3-18B**). Based on all these observations, we propose that the expression of KIR family of receptors, together with CD45RA (127), may serve as better markers for terminally-differentiated and senescent $CD8^+$ T cells in humans.

Figure 3-18: **Terminally-differentiated $CD8^+$ T cells in humans express KIRs and other natural-killer (NK) cell's receptors.** (**A**) $CD8^+$ T cell subsets in normal human PBMC, as defined by CCR7 and CD45RA expressions, were sorted on a MoFlow Cytometer (DakoCytomation), with purity of the isolated subpopulations between 93%-98% as described in Willinger, T., *et al*. 2005. *J. Immunol*. 175: 5895–5903. (**B**) Microarray data on the sorted $CD8^+$ T cell subsets corresponding to the aforementioned publication was obtained from European Bioinformatics Institute ArrayExpress public database (Accession **#E-TABM-40**). We used a comprehensive software package, BRB-ArrayTools v4.2.1 (NCI, Bethesda, MD), to determine a list of genes that are statistically different ($p < 0.01$) between T_N, T_{EM}, and T_{EMRA} subsets using a random variance F-test. Two-way hierarchical clustering was performed using centered correlation and average linkage. The resulting heatmap was generated by BRB-ArrayTools v4.2.1.

Figure 3-18:

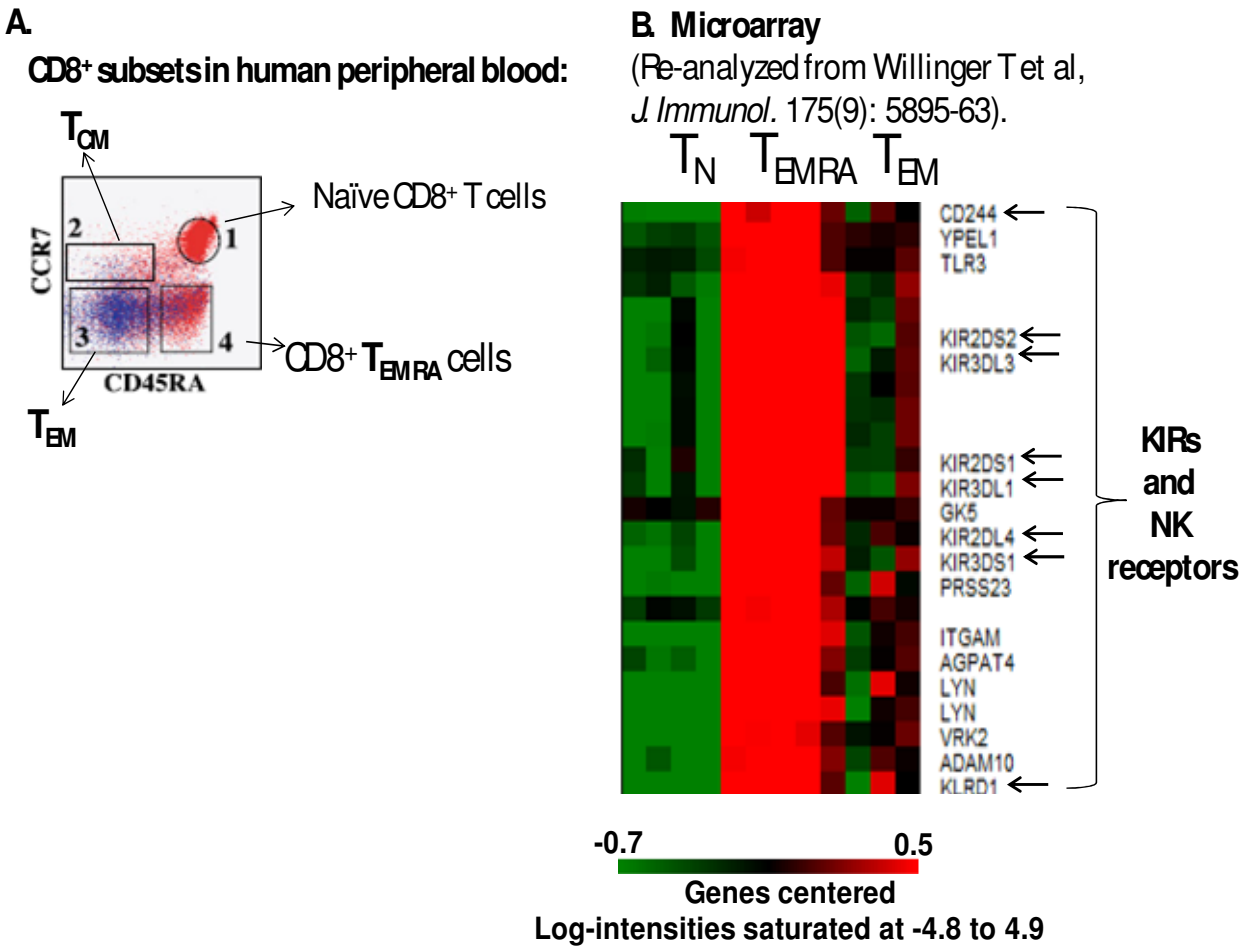
A.
CD8+ subsets in human peripheral blood:
TCM
CCR7
2
1
3
4
CD45RA
TEM
Naïve CD8+ T cells
CD8+ TEMRA cells
B. Microarray
(Re-analyzed from Willinger T et al,
J. Immunol. 175(9): 5895-63).
TN
TEMRA
TEM
CD244
YPEL1
TLR3
KIR2DS2
KIR3DL3
KIR2DS1
KIR3DL1
GK5
KIR2DL4
KIR3DS1
PRSS23
ITGAM
AGPAT4
LYN
LYN
VRK2
ADAM10
KLRD1
KIRs and NK receptors
-0.7
0.5
Genes centered
Log-intensities saturated at -4.8 to 4.9

We also observed that $CD8^+BTLA^-$ TIL, though hypo-responsive to proliferative signals, nevertheless maintained a similar cytotoxic capability as the $CD8^+BTLA^+$ TIL. This phenomenon may be due to the unique signaling of KIRs on human $CD8^+$ T cells; other previous studies have found that their presence on $CD8^+CD28^-$ T cells, unlike NK cells, only inhibits complex cellular functions, such as proliferation, while leaving certain effector functions, such as cytotoxicity, essentially intact, presumably due to delayed recruitment to the TCR synapse after activation (229). Additionally, although there was discordance between enrichment of multiple KIRs' gene transcripts in the $CD8^+BTLA^-$ TIL and a few KIR actually being expressed at the protein level in our present study, this may be explained by a recent finding where it was shown that human $CD8^+$ T cells, distinct unlike NK cells, generally express only one activating or inhibitory KIR (230). This suggests that post-transcriptional regulation may play a role in limiting the expression of a full repertoire of active KIR transcripts in the $CD8^+BTLA^-$ TIL, although such potential mechanism will need to be addressed in a future study.

We have discovered that BTLA, upon binding to its cognate receptor, HVEM, delivered a pro-survival signal in $CD8^+$ TIL. The prosurvival role of BTLA was initially suggested in a study by Hurchla *et al*., who found, in a GvHD model, that the transferred $BTLA^{-/-}$ splenocytes in a new host were unable to sustain its proliferation and the GvHD response compared with wild-type counterparts (231). Moreover, it was reported that BTLA has a third conserved tyrosine-containing motif within the cytoplasmic domain that could recruit Grb-2 and p85 subunit of PI3K *in vitro* (51). Interestingly, a recent study demonstrated that ligation of BTLA *in vitro* results in a signaling cascade similar to but weaker than that seen with CD28 and ICOS signaling (232). Based on these observations, it

seems likely that BTLA may exert inhibitory activity on T cells while simultaneously promote their survival (219) (**Fig. 3-19**). We initially tested this hypothesis by co-culturing bulk TIL with HVEM-expressing vs. control L cells loaded with αCD3 antibody for 5 days. We consistently found that TIL co-cultured with $HVEM^+$ L cells had significantly lower percentage of apoptotic cells compared to that of the control L cells. We further explored this phenomenon in sorted $CD8^+BTLA^+$ vs $CD8^+BTLA^-$ TIL in a cleaner system by stimulating them with plate-bound HVEM-Fc fusion protein and αCD3. We found that TCR stimulation together with ligation of BTLA on $CD8^+BTLA^+$ TIL with HVEM-Fc led to higher level of phosphorylated Akt (Ser473), when compared to that of the control-Fc fusion protein, as early as 2 h after stimulation. This enhanced Akt activation was abrogated with the addition of a BTLA blocking antibody. Also, we did not see the enhanced Akt activation in $CD8^+BTLA^-$ TIL after stimulation with HVEM-Fc. We speculate that the loss of BTLA in a highly-differentiation state, hence a loss of pro-survival Akt activation, may contribute to the enrichment of T cell deletion gene signature (198), in the $CD8^+BTLA^-$ TIL.

Figure 3-19: BTLA, a dual signaling molecular rheostat? Analogous to PD-1, the cytoplasmic domain of BTLA contains two immunotyrosine-based inhibitory motifs (ITIMs). Binding of PD-1 and BTLA to PDL1/2 and HVEM, respectively, generally activate inhibitory signaling pathways in T cells, as their two ITIM motifs in the cytoplasmic tails recruit SHP1/2 phosphatases and dephosphorylate TCR signaling molecules. This leads to decreases in T-cell's proliferation and cytokine secretion. Additionally, in the case of PD-1 signaling, it leads to both $CD8^+$ T cell anergy (233) and deletion (234, 235). However, unlike PD-1, the cytoplastmic domain of BTLA has been reported to contain a third conserved tyrosine-containing motif, which has been shown to recruit Grb-2 and p85 subunit of PI3K *in vitro*. We think that BTLA plays a more complex role in T-cell than simply acting as an inhibitory receptor. We propose that it acts as a molecular rheostat by regulating the degree of T-cell activation depending on the relative TCR signaling strengths. When the TCR signaling strength is low, inhibitory signaling through BTLA predominates. When the TCR signaling strength is high such that T-cell is prone to die by activation-induced cell death (AICD) (61, 236), BTLA promotes the survival of T-cells by attenuating TCR signaling and by activating the pro-survival Akt/PKB signaling pathway.

Figure 3-19:

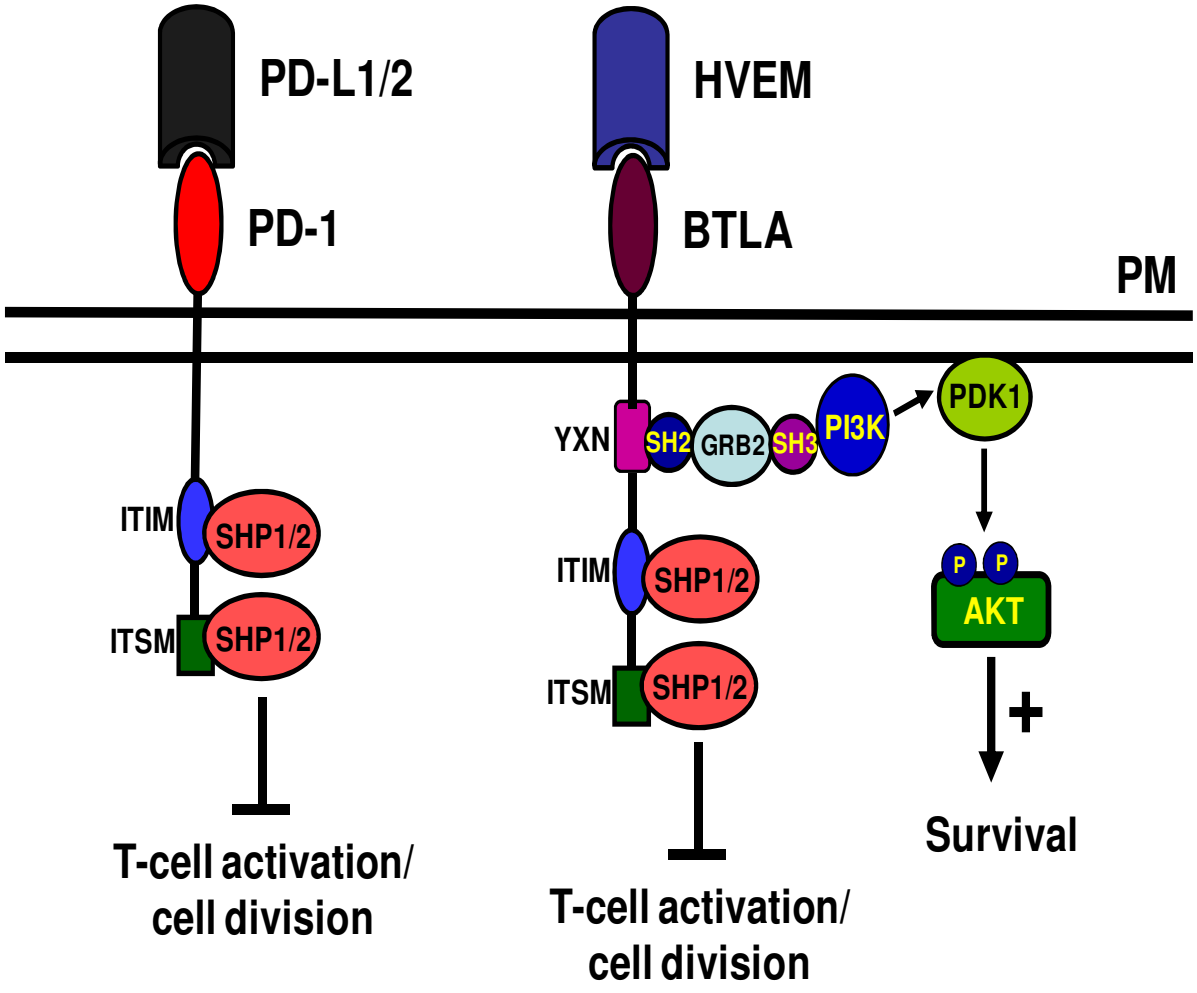
PD-L1/2
PD-1
HVEM
BTLA
PM
YXN
SH2
GRB2
SH3
PI3K
PDK1
ITIM
SHP1/2
ITSM
SHP1/2
ITIM
SHP1/2
ITSM
SHP1/2
P
P
AKT
+
Survival
T-cell activation/
cell division
T-cell activation/
cell division

These findings in our study demonstrated the specificity of the interaction between BTLA and HVEM. Although we found that LIGHT was up-regulated on $CD8^+$ TIL after TCR activation and could potentially interact with HVEM, we did not think that the pro-survival effect could be mediated through LIGHT since it has no obvious signaling motif (237), and it has been reported that signaling through HVEM upon binding to LIGHT was required to influence T cell's survival *in vivo* (238). Lastly, in agreement with other studies on BTLA's inhibitory role (50, 52, 239), we found that TCR stimulation, together with ligation of BTLA on $CD8^+BTLA^+$ TIL with HVEM-Fc fusion protein, led to significant decreases in proliferation and productions of IFN-γ and TNF-α.

In an attempt to determine the difference in persistence between the $CD8^+BTLA^+$ vs. $CD8^+BTLA^-$ TIL subsets *in vivo,* we, in collaboration with Adaptive Biotechnology™, had performed high-throughput DNA sequencing of TCR clonotypes deriving from $CD8^+BTLA^+$ vs. $CD8^+BTLA^-$ TIL before infusion and at various time points after infusion in two melanoma patients. Our preliminary study on two patients who had received infusion with TIL showed that there were more persisting T cell clones from $CD8^+BTLA^+$ than $BTLA^-$ TIL (data not shown). We anticipate that, by having more patient samples available in the near future, there will be more statistical power to link the persistence of $CD8^+$ T cell clones with the CD8+$BTLA^+$ TIL subset. At this point, our preliminary results have shown a conceptual agreement with other reports demonstrating that the persistence of the infused TIL clones was one of the most important factors associated with positive clinical response after ACT (102, 103).

In summary, our study provides a molecular basis for our previously observed positive clinical correlation with $CD8^+BTLA^+$ TIL after adoptive transfer in metastatic

melanoma patients. This is due to the less differentiated state of $CD8^+BTLA^+$ TIL subset, their ability to receive pro-survival signal through BTLA, as well as their ability to persist better after adoptive transfer *in vivo*. Our study provides a rationale to improve persistence of the T cell clones *in vivo* by selectively isolating the $CD8^+BTLA^+$ TIL prior to infusion into melanoma patients. Based on our novel discovery of BTLA's pro-survival effect, it will be of interest to further modify the domains within the cytoplasmic tail of BTLA, which can help dissect its inhibitory from prosurvival roles (219). We speculate that, by transducing TIL with a modified form of BTLA in which only Grb2-recruitment domain exists, it may help to remove the inhibitory influence from the tumor microenvironment while promoting $CD8^+$ TIL's survival and normal differentiation.

Chapter 4

General Discussion

Taken together, the two studies described in this dissertation provided a comprehensive characterization of the changes in $CD8^+$ T-cell differentiation markers in TIL from metastatic melanoma and the functional characterization of two unique TIL subsets, of which one ($CD8^+BTLA^+$) is associated with clinical tumor regression during adoptive cell therapy with TIL. In the first study (**Chapter 2**), we initially hypothesized that CD57 marked senescent and terminally-differentiated $CD8^+$ TIL, similar to those found in HIV patients (131). When we examined the $CD8^+$ T cells in the peripheral blood of normal donors as well as melanoma patients, we found that the $CD8^+CD57^+$ T cells showed highly differentiated phenotype ($CD27^-CD28^-$), exhibited high level of cytotoxic (GB^{Hi}, $Perf^{Hi}$) and effector (IFN-γ production) activities, in agreement with what was known about this subset of $CD8^+$ T-cells from the literature (127). However, when we looked at the $CD8^+$ TIL residing in melanoma metastases, the simplistic description of CD57 as a senescent marker became much more complex. We found that the $CD8^+CD57^+$ TIL co-expressed early T_{EM} markers (CD27 and CD28) and were GB^+ but $Perf^{Lo}$, unlike the $CD8^+CD57^+$ T cells found in the peripheral blood of melanoma patients' peripheral blood (202). We have also shown that $CD8^+CD57^+$ TIL could be induced to divide and produce cytokines after TCR stimulation (202) similar to other recent studies on $CD8^+CD57^+$ T cells in humans (127, 181). This $CD8^+CD57^+$ TIL subset that had high CD28 as well as CD27 expressions, were not senescent and retained functional characteristics of early T_{EM} cells. We believe this novel TIL subset may functionally resemble the $CD8^+BTLA^+$ TIL we described in the second study (**Chapter 3**). We found that $CD8^+BTLA^+$ TIL subset exhibited high degree of effector functions and also co-expressed early T_{EM} markers (CD27, CD28) and late-differentiation markers, such as

CD57, CX3CR1 [ref. (167, 209)], and ITGAM [integrin, alpha M, **Table 3-II** and **Fig. 3-14].** We believe that this unique incompletely-differentiated phenotype may have arisen as a consequence of the altered differentiation program in the $CD8^+$ TIL within the tumor microenvironment (202, 240) (**Fig. 4-1**)

One of the incompletely answered questions from the first study was what immunosuppressive factors within the tumor microenvironment could promote the $CD8^+$ TIL to accumulate in an incompletely differentiated state. Although we have established TGF-β1 as one possible factor in this process (**Chapter 2**), we think that inhibitory signaling through PD-1 or BTLA (similar structural monomeric members of the Ig family of negative costimulatory molecules) may also play a role. PD-1 signaling generally leads to decreases in $CD8^+$ T-cell effector function (241), and induction of anergy (233) and deletion (234, 235). On the other hand, BTLA signaling also regulates $CD8^+$ T cell effector function (52), however in a more unique way than PD-1 because it also seems to promote cell survival via the Akt/PKB pathway (**Chapter 3**). It has been reported that the ligands for PD-1 and BTLA, PD-L1 and HVEM, respectively, are expressed by melanoma tumors (43, 52). Therefore it is likely that, within the tumor microenvironment, both signaling pathways through PD-1 and BTLA are active in $CD8^+$ TIL. It has been shown that PD-1 and BTLA are recruited to the immune synapse during T-cell-APC interaction (242, 243). These findings suggest an intriguing possibility that, in the context of chronic antigen stimulation within the tumor microenvironment, PD-1 and BTLA ligations by PD-L1-expressing or HVEM-expressing melanoma cancer cells may arrest the differentiation of $CD8^+$ TIL while enhancing their survival, leading to their accumulation in an incomplete-differentiated state (202, 240) (**Fig. 4-1**).

One of the most intriguing questions raised in this dissertation is whether $CD8^+$ TIL in melanoma can be adequately defined as exhausted. T-cell exhaustion was originally described more than a decade ago as dysfunction and subsequent physical deletion of antigen-specific T cells during chronic viral infection by lymphocytic choriomeningitis (LCMV) clone 13 in mice (244), and has since been reported in $CD8^+$ T cells in melanoma (164, 217). However, if exhaustion is defined as a permanent state of $CD8^+$ T-cell differentiation, it would not explain the feasibility of expanding the TIL with high-dose IL-2 *ex vivo*, as well as some of our findings here with highly proliferative and functional $BTLA^+$ TIL that nevertheless express high levels of PD-1 and TIM-3. TIL generally recover their proliferation and other effector functions with IL-2 culture and are capable being expanded 1 to 2,000-fold *ex vivo* after the REP. A characteristic feature often used to define exhausted $CD8^+$ T cells in chronic viral infection and cancer has been the co-expression of multiple inhibitory receptors such as PD-1, TIM-3, BTLA, LAG3, CD160, and 2B4 (53, 217, 221, 222). In contrast, in our second study (**Chapter 3**), we found that $CD8^+BTLA^+$ TIL, which also co-expressed PD-1 and TIM-3, had intact effector functions and are positively correlated to clinical response to ACT. We surmise that the reason why T-cell exhaustion is more readily observed in chronic viral infection, as opposed to cancer, may be due to the nature of the antigens. Antigens from viruses such as HIV and EBV are completely foreign to the host, and therefore exhibit high affinity and avidity for host's TCR. The persistence of these antigens in chronic viral infection continuously induces strong TCR signaling in the responding $CD8^+$ T cells. PD-1 is induced and maintained persistently due to continuous induction of a transcription factor downstream from TCR signaling, nuclear factor of activated T-cells, cytoplasmic 1 (NFATc1) (245), which is also one of the genes highly

expressed in exhausted T-cells in chronic viral infection (218). In this setting, the high PD-1 expression by $CD8^+$ T cells truly defines exhausted T cells. In contrast, because many of the melanoma-associated antigens are self-proteins, they do not bind as avidly to TCR and thus do not induce strong effector T-cell response from the host, as a consequence of immune tolerance (246). This often allows melanoma cells to escape from immune responses. At the same time, the weak TCR signaling by the tumor antigens in TIL do not trigger NFATc1 as strongly. Thus, $CD8^+$ TIL naturally express PD-1 as a reflection of their state of differentiation, not due to the persistence of NFATc1. We think the lack of a true exhausted state in TIL may help explain why they can often be harvested for adoptive cell therapy. From a basic science point of view, it will be interesting to examine how the *PDCD1* gene locus (corresponding to the PD-1 protein) is differentially regulated by transcription factors in chronic viral infection vs. cancer.

However, how this model applies to TIL reactive against epitopes generated from mutated tumor antigens [so-called "mutatopes" (247)], where prior self-tolerance would not play a role and TCR affinities for these epitopes would be much higher, is not known. Other immunosuppressive factors in the tumor environment, such as TGF-β, adenosine, hypoxia, IDO, may also regulate the state of TIL activation or "exhaustion" through the expression of these negatively signaling co-receptors. Also, it is possible that many of these tumor neo-epitoe or mutatope specific T cells are deleted through AICD or are lost as the tumor progresses and loses the expression of these epitopes due to immunoediting (248). Thus, what we see by the time we have access to a cancer (melanoma) patient is a highly immunoedited situation with constant selective pressure to "reign in" these highly reactive T-cells through these inhibitory pathways, which may be mistaken as "exhaustion." Thus,

these T-cells are highly activated cells being subjected to negative regulation, a natural response of the immune system to prevent runaway immune responses and autoimmunity. This would explain why the $CD8^+BTLA^+$ (and PD-1^+ and TIM-3^+) TIL were such highly active cells *ex vivo* out of the host's tumor microenvironment. Future studies, however, will be need to determine whether these infused T-cell clones arising from these *ex vivo* highly active subsets are also more active *in vivo* during adoptive cell therapy, and whether this negative regulation still exists to try to "reign them in." This new viewpoint can then lead us to a newer perspective by which we view this system and novel approaches to further facilitate the functioning of these cells to improve clinical response rates.

Future Directions

Throughout this dissertation, we have used the term "tumor-infiltrating lymphocytes (TIL)" loosely. A recent study has revealed distinct histologic infiltrative patterns of T-cells within melanocytic lesions in humans (43) (**Fig. 4-2**). We think that the term, TIL, can be misleading in that it gives the impression that the T-cells isolated from melanoma metastases always infiltrate deeply into tumor mass, when in fact T-cells in a melanocytic lesions can be found either inside the tumor mass, at the advancing edge of an invasive tumor, or at the perivascular area (**Fig. 4-2**). Therefore, we think that a more general terminology to describe these T-cells within melanoma tumor mass, tumor-associatd lymphocytes (TAL), is more appropriate at capturing the complexity of the T-cells-tumor interaction in the tumor microenvironment.

In the first study (**Chapter 2**), we have identified a unique subset of $CD8^+CD27^+CD57^+$ T-cells in melanoma metastases by flow cytometry. However, we are not certain of the location of this unique TIL subset within the tumor mass. Therefore, one future direction of this project will be to utilize double or triple immunofluoresence staining in combination with hematoxylin/eosin staining of melanoma tumor sections in order to precisely determine the infiltrative pattern of the $CD8^+CD27^+CD57^+$ T cells. This will allow us to determine whether this subset of T-cells is actively interacting with tumor cells either within the tumor mass or at the advancing edge of an invasive primary melanoma (**Fig. 4-2A and B**), or they are merely "bystander" T-cells in the perivascular area (**Fig. 4-2C**). Additionally, we hypothesize that it is likely that there is a correlation between the patterns of T-cell infiltration in tumors and melanoma patients' prognosis after adoptive T-cell therapy. We think that the infused TIL may exert the greatest efficacy at controlling tumor growth when they are present at the invasive edge of the tumor mass, which will limit tumor's growth or metastatic potential. However, another recent study has shown that the edges of melanoma tumors were often surrounded by immunosupressive tumor-associated fibroblasts (TAF), which could upregulate inhibitory receptor ligands, PD-L1 and PD-L2, under the influence of IL-1 produced by melanoma cells with BRAF V600E mutation (249). Thus, it remains an open question which T-cells' infiltrative patterns are related to the optimal control of tumor growth.

Also, we do not know why $CD8^+CD27^+$ T-cells prematurely expressed CD57, a marker of highly-differentiated T-cells, in the tumor microenvironment. We think that TGF-β may play a role in inducing CD57 expression. Furthermore, it would be helpful to know if there was a correlation between the presence of TGF-β and the amount of $CD8^+CD57^+$ T

cells in the histologic melanoma tumor specimen. Also, CD57 has been shown to have cell-adhesion function for motor neurons in the central nervous system (**Chapter 2, Discussion**). It is possible that the CD57 expressed by T-cells may play a role in enhacing the attachment of infiltrating T-cells to tumor cells, in addition to its role as a differentiation marker. Therefore, it will be of interest to examine the transcription factors controlling the CD57 locus in $CD8^+$ TIL vs. $CD8^+$ T-cells in the peripheral blood.

The last key question raised in this dissertation was which set of markers defined terminally-differentiated and senescent $CD8^+$ T cells in humans. In our first study, we found that the $CD8^+CD27^+CD57^+$ TIL could be induced to differentiate into $CD27^-CD57^+$ TIL, or, in some patients, into $CD27^-CD57^-$ TIL. Therefore, we think that CD57 does not define the penultimate state of human $CD8^+$ T-cell's differentiation. From our current study (**Chapter 3**) and an earlier study by our group (96), we observed that the loss of CD28 and BTLA on $CD8^+$ TIL corresponded to their loss of proliferative and other effector functions. This is associated with the re-expression of CD45RA and acquisition of NKR (Chapter 3, **Fig. 3-14**), such as the KLRG-1 (171) and KIRs (96, 166). Among all the NKRs, We found that KIRs were the most highly expressed genes in the $CD8^+BTLA^-$ TIL subset. Thus we think the truly senescent $CD8^+$ T cells in humans, or those that are the immediate precursors of terminally-differentiated /senescent $CD8^+$ T cells, are mainly defined by CD45RA and KIRs. Because most of the ligands [e.g., nonclassical HLA-G (250)] for these KIRs are expressed on somatic cells, it is possible that the activation of these $CD8^+$ T cells is no longer under the control of pAPC, and instead under the control of the tissue microenviroment, similar to NK cells (195). At the present time, we do not know whether these NKR-expressing, senescent $CD8^+$, despite being $CD3^+$ (TCR^+), exhibited HLA-unrestricted cytotoxicity like NK cells,

(**Chapter 3**). It will be of interest in a future experiment to co-incubate KIR-expressing $CD8^+$ TIL with NK-sensitive cell line such as the K562 (human myelogenous leukemia) (251), and determine whether these target cells can be killed independently of TCR triggering.

Figure 4-1: Proposed differentiation pathway of the tumor-infiltrating $CD8^+$ T cells in metastatic cancer. In situations where $CD8^+$ T cells encounter persistent, chronic antigenic stimulation such as metastatic cancer or uncontrolled chronic viral infections, $CD8^+$ effector-memory (T_{EM}) cells fail to coordinate down-regulation of CD27 with up-regulation of an end-stage CTL marker, CD57. Thus T_{EM} fail to transition from a granzyme B (GB^+) $perforin^{lo}$ ($Perf^{lo}$) cells into $Perf^{hi}$, highly cytotoxic end-stage CTL. This resulted in accumulation of $CD8^+$ T cells at a transitional stage where markers for early effector-memory T cells, CD27, CD28, BTLA, and PD-1, are co-expressed with CD57, even though the cells remain $Perf^{Lo}$. We think that TGF-β1 or signaling through PD-1 and BTLA may contribute to the arrested differentiation and accumulations of $CD27^+CD57^-$ precursor T cells and $CD27^+CD57^+$ T cell. $CD27^+CD57^+$ T cells highly express inhibitory receptors, PD-1 and BTLA, which implies that they may exhibit a higher level of effector activity. When these tumor-infiltrating lymphocytes (TIL) are expanded with IL-2, a minor fraction (~30%) of $CD27^+CD57^-$ subset differentiated into $CD27^+CD57^+$ T cells. After TCR stimulation *ex vivo*, the $CD27^+$ $CD57^-$ subset directly differentiated to become $CD27^-CD57^-$ T cells, while the $CD27^+CD57^+$ subset differentiated to become $CD27^-CD57^+$, and, in some patients, $CD27^-CD57^-$, with down-regulation of PD-1 and BTLA with progressive differentiation. These phenotypic changes were accompanied by increased perforin expression and acquisition of potent cytotoxicity against tumor cells. We think that CD57 is not a marker for T-cell senescence, but rather marks highly differentiated T cells that is in the process of transitioning into a truly end-stage, senescent effector CTL. We propose that the truly end-stage CTL is more NK-like, and could be defined by a $CD45RA^+$, $KIRs^{++}$, $KLRG\text{-}1^+$, $CD56^+$, and $CD122^+$ (?) phenotype (conventional $CD8^+$ T cells are $CD122^-$). CTL: cytotoxic T lymphocytes; Ag: antigen; CD122: IL-2Rβ; CD56: Neural cell adhesion molecule; KIRs: killer-cell immunoglobulin-like receptors. KLRG-1: killer-cell lectin-like receptor G1.

Reprinted with permission from: Wu RC, Hwu P, and Radvanyi LG. 2012. New insights on the role of $CD8^+CD57^+$ T cells in cancer. *Oncoimmunology*. 1(6): 954-956. http://dx.doi.org/10.4161/onci.20307

Figure 4-1:

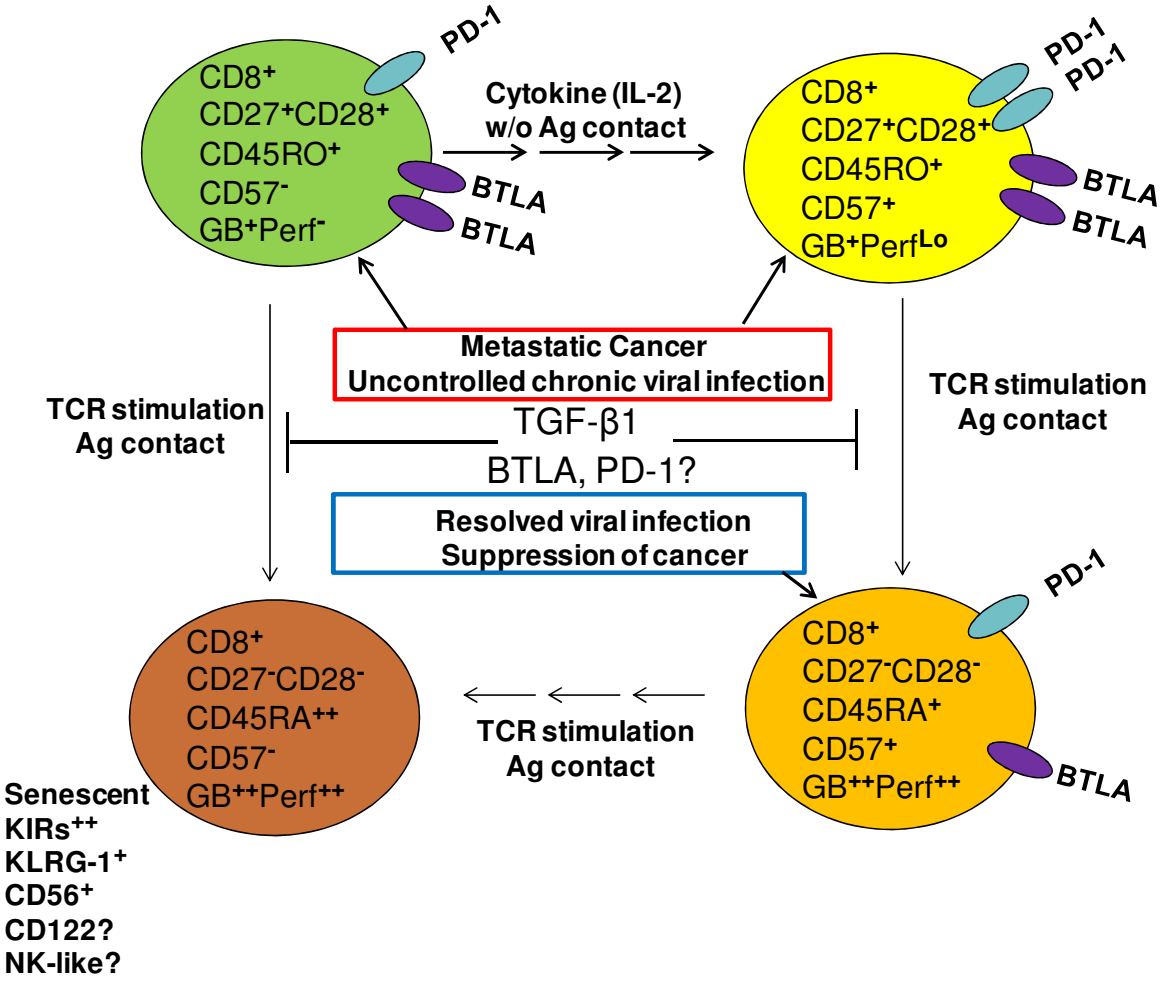
PD-1
CD8+
CD27+CD28+
CD45RO+
CD57-
GB+Perf-
BTLA
BTLA
Cytokine (IL-2)
w/o Ag contact
PD-1
PD-1
CD8+
CD27+CD28+
CD45RO+
CD57+
GB+PerfLo
BTLA
BTLA
Metastatic Cancer
Uncontrolled chronic viral infection
TGF-β1
BTLA, PD-1?
Resolved viral infection
Suppression of cancer
TCR stimulation
Ag contact
TCR stimulation
Ag contact
PD-1
CD8+
CD27-CD28-
CD45RA++
CD57-
GB++Perf++
TCR stimulation
Ag contact
CD8+
CD27-CD28-
CD45RA+
CD57+
GB++Perf++
BTLA
Senescent
KIRs++
KLRG-1+
CD56+
CD122?
NK-like?

Figure 4-2: Distinct geographic infiltrative patterns of T-cells within melanoma metastases. (**A**) Rare $CD3^+$ TILs identified by IHC in a benign nevus, indicated by arrows. 200x original magnification (size bar 50 um). (**B**) A 'moderate' infiltrate of $CD3^+$ TILs at the advancing edge of an invasive primary melanoma, nodular histologic subtype, 40x original magnification (size bar 200 um). (**C**) 400x original magnification (20 um size bar) of the boxed area shown in panel **B**. (**D**) Only singular $CD3^+$ TILs were observed, predominantly in perivascular areas and not infiltrating among tumor cells, in a melanoma metastasis. 200x original magnification (size bar 50 um).

"From Taube JM, Anders RA, Young GD, Xu H, Sharma R, McMiller TL, Chen S, Klein AP, Pardoll DM, Topalian SL, and Chen L. 2012. Colocalization of inflammatory response with B7-h1 expression in human melanocytic lesions supports an adaptive resistance mechanism of immune escape. *Sci. Transl. Med.* 4(127): 127ra37. Reprinted with permission from AAAS."

Figure 4-2:

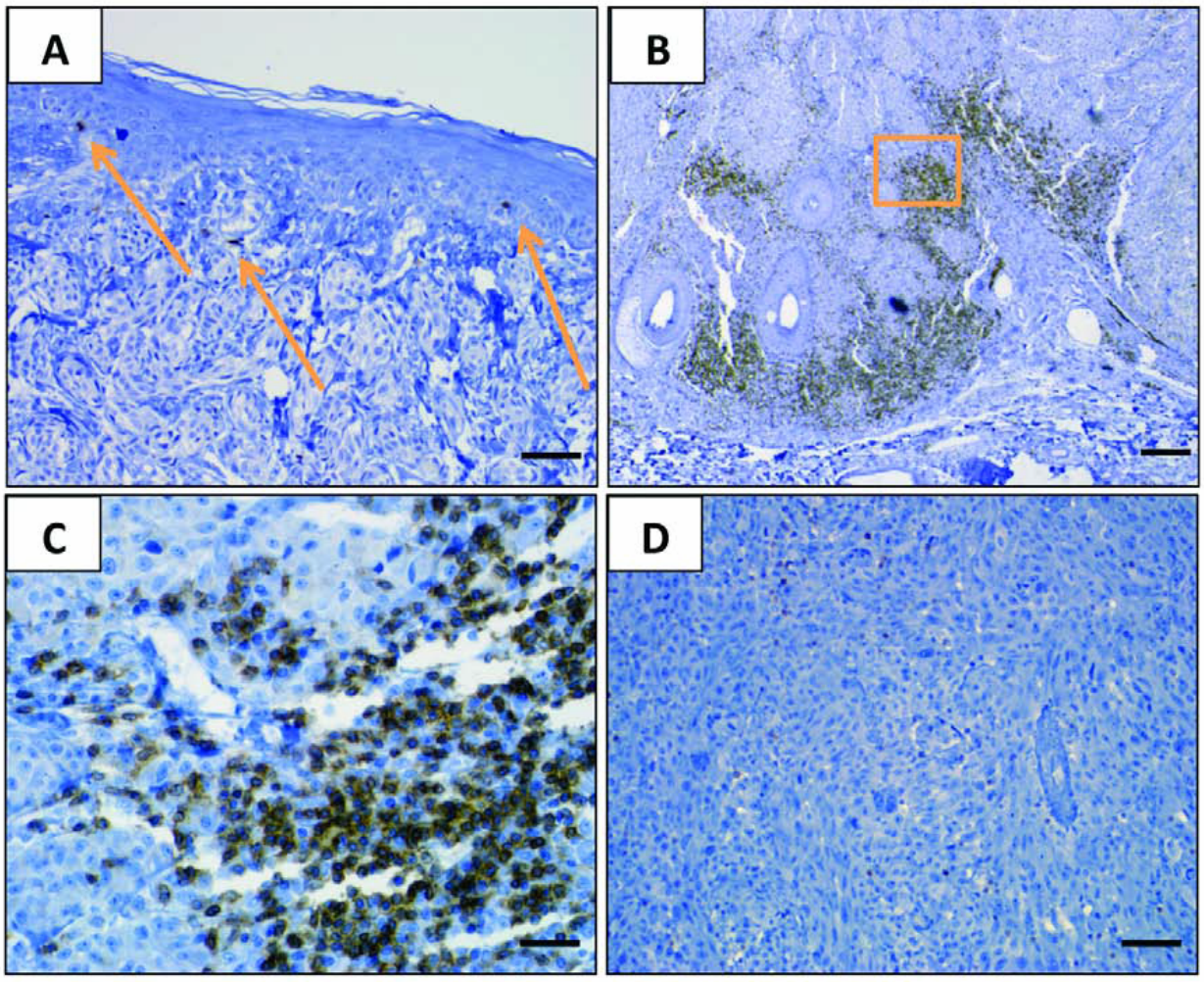

Bibliography:

1. American Cancer Society. "Cancer facts & figures 2012." Retrieved January 27th, 2013, from http://www.cancer.org/acs/groups/content/@epidemiologysurveilance/documents/document/acspc-031941.pdf.
2. National Cancer Institute. (2012). "General Information about melanoma." Retrieved January 27th, 2013, from http://www.cancer.gov/cancertopics/pdq/treatment/melanoma/healthprofessional.
3. Howell, P. M., Jr., S. Liu, S. Ren, C. Behlen, O. Fodstad, and A. I. Riker. 2009. Epigenetics in human melanoma. *Cancer Control* 16:200-218.
4. Legha, S. S. 2009. Treating metastatic melanoma: further considerations. *Oncology (Williston Park)* 23:500, 508.
5. Flockhart, R. J., J. L. Armstrong, N. J. Reynolds, and P. E. Lovat. 2009. NFAT signalling is a novel target of oncogenic BRAF in metastatic melanoma. *British journal of cancer*.
6. Hersey, P., L. Bastholt, V. Chiarion-Sileni, G. Cinat, R. Dummer, A. M. Eggermont, E. Espinosa, A. Hauschild, I. Quirt, C. Robert, and D. Schadendorf. 2009. Small molecules and targeted therapies in distant metastatic disease. *Ann Oncol* 20 Suppl 6:vi35-40.
7. Jaiswal, B. S., V. Janakiraman, N. M. Kljavin, J. Eastham-Anderson, J. E. Cupp, Y. Liang, D. P. Davis, K. P. Hoeflich, and S. Seshagiri. 2009. Combined targeting of BRAF and CRAF or BRAF and PI3K effector pathways is required for efficacy in NRAS mutant tumors. *PloS one* 4:e5717.

8. Kido, K., H. Sumimoto, S. Asada, S. M. Okada, T. Yaguchi, N. Kawamura, M. Miyagishi, T. Saida, and Y. Kawakami. 2009. Simultaneous suppression of MITF and BRAF V600E enhanced inhibition of melanoma cell proliferation. *Cancer science* 100:1863-1869.

9. American Cancer Society. (2012). "Melanoma Skin Cancer: How is melanoma skin cancer staged?". Retrieved January 27th, 2013, from http://www.cancer.org/cancer/skincancer-melanoma/detailedguide/melanoma-skin-cancer-staging.

10. National Cancer Institute. (2012). "Melanoma Treatment (PDQ)." Retrieved January 27th, 2013, from http://www.cancer.gov/cancertopics/pdq/treatment/melanoma/HealthProfessional/page4.

11. Kirkwood, J. M., M. H. Strawderman, M. S. Ernstoff, T. J. Smith, E. C. Borden, and R. H. Blum. 1996. Interferon alfa-2b adjuvant therapy of high-risk resected cutaneous melanoma: the Eastern Cooperative Oncology Group Trial EST 1684. *J Clin Oncol* 14:7-17.

12. Chapman, P. B., L. H. Einhorn, M. L. Meyers, S. Saxman, A. N. Destro, K. S. Panageas, C. B. Begg, S. S. Agarwala, L. M. Schuchter, M. S. Ernstoff, A. N. Houghton, and J. M. Kirkwood. 1999. Phase III multicenter randomized trial of the Dartmouth regimen versus dacarbazine in patients with metastatic melanoma. *J Clin Oncol* 17:2745-2751.

13. Middleton, M. R., J. J. Grob, N. Aaronson, G. Fierlbeck, W. Tilgen, S. Seiter, M. Gore, S. Aamdal, J. Cebon, A. Coates, B. Dreno, M. Henz, D. Schadendorf, A. Kapp, J. Weiss, U. Fraass, P. Statkevich, M. Muller, and N. Thatcher. 2000. Randomized

phase III study of temozolomide versus dacarbazine in the treatment of patients with advanced metastatic malignant melanoma. *J Clin Oncol* 18:158-166.

14. Robert, C., L. Thomas, I. Bondarenko, S. O'Day, D. J. M, C. Garbe, C. Lebbe, J. F. Baurain, A. Testori, J. J. Grob, N. Davidson, J. Richards, M. Maio, A. Hauschild, W. H. Miller, Jr., P. Gascon, M. Lotem, K. Harmankaya, R. Ibrahim, S. Francis, T. T. Chen, R. Humphrey, A. Hoos, and J. D. Wolchok. Ipilimumab plus dacarbazine for previously untreated metastatic melanoma. *N Engl J Med* 364:2517-2526.

15. Chapman, P. B., A. Hauschild, C. Robert, J. B. Haanen, P. Ascierto, J. Larkin, R. Dummer, C. Garbe, A. Testori, M. Maio, D. Hogg, P. Lorigan, C. Lebbe, T. Jouary, D. Schadendorf, A. Ribas, S. J. O'Day, J. A. Sosman, J. M. Kirkwood, A. M. Eggermont, B. Dreno, K. Nolop, J. Li, B. Nelson, J. Hou, R. J. Lee, K. T. Flaherty, and G. A. McArthur. 2011. Improved survival with vemurafenib in melanoma with BRAF V600E mutation. *N Engl J Med* 364:2507-2516.

16. Weber, J. 2007. Review: anti-CTLA-4 antibody ipilimumab: case studies of clinical response and immune-related adverse events. *Oncologist* 12:864-872.

17. Manola, J., M. Atkins, J. Ibrahim, and J. Kirkwood. 2000. Prognostic factors in metastatic melanoma: a pooled analysis of Eastern Cooperative Oncology Group trials. *J Clin Oncol* 18:3782-3793.

18. Sullivan, R. J., and K. T. Flaherty. Resistance to BRAF-targeted therapy in melanoma. *Eur J Cancer*.

19. Liu ZJ, H. M. 2005. Melanoma. In *Cancer: Principles and Practice of Oncology*, 7th ed. H. S. DeVita VT Jr., Rosenberg SA., ed. Lippincott Williams & Wilkins, Philadelphia, PA. 1745-1824.

20. Tarazona, R., J. G. Casado, R. Soto, O. DelaRosa, E. Peralbo, L. Rioja, J. Pena, and R. Solana. 2004. Expression of NK-associated receptors on cytotoxic T cells from melanoma patients: a two-edged sword? *Cancer Immunol Immunother* 53:911-924.

21. Kawakami, Y., S. Eliyahu, K. Sakaguchi, P. F. Robbins, L. Rivoltini, J. R. Yannelli, E. Appella, and S. A. Rosenberg. 1994. Identification of the immunodominant peptides of the MART-1 human melanoma antigen recognized by the majority of HLA-A2-restricted tumor infiltrating lymphocytes. *J Exp Med* 180:347-352.

22. Jager, E., D. Jager, J. Karbach, Y. T. Chen, G. Ritter, Y. Nagata, S. Gnjatic, E. Stockert, M. Arand, L. J. Old, and A. Knuth. 2000. Identification of NY-ESO-1 epitopes presented by human histocompatibility antigen (HLA)-DRB4*0101-0103 and recognized by CD4(+) T lymphocytes of patients with NY-ESO-1-expressing melanoma. *J Exp Med* 191:625-630.

23. Radvanyi, L. 2004. Discovery and immunologic validation of new antigens for therapeutic cancer vaccines. *Int Arch Allergy Immunol* 133:179-197.

24. Robbins, P. F., M. El-Gamil, Y. F. Li, Y. Kawakami, D. Loftus, E. Appella, and S. A. Rosenberg. 1996. A mutated beta-catenin gene encodes a melanoma-specific antigen recognized by tumor infiltrating lymphocytes. *J Exp Med* 183:1185-1192.

25. Heinzel, S., D. Rea, R. Offringa, and G. Pawelec. 2001. The self peptide annexin II (208-223) presented by dendritic cells sensitizes autologous CD4+ T lymphocytes to recognize melanoma cells. *Cancer Immunol Immunother* 49:671-678.

26. Li, K., M. Adibzadeh, T. Halder, H. Kalbacher, S. Heinzel, C. Muller, J. Zeuthen, and G. Pawelec. 1998. Tumour-specific MHC-class-II-restricted responses after in vitro

sensitization to synthetic peptides corresponding to gp100 and Annexin II eluted from melanoma cells. *Cancer Immunol Immunother* 47:32-38.

27. Topalian, S. L., L. Rivoltini, M. Mancini, N. R. Markus, P. F. Robbins, Y. Kawakami, and S. A. Rosenberg. 1994. Human CD4+ T cells specifically recognize a shared melanoma-associated antigen encoded by the tyrosinase gene. *Proc Natl Acad Sci U S A* 91:9461-9465.

28. Topalian, S. L., M. I. Gonzales, M. Parkhurst, Y. F. Li, S. Southwood, A. Sette, S. A. Rosenberg, and P. F. Robbins. 1996. Melanoma-specific CD4+ T cells recognize nonmutated HLA-DR-restricted tyrosinase epitopes. *J Exp Med* 183:1965-1971.

29. Touloukian, C. E., W. W. Leitner, S. L. Topalian, Y. F. Li, P. F. Robbins, S. A. Rosenberg, and N. P. Restifo. 2000. Identification of a MHC class II-restricted human gp100 epitope using DR4-IE transgenic mice. *J Immunol* 164:3535-3542.

30. 2010. Trial watch: ipilimumab success in melanoma provides boost for cancer immunotherapy. *Nat Rev Drug Discov* 9:584.

31. Callahan, M. K., J. D. Wolchok, and J. P. Allison. 2011. Anti-CTLA-4 antibody therapy: immune monitoring during clinical development of a novel immunotherapy. *Semin Oncol* 37:473-484.

32. Korman, A. J., K. S. Peggs, and J. P. Allison. 2006. Checkpoint blockade in cancer immunotherapy. *Adv Immunol* 90:297-339.

33. Wang, L., R. Rubinstein, J. L. Lines, A. Wasiuk, C. Ahonen, Y. Guo, L. F. Lu, D. Gondek, Y. Wang, R. A. Fava, A. Fiser, S. Almo, and R. J. Noelle. VISTA, a novel mouse Ig superfamily ligand that negatively regulates T cell responses. *J Exp Med* 208:577-592.

34. Ngiow, S. F., B. von Scheidt, H. Akiba, H. Yagita, M. W. Teng, and M. J. Smyth. Anti-TIM3 antibody promotes T cell IFN-gamma-mediated antitumor immunity and suppresses established tumors. *Cancer Res* 71:3540-3551.

35. Sedy, J. R., M. Gavrieli, K. G. Potter, M. A. Hurchla, R. C. Lindsley, K. Hildner, S. Scheu, K. Pfeffer, C. F. Ware, T. L. Murphy, and K. M. Murphy. 2005. B and T lymphocyte attenuator regulates T cell activation through interaction with herpesvirus entry mediator. *Nat Immunol* 6:90-98.

36. Ahmadzadeh, M., L. A. Johnson, B. Heemskerk, J. R. Wunderlich, M. E. Dudley, D. E. White, and S. A. Rosenberg. 2009. Tumor antigen-specific CD8 T cells infiltrating the tumor express high levels of PD-1 and are functionally impaired. *Blood* 114:1537-1544.

37. Fourcade, J., P. Kudela, Z. Sun, H. Shen, S. R. Land, D. Lenzner, P. Guillaume, I. F. Luescher, C. Sander, S. Ferrone, J. M. Kirkwood, and H. M. Zarour. 2009. PD-1 is a regulator of NY-ESO-1-specific CD8+ T cell expansion in melanoma patients. *J Immunol* 182:5240-5249.

38. Keir, M. E., L. M. Francisco, and A. H. Sharpe. 2007. PD-1 and its ligands in T-cell immunity. *Current opinion in immunology* 19:309-314.

39. Butte, M. J., M. E. Keir, T. B. Phamduy, A. H. Sharpe, and G. J. Freeman. 2007. Programmed death-1 ligand 1 interacts specifically with the B7-1 costimulatory molecule to inhibit T cell responses. *Immunity* 27:111-122.

40. Hamanishi, J., M. Mandai, M. Iwasaki, T. Okazaki, Y. Tanaka, K. Yamaguchi, T. Higuchi, H. Yagi, K. Takakura, N. Minato, T. Honjo, and S. Fujii. 2007. Programmed

cell death 1 ligand 1 and tumor-infiltrating CD8+ T lymphocytes are prognostic factors of human ovarian cancer. *Proc Natl Acad Sci U S A* 104:3360-3365.

41. Nomi, T., M. Sho, T. Akahori, K. Hamada, A. Kubo, H. Kanehiro, S. Nakamura, K. Enomoto, H. Yagita, M. Azuma, and Y. Nakajima. 2007. Clinical significance and therapeutic potential of the programmed death-1 ligand/programmed death-1 pathway in human pancreatic cancer. *Clin Cancer Res* 13:2151-2157.

42. Hino, R., K. Kabashima, Y. Kato, H. Yagi, M. Nakamura, T. Honjo, T. Okazaki, and Y. Tokura. Tumor cell expression of programmed cell death-1 ligand 1 is a prognostic factor for malignant melanoma. *Cancer* 116:1757-1766.

43. Taube, J. M., R. A. Anders, G. D. Young, H. Xu, R. Sharma, T. L. McMiller, S. Chen, A. P. Klein, D. M. Pardoll, S. L. Topalian, and L. Chen. Colocalization of inflammatory response with B7-h1 expression in human melanocytic lesions supports an adaptive resistance mechanism of immune escape. *Sci Transl Med* 4:127ra137.

44. Droeser, R. A., C. Hirt, C. T. Viehl, D. M. Frey, C. Nebiker, X. Huber, I. Zlobec, S. Eppenberger-Castori, A. Tzankov, R. Rosso, M. Zuber, M. G. Muraro, F. Amicarella, E. Cremonesi, M. Heberer, G. Iezzi, A. Lugli, L. Terracciano, G. Sconocchia, D. Oertli, G. C. Spagnoli, and L. Tornillo. Clinical impact of programmed cell death ligand 1 expression in colorectal cancer. *Eur J Cancer*.

45. Chen, J., Y. Feng, L. Lu, H. Wang, L. Dai, Y. Li, and P. Zhang. Interferon-gamma-induced PD-L1 surface expression on human oral squamous carcinoma via PKD2 signal pathway. *Immunobiology* 217:385-393.

46. Brahmer, J. R., C. G. Drake, I. Wollner, J. D. Powderly, J. Picus, W. H. Sharfman, E. Stankevich, A. Pons, T. M. Salay, T. L. McMiller, M. M. Gilson, C. Wang, M. Selby,

J. M. Taube, R. Anders, L. Chen, A. J. Korman, D. M. Pardoll, I. Lowy, and S. L. Topalian. Phase I study of single-agent anti-programmed death-1 (MDX-1106) in refractory solid tumors: safety, clinical activity, pharmacodynamics, and immunologic correlates. *J Clin Oncol* 28:3167-3175.

47. Topalian, S. L., F. S. Hodi, J. R. Brahmer, S. N. Gettinger, D. C. Smith, D. F. McDermott, J. D. Powderly, R. D. Carvajal, J. A. Sosman, M. B. Atkins, P. D. Leming, D. R. Spigel, S. J. Antonia, L. Horn, C. G. Drake, D. M. Pardoll, L. Chen, W. H. Sharfman, R. A. Anders, J. M. Taube, T. L. McMiller, H. Xu, A. J. Korman, M. Jure-Kunkel, S. Agrawal, D. McDonald, G. D. Kollia, A. Gupta, J. M. Wigginton, and M. Sznol. Safety, activity, and immune correlates of anti-PD-1 antibody in cancer. *N Engl J Med* 366:2443-2454.

48. Brahmer, J. R., S. S. Tykodi, L. Q. Chow, W. J. Hwu, S. L. Topalian, P. Hwu, C. G. Drake, L. H. Camacho, J. Kauh, K. Odunsi, H. C. Pitot, O. Hamid, S. Bhatia, R. Martins, K. Eaton, S. Chen, T. M. Salay, S. Alaparthy, J. F. Grosso, A. J. Korman, S. M. Parker, S. Agrawal, S. M. Goldberg, D. M. Pardoll, A. Gupta, and J. M. Wigginton. Safety and activity of anti-PD-L1 antibody in patients with advanced cancer. *N Engl J Med* 366:2455-2465.

49. Sierro, S., P. Romero, and D. E. Speiser. The CD4-like molecule LAG-3, biology and therapeutic applications. *Expert Opin Ther Targets* 15:91-101.

50. Watanabe, N., M. Gavrieli, J. R. Sedy, J. Yang, F. Fallarino, S. K. Loftin, M. A. Hurchla, N. Zimmerman, J. Sim, X. Zang, T. L. Murphy, J. H. Russell, J. P. Allison, and K. M. Murphy. 2003. BTLA is a lymphocyte inhibitory receptor with similarities to CTLA-4 and PD-1. *Nat Immunol* 4:670-679.

51. Gavrieli, M., and K. M. Murphy. 2006. Association of Grb-2 and PI3K p85 with phosphotyrosile peptides derived from BTLA. *Biochem Biophys Res Commun* 345:1440-1445.

52. Derre, L., J. P. Rivals, C. Jandus, S. Pastor, D. Rimoldi, P. Romero, O. Michielin, D. Olive, and D. E. Speiser. BTLA mediates inhibition of human tumor-specific CD8+ T cells that can be partially reversed by vaccination. *J Clin Invest* 120:157-167.

53. Fourcade, J., Z. Sun, O. Pagliano, P. Guillaume, I. F. Luescher, C. Sander, J. M. Kirkwood, D. Olive, V. Kuchroo, and H. M. Zarour. CD8(+) T cells specific for tumor antigens can be rendered dysfunctional by the tumor microenvironment through upregulation of the inhibitory receptors BTLA and PD-1. *Cancer Res* 72:887-896.

54. Serriari, N. E., F. Gondois-Rey, Y. Guillaume, E. B. Remmerswaal, S. Pastor, N. Messal, A. Truneh, I. Hirsch, R. A. van Lier, and D. Olive. B and T lymphocyte attenuator is highly expressed on CMV-specific T cells during infection and regulates their function. *J Immunol* 185:3140-3148.

55. Radvanyi, L. G., C. Bernatchez, M. Zhang, P. S. Fox, P. Miller, J. Chacon, R. Wu, G. Lizee, S. Mahoney, G. Alvarado, M. Glass, V. E. Johnson, J. D. McMannis, E. Shpall, V. Prieto, N. Papadopoulos, K. Kim, J. Homsi, A. Bedikian, W. J. Hwu, S. Patel, M. I. Ross, J. E. Lee, J. E. Gershenwald, A. Lucci, R. Royal, J. N. Cormier, M. A. Davies, R. Mansaray, O. J. Fulbright, C. Toth, R. Ramachandran, S. Wardell, A. Gonzalez, and P. Hwu. 2012. Specific lymphocyte subsets predict response to adoptive cell therapy using expanded autologous tumor-infiltrating lymphocytes in metastatic melanoma patients. *Clin Cancer Res* 18:6758-6770.

56. Atkins, M. B., L. Kunkel, M. Sznol, and S. A. Rosenberg. 2000. High-dose recombinant interleukin-2 therapy in patients with metastatic melanoma: long-term survival update. *Cancer J Sci Am* 6 Suppl 1:S11-14.

57. Schwartzentruber, D. J., D. H. Lawson, J. M. Richards, R. M. Conry, D. M. Miller, J. Treisman, F. Gailani, L. Riley, K. Conlon, B. Pockaj, K. L. Kendra, R. L. White, R. Gonzalez, T. M. Kuzel, B. Curti, P. D. Leming, E. D. Whitman, J. Balkissoon, D. S. Reintgen, H. Kaufman, F. M. Marincola, M. J. Merino, S. A. Rosenberg, P. Choyke, D. Vena, and P. Hwu. 2011. gp100 peptide vaccine and interleukin-2 in patients with advanced melanoma. *N Engl J Med* 364:2119-2127.

58. Besser, M. J., R. Shapira-Frommer, A. J. Treves, D. Zippel, O. Itzhaki, L. Hershkovitz, D. Levy, A. Kubi, E. Hovav, N. Chermoshniuk, B. Shalmon, I. Hardan, R. Catane, G. Markel, S. Apter, A. Ben-Nun, I. Kuchuk, A. Shimoni, A. Nagler, and J. Schachter. 2010. Clinical responses in a phase II study using adoptive transfer of short-term cultured tumor infiltration lymphocytes in metastatic melanoma patients. *Clin Cancer Res* 16:2646-2655.

59. Dudley, M. E., J. R. Wunderlich, J. C. Yang, R. M. Sherry, S. L. Topalian, N. P. Restifo, R. E. Royal, U. Kammula, D. E. White, S. A. Mavroukakis, L. J. Rogers, G. J. Gracia, S. A. Jones, D. P. Mangiameli, M. M. Pelletier, J. Gea-Banacloche, M. R. Robinson, D. M. Berman, A. C. Filie, A. Abati, and S. A. Rosenberg. 2005. Adoptive cell transfer therapy following non-myeloablative but lymphodepleting chemotherapy for the treatment of patients with refractory metastatic melanoma. *J Clin Oncol* 23:2346-2357.

60. Radvanyi, L. G., C. Bernatchez, M. Zhang, P. Miller, M. Glass, N. Papadopoulos, and P. Hwu. 2010. Adoptive T-cell therapy for metastatic melanoma: The MD Anderson experience. *J Immunother* 33:863.

61. Hernandez-Chacon, J. A., Y. Li, R. C. Wu, C. Bernatchez, Y. Wang, J. S. Weber, P. Hwu, and L. G. Radvanyi. Costimulation through the CD137/4-1BB pathway protects human melanoma tumor-infiltrating lymphocytes from activation-induced cell death and enhances antitumor effector function. *J Immunother* 34:236-250.

62. Vinay, D. S., and B. S. Kwon. Immunotherapy of cancer with 4-1BB. *Mol Cancer Ther* 11:1062-1070.

63. Ueki, T., S. Murata, N. Kitamura, E. Mekata, and T. Tani. 2009. Pre-treatment with cyclophosphamide or OX40 (CD134) costimulation targeting regulatory T cell function enhances the anti-tumor immune effect of adoptively transferred CD8+ T cells from wild-type mice. *Mol Med Report* 2:615-620.

64. Sumimoto, H., F. Imabayashi, T. Iwata, and Y. Kawakami. 2006. The BRAF-MAPK signaling pathway is essential for cancer-immune evasion in human melanoma cells. *J Exp Med* 203:1651-1656.

65. Boni, A., A. P. Cogdill, P. Dang, D. Udayakumar, C. N. Njauw, C. M. Sloss, C. R. Ferrone, K. T. Flaherty, D. P. Lawrence, D. E. Fisher, H. Tsao, and J. A. Wargo. 2010. Selective BRAFV600E inhibition enhances T-cell recognition of melanoma without affecting lymphocyte function. *Cancer Res* 70:5213-5219.

66. Zitvogel, L., L. Apetoh, F. Ghiringhelli, and G. Kroemer. 2008. Immunological aspects of cancer chemotherapy. *Nat Rev Immunol* 8:59-73.

67. Locher, C., R. Conforti, L. Aymeric, Y. Ma, T. Yamazaki, S. Rusakiewicz, A. Tesniere, F. Ghiringhelli, L. Apetoh, Y. Morel, J. P. Girard, G. Kroemer, and L. Zitvogel. 2010. Desirable cell death during anticancer chemotherapy. *Ann N Y Acad Sci* 1209:99-108.

68. Obeid, M., A. Tesniere, F. Ghiringhelli, G. M. Fimia, L. Apetoh, J. L. Perfettini, M. Castedo, G. Mignot, T. Panaretakis, N. Casares, D. Metivier, N. Larochette, P. van Endert, F. Ciccosanti, M. Piacentini, L. Zitvogel, and G. Kroemer. 2007. Calreticulin exposure dictates the immunogenicity of cancer cell death. *Nat Med* 13:54-61.

69. Tompers Frederick, D., A. Piris, A. P. Cogdill, Z. A. Cooper, C. Lezcano, C. R. Ferrone, D. Mitra, A. Boni, L. P. Newton, C. Liu, W. Peng, R. J. Sullivan, D. P. Lawrence, F. S. Hodi, W. W. Overwijk, G. Lizee, G. F. Murphy, P. Hwu, K. T. Flaherty, D. E. Fisher, and J. A. Wargo. BRAF inhibition is associated with enhanced melanoma antigen expression and a more favorable tumor microenvironment in patients with metastatic melanoma. *Clin Cancer Res*.

70. Yang, J. C., and S. A. Rosenberg. 1988. Current approaches to the adoptive immunotherapy of cancer. *Advances in experimental medicine and biology* 233:459-467.

71. Radvanyi, L. G., C. Bernatchez, M. Zhang, P. S. Fox, P. Miller, J. Chacon, R. Wu, G. Lizee, S. Mahoney, G. Alvarado, M. Glass, V. E. Johnson, J. D. McMannis, E. Shpall, V. Prieto, N. Papadopoulos, K. Kim, J. Homsi, A. Bedikian, W. J. Hwu, S. Patel, M. I. Ross, J. E. Lee, J. E. Gershenwald, A. Lucci, R. Royal, J. N. Cormier, M. A. Davies, R. Mansaray, O. J. Fulbright, C. Toth, R. Ramachandran, S. Wardell, A. Gonzalez, and P. Hwu. Specific lymphocyte subsets predict response to adoptive cell

therapy using expanded autologous tumor-infiltrating lymphocytes in metastatic melanoma patients. *Clin Cancer Res* 18:6758-6770.

72. Mackensen, A., N. Meidenbauer, S. Vogl, M. Laumer, J. Berger, and R. Andreesen. 2006. Phase I study of adoptive T-cell therapy using antigen-specific CD8+ T cells for the treatment of patients with metastatic melanoma. *J Clin Oncol* 24:5060-5069.

73. Mitchell, M. S., D. Darrah, D. Yeung, S. Halpern, A. Wallace, J. Voland, V. Jones, and J. Kan-Mitchell. 2002. Phase I trial of adoptive immunotherapy with cytolytic T lymphocytes immunized against a tyrosinase epitope. *J Clin Oncol* 20:1075-1086.

74. Yee, C., J. A. Thompson, D. Byrd, S. R. Riddell, P. Roche, E. Celis, and P. D. Greenberg. 2002. Adoptive T cell therapy using antigen-specific CD8+ T cell clones for the treatment of patients with metastatic melanoma: in vivo persistence, migration, and antitumor effect of transferred T cells. *Proc Natl Acad Sci U S A* 99:16168-16173.

75. Morgan, R. A., M. E. Dudley, J. R. Wunderlich, M. S. Hughes, J. C. Yang, R. M. Sherry, R. E. Royal, S. L. Topalian, U. S. Kammula, N. P. Restifo, Z. Zheng, A. Nahvi, C. R. de Vries, L. J. Rogers-Freezer, S. A. Mavroukakis, and S. A. Rosenberg. 2006. Cancer regression in patients after transfer of genetically engineered lymphocytes. *Science* 314:126-129.

76. Morgan, R. A., M. E. Dudley, Y. Y. Yu, Z. Zheng, P. F. Robbins, M. R. Theoret, J. R. Wunderlich, M. S. Hughes, N. P. Restifo, and S. A. Rosenberg. 2003. High efficiency TCR gene transfer into primary human lymphocytes affords avid recognition of melanoma tumor antigen glycoprotein 100 and does not alter the recognition of autologous melanoma antigens. *J Immunol* 171:3287-3295.

77. Kalos, M., B. L. Levine, D. L. Porter, S. Katz, S. A. Grupp, A. Bagg, and C. H. June. 2011. T cells with chimeric antigen receptors have potent antitumor effects and can establish memory in patients with advanced leukemia. *Sci Transl Med* 3:95ra73.

78. Yvon, E., M. Del Vecchio, B. Savoldo, V. Hoyos, A. Dutour, A. Anichini, G. Dotti, and M. K. Brenner. 2009. Immunotherapy of metastatic melanoma using genetically engineered GD2-specific T cells. *Clin Cancer Res* 15:5852-5860.

79. Porter, D. L., B. L. Levine, M. Kalos, A. Bagg, and C. H. June. Chimeric antigen receptor-modified T cells in chronic lymphoid leukemia. *N Engl J Med* 365:725-733.

80. Cell Signaling Technology. 2010. T-cell Receptor Signaling. Cell Signaling Technology. .

81. Chekmasova, A. 2010. Adoptive T-cell Immunotherapy Strategies for the Treatment of Patients with Ovarian Cancer. Discovery Magazine.

82. Dudley, M. E., C. A. Gross, M. M. Langhan, M. R. Garcia, R. M. Sherry, J. C. Yang, G. Q. Phan, U. S. Kammula, M. S. Hughes, D. E. Citrin, N. P. Restifo, J. R. Wunderlich, P. A. Prieto, J. J. Hong, R. C. Langan, D. A. Zlott, K. E. Morton, D. E. White, C. M. Laurencot, and S. A. Rosenberg. 2010. CD8+ enriched "young" tumor infiltrating lymphocytes can mediate regression of metastatic melanoma. *Clin Cancer Res* 16:6122-6131.

83. Dudley, M. E., J. C. Yang, R. Sherry, M. S. Hughes, R. Royal, U. Kammula, P. F. Robbins, J. Huang, D. E. Citrin, S. F. Leitman, J. Wunderlich, N. P. Restifo, A. Thomasian, S. G. Downey, F. O. Smith, J. Klapper, K. Morton, C. Laurencot, D. E. White, and S. A. Rosenberg. 2008. Adoptive cell therapy for patients with metastatic

melanoma: evaluation of intensive myeloablative chemoradiation preparative regimens. *J Clin Oncol* 26:5233-5239.

84. Rosenberg, S. A., and M. E. Dudley. 2004. Cancer regression in patients with metastatic melanoma after the transfer of autologous antitumor lymphocytes. *Proc Natl Acad Sci U S A* 101 Suppl 2:14639-14645.

85. Rosenberg, S. A., J. C. Yang, R. M. Sherry, U. S. Kammula, M. S. Hughes, G. Q. Phan, D. E. Citrin, N. P. Restifo, P. F. Robbins, J. R. Wunderlich, K. E. Morton, C. M. Laurencot, S. M. Steinberg, D. E. White, and M. E. Dudley. 2011. Durable complete responses in heavily pretreated patients with metastatic melanoma using T-cell transfer immunotherapy. *Clin Cancer Res* 17:4550-4557.

86. Besser, M. J., R. Shapira-Frommer, A. J. Treves, D. Zippel, O. Itzhaki, E. Schallmach, A. Kubi, B. Shalmon, I. Hardan, R. Catane, E. Segal, G. Markel, S. Apter, A. B. Nun, I. Kuchuk, A. Shimoni, A. Nagler, and J. Schachter. 2009. Minimally cultured or selected autologous tumor-infiltrating lymphocytes after a lympho-depleting chemotherapy regimen in metastatic melanoma patients. *J Immunother* 32:415-423.

87. Hunder, N. N., H. Wallen, J. Cao, D. W. Hendricks, J. Z. Reilly, R. Rodmyre, A. Jungbluth, S. Gnjatic, J. A. Thompson, and C. Yee. 2008. Treatment of metastatic melanoma with autologous CD4+ T cells against NY-ESO-1. *N Engl J Med* 358:2698-2703.

88. Verdegaal, E. M., M. Visser, T. H. Ramwadhdoebe, C. E. van der Minne, J. A. van Steijn, E. Kapiteijn, J. B. Haanen, S. H. van der Burg, J. W. Nortier, and S. Osanto. 2011. Successful treatment of metastatic melanoma by adoptive transfer of blood-

derived polyclonal tumor-specific CD4+ and CD8+ T cells in combination with low-dose interferon-alpha. *Cancer Immunol Immunother* 60:953-963.

89. Butler, M. O., P. Friedlander, M. I. Milstein, M. M. Mooney, G. Metzler, A. P. Murray, M. Tanaka, A. Berezovskaya, O. Imataki, L. Drury, L. Brennan, M. Flavin, D. Neuberg, K. Stevenson, D. Lawrence, F. S. Hodi, E. F. Velazquez, M. T. Jaklitsch, S. E. Russell, M. Mihm, L. M. Nadler, and N. Hirano. 2011. Establishment of antitumor memory in humans using in vitro-educated CD8+ T cells. *Sci Transl Med* 3:80ra34.

90. Johnson, L. A., R. A. Morgan, M. E. Dudley, L. Cassard, J. C. Yang, M. S. Hughes, U. S. Kammula, R. E. Royal, R. M. Sherry, J. R. Wunderlich, C. C. Lee, N. P. Restifo, S. L. Schwarz, A. P. Cogdill, R. J. Bishop, H. Kim, C. C. Brewer, S. F. Rudy, C. VanWaes, J. L. Davis, A. Mathur, R. T. Ripley, D. A. Nathan, C. M. Laurencot, and S. A. Rosenberg. 2009. Gene therapy with human and mouse T-cell receptors mediates cancer regression and targets normal tissues expressing cognate antigen. *Blood* 114:535-546.

91. Robbins, P. F., R. A. Morgan, S. A. Feldman, J. C. Yang, R. M. Sherry, M. E. Dudley, J. R. Wunderlich, A. V. Nahvi, L. J. Helman, C. L. Mackall, U. S. Kammula, M. S. Hughes, N. P. Restifo, M. Raffeld, C. C. Lee, C. L. Levy, Y. F. Li, M. El-Gamil, S. L. Schwarz, C. Laurencot, and S. A. Rosenberg. 2011. Tumor regression in patients with metastatic synovial cell sarcoma and melanoma using genetically engineered lymphocytes reactive with NY-ESO-1. *J Clin Oncol* 29:917-924.

92. Lo, A. S., Q. Ma, D. L. Liu, and R. P. Junghans. 2010. Anti-GD3 chimeric sFv-CD28/T-cell receptor zeta designer T cells for treatment of metastatic melanoma and other neuroectodermal tumors. *Clin Cancer Res* 16:2769-2780.

93. Burns, W. R., Y. Zhao, T. L. Frankel, C. S. Hinrichs, Z. Zheng, H. Xu, S. A. Feldman, S. Ferrone, S. A. Rosenberg, and R. A. Morgan. 2010. A high molecular weight melanoma-associated antigen-specific chimeric antigen receptor redirects lymphocytes to target human melanomas. *Cancer Res* 70:3027-3033.

94. Dudley, M. E., J. R. Wunderlich, T. E. Shelton, J. Even, and S. A. Rosenberg. 2003. Generation of tumor-infiltrating lymphocyte cultures for use in adoptive transfer therapy for melanoma patients. *J Immunother* 26:332-342.

95. Hernandez-Chacon, J. A., Y. Li, R. C. Wu, C. Bernatchez, Y. Wang, J. S. Weber, P. Hwu, and L. G. Radvanyi. 2011. Costimulation through the CD137/4-1BB pathway protects human melanoma tumor-infiltrating lymphocytes from activation-induced cell death and enhances antitumor effector function. *J Immunother* 34:236-250.

96. Li, Y., S. Liu, J. Hernandez, L. Vence, P. Hwu, and L. Radvanyi. 2010. MART-1-specific melanoma tumor-infiltrating lymphocytes maintaining CD28 expression have improved survival and expansion capability following antigenic restimulation in vitro. *J Immunol* 184:452-465.

97. Riddell, S. R., and P. D. Greenberg. 1990. The use of anti-CD3 and anti-CD28 monoclonal antibodies to clone and expand human antigen-specific T cells. *J Immunol Methods* 128:189-201.

98. Dudley, M. E., and S. A. Rosenberg. 2003. Adoptive-cell-transfer therapy for the treatment of patients with cancer. *Nat Rev Cancer* 3:666-675.

99. Dudley, M. E., and S. A. Rosenberg. 2007. Adoptive cell transfer therapy. *Semin Oncol* 34:524-531.

100. Phan, G. Q., P. Attia, S. M. Steinberg, D. E. White, and S. A. Rosenberg. 2001. Factors associated with response to high-dose interleukin-2 in patients with metastatic melanoma. *J Clin Oncol* 19:3477-3482.

101. Zhou, J., M. E. Dudley, S. A. Rosenberg, and P. F. Robbins. 2004. Selective growth, in vitro and in vivo, of individual T cell clones from tumor-infiltrating lymphocytes obtained from patients with melanoma. *J Immunol* 173:7622-7629.

102. Huang, J., H. T. Khong, M. E. Dudley, M. El-Gamil, Y. F. Li, S. A. Rosenberg, and P. F. Robbins. 2005. Survival, persistence, and progressive differentiation of adoptively transferred tumor-reactive T cells associated with tumor regression. *J Immunother* 28:258-267.

103. Robbins, P. F., M. E. Dudley, J. Wunderlich, M. El-Gamil, Y. F. Li, J. Zhou, J. Huang, D. J. Powell, Jr., and S. A. Rosenberg. 2004. Cutting edge: persistence of transferred lymphocyte clonotypes correlates with cancer regression in patients receiving cell transfer therapy. *J Immunol* 173:7125-7130.

104. Klebanoff, C. A., H. T. Khong, P. A. Antony, D. C. Palmer, and N. P. Restifo. 2005. Sinks, suppressors and antigen presenters: how lymphodepletion enhances T cell-mediated tumor immunotherapy. *Trends in immunology* 26:111-117.

105. Wang, L. X., S. Shu, and G. E. Plautz. 2005. Host lymphodepletion augments T cell adoptive immunotherapy through enhanced intratumoral proliferation of effector cells. *Cancer Res* 65:9547-9554.

106. Lake, R. A., and B. W. Robinson. 2005. Immunotherapy and chemotherapy--a practical partnership. *Nat Rev Cancer* 5:397-405.

107. Wallen, H., J. A. Thompson, J. Z. Reilly, R. M. Rodmyre, J. Cao, and C. Yee. 2009. Fludarabine modulates immune response and extends in vivo survival of adoptively transferred CD8 T cells in patients with metastatic melanoma. *PloS one* 4:e4749.

108. Poehlein, C. H., D. P. Haley, E. B. Walker, and B. A. Fox. 2009. Depletion of tumor-induced Treg prior to reconstitution rescues enhanced priming of tumor-specific, therapeutic effector T cells in lymphopenic hosts. *European journal of immunology* 39:3121-3133.

109. Powell, D. J., Jr., C. R. de Vries, T. Allen, M. Ahmadzadeh, and S. A. Rosenberg. 2007. Inability to mediate prolonged reduction of regulatory T Cells after transfer of autologous CD25-depleted PBMC and interleukin-2 after lymphodepleting chemotherapy. *J Immunother* 30:438-447.

110. Turk, M. J., J. A. Guevara-Patino, G. A. Rizzuto, M. E. Engelhorn, S. Sakaguchi, and A. N. Houghton. 2004. Concomitant tumor immunity to a poorly immunogenic melanoma is prevented by regulatory T cells. *J Exp Med* 200:771-782.

111. Condamine, T., and D. I. Gabrilovich. Molecular mechanisms regulating myeloid-derived suppressor cell differentiation and function. *Trends in immunology* 32:19-25.

112. Rosenberg, S. A., and M. E. Dudley. 2009. Adoptive cell therapy for the treatment of patients with metastatic melanoma. *Current opinion in immunology* 21:233-240.

113. Dudley, M. E. 2011. Adoptive cell therapy for patients with melanoma. *J Cancer* 2:360-362.

114. Trapani, J. A. 1995. Target cell apoptosis induced by cytotoxic T cells and natural killer cells involves synergy between the pore-forming protein, perforin, and the serine protease, granzyme B. *Aust N Z J Med* 25:793-799.

115. Young, J. D., H. Hengartner, E. R. Podack, and Z. A. Cohn. 1986. Purification and characterization of a cytolytic pore-forming protein from granules of cloned lymphocytes with natural killer activity. *Cell* 44:849-859.

116. Andersen, M. H., D. Schrama, P. Thor Straten, and J. C. Becker. 2006. Cytotoxic T cells. *J Invest Dermatol* 126:32-41.

117. Goff, S. L., F. O. Smith, J. A. Klapper, R. Sherry, J. R. Wunderlich, S. M. Steinberg, D. White, S. A. Rosenberg, M. E. Dudley, and J. C. Yang. 2010. Tumor infiltrating lymphocyte therapy for metastatic melanoma: analysis of tumors resected for TIL. *J Immunother* 33:840-847.

118. Muranski, P., and N. P. Restifo. 2009. Adoptive immunotherapy of cancer using CD4(+) T cells. *Current opinion in immunology* 21:200-208.

119. Weber, J., M. Atkins, P. Hwu, L. Radvanyi, M. Sznol, and C. Yee. 2011. White paper on adoptive cell therapy for cancer with tumor-infiltrating lymphocytes: a report of the CTEP subcommittee on adoptive cell therapy. *Clin Cancer Res* 17:1664-1673.

120. Appay, V., J. J. Zaunders, L. Papagno, J. Sutton, A. Jaramillo, A. Waters, P. Easterbrook, P. Grey, D. Smith, A. J. McMichael, D. A. Cooper, S. L. Rowland-Jones, and A. D. Kelleher. 2002. Characterization of CD4(+) CTLs ex vivo. *J Immunol* 168:5954-5958.

121. Qui, H. Z., A. T. Hagymasi, S. Bandyopadhyay, M. C. St Rose, R. Ramanarasimhaiah, A. Menoret, R. S. Mittler, S. M. Gordon, S. L. Reiner, A. T.

Vella, and A. J. Adler. 2011. CD134 plus CD137 dual costimulation induces Eomesodermin in CD4 T cells to program cytotoxic Th1 differentiation. *J Immunol* 187:3555-3564.

122. Merkenschlager, M., L. Terry, R. Edwards, and P. C. Beverley. 1988. Limiting dilution analysis of proliferative responses in human lymphocyte populations defined by the monoclonal antibody UCHL1: implications for differential CD45 expression in T cell memory formation. *European journal of immunology* 18:1653-1661.

123. Sallusto, F., J. Geginat, and A. Lanzavecchia. 2004. Central memory and effector memory T cell subsets: function, generation, and maintenance. *Annu Rev Immunol* 22:745-763.

124. Gattinoni, L., E. Lugli, Y. Ji, Z. Pos, C. M. Paulos, M. F. Quigley, J. R. Almeida, E. Gostick, Z. Yu, C. Carpenito, E. Wang, D. C. Douek, D. A. Price, C. H. June, F. M. Marincola, M. Roederer, and N. P. Restifo. A human memory T cell subset with stem cell-like properties. *Nat Med* 17:1290-1297.

125. Klebanoff, C. A., L. Gattinoni, D. C. Palmer, P. Muranski, Y. Ji, C. S. Hinrichs, Z. A. Borman, S. P. Kerkar, C. D. Scott, S. E. Finkelstein, S. A. Rosenberg, and N. P. Restifo. 2011. Determinants of successful CD8+ T-cell adoptive immunotherapy for large established tumors in mice. *Clin Cancer Res* 17:5343-5352.

126. Vallejo, A. N. 2005. CD28 extinction in human T cells: altered functions and the program of T-cell senescence. *Immunol Rev* 205:158-169.

127. Strioga, M., V. Pasukoniene, and D. Characiejus. CD8+ CD28- and CD8+ CD57+ T cells and their role in health and disease. *Immunology* 134:17-32.

128. Plunkett, F. J., O. Franzese, H. M. Finney, J. M. Fletcher, L. L. Belaramani, M. Salmon, I. Dokal, D. Webster, A. D. Lawson, and A. N. Akbar. 2007. The loss of telomerase activity in highly differentiated CD8+CD28-CD27- T cells is associated with decreased Akt (Ser473) phosphorylation. *J Immunol* 178:7710-7719.

129. Appay, V., L. Papagno, C. A. Spina, P. Hansasuta, A. King, L. Jones, G. S. Ogg, S. Little, A. J. McMichael, D. D. Richman, and S. L. Rowland-Jones. 2002. Dynamics of T cell responses in HIV infection. *J Immunol* 168:3660-3666.

130. Papagno, L., C. A. Spina, A. Marchant, M. Salio, N. Rufer, S. Little, T. Dong, G. Chesney, A. Waters, P. Easterbrook, P. R. Dunbar, D. Shepherd, V. Cerundolo, V. Emery, P. Griffiths, C. Conlon, A. J. McMichael, D. D. Richman, S. L. Rowland-Jones, and V. Appay. 2004. Immune activation and CD8+ T-cell differentiation towards senescence in HIV-1 infection. *PLoS Biol* 2:E20.

131. Brenchley, J. M., N. J. Karandikar, M. R. Betts, D. R. Ambrozak, B. J. Hill, L. E. Crotty, J. P. Casazza, J. Kuruppu, S. A. Migueles, M. Connors, M. Roederer, D. C. Douek, and R. A. Koup. 2003. Expression of CD57 defines replicative senescence and antigen-induced apoptotic death of CD8+ T cells. *Blood* 101:2711-2720.

132. Gattinoni, L., X. S. Zhong, D. C. Palmer, Y. Ji, C. S. Hinrichs, Z. Yu, C. Wrzesinski, A. Boni, L. Cassard, L. M. Garvin, C. M. Paulos, P. Muranski, and N. P. Restifo. 2009. Wnt signaling arrests effector T cell differentiation and generates CD8+ memory stem cells. *Nat Med* 15:808-813.

133. Wu, R., M. A. Forget, J. Chacon, C. Bernatchez, C. Haymaker, J. Q. Chen, P. Hwu, and L. G. Radvanyi. Adoptive T-cell therapy using autologous tumor-infiltrating

lymphocytes for metastatic melanoma: current status and future outlook. *Cancer J* 18:160-175.

134. Huang, J., K. W. Kerstann, M. Ahmadzadeh, Y. F. Li, M. El-Gamil, S. A. Rosenberg, and P. F. Robbins. 2006. Modulation by IL-2 of CD70 and CD27 expression on CD8+ T cells: importance for the therapeutic effectiveness of cell transfer immunotherapy. *J Immunol* 176:7726-7735.

135. Zhou, J., M. E. Dudley, S. A. Rosenberg, and P. F. Robbins. 2005. Persistence of multiple tumor-specific T-cell clones is associated with complete tumor regression in a melanoma patient receiving adoptive cell transfer therapy. *J Immunother* 28:53-62.

136. Zhou, J., X. Shen, J. Huang, R. J. Hodes, S. A. Rosenberg, and P. F. Robbins. 2005. Telomere length of transferred lymphocytes correlates with in vivo persistence and tumor regression in melanoma patients receiving cell transfer therapy. *J Immunol* 175:7046-7052.

137. Kern, F., S. Ode-Hakim, K. Vogt, C. Hoflich, P. Reinke, and H. D. Volk. 1996. The enigma of CD57+CD28- T cell expansion--anergy or activation? *Clin Exp Immunol* 104:180-184.

138. Dolstra, H., F. Preijers, E. Van de Wiel-van Kemenade, A. Schattenberg, J. Galama, and T. de Witte. 1995. Expansion of CD8+CD57+ T cells after allogeneic BMT is related with a low incidence of relapse and with cytomegalovirus infection. *Br J Haematol* 90:300-307.

139. Kagi, D., B. Ledermann, K. Burki, P. Seiler, B. Odermatt, K. J. Olsen, E. R. Podack, R. M. Zinkernagel, and H. Hengartner. 1994. Cytotoxicity mediated by T cells and natural killer cells is greatly impaired in perforin-deficient mice. *Nature* 369:31-37.

140. Lieberman, J., L. A. Trimble, R. S. Friedman, J. Lisziewicz, F. Lori, P. Shankar, and H. Jessen. 1999. Expansion of CD57 and CD62L-CD45RA+ CD8 T lymphocytes correlates with reduced viral plasma RNA after primary HIV infection. *AIDS* 13:891-899.

141. Lynne, J. E., I. Schmid, J. L. Matud, K. Hirji, S. Buessow, D. M. Shlian, and J. V. Giorgi. 1998. Major expansions of select CD8+ subsets in acute Epstein-Barr virus infection: comparison with chronic human immunodeficiency virus disease. *J Infect Dis* 177:1083-1087.

142. Ohkawa, T., S. Seki, H. Dobashi, Y. Koike, Y. Habu, K. Ami, H. Hiraide, and I. Sekine. 2001. Systematic characterization of human CD8+ T cells with natural killer cell markers in comparison with natural killer cells and normal CD8+ T cells. *Immunology* 103:281-290.

143. Takayama, E., Y. Koike, T. Ohkawa, T. Majima, M. Fukasawa, N. Shinomiya, T. Yamaguchi, M. Konishi, H. Hiraide, T. Tadakuma, and S. Seki. 2003. Functional and Vbeta repertoire characterization of human CD8+ T-cell subsets with natural killer cell markers, CD56+ CD57- T cells, CD56+ CD57+ T cells and CD56- CD57+ T cells. *Immunology* 108:211-219.

144. Appay, V., P. R. Dunbar, M. Callan, P. Klenerman, G. M. Gillespie, L. Papagno, G. S. Ogg, A. King, F. Lechner, C. A. Spina, S. Little, D. V. Havlir, D. D. Richman, N. Gruener, G. Pape, A. Waters, P. Easterbrook, M. Salio, V. Cerundolo, A. J. McMichael, and S. L. Rowland-Jones. 2002. Memory CD8+ T cells vary in differentiation phenotype in different persistent virus infections. *Nat Med* 8:379-385.

145. Hoji, A., N. C. Connolly, W. G. Buchanan, and C. R. Rinaldo, Jr. 2007. CD27 and CD57 expression reveals atypical differentiation of human immunodeficiency virus type 1-specific memory CD8+ T cells. *Clin Vaccine Immunol* 14:74-80.

146. van Baarle, D., S. Kostense, E. Hovenkamp, G. Ogg, N. Nanlohy, M. F. Callan, N. H. Dukers, A. J. McMichael, M. H. van Oers, and F. Miedema. 2002. Lack of Epstein-Barr virus- and HIV-specific CD27- CD8+ T cells is associated with progression to viral disease in HIV-infection. *AIDS* 16:2001-2011.

147. Kaech, S. M., and E. J. Wherry. 2007. Heterogeneity and cell-fate decisions in effector and memory CD8+ T cell differentiation during viral infection. *Immunity* 27:393-405.

148. Casado, J. G., R. Soto, O. DelaRosa, E. Peralbo, M. del Carmen Munoz-Villanueva, L. Rioja, J. Pena, R. Solana, and R. Tarazona. 2005. CD8 T cells expressing NK associated receptors are increased in melanoma patients and display an effector phenotype. *Cancer Immunol Immunother* 54:1162-1171.

149. Akagi, J., and H. Baba. 2008. Prognostic value of CD57(+) T lymphocytes in the peripheral blood of patients with advanced gastric cancer. *Int J Clin Oncol* 13:528-535.

150. Characiejus, D., V. Pasukoniene, R. Jonusauskaite, N. Azlauskaite, E. Aleknavicius, M. Mauricas, and W. D. Otter. 2008. Peripheral blood CD8highCD57+ lymphocyte levels may predict outcome in melanoma patients treated with adjuvant interferon-alpha. *Anticancer Res* 28:1139-1142.

151. Characiejus, D., V. Pasukoniene, N. Kazlauskaite, K. P. Valuckas, T. Petraitis, M. Mauricas, and W. Den Otter. 2002. Predictive value of CD8highCD57+ lymphocyte

subset in interferon therapy of patients with renal cell carcinoma. *Anticancer Res* 22:3679-3683.

152. Chochi, K., T. Ichikura, T. Majima, T. Kawabata, A. Matsumoto, H. Sugasawa, N. Kawarabayashi, E. Takayama, H. Hiraide, S. Seki, and H. Mochizuki. 2003. The increase of CD57+ T cells in the peripheral blood and their impaired immune functions in patients with advanced gastric cancer. *Oncol Rep* 10:1443-1448.

153. Bandres, E., J. Merino, B. Vazquez, S. Inoges, C. Moreno, M. L. Subira, and A. Sanchez-Ibarrola. 2000. The increase of IFN-gamma production through aging correlates with the expanded CD8(+high)CD28(-)CD57(+) subpopulation. *Clin Immunol* 96:230-235.

154. Gorochov, G., P. Debre, V. Leblond, B. Sadat-Sowti, F. Sigaux, and B. Autran. 1994. Oligoclonal expansion of CD8+ CD57+ T cells with restricted T-cell receptor beta chain variability after bone marrow transplantation. *Blood* 83:587-595.

155. Pittet, M. J., D. E. Speiser, D. Valmori, J. C. Cerottini, and P. Romero. 2000. Cutting edge: cytolytic effector function in human circulating CD8+ T cells closely correlates with CD56 surface expression. *J Immunol* 164:1148-1152.

156. Mortarini, R., A. Piris, A. Maurichi, A. Molla, I. Bersani, A. Bono, C. Bartoli, M. Santinami, C. Lombardo, F. Ravagnani, N. Cascinelli, G. Parmiani, and A. Anichini. 2003. Lack of terminally differentiated tumor-specific CD8+ T cells at tumor site in spite of antitumor immunity to self-antigens in human metastatic melanoma. *Cancer Res* 63:2535-2545.

157. Takata, H., and M. Takiguchi. 2006. Three memory subsets of human CD8+ T cells differently expressing three cytolytic effector molecules. *J Immunol* 177:4330-4340.

158. Ahmadzadeh, M., and S. A. Rosenberg. 2005. TGF-beta 1 attenuates the acquisition and expression of effector function by tumor antigen-specific human memory CD8 T cells. *J Immunol* 174:5215-5223.

159. Bennicelli, J. L., and D. t. Guerry. 1993. Production of multiple cytokines by cultured human melanomas. *Exp Dermatol* 2:186-190.

160. Derynck, R., J. A. Jarrett, E. Y. Chen, D. H. Eaton, J. R. Bell, R. K. Assoian, A. B. Roberts, M. B. Sporn, and D. V. Goeddel. 1985. Human transforming growth factor-beta complementary DNA sequence and expression in normal and transformed cells. *Nature* 316:701-705.

161. Polak, M. E., N. J. Borthwick, F. G. Gabriel, P. Johnson, B. Higgins, J. Hurren, D. McCormick, M. J. Jager, and I. A. Cree. 2007. Mechanisms of local immunosuppression in cutaneous melanoma. *Br J Cancer* 96:1879-1887.

162. Currier, J. R., H. Deulofeut, K. S. Barron, P. J. Kehn, and M. A. Robinson. 1996. Mitogens, superantigens, and nominal antigens elicit distinctive patterns of TCRB CDR3 diversity. *Hum Immunol* 48:39-51.

163. He, L., J. Hakimi, D. Salha, I. Miron, P. Dunn, and L. Radvanyi. 2005. A sensitive flow cytometry-based cytotoxic T-lymphocyte assay through detection of cleaved caspase 3 in target cells. *J Immunol Methods* 304:43-59.

164. Sakuishi, K., L. Apetoh, J. M. Sullivan, B. R. Blazar, V. K. Kuchroo, and A. C. Anderson. Targeting Tim-3 and PD-1 pathways to reverse T cell exhaustion and restore anti-tumor immunity. *J Exp Med* 207:2187-2194.

165. Quigley, M., F. Pereyra, B. Nilsson, F. Porichis, C. Fonseca, Q. Eichbaum, B. Julg, J. L. Jesneck, K. Brosnahan, S. Imam, K. Russell, I. Toth, A. Piechocka-Trocha, D.

Dolfi, J. Angelosanto, A. Crawford, H. Shin, D. S. Kwon, J. Zupkosky, L. Francisco, G. J. Freeman, E. J. Wherry, D. E. Kaufmann, B. D. Walker, B. Ebert, and W. N. Haining. Transcriptional analysis of HIV-specific CD8+ T cells shows that PD-1 inhibits T cell function by upregulating BATF. *Nat Med* 16:1147-1151.

166. Duraiswamy, J., C. C. Ibegbu, D. Masopust, J. D. Miller, K. Araki, G. H. Doho, P. Tata, S. Gupta, M. J. Zilliox, H. I. Nakaya, B. Pulendran, W. N. Haining, G. J. Freeman, and R. Ahmed. Phenotype, function, and gene expression profiles of programmed death-1(hi) CD8 T cells in healthy human adults. *J Immunol* 186:4200-4212.

167. Le Priol, Y., D. Puthier, C. Lecureuil, C. Combadiere, P. Debre, C. Nguyen, and B. Combadiere. 2006. High cytotoxic and specific migratory potencies of senescent CD8+ CD57+ cells in HIV-infected and uninfected individuals. *J Immunol* 177:5145-5154.

168. Dudley, M. E., J. R. Wunderlich, P. F. Robbins, J. C. Yang, P. Hwu, D. J. Schwartzentruber, S. L. Topalian, R. Sherry, N. P. Restifo, A. M. Hubicki, M. R. Robinson, M. Raffeld, P. Duray, C. A. Seipp, L. Rogers-Freezer, K. E. Morton, S. A. Mavroukakis, D. E. White, and S. A. Rosenberg. 2002. Cancer regression and autoimmunity in patients after clonal repopulation with antitumor lymphocytes. *Science* 298:850-854.

169. Bannard, O., M. Kraman, and D. T. Fearon. Cutting edge: Virus-specific CD8+ T cell clones and the maintenance of replicative function during a persistent viral infection. *J Immunol* 185:7141-7145.

170. Ibegbu, C. C., Y. X. Xu, W. Harris, D. Maggio, J. D. Miller, and A. P. Kourtis. 2005. Expression of killer cell lectin-like receptor G1 on antigen-specific human CD8+ T lymphocytes during active, latent, and resolved infection and its relation with CD57. *J Immunol* 174:6088-6094.

171. Voehringer, D., M. Koschella, and H. Pircher. 2002. Lack of proliferative capacity of human effector and memory T cells expressing killer cell lectinlike receptor G1 (KLRG1). *Blood* 100:3698-3702.

172. Morley, J. K., F. M. Batliwalla, R. Hingorani, and P. K. Gregersen. 1995. Oligoclonal CD8+ T cells are preferentially expanded in the CD57+ subset. *J Immunol* 154:6182-6190.

173. Kim, Y. J., T. M. Stringfield, Y. Chen, and H. E. Broxmeyer. 2005. Modulation of cord blood CD8+ T-cell effector differentiation by TGF-beta1 and 4-1BB costimulation. *Blood* 105:274-281.

174. Smyth, M. J., S. L. Strobl, H. A. Young, J. R. Ortaldo, and A. C. Ochoa. 1991. Regulation of lymphokine-activated killer activity and pore-forming protein gene expression in human peripheral blood CD8+ T lymphocytes. Inhibition by transforming growth factor-beta. *J Immunol* 146:3289-3297.

175. Willinger, T., T. Freeman, M. Herbert, H. Hasegawa, A. J. McMichael, and M. F. Callan. 2006. Human naive CD8 T cells down-regulate expression of the WNT pathway transcription factors lymphoid enhancer binding factor 1 and transcription factor 7 (T cell factor-1) following antigen encounter in vitro and in vivo. *J Immunol* 176:1439-1446.

176. Walker, E. B., D. Haley, U. Petrausch, K. Floyd, W. Miller, N. Sanjuan, G. Alvord, B. A. Fox, and W. J. Urba. 2008. Phenotype and functional characterization of long-term gp100-specific memory CD8+ T cells in disease-free melanoma patients before and after boosting immunization. *Clin Cancer Res* 14:5270-5283.

177. Anichini, A., A. Molla, C. Vegetti, I. Bersani, R. Zappasodi, F. Arienti, F. Ravagnani, A. Maurichi, R. Patuzzo, M. Santinami, H. Pircher, M. Di Nicola, and R. Mortarini. Tumor-reactive CD8+ early effector T cells identified at tumor site in primary and metastatic melanoma. *Cancer Res* 70:8378-8387.

178. Lopez-Verges, S., J. M. Milush, S. Pandey, V. A. York, J. Arakawa-Hoyt, H. Pircher, P. J. Norris, D. F. Nixon, and L. L. Lanier. CD57 defines a functionally distinct population of mature NK cells in the human CD56dimCD16+ NK-cell subset. *Blood* 116:3865-3874.

179. Jungalwala, F. B. 1994. Expression and biological functions of sulfoglucuronyl glycolipids (SGGLs) in the nervous system--a review. *Neurochem Res* 19:945-957.

180. Cebo, C., T. Dambrouck, E. Maes, C. Laden, G. Strecker, J. C. Michalski, and J. P. Zanetta. 2001. Recombinant human interleukins IL-1alpha, IL-1beta, IL-4, IL-6, and IL-7 show different and specific calcium-independent carbohydrate-binding properties. *J Biol Chem* 276:5685-5691.

181. Chong, L. K., R. J. Aicheler, S. Llewellyn-Lacey, P. Tomasec, P. Brennan, and E. C. Wang. 2008. Proliferation and interleukin 5 production by CD8hi CD57+ T cells. *Eur J Immunol* 38:995-1000.

182. Zhang, J., I. Scordi, M. J. Smyth, and M. G. Lichtenheld. 1999. Interleukin 2 receptor signaling regulates the perforin gene through signal transducer and activator of transcription (Stat)5 activation of two enhancers. *J Exp Med* 190:1297-1308.

183. Godin-Ethier, J., S. Pelletier, L. A. Hanafi, P. O. Gannon, M. A. Forget, J. P. Routy, M. R. Boulassel, U. Krzemien, S. Tanguay, J. B. Lattouf, N. Arbour, and R. Lapointe. 2009. Human activated T lymphocytes modulate IDO expression in tumors through Th1/Th2 balance. *J Immunol* 183:7752-7760.

184. Takikawa, O. 2005. Biochemical and medical aspects of the indoleamine 2,3-dioxygenase-initiated L-tryptophan metabolism. *Biochem Biophys Res Commun* 338:12-19.

185. Okada, T., T. Iiai, Y. Kawachi, T. Moroda, Y. Takii, K. Hatakeyama, and T. Abo. 1995. Origin of CD57+ T cells which increase at tumour sites in patients with colorectal cancer. *Clin Exp Immunol* 102:159-166.

186. Thomas, D. A., and J. Massague. 2005. TGF-beta directly targets cytotoxic T cell functions during tumor evasion of immune surveillance. *Cancer Cell* 8:369-380.

187. Gorelik, L., and R. A. Flavell. 2001. Immune-mediated eradication of tumors through the blockade of transforming growth factor-beta signaling in T cells. *Nat Med* 7:1118-1122.

188. Haas, A. R., J. Sun, A. Vachani, A. F. Wallace, M. Silverberg, V. Kapoor, and S. M. Albelda. 2006. Cycloxygenase-2 inhibition augments the efficacy of a cancer vaccine. *Clin Cancer Res* 12:214-222.

189. Besser, M. J., R. Shapira-Frommer, A. J. Treves, D. Zippel, O. Itzhaki, L. Hershkovitz, D. Levy, A. Kubi, E. Hovav, N. Chermoshniuk, B. Shalmon, I. Hardan,

R. Catane, G. Markel, S. Apter, A. Ben-Nun, I. Kuchuk, A. Shimoni, A. Nagler, and J. Schachter. Clinical responses in a phase II study using adoptive transfer of short-term cultured tumor infiltration lymphocytes in metastatic melanoma patients. *Clin Cancer Res* 16:2646-2655.

190. Eisenhauer, E. A., P. Therasse, J. Bogaerts, L. H. Schwartz, D. Sargent, R. Ford, J. Dancey, S. Arbuck, S. Gwyther, M. Mooney, L. Rubinstein, L. Shankar, L. Dodd, R. Kaplan, D. Lacombe, and J. Verweij. 2009. New response evaluation criteria in solid tumours: revised RECIST guideline (version 1.1). *Eur J Cancer* 45:228-247.

191. Hinrichs, C. S., Z. A. Borman, L. Gattinoni, Z. Yu, W. R. Burns, J. Huang, C. A. Klebanoff, L. A. Johnson, S. P. Kerkar, S. Yang, P. Muranski, D. C. Palmer, C. D. Scott, R. A. Morgan, P. F. Robbins, S. A. Rosenberg, and N. P. Restifo. Human effector CD8+ T cells derived from naive rather than memory subsets possess superior traits for adoptive immunotherapy. *Blood* 117:808-814.

192. Klebanoff, C. A., L. Gattinoni, and N. P. Restifo. Sorting through subsets: which T-cell populations mediate highly effective adoptive immunotherapy? *J Immunother* 35:651-660.

193. Baitsch, L., A. Legat, L. Barba, S. A. Fuertes Marraco, J. P. Rivals, P. Baumgaertner, C. Christiansen-Jucht, H. Bouzourene, D. Rimoldi, H. Pircher, N. Rufer, M. Matter, O. Michielin, and D. E. Speiser. 2012. Extended co-expression of inhibitory receptors by human CD8 T-cells depending on differentiation, antigen-specificity and anatomical localization. *PLoS One* 7:e30852.

194. Smyth, M. J., Y. Hayakawa, K. Takeda, and H. Yagita. 2002. New aspects of natural-killer-cell surveillance and therapy of cancer. *Nat Rev Cancer* 2:850-861.

195. Weng, N. P., A. N. Akbar, and J. Goronzy. 2009. CD28(-) T cells: their role in the age-associated decline of immune function. *Trends Immunol* 30:306-312.

196. Willinger, T., T. Freeman, H. Hasegawa, A. J. McMichael, and M. F. Callan. 2005. Molecular signatures distinguish human central memory from effector memory CD8 T cell subsets. *J Immunol* 175:5895-5903.

197. Parish, I. A., and S. M. Kaech. 2009. Diversity in CD8(+) T cell differentiation. *Curr Opin Immunol* 21:291-297.

198. Parish, I. A., S. Rao, G. K. Smyth, T. Juelich, G. S. Denyer, G. M. Davey, A. Strasser, and W. R. Heath. 2009. The molecular signature of CD8+ T cells undergoing deletional tolerance. *Blood* 113:4575-4585.

199. Martin-Orozco, N., Y. Li, Y. Wang, S. Liu, P. Hwu, Y. J. Liu, C. Dong, and L. Radvanyi. Melanoma cells express ICOS ligand to promote the activation and expansion of T-regulatory cells. *Cancer Res* 70:9581-9590.

200. Vendel, A. C., J. Calemine-Fenaux, A. Izrael-Tomasevic, V. Chauhan, D. Arnott, and D. L. Eaton. 2009. B and T lymphocyte attenuator regulates B cell receptor signaling by targeting Syk and BLNK. *J Immunol* 182:1509-1517.

201. Baitsch, L., A. Legat, L. Barba, S. A. Fuertes Marraco, J. P. Rivals, P. Baumgaertner, C. Christiansen-Jucht, H. Bouzourene, D. Rimoldi, H. Pircher, N. Rufer, M. Matter, O. Michielin, and D. E. Speiser. Extended co-expression of inhibitory receptors by human CD8 T-cells depending on differentiation, antigen-specificity and anatomical localization. *PLoS One* 7:e30852.

202. Wu, R. C., S. Liu, J. A. Chacon, S. Wu, Y. Li, P. Sukhumalchandra, J. L. Murray, J. J. Molldrem, P. Hwu, H. Pircher, G. Lizee, and L. G. Radvanyi. Detection and

characterization of a novel subset of CD8(+)CD57(+) T cells in metastatic melanoma with an incompletely differentiated phenotype. *Clin Cancer Res* 18:2465-2477.

203. Herndler-Brandstetter, D., S. Schwaiger, E. Veel, C. Fehrer, D. P. Cioca, G. Almanzar, M. Keller, G. Pfister, W. Parson, R. Wurzner, D. Schonitzer, S. M. Henson, R. Aspinall, G. Lepperdinger, and B. Grubeck-Loebenstein. 2005. CD25-expressing CD8+ T cells are potent memory cells in old age. *J Immunol* 175:1566-1574.

204. McDonald, D. R., F. Goldman, O. D. Gomez-Duarte, A. C. Issekutz, D. S. Kumararatne, R. Doffinger, and R. S. Geha. Impaired T-cell receptor activation in IL-1 receptor-associated kinase-4-deficient patients. *J Allergy Clin Immunol* 126:332-337, 337 e331-332.

205. Morel, Y., J. M. Schiano de Colella, J. Harrop, K. C. Deen, S. D. Holmes, T. A. Wattam, S. S. Khandekar, A. Truneh, R. W. Sweet, J. A. Gastaut, D. Olive, and R. T. Costello. 2000. Reciprocal expression of the TNF family receptor herpes virus entry mediator and its ligand LIGHT on activated T cells: LIGHT down-regulates its own receptor. *J Immunol* 165:4397-4404.

206. Collins, N. D., C. D'Souza, B. Albrecht, M. D. Robek, L. Ratner, W. Ding, P. L. Green, and M. D. Lairmore. 1999. Proliferation response to interleukin-2 and Jak/Stat activation of T cells immortalized by human T-cell lymphotropic virus type 1 is independent of open reading frame I expression. *J Virol* 73:9642-9649.

207. Kim, T. K., L. S. St John, E. D. Wieder, J. Khalili, Q. Ma, and K. V. Komanduri. 2009. Human late memory CD8+ T cells have a distinct cytokine signature

characterized by CC chemokine production without IL-2 production. *J Immunol* 183:6167-6174.

208. Makedonas, G., and M. R. Betts. Living in a house of cards: re-evaluating CD8+ T-cell immune correlates against HIV. *Immunol Rev* 239:109-124.

209. Appay, V., A. Bosio, S. Lokan, Y. Wiencek, C. Biervert, D. Kusters, E. Devevre, D. Speiser, P. Romero, N. Rufer, and S. Leyvraz. 2007. Sensitive gene expression profiling of human T cell subsets reveals parallel post-thymic differentiation for CD4+ and CD8+ lineages. *J Immunol* 179:7406-7414.

210. Turnbull, I. R., and M. Colonna. 2007. Activating and inhibitory functions of DAP12. *Nat Rev Immunol* 7:155-161.

211. Ito, M., T. Maruyama, N. Saito, S. Koganei, K. Yamamoto, and N. Matsumoto. 2006. Killer cell lectin-like receptor G1 binds three members of the classical cadherin family to inhibit NK cell cytotoxicity. *J Exp Med* 203:289-295.

212. Brumbaugh, K. M., B. A. Binstadt, D. D. Billadeau, R. A. Schoon, C. J. Dick, R. M. Ten, and P. J. Leibson. 1997. Functional role for Syk tyrosine kinase in natural killer cell-mediated natural cytotoxicity. *J Exp Med* 186:1965-1974.

213. Poli, A., T. Michel, M. Theresine, E. Andres, F. Hentges, and J. Zimmer. 2009. CD56bright natural killer (NK) cells: an important NK cell subset. *Immunology* 126:458-465.

214. Sugimoto, N., T. Oida, K. Hirota, K. Nakamura, T. Nomura, T. Uchiyama, and S. Sakaguchi. 2006. Foxp3-dependent and -independent molecules specific for CD25+CD4+ natural regulatory T cells revealed by DNA microarray analysis. *Int Immunol* 18:1197-1209.

215. Safford, M., S. Collins, M. A. Lutz, A. Allen, C. T. Huang, J. Kowalski, A. Blackford, M. R. Horton, C. Drake, R. H. Schwartz, and J. D. Powell. 2005. Egr-2 and Egr-3 are negative regulators of T cell activation. *Nat Immunol* 6:472-480.

216. Calnan, B. J., S. Szychowski, F. K. Chan, D. Cado, and A. Winoto. 1995. A role for the orphan steroid receptor Nur77 in apoptosis accompanying antigen-induced negative selection. *Immunity* 3:273-282.

217. Baitsch, L., P. Baumgaertner, E. Devevre, S. K. Raghav, A. Legat, L. Barba, S. Wieckowski, H. Bouzourene, B. Deplancke, P. Romero, N. Rufer, and D. E. Speiser. Exhaustion of tumor-specific CD8(+) T cells in metastases from melanoma patients. *J Clin Invest* 121:2350-2360.

218. Wherry, E. J., S. J. Ha, S. M. Kaech, W. N. Haining, S. Sarkar, V. Kalia, S. Subramaniam, J. N. Blattman, D. L. Barber, and R. Ahmed. 2007. Molecular signature of CD8+ T cell exhaustion during chronic viral infection. *Immunity* 27:670-684.

219. Murphy, T. L., and K. M. Murphy. Slow down and survive: Enigmatic immunoregulation by BTLA and HVEM. *Annu Rev Immunol* 28:389-411.

220. Wherry, E. J. T cell exhaustion. *Nat Immunol* 12:492-499.

221. Fourcade, J., Z. Sun, M. Benallaoua, P. Guillaume, I. F. Luescher, C. Sander, J. M. Kirkwood, V. Kuchroo, and H. M. Zarour. Upregulation of Tim-3 and PD-1 expression is associated with tumor antigen-specific CD8+ T cell dysfunction in melanoma patients. *J Exp Med* 207:2175-2186.

222. Blackburn, S. D., H. Shin, W. N. Haining, T. Zou, C. J. Workman, A. Polley, M. R. Betts, G. J. Freeman, D. A. Vignali, and E. J. Wherry. 2009. Coregulation of CD8+ T

cell exhaustion by multiple inhibitory receptors during chronic viral infection. *Nat Immunol* 10:29-37.

223. Inozume, T., K. Hanada, Q. J. Wang, M. Ahmadzadeh, J. R. Wunderlich, S. A. Rosenberg, and J. C. Yang. Selection of CD8+PD-1+ lymphocytes in fresh human melanomas enriches for tumor-reactive T cells. *J Immunother* 33:956-964.

224. Schwartz, R. H. 2003. T cell anergy. *Annu Rev Immunol* 21:305-334.

225. Haymaker, C., R. Wu, C. Bernatchez, and L. Radvanyi. 2012. PD-1 and BTLA and CD8(+) T-cell "exhaustion" in cancer: "Exercising" an alternative viewpoint. *Oncoimmunology* 1:735-738.

226. Peng, W., C. Liu, C. Xu, Y. Lou, J. Chen, Y. Yang, H. Yagita, W. W. Overwijk, G. Lizee, L. Radvanyi, and P. Hwu. 2012. PD-1 blockade enhances T-cell migration to tumors by elevating IFN-gamma inducible chemokines. *Cancer Res* 72:5209-5218.

227. Wong, R. M., R. R. Scotland, R. L. Lau, C. Wang, A. J. Korman, W. M. Kast, and J. S. Weber. 2007. Programmed death-1 blockade enhances expansion and functional capacity of human melanoma antigen-specific CTLs. *Int Immunol* 19:1223-1234.

228. Mujib, S., R. B. Jones, C. Lo, N. Aidarus, K. Clayton, A. Sakhdari, E. Benko, C. Kovacs, and M. A. Ostrowski. Antigen-independent induction of Tim-3 expression on human T cells by the common gamma-chain cytokines IL-2, IL-7, IL-15, and IL-21 is associated with proliferation and is dependent on the phosphoinositide 3-kinase pathway. *J Immunol* 188:3745-3756.

229. Henel, G., K. Singh, D. Cui, S. Pryshchep, W. W. Lee, C. M. Weyand, and J. J. Goronzy. 2006. Uncoupling of T-cell effector functions by inhibitory killer immunoglobulin-like receptors. *Blood* 107:4449-4457.

230. Bjorkstrom, N. K., V. Beziat, F. Cichocki, L. L. Liu, J. Levine, S. Larsson, R. A. Koup, S. K. Anderson, H. G. Ljunggren, and K. J. Malmberg. 2012. CD8 T cells express randomly selected KIRs with distinct specificities compared with NK cells. *Blood* 120:3455-3465.

231. Hurchla, M. A., J. R. Sedy, and K. M. Murphy. 2007. Unexpected role of B and T lymphocyte attenuator in sustaining cell survival during chronic allostimulation. *J Immunol* 178:6073-6082.

232. Wakamatsu, E., D. Mathis, and C. Benoist. 2013. Convergent and divergent effects of costimulatory molecules in conventional and regulatory CD4+ T cells. *Proc Natl Acad Sci U S A* 110:1023-1028.

233. Tsushima, F., S. Yao, T. Shin, A. Flies, S. Flies, H. Xu, K. Tamada, D. M. Pardoll, and L. Chen. 2007. Interaction between B7-H1 and PD-1 determines initiation and reversal of T-cell anergy. *Blood* 110:180-185.

234. Goldberg, M. V., C. H. Maris, E. L. Hipkiss, A. S. Flies, L. Zhen, R. M. Tuder, J. F. Grosso, T. J. Harris, D. Getnet, K. A. Whartenby, D. G. Brockstedt, T. W. Dubensky, Jr., L. Chen, D. M. Pardoll, and C. G. Drake. 2007. Role of PD-1 and its ligand, B7-H1, in early fate decisions of CD8 T cells. *Blood* 110:186-192.

235. Keir, M. E., G. J. Freeman, and A. H. Sharpe. 2007. PD-1 regulates self-reactive CD8+ T cell responses to antigen in lymph nodes and tissues. *J Immunol* 179:5064-5070.

236. Radvanyi, L. G., G. B. Mills, and R. G. Miller. 1993. Religation of the T cell receptor after primary activation of mature T cells inhibits proliferation and induces apoptotic cell death. *J Immunol* 150:5704-5715.

237. Mauri, D. N., R. Ebner, R. I. Montgomery, K. D. Kochel, T. C. Cheung, G. L. Yu, S. Ruben, M. Murphy, R. J. Eisenberg, G. H. Cohen, P. G. Spear, and C. F. Ware. 1998. LIGHT, a new member of the TNF superfamily, and lymphotoxin alpha are ligands for herpesvirus entry mediator. *Immunity* 8:21-30.

238. Soroosh, P., T. A. Doherty, T. So, A. K. Mehta, N. Khorram, P. S. Norris, S. Scheu, K. Pfeffer, C. Ware, and M. Croft. Herpesvirus entry mediator (TNFRSF14) regulates the persistence of T helper memory cell populations. *J Exp Med* 208:797-809.

239. Chemnitz, J. M., A. R. Lanfranco, I. Braunstein, and J. L. Riley. 2006. B and T lymphocyte attenuator-mediated signal transduction provides a potent inhibitory signal to primary human CD4 T cells that can be initiated by multiple phosphotyrosine motifs. *J Immunol* 176:6603-6614.

240. Wu, R. C., P. Hwu, and L. G. Radvanyi. New insights on the role of CD8(+)CD57(+) T-cells in cancer. *Oncoimmunology* 1:954-956.

241. Jin, H. T., R. Ahmed, and T. Okazaki. Role of PD-1 in regulating T-cell immunity. *Curr Top Microbiol Immunol* 350:17-37.

242. Wu, T. H., Y. Zhen, C. Zeng, H. F. Yi, and Y. Zhao. 2007. B and T lymphocyte attenuator interacts with CD3zeta and inhibits tyrosine phosphorylation of TCRzeta complex during T-cell activation. *Immunol Cell Biol* 85:590-595.

243. Keir, M. E., M. J. Butte, G. J. Freeman, and A. H. Sharpe. 2008. PD-1 and its ligands in tolerance and immunity. *Annu Rev Immunol* 26:677-704.

244. Wherry, E. J., J. N. Blattman, K. Murali-Krishna, R. van der Most, and R. Ahmed. 2003. Viral persistence alters CD8 T-cell immunodominance and tissue distribution and results in distinct stages of functional impairment. *J Virol* 77:4911-4927.

245. Oestreich, K. J., H. Yoon, R. Ahmed, and J. M. Boss. 2008. NFATc1 regulates PD-1 expression upon T cell activation. *J Immunol* 181:4832-4839.

246. Ferrone, S., J. F. Finerty, E. M. Jaffee, and G. J. Nabel. 2000. How much longer will tumour cells fool the immune system? *Immunol Today* 21:70-72.

247. Castle, J. C., S. Kreiter, J. Diekmann, M. Lower, N. van de Roemer, J. de Graaf, A. Selmi, M. Diken, S. Boegel, C. Paret, M. Koslowski, A. N. Kuhn, C. M. Britten, C. Huber, O. Tureci, and U. Sahin. Exploiting the mutanome for tumor vaccination. *Cancer Res* 72:1081-1091.

248. Schreiber, R. D., L. J. Old, and M. J. Smyth. Cancer immunoediting: integrating immunity's roles in cancer suppression and promotion. *Science* 331:1565-1570.

249. Khalili, J. S., S. Liu, T. G. Rodriguez-Cruz, M. Whittington, S. Wardell, C. Liu, M. Zhang, Z. A. Cooper, D. T. Frederick, Y. Li, R. W. Joseph, C. Bernatchez, S. Ekmekcioglu, E. Grimm, L. G. Radvanyi, R. E. Davis, M. A. Davies, J. A. Wargo, P. Hwu, and G. Lizee. Oncogenic BRAF(V600E) promotes stromal cell-mediated immunosuppression via induction of interleukin-1 in melanoma. *Clin Cancer Res* 18:5329-5340.

250. Lanier, L. L. 2008. Up on the tightrope: natural killer cell activation and inhibition. *Nat Immunol* 9:495-502.

251. North, J., I. Bakhsh, C. Marden, H. Pittman, E. Addison, C. Navarrete, R. Anderson, and M. W. Lowdell. 2007. Tumor-primed human natural killer cells lyse NK-resistant tumor targets: evidence of a two-stage process in resting NK cell activation. *J Immunol* 178:85-94.

VITA

Richard C. Wu was born in Taipei, Taiwan on Dec. 4th, 1982, the son of Dr. Chen-Jung Wu and Dr. Li-Cheng Lee. After completing Bachelor of Science in Biochemistry, *summa cum laude*, at the Southern Methodist University in Dallas, TX, he attened the M.D./Ph.D program at the University of Texas Medical School at Houston and M.D. Anderson Cancer Center, in June of 2005. Richard carried out this dissertation work in the Department of Melanoma Medical Oncology at the University of Texas M.D. Anderson Cancer Center under the guidance of Dr. Laszlo Radvanyi, Ph.D. After completing the M.D./Ph.D. program, he will start his clinical training in internal medicine at the University of Texas Southwestern Medical Center in Dallas, TX.